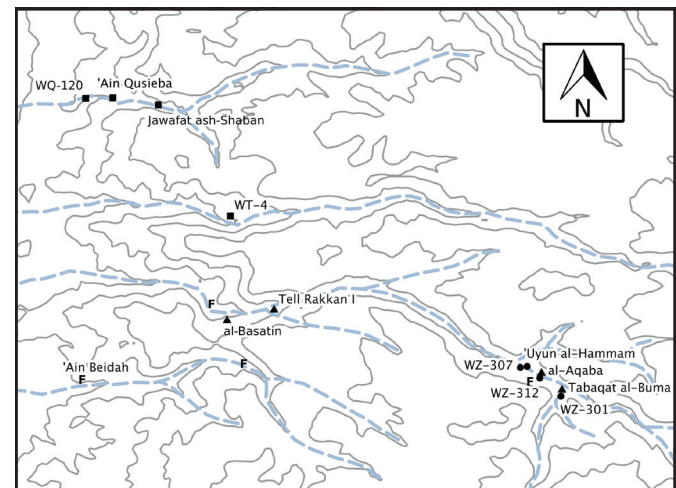




THE CONSEQUENCES OF HUMAN LAND-USE STRATEGIES DURING THE PPNB-LN TRANSITION: A SIMULATION MODELING APPROACH

ISAAC I.T. ULLAH



2017

ARIZONA STATE UNIVERSITY

ANTHROPOLOGICAL RESEARCH PAPERS SERIES NO. 60

About the Author.

Isaac I.T. Ullah is an Assistant Professor at San Diego State University. He received his M.A. in anthropology from the University of Toronto in 2003 and his Ph.D. in anthropology at Arizona State University in 2013. He is a computational archaeologist who employs GIS and simulation modeling to understand the long-term dynamics of humans and the Earth System. He is particularly interested in the social and environmental changes surrounding the advent of farming and animal husbandry. His focus is on Mediterranean and other semi-arid landscapes, and he conducts fieldwork in Jordan, Italy, and Kazakhstan. His field work includes survey for and excavation of early agricultural sites as well as geoarchaeological analyses of anthropogenic landscapes. His specialties include landscape evolution, complex adaptive systems science, computational methods, geospatial analysis, and imagery analysis.

The logo for *Anthropological Research Papers No. 60* is a map showing the known Neolithic sites and potential flint sources in Wadi Ziqlâb and the neighboring Wadis.

Copyright © 2017
The Arizona Board of Regents

All Rights Reserved
Manufactured in the U.S.A.

Library of Congress Cataloging in Publication Data

Ullah, Isaac I. T. (b. 1979)
The Consequences of Human Land-Use Strategies
During the PPNB-LN Transition: A Simulation Modeling Approach

(*Arizona State University Anthropological Research Papers No. 60*)

Includes bibliography

1. Wadi Ziqlâb, (Jordan). 2. Middle East (Jordan)-Antiquities. 3. Neolithic period-Middle East. 4. Dynamical Systems Theory-Complex Adaptive Systems. 5. Survey (Archaeology)-Jordan. 6. Socio-environmental Systems-Middle East. I. Title. II. Series.

2017

Library of Congress Control Number 2016936117

ISBN 0-936249-40-4

ISBN 978-0-936249-40-4

ABSTRACT

This monograph investigates the long-term consequences of human land-use practices generally, and in early agricultural villages specifically. This pioneering case study investigates the “collapse” of the Early (Pre-Pottery) Neolithic lifeway, which was a major transformational event marked by significant changes in settlement patterns, material culture, and social markers. To move beyond traditional narratives of cultural collapse, I apply a Complex Adaptive Systems (CAS) approach—a special subset of Dynamical Systems Theory—to this research, and combine agent-based computer simulations of Neolithic land-use with dynamic and spatially-explicit GIS-based environmental models to conduct experiments into long-term trajectories of different potential Neolithic socio-environmental systems. My analysis outlines how the Early Neolithic “collapse” was likely instigated by a non-linear sequence of events, and that it would have been impossible for Neolithic peoples to recognize the long-term outcome of their actions.

The experiment-based simulation approach shows that, starting from the same initial conditions, complex combinations of feedback amplification, stochasticity, responses to internal and external stimuli, and the accumulation of incremental changes to the socio-natural landscape, can lead to widely divergent outcomes over time. Thus, rather than being an inevitable consequence of specific Neolithic land-use choices, the “catastrophic” transformation at the end of the Early Neolithic was an emergent property of the Early Neolithic socio-natural system itself. Thus, it was likely not an easily predictable event. In this way, I use the technique of simulation modeling to connect CAS theory with the archaeological and geoarchaeological record to help understand the causes and consequences of socio-ecological transformation at a regional scale. The research is broadly applicable to other archaeological studies of resilience and collapse, and is truly interdisciplinary in that it draws on fields such as geomorphology, computer science, and agronomy, in addition to archaeology.

ACKNOWLEDGEMENTS

I owe a great debt to the many friends, colleagues, and mentors who supported my research over the years. Michael Barton supported my graduate career by providing excellent research opportunities, funding, mentorship, and advice, and allowed me to take a leadership role in the Mediterranean Landscape Dynamics Project. This research would not have been possible with his support, direction, and instruction. Ted Banning has supported my research over numerous years, and introduced me to the Neolithic Archaeology of Wadi Ziqlâb. My participation in the Wadi Ziqlâb Project, including fieldwork opportunities, directly facilitated much of my dissertation research. Geoff Clark has provided abundant advice and mentoring, and his guidance greatly aided the structure and nature of this monograph. Ramon Arrowsmith provided essential instruction and advice on field geomorphology and erosion modeling, which became core aspects of my research agenda.

Helena Mitasova provided invaluable advice on the landscape evolution modeling aspects of this research. Alexandra Miller compiled and facilitated the climate modeling that is used in this research. Mariela Soto-Berelov provided the paleovegetation modeling that is used in this research. Erin Dimaggio and Sidney Remple georectified much of the imagery and other GIS

data. Gary Mayer, Hessam Sarjoughian, and especially Sean Bergin were instrumental in the construction of the Agent-Based simulation environment used in this research. Gabriel Popescu helped to compile some of the ethnographic data used to parameterize the simulation. Much of the archaeological data used in this dissertation was compiled and analyzed by Wadi Ziqlâb Project members Seiji Kadowaki, Kevin Gibbs, Lisa Maher, and Danielle MacDonald.

I would also like to thank Sean Bergin, Christopher Roberts, Bulent Arikán, Alexandra Miller, Mason Thompson, Sophia Kelly, Matt Peeples, Melissa Kruse-Peeples, Julien Riel-Salvatore, Ian Kuijt, Meredith Chesson, Loukas Barton, Claudia Chang, Perry Tourtelotte, Bryan Hanks, and Dick Drennan for stimulating discussion, general collegiality, advice, critiques, support, and friendship. Finally, without my wife, Leah Abriani, none of this would have been possible.

Significant financial support for this dissertation came from NSF award BCS-0410269, the Arizona State University Dean's Advanced Scholarship, and the Arizona State University Dean's Dissertation Writing Fellowship. Fieldwork was supported by various grants from the Social Studies and Humanities Research Council of Canada.

TABLE OF CONTENTS

ABSTRACT	i
ACKNOWLEDGEMENTS.....	iii
TABLE OF CONTENTS.....	v
LIST OF TABLES	ix
LIST OF FIGURES.....	x

CHAPTER 1

INTRODUCTION	1
1.1 Introduction	1
1.2. The Geography, Climate, and Geology of Northern Jordan.....	2
1.3. Organization of the Monograph	3

CHAPTER 2

THE NEOLITHIC PERIOD IN NORTHERN JORDAN	5
2.1 Chapter Introduction	5
2.2. The Neolithic Period in the Northern Jordanian Highlands	5
2.2.1. Final Natufian/PPNA.....	5
2.2.2. Early PPNB	8
2.2.3. Middle PPNB	8
2.2.4. Late PPNB	10
2.2.5. PPNC/Final PPNB.....	13
2.2.6. Late Neolithic (Yarmoukian and Wadi Rabah)	15
2.2.7. The End of the Late Neolithic	20
2.3. Neolithic Sites in Wadi Ziqlâb	20
2.3.1. Tell Rakkan I	21
2.3.2. LN Tabaqat al-Bûma	22
2.3.3. LN al-Basatîn	23
2.3.4. Al-Aqaba	25
2.3.5. Other Locations in Wadi Ziqlâb with Neolithic Material.....	25
2.3.6. Neolithic Sites in Neighboring Wadis	27
2.4. Chapter Summary.....	27

CHAPTER 3

THEORETICAL APPROACHES TO THE PPN-LN TRANSITION	29
3.1. Chapter Introduction	29
3.2. Existing Hypotheses About the PPN-LN Transition.....	29
3.2.1. The Climatic-Forcing Hypothesis	29

3.2.2. The Anthropogenic Catastrophe Hypothesis	31
3.2.3. The Epidemiological Hypothesis	33
3.2.4. The Social Breakdown Hypothesis	34
3.2.5. The Settlement Reorganization Hypothesis	34
3.2.6. Summary and Critique of Existing Hypotheses	35
3.3. The Dynamical Systems Approach	35
3.3.1. Change in Non-Linear Systems.....	36
3.3.2. Are There Alternative Stable States of Human Subsistence?.....	41
3.4. A Dynamical Systems Hypothesis for the PPN-LN Transition.....	42
3.4.1. A Narrative DST Model of PPN Regional Social-Ecological Systems.....	42
3.4.2. Gradual and Punctuated Change in PPN Regional Social-ecological Systems	43
3.5. Chapter Summary.....	46

CHAPTER 4

MODELING SOCIAL AND NATURAL PROCESSES 49

4.1. Modeling Social and Natural Processes	49
4.1.1. Overview of the Mediterranean Modeling Laboratory	49
4.1.2 Comparison to Other Land-use Simulation Models.....	50
4.2. Modeling Agropastoral Subsistence Planning in the MML	53
4.2.1. Choosing the Number of Farmed Plots	53
4.2.2. Choosing the Amount of Grazing Land	54
4.2.3. Choosing the Amount of Firewood Gathering Patches	54
4.2.4. Simulating Farmer/Herder Knowledge Biases.....	54
4.3. Modeling the Location of Agropastoral Subsistence Activities in the MML.....	55
4.3.1. Choosing the Location of Farm Plots.....	55
4.3.2 Choosing Grazing Patches	56
4.3.3 Choosing Firewood Gathering Patches	56
4.4. Modeling Agropastoral Subsistence Returns in the MML	57
4.4.1. Calculating Farming Returns	57
4.4.2. Calculating Grazing Returns	58
4.4.3. Calculating Woodgathering Returns	59
4.5. Simulating Soil Fertility and Vegetation Dynamics, and the Direct Impacts of Subsistence Activities in the MML.....	59
4.5.1. Modeling Soil Fertility Impacts and Dynamics	59
4.5.2. Modeling Vegetation Impacts and Dynamics.....	60
4.6. Modeling Population Dynamics in the MML	64
4.7. Modeling Landscape Evolution in the MML.....	65
4.7.1. Estimating Elevation Changes Due to Soil Creep.....	65
4.7.2. Estimating Transport-Capacity on Hillslopes	65
4.7.3. Estimating Transport-Capacity in Streams.....	66
4.7.4. Estimating Erosion/Deposition Potential from Transport-Capacity.....	67
4.7.5. Converting Erosion/Deposition Potential to Net Elevation Change	67
4.7.6. Implementing Landscape Evolution.....	67
4.8. Chapter Summary.....	68

CHAPTER 5

PALEOENVIRONMENTAL RECONSTRUCTION	69
5.1. Chapter Introduction	69
5.2. Reconstruction of Ancient Topography	69
5.2.1. Landscape Evolution Research in Wadi Ziqlâb.....	69
5.2.2. Considerations for Paleotopographic Reconstruction in Wadi Ziqlâb	73
5.2.3. Existing Methods of Paleotopographic Reconstruction	75
5.2.4. A New Method for Reconstructing Paleotopography	76
5.2.5. Neolithic Paleotopographic Reconstruction of the Ziqlâb Area.....	78
5.3. Reconstructing Ancient Soils	79
5.3.1. Sources of Soil Data in the Region	80
5.3.2. Modeling the Depth of Soils Across the Landscape	80
5.3.3. Modeling Soil Erodibility.....	82
5.3.4. Modeling Soil Fertility	84
5.4. Paleoclimate Reconstruction	84
5.4.1. Methods of Paleoclimatological Modeling	85
5.4.2. The Archaeoclimatology Macrophysical Climate Model	86
5.4.3. Conversion to MML Climatological Input.....	88
5.4.4. Conversion to Full-coverage Climate Maps.....	89
5.5. Paleovegetation Reconstruction	89
5.5.1. Methods of Paleovegetation Modeling	90
5.5.2. Paleovegetation Modeling in the Southern Levant	91
5.5.3. Conversion to MML Vegetation Input	92
5.6. Chapter Summary.....	93

CHAPTER 6

MODELING THE PPN-LN TRANSITION IN WADI ZIQLÂB	95
6.1 Chapter Introduction	95
6.2. Composing PPN Land-Use Modeling Experiments.....	95
6.2.1. Parameterizing Neolithic Subsistence Behavior	96
6.2.2. Parameterizing Neolithic Wood Gathering Behavior.....	96
6.2.3. Parameterizing Neolithic Population Dynamics	97
6.2.4. Constructing Simulation Experiments for the PPN/LN Transition.....	98
6.2.5. Emergence and Experiment Repetition.....	99
6.3. Chapter Summary.....	100

CHAPTER 7

RESULTS AND DISCUSSION	101
7.1 Chapter Introduction	101
7.2. Population.....	101
7.2.1. Average Population Levels	101
7.2.2. Population Stability	102
7.2.3. Population Cyclicity	103
7.2.4. Inter-Run Variability in Population Trends	105
7.3. Vegetation Dynamics.....	105
7.3.1. Spatial Patterning of Vegetation	105

7.3.2. Temporal Patterning of Vegetation.....	106
7.3.3. Landcover Dynamics and Population Stability Patterns	111
7.3.4. Land-Cover Dynamics and Alternative Stable States	115
7.4. Landscape Evolution Dynamics.....	116
7.4.1. Landscape Evolution Control Model and Sensitivity Analysis.....	116
7.4.2. Overall Human Affect on Sediment Balance	119
7.4.3. Spatial Patterning of Landscape Evolution	121
7.4.4. Temporal Patterning of Landscape Evolution	122
7.5. Soil Dynamics	124
7.5.1. Temporal Variability in Soil Depth.....	124
7.5.2. Spatial Patterning in Soil Depth.....	126
7.5.3. Temporal Patterning in Soil Fertility.....	128
7.6. Discussion	129
7.7. Summary	133

CHAPTER 8

CONCLUSION 135

8.1. Implications for Societal Transition in the Neolithic and Beyond	135
8.1.1. Implications for the PPN-LN Transition in Wadi Ziqlâb	135
8.1.2. Implications for the PPN-LN Transition in General	136
8.2. Future Research Directions	137
8.3. Conclusion.....	138

BIBLIOGRAPHY 139

APPENDIX A

Subsidiary Formulas and Modeling Routines 163

A.1. Estimating Stream Depths	163
A.2. Determining Breakpoints in Net Accumulated Flow for Process Phase Changes	163
A.3. The Adaptive “Soft-Knee” Net- <i>dz</i> Smoothing Algorithm.....	164
A.4. Calculation of Soil-Depth “Rates”	165

APPENDIX B

A Geoarchaeological Gazetteer of the wadi Ziqlâb region..... 167

B.1. Geoarchaeological Survey of Wadi-Ziqlâb.....	167
B.2. Geoarchaeological Survey of Wadi Tayyiba.....	172
B.3. Geoarchaeological Survey of Wadi Abu Ziad	175

LIST OF TABLES

Table 4.1. Table of vegetation succession stages in the MML vegetation dynamics model, and their corresponding vegetation communities.....	61
Table 4.2. Table of equivalences showing between MML vegetation community/succession value and above-ground biomass (kg/m ²).....	62
Table 4.3. Table of equivalences between MML vegetation community types/succession stages and C-factor values.....	63
Table 5.1. Areal (ha) statistics for middle terrace remnants in all three of the Wadis of the project area.....	77
Table 5.2. Climate variables as input to the MML for the LPPNB/PPNC and Yarmoukian periods.	89
Table 5.3. Table of equivalences used to convert the MAXENT climax vegetation types to stages in the vegetation succession order used in the MML.....	92
Table 6.1. Table of economic and ecological data used to parameterize the models of PPN subsistence systems.....	97
Table 6.2. Table showing the values of the independent variables used to create the six modeling experiments.....	98
Table 7.1. Table of population sizes and population stability measurements for each experiment.	103
Table 7.2. Summary of demographic stability patterns for all experiments.....	103
Table 7.3. Summary of general trends in population dynamics for each experiment type as revealed by Lag-1 Autocorrelation (see Figure 7.2).	110
Table 7.4. Summary of inter-realization variation in population for each experiment.....	111
Table 7.5. Table of average total sediment balance (sum of cumulative erosion and deposition) and average anthropogenic changes to sediment balance (compared to a control model) after 700 years for each experiment.....	118
Table 7.6. Summary of general system potential, resilience, and connectedness in each of the modeling experiments, based on the measures presented in this chapter.....	132

LIST OF FIGURES

Fig. 1.1. Composite satellite image of Jordan, showing the physical terrain.	3
Fig. 2.1. Chronological diagram of the Neolithic in Northern Jordan.	6
Fig. 2.2. Map of Neolithic sites mentioned in the text.	7
Fig. 2.3. Map showing the known Neolithic sites and potential flint sources in Wadi Ziqlab and the neighboring Wadis.	20
Fig. 2.4. Overview of Tell Rakkan I.	21
Fig. 2.5. Overview of Tabaqat al-Bûma.	22
Fig. 2.6. Overview of the al-Basafîn terrace.	24
Fig. 2.7. The al-Aqaba terrace.	25
Fig. 2.8. Site WZ-301, one of the terraces where small amounts of Neolithic material was recovered in test trenches.	25
Fig. 2.9. Overview of the WT-4 terrace, showing the long bulldozer cut that bisects the site.	26
Fig. 3.1. Representations of adaptive cycles.	37
Fig. 3.2. The adaptive cycle plotted as a time series graph.	38
Fig. 3.3. Diagram of potential trajectories of an adaptive system over time.	39
Fig. 3.4. Diagram of different types of system state change.	39
Fig. 3.5. A time series of “stability” landscapes crossing over a critical transition point.	40
Fig. 3.6. Heuristic graphs showing the time-series indicators for a “stable” system (a) and for a system that is approaching a critical transition (b).	40
Fig. 3.7. The differences in system connectivity and heterogeneity between steady-state change (continual revolt, remember, or remain) and rapid change (critical transitions).	41
Fig. 4.1. The regressive relationship between precipitation and a) wheat yield, and b) barley yield.	58
Fig. 4.2. The regressive relationship between soil depth and a) wheat yields, and b) barley yields.	58
Fig. 4.3. The regressive relationship between soil organic matter (fertility) and a) wheat yield, and b) barley yield.	59
Fig. 5.1. Outline of the project area on GeoEye imagery.	73
Fig. 5.2. GeoEye imagery of the project areas with the knick points and wadi outlets marked, and the middle terrace remnants outlined in red.	74
Fig. 5.3. Detail of the flow accumulation map near Tell Rakkan.	77
Fig. 5.4. Map of the portions of the project area detected by the automated detection routine.	79
Fig. 5.5. 3-D perspective views of the modern DEM (left) and the interpolated “PaleoDEM” (right).	79
Fig. 5.6. 3-D perspective view of the project area, colored by the difference in elevation between the Modern DEM and the “PaleoDEM”.	80
Fig. 5.7. The Fisher et al. (1964) soils map of Wadi Ziqlâb.	81
Fig. 5.8. The Fisher et al. (1964) bedrock geology map of Wadi Ziqlâb.	81
Fig. 5.9. Detail of the map of modeled soil depths in the vicinity of Tell Rakkan.	83
Fig. 5.10. Detail of the K-factor map in the vicinity of Tell Rakkan. Inset shows the entire project area.	85
Fig. 5.11. Holocene temperature history for the Wadi Ziqlâb region, as modeled by the AMCM.	87
Fig. 5.12. Holocene precipitation history for the Wadi Ziqlâb region as modeled by the AMCM.	87
Fig. 5.13. Holocene precipitation variability history for the Wadi Ziqlâb region as modeled by the AMCM.	88
Fig. 5.14. Vegetation maps of the southern Levant as created by the MAXENT PVM for the year 8500 BP (left) and 7500 BP (right). After Soto-Berelov (2011).	91

Fig. 5.15. Detail of the input LPPNB/PPNC vegetation map in the vicinity of Tell Rakkan	92
Fig. 7.1. Time-series plots show the trends in human population dynamics for Agriculturalists, Agropastoralists, and Pastoralists in each experiment	102
Fig. 7.2. Lag-1 autocorrelation plots of human population time-series shown in figure 7.1.....	104
Fig. 7.3. Average inter-realization variability in human population across all 700 years for each of the experiments.....	105
Fig. 7.4. Example “high population” landcover maps for all runs of all models.....	106
Fig. 7.5. The coefficient of variation in the spatial extent of each of the 50 landcover types over the entire 700 years for each of the modeled subsistence strategies shows which vegetation types are most affected by each subsistence variant.....	107
Fig. 7.6. Time series plots of the “Simpsons D” statistic derived from the maps of vegetation in every year show how plant biodiversity changes over time in each experiment	108
Fig. 7.7. “Heatmap” plots of the frequency of each vegetation type over time reveals temporal dynamics in vegetation impacts.....	109
Fig. 7.8. A) A principle components analysis of the temporal patterning of vegetation variation for an example “metastable” experiment run shows how the vegetation adjusts over time to a relatively small region of stability. Each dot represents an individual year of the experiment. B) The loadings for each vegetation class along principle component 1 (y-axis in PC plot). C) The loadings for each vegetation class along principle component 2 (x-axis in PC plot).....	112
Fig. 7.9. A) A principle components analysis of the temporal patterning of vegetation variation for an example “multi-stable” experiment run shows two distinct configurations of vegetation. These zones represent alternative stable states of the model. Each dot represents an individual year of the experiment. B) The loadings for each vegetation class along principle component 1 (y-axis in PC plot). C) The loadings for each vegetation class along principle component 2 (x-axis in PC plot).....	113
Fig. 7.10. A) A principle components analysis of the temporal patterning of vegetation variation for an example “unstable” experiment run shows that the experiment rarely attained the same configuration of vegetation more than once. Each dot represents an individual year of the experiment. B) The loadings for each vegetation class along principle component 1 (y-axis in PC plot). C) The loadings for each vegetation class along principle component 2 (x-axis in PC plot).....	114
Fig. 7.11. A) A principle components analysis of the temporal patterning of vegetation variation for an example “stable trending to unstable” experiment run shows a small zone of initial vegetation stability followed by general instability. Each dot represents an individual year of the experiment. B) The loadings for each vegetation class along principle component 1 (y-axis in PC plot). C) The loadings for each vegetation class along principle component 2 (x-axis in PC plot).....	115
Fig. 7.12. Comparison of the landcover maps from a low population stable state (left) and a high population stable state (right) for the "Good" pastoralist experiment shows how population levels relate to vegetation impact. Higher population requires a larger footprint, which reduces vegetation cover in the area around the site.	116
Fig. 7.13. “Heatmap” plots of the frequency of each vegetation type over time for six realizations runs of the “Good” pastoralism experiment.	117
Fig. 7.14. Time-series trends for a series of short-term landscape evolution control models under different, but spatially homogeneous vegetation regimes show how vegetation influences rates of erosion and deposition.	118

Fig. 7.15. The average (of all raster cells) temporal variance in net elevation change for each of the short -term homogeneous vegetation landscape evolution model runs show how the C-factor influences the stability of erosion and deposition rates over time.....	119
Fig. 7.16. Box-plots summarize the range of cumulative net elevation change values after 700 years in each of the modeling experiments.	119
Fig. 7.17 Maps of the cumulative human-caused elevation change show the severity and extent of human impact on surface processes for each of the modeled scenarios.....	120
Fig. 7.18. Maps of the inter-realization variance in cumulative elevation change show the portions of the landscape most sensitive to variability in human land-use in each of the modeled scenarios.	121
Fig. 7.19. Plotting the cumulative human-caused deposition for each modeled scenario shows how human land-use influences deposition rates over time.	122
Fig. 7.20. Plotting the cumulative human-caused erosion for each modeled scenario shows how human land-use influences erosion rates over time.	123
Fig. 7.21. Plotting the deviation in depth of anthropogenic soils from natural soils for each modeled scenario shows how human land-use influences soil availability over time.	124
Fig. 7.22. Human land-use affects soil depths on some landforms more than others.....	125
Fig. 7.23. Viewing the total human impact on soil depths as box-plots for the different landforms shows that human land-use mostly affects the upper slopes.	126
Fig. 7.24. Human land-use alters the relationship of slope to erosion.....	127
Fig. 7.25. Viewing the total human impact on soil depths as box-plots for the different slope intervals shows that there is a wide range of variability in the human impact on soil depths in shallow areas.	128
Fig. 7.26. Plotting the average fertility of soils shows the temporal dynamics of soil degradation and regeneration for each modeled scenario over time.	129
Fig. A.1. Method of approximation of peak flow depth from an idealize unit hydrograph.....	163
Fig. A.2. Graphical display of profile curvature and tangential curvature versus log flow accumulation.....	164
Fig. A.3. Map showing the locations of surface process transitions as determined from the graphs in Figure A.2.	165
Fig B.1. Upper section of Wadi ‘Ayn Zubia.	167
Fig B.2. Cutbank into a middle terrace remnant in the Upper Ziqlâb, showing the stratigraphy of the terrace.	167
Fig B.3. An example of a remnant of the upper terrace in the Upper Ziqlâb region.	168
Fig B.4. A filled gully on the slopes of the Upper Ziqlâb.	168
Fig B.5. This recent agricultural terrace cut in the Upper Ziqlâb region has exposed a section showing the red Epipaleolithic paleosol directly (and unconformably) overlain by tan Holocene colluvium.	168
Fig B.6. Overview of the middle section of the Wadi Ziqlâb drainage.	169
Fig B.7. This cutbank has exposed a small stratigraphic section of the middle terrace in the mid-reaches of the Ziqlâb drainage.	169
Fig B.8. An excellent example of terrace edge-slump caused by bank undercut in the middle section of the Ziqlâb drainage.	169
Fig B.9. An example of Late Holocene colluvium directly overlying alluvial deposits of the middle terrace in the mid-section of the Ziqlâb drainage.	169
Fig B.10. An example of the Late Holocene colluvium directly and unconformably overlying the Epipaleolithic red paleosol in the middle section of the Wadi Ziqlâb drainage.	170

Fig B.11. The outlined band of red alluvium likely represents reworked sediments eroded from the red Epipaleolithic paleosol further up the Wadi.	170
Fig B.12. This photograph shows multiple slumps on the flank of the middle section of the Ziqlâb drainage.	170
Fig B.13. This photograph shows a small alluvial fan in the middle section of the Ziqlâb drainage.	171
Fig B.14. A photograph of the spectacular waterfall that occurs at the Tell Rakkan knick point.	171
Fig B.15. This bulldozer cut on the Tell Rakkan terrace exposes a large section of the Late Holocene colluvium.	171
Fig B.16. An overview of the lower portion of the Ziqlâb drainage, showing how incised the channel is at this point.	171
Fig B.17. Several ancient rills/gullies are preserved in the al-Basatin terrace. The dashed line outlines an ancient gully that cut into the Late Neolithic layers.	172
Fig B.18. Photographs of the waterfall that forms at the lower knick point in Wadi Ziqlâb.	172
Fig B.19. Overview of the middle section of Wadi Tayyiba.	173
Fig B.20. Close up of a section of the middle Wadi Tayyiba drainage.	173
Fig B.21. Overview of lower Tayyiba knickpoint. Notice the presence of an Ottoman period mill.	173
Fig B.22. Overview of the lower section of the Wadi Tayyiba drainage.	174
Fig B.23. CORONA (left) and GeoEye (right) imagery of the WT-4 terrace landform.	174
Fig B.24. Close up of the stratigraphy of the “toe” of the WT-4 landform.	175
Fig B.25. Overview of the middle Wadi Abu Ziad drainage.	175
Fig B.26. Arrows point to probable ancient flint quarries at ‘Ain Beidha.	176
Fig B.27. Overview of large alluvial deposits at the mouth of Wadi Abu Ziad.	176
Fig B.28. The large exposed section of alluvium at the mouth of Wadi Abu Ziad.	176
Fig B.29. Close up of the dated strata from the large alluvial deposit at the mouth of Wadi Abu Ziad.	176

CHAPTER 1

INTRODUCTION

1.1 INTRODUCTION

This monograph investigates the “collapse” of the Early (Pre-Pottery) Neolithic lifeway, a major transformational event that occurred approximately 8500 years ago, which was marked by significant changes in settlement patterns, material culture, and social markers.

The instigation for this transition remains unclear, but human-caused landscape degradation, rapid climate change, social upheaval, the rise of pandemic disease, conscious reorganization for effective resource use have all been suggested as likely candidates. Little consensus exists among scholars, mainly because the fragmentary nature of the archaeological record from this period prohibits a conclusive understanding of this transition using traditional archaeological techniques alone. To move beyond traditional narratives of cultural collapse, I employ a Complex Adaptive Systems (CAS) approach to this research, and combine agent-based computer simulation models of Neolithic land-use with dynamic and spatially-explicit GIS-based environmental models to conduct experiments into the long-term trajectories of different potential Neolithic socio-environmental systems.

The goal of all archaeological modeling is to better understand the trajectory of events that created the archaeological record, but for years archaeologists have relied on narrative models that attempt to draw together the disparate bits of archaeological evidence that we uncover, and somehow bridge them into a cohesive whole within paradigmatic understandings of the nature of human systems. The archaeological record is fragmentary, however, and at best only provides partial clues into ancient peoples’ actual daily activities. Furthermore, it is exceedingly difficult, and usually impossible, for archaeologists to

know—based on the archaeological data alone—if the clues they have recovered actually reflect real day-to-day economic patterns, or are a consequence of discard biases and site formation processes (Hayden and Cannon, 1983; Schiffer, 1987). Whole subdisciplines of archaeology (e.g., geoarchaeology, ethnoarchaeology, microarchaeology, etc.) have arisen as ways of mitigating these issues, but still typically culminate in narrations of potential past lifeways. The simulation approach used in this research differs from the narrative approach in that it uses computer simulation modeling techniques as the bridge between the various pieces of proxy data found in archaeological research. This is a way to move beyond the limitations of archaeological narration because simulation allows a quantitative examination of the kinds of socio-natural processes that we know must have operated in the past, but for which we have little direct evidence.

My analysis outlines how the Early Neolithic “collapse” was likely instigated by a non-linear sequence of events, and that it would have been impossible for Neolithic peoples to recognize the long-term outcome of their actions. The experiment-based simulation approach shows that, starting from the same initial conditions, complex combinations of feedback amplification, stochasticity, responses to internal and external stimuli, and the accumulation of incremental changes to the socio-natural landscape, can lead to widely divergent outcomes over time. Thus, rather than being an inevitable consequence of specific Neolithic land-use choices, the “catastrophic” transformation at the end of the Early Neolithic was an emergent property of the Early Neolithic socio-natural system itself. It was, thus, an event likely unforeseeable to Neolithic peoples. I use the technique of simulation modeling to connect CAS theory with the archaeological

and geoarchaeological record to help better understand the causes and consequences of socio-ecological transformation at a regional scale, and what these changes may implicate for the sustainability of the Neolithic way of life.

Studying this phenomenon in the Neolithic period provides a great time-depth, which allows me to examine change at several different temporal scales. This deep-time perspective may be necessary to understand the long-term trajectory of changes that can cascade from deleterious consequences of subsistence decisions. Many people in the developing world continue to live a lifestyle of subsistence farming and herding, and so face similar dilemmas to their Neolithic ancestors. A better understanding of the consequences of the cumulative actions of ancient farmers and herders will help us to better predict the future effects of agropastoralism in developing countries today.

1.2. THE GEOGRAPHY, CLIMATE, AND GEOLOGY OF NORTHERN JORDAN

Wadi Ziqlâb is one of a series of linear incised valleys that line the western edge of the northernmost reaches of the Jordanian Highlands (Figure 1.1). These crosscutting wadis are tributaries of the Jordan River, ultimately draining into the Dead Sea. Most of the Wadis, including those in the Ziqlâb region, have perennially flowing streams in their lower portions (below about 200 masl), fed by a multitude of springs emerging from the limestone bedrock of the wadis (Maher, 2005), whereas their upper portions are seasonally inundated dry riverbeds.

The natural geography, general geology, and modern climate of northern Jordan has been described by numerous authors (Al-Jaloudy, 2006; Bender, 1975; Bender and Khdeir, 1974; e.g., Burdon and Quennell, 1959, 1959; Cordova, 2007; C. P. Davies and P.L. Fall, 2001; W. Fisher et al., 1966; Horowitz, 2001; Schulman, 1962; Sneh et al., 1998; Wagner, 2011), and the brief overview provided here draws from these sources. The bedrock in northern Jordan is largely calcareous lightly metamorphosed sedimentary rocks dating to the Cretaceous and Late Tertiary.

The sediment from which these rocks are formed derives mainly from oceanic sedimentation on the floor of the Tethys Sea, and these rocks are sometimes unconformably overlain by early quaternary conglomeritic rocks of terrestrial origin, especially along the margins of the Jordan Valley. The Jordan Valley—locally referred to as al-Ghôr—is composed of recent fine-grained alluvial soils with high organic content, which overlay marl and shale lake sediments deriving from the ancient Lake Lisan that filled the valley in the Late Pleistocene. The Jordan Valley is part of the greater Jordan Rift zone, which formed as the Arabian Plate moved away from the African Plate, and which stretches from the Red Sea in the south, through the Wadi al Arabah and the Dead Sea, up through the Jordan Valley to the Sea of Galilee, and thence to the Hula Basin in the north. The Valley itself is entirely below sea level, measuring 212 mbsl at its north end and 423 mbsl at its south, and the Jordan River flows along its length, channeling water from Galilee and the Yarmouk River to the Dead Sea. The modern alluvial soils of the valley are a combination of overbank deposits from the Jordan River and outwash deposits from the numerous tributary streams and seasonal washes that empty into the Valley from both the Judean and Samaran Hills to the west, and the Jordanian Highlands to the east.

The Jordanian Highlands—also referred to as the Mountain Ridge Province—form the eastern edge of the Jordan-Arabah rift zone, and were formed by a combination of synclinal horst and graben subsidence along the strike/slip fault in the Rift Zone and local uplift related to constriction along the fault. Thus, numerous structural features are present in the uplands, including localized and regional deformation and tilting of bedding planes, and a series of translational faults running perpendicular to the main Jordan Rift fault.

The Northern Highlands region encompasses most of the area between Umm Qais and Madaba (Figure 1.1), but is most typically associated with the “heartland” between the Yarmouk and Zarqa rivers. The Northern Highlands are composed primarily of calcareous sedimentary rocks of marine origin. The limestones of the upper

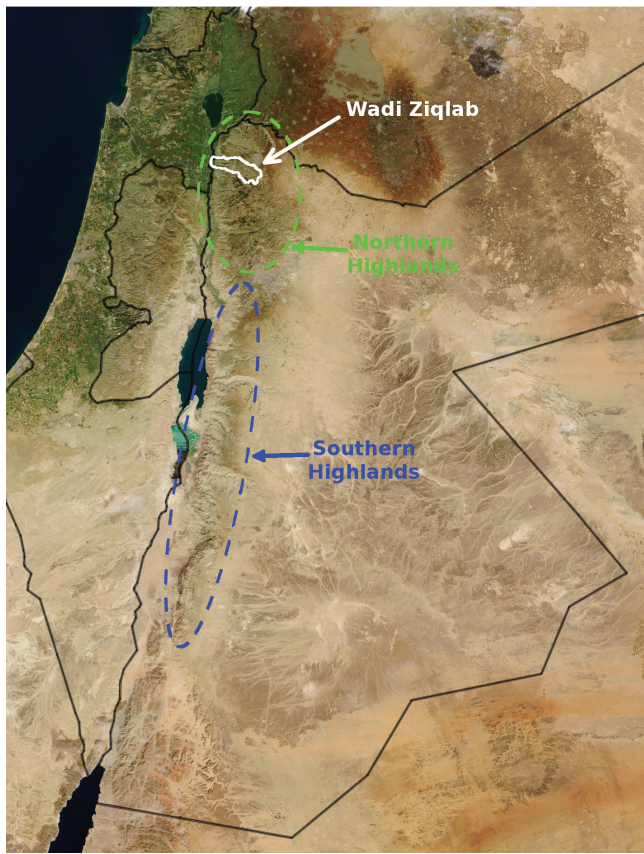


Fig. 1.1. Composite satellite image of Jordan, showing the physical terrain. The green dashed line delimits the approximate extent of the Northern Highlands region, the blue dashed line delimits the approximate extent of the Southern Highlands region, and the solid white line delimits the Wadi Ziqlab catchment.

member of the Northern Highlands formation are crystalline, and are thus more resistant to erosion than the chalk/marls found in the lower member. The differing hardness of these members creates a narrow, highly incised, relatively flat-topped plateau of marls directly bordering the Jordan Valley, from which rises the steeper slopes of the harder crystalline limestones to the east. A band of flint-bearing limestones lies between the upper and lower members, providing easy access to tool-stone across the entire region. On their eastern side, the Northern Highlands slope more gently towards the central Jordanian Plateau.

The elevation of the Northern Highlands region ranges from 700-1200 meters above sea level. The Northern Highlands region is

characterized by a Mediterranean climate with cool wet winters, and hot dry summers, and an average precipitation of between 300-600 mm. The higher elevations are mantled in an oak and pistachio woodland, with interspersed pines and junipers becoming more dominant in the lower elevations. Portions of these areas are covered in fairly dense oak/pistachio Maquis or scrub Garrigue, and large tracts have been converted to olive-growing or cultivation of cereal crops. The lowest portions of the Northern Highlands are dominated by open grasslands, especially on the eastern flanks descending through the Northern Steppes towards the Hamada. Vegetation in the wadi-bottoms includes cane, oleanders, and a variety of leafy shrubs and forbs. This wadi-bottom vegetation can be quite dense, especially near springs and around perennially-flowing streams.

In contrast, the Southern Highlands—which span from Wadi Zarqa to Wadi Rumm (Figure 1.1)—are dominated by sandstones, basalts, and granitic bedrocks, and are more highly incised by wadi systems than are the Northern Highlands. These wadis typically drain into the Dead Sea via the Wadi al Arabah, although those that drain the southernmost stretches of the highlands empty southward into the Red Sea. Although occasional peaks in this region reach heights of almost 1800 meters, the region is generally at a lower average elevation than are the Northern Highlands, though the topography is considerably rougher and more varied. Although a significant proportion of the region is still considered to have a Mediterranean climate, the region receives quite a bit less rainfall than the north. Those parts of the region below about 700 meters receive a precipitation of only 150-300 mm per year, thus, falling into the Iran-Turanian climate zone. Consequently, there is a wide range of vegetation community types across the region, with much of the area currently covered by shrub-steppe and scrublands.

1.3. ORGANIZATION OF THE MONOGRAPH

In Chapter 2, I examine the archaeological record of the Neolithic period in the Northern

Highlands, and provide a traditional narrative model of the sequence of events that led to the PPN-LN transition. In Chapter 3, I examine the existing ideas about the character of the transition, and the motivating/instigating factors that caused it. I critique these ideas, and present a new approach to understanding the PPN-LN transition based on Complex Adaptive Systems (CAS) theory and the idea of Soical-Ecological Systems (SES). I discuss the basic concepts of CAS theory, examine the evidence for complexity in human subsistence systems, and provide a heuristic model of the PPNB subsistence system as a regional SES. I also provide some test implications and guiding questions that frame the research presented in the remaining portions of the dissertation. In Chapter 4, I introduce the idea of simulation modeling and discuss the basics of the simulation modeling approach. I then describe the components and structure of the MedLanD Modeling Laboratory (MML), which is the simulation modeling platform used in this research (an agent-based model of subsistence agropastoralism, a vegetation dynamics modeling engine, a soil dynamics modeling engine, a climate modeling engine, and a landscape-evolution

modeling engine). In Chapter 5, I discuss the concept of spatially explicit paleoenvironmental reconstruction, and discuss the methods I use to achieve it. I also discuss the results of previous and new geoarchaeolgical fieldwork conducted in Wadi Ziqlâb, and examine their implications for paleoenvironmental reconstruction and as a source of comparison for the simulation model-output. In Chapter 6, I describe how I used ethnographic and archaeological data to parameterize the MML to simulate Neolithic subsistence. I form a series of twelve modeling experiments to better understand the long-term dynamics of potential Neolithic subsistence strategies. In Chapter 7, I examine the output of these modeling experiments to look for patterns relating to issues of resilience, vulnerability, flexibility, rigidity, and other CAS concepts. I examine the dynamic and recursive interconnections in the simulations, and examine how similar initial conditions could lead to vastly different outcomes. In Chapter 8, I investigate the implications of this research for our understanding of the PPN-LN transition in specific, but also of the concept of “collapse” and the long-term sustainability of SES in general.

CHAPTER 2

THE NEOLITHIC PERIOD IN NORTHERN JORDAN

2.1 CHAPTER INTRODUCTION

This chapter describes the basic sequence of the Neolithic period in the Northern Jordanian Highlands region, with special regard to the archaeological record from the Wadi Ziqlâb. The purpose of this narrative is to provide a basic descriptive model of the PPN/LN transition that is the main focus of this monograph. This is meant to contextualize the simulation experiments described in later chapters. Here, I provide the archaeological facts upon which those simulations are based, and go through the traditional archaeological narrative that they are meant to compliment. In my overview, I therefore focus only on those aspects of the archaeological record that inform us about society, economy, and the relationship between people and their surrounding environment. I have not covered all the specifics of every site in the region; such a detailed review is outside the purview of this monograph. I do, however, summarize the major diachronic trends over the Neolithic period, identifying aspects of Neolithic material culture and economy that changed drastically at the PPN/LN transition. I provide extra details about the known Neolithic sites in Wadi Ziqlâb.

2.2. THE NEOLITHIC PERIOD IN THE NORTHERN JORDANIAN HIGHLANDS

Although a range of alternative chronological sequences are used across Southwest Asia, in this research I have chosen to follow the most widely used scheme for the Neolithic of the Southern Levant. The scheme has two major divisions – Pre-Pottery Neolithic (PPN) and Late Neolithic (LN) – each with their own internal divisions, so that the sequence of named periods proceeds: PPNA, EPPNB, MPPNP, LPPNB, PPNC, Yarmoukian (LN), and Wadi Rabah (LN).

In this dating schema, the PPN/LN transition occurs during the PPNC period. These periods are assigned generally-accepted date-ranges (Figure 2.1), but the actual timing of occupation phases can be quite different in the various sub-regions of the Levant, and even from site to site within a particular sub-region (Banning, 2007a). I provide here a brief outline of the course of the Neolithic in the Northern Jordanian Highlands (see Chapter 1 for a location map) in the vicinity of Wadi Ziqlâb, with particular emphasis on the events preceding the PPN/LN transition in the PPNC and those that immediately followed in the Yarmoukian¹.

2.2.1. Final Natufian/PPNA

Although there are abundant earlier Epipaleolithic remains in the region (Maher, 2011, 2005; Maher et al., 2002; Maher and Banning, 2001), there is very little evidence for Natufian or PPNA occupation in northern Jordan. This is likely more to do with preservation biases due to erosion of the landforms most used in these periods than that the region was actually abandoned (see Chapter 3 for more information about the source of these biases). The evidence from Iraq ed-Dubb—the only site in the region with preserved Late Natufian and PPNA occupations—corroborates this, and suggests that a network of small PPNA sites likely existed throughout the region (Goodale and Kuijt, 2006; Kuijt, 2004; Kuijt et al., 1991). Located in the upper portion of Wadi el-Yabis, about 10 kilometers due south of Wadi Ziqlâb, Iraq ed-Dubb is a cave site situated high up on

¹ This summary will specifically focus on the archaeology of northern Jordan. Several excellent recent general summaries of the Neolithic in all parts of the Levant already exist (e.g., Banning, 1998; Kuijt, 2000; Rollefson, 2001; Kuijt and Goring-Morris, 2002; Simmons, 2007; Twiss, 2007), and much of the detail presented in them will not be replicated here.

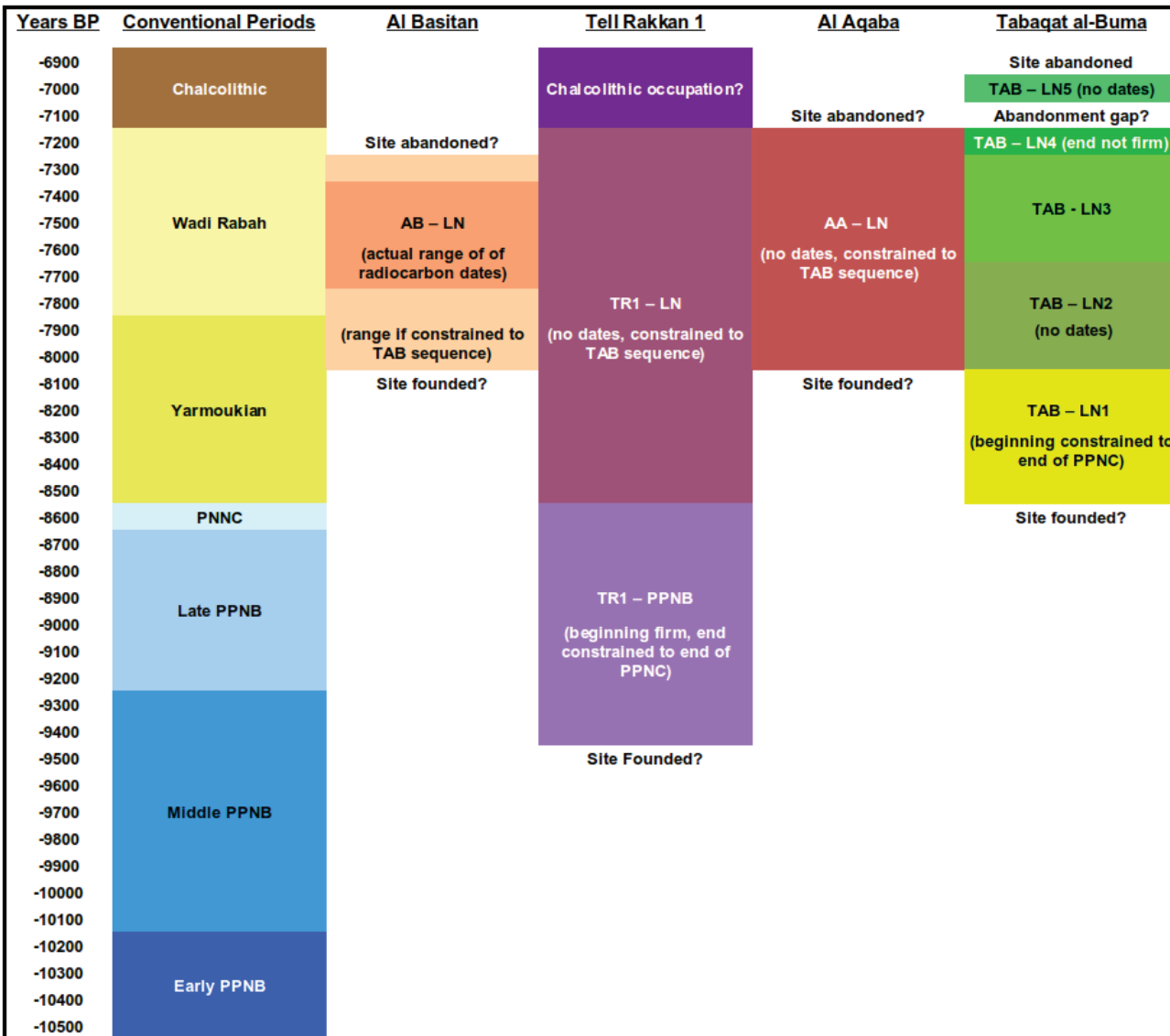


Fig. 2.1. Chronological diagram of the Neolithic in Northern Jordan. The regional “techno-typological” chronology appears on the left, and the absolute or inferred chronology of each of the excavated Ziqlâb Neolithic sites appears as a separate column on the right.

the southern flank of the Wadi, and this unique location is likely the reason this site was preserved while most other sites of this period were not. Two circular, semi-subterranean houses, and the intervening intramural area were excavated, and statistical and spatial analysis of the faunal remains at Iraq ed-Dubb (Martin and Edwards, 2007) suggests that the site was occupied year round, though possibly only periodically². No domestic fauna were discovered, but a high diversity of wild

species were present in the faunal assemblage, with an emphasis on hunted and trapped mammals (especially gazelle, squirrel, fox, hare, and boar) (Martin and Edwards, 2007). Interestingly, the pattern of animal exploitation did not change significantly between the Late Natufian and PPNA layers, indicating both a high degree of continuity between the periods, and that floral and faunal resources were not depleted by the occupants of the site (i.e., they were living below the carrying capacity of the local catchment). Iraq ed-Dubb also

² Originally, it was thought that the site was a seasonally-occupied hunting camp (Kuijt et al., 1991).

boasts some of the earliest evidence of domesticated cereals (carbonized wheat and barley grains dated to 11600 – 11475 cal. BP [Colledge, 2001; Colledge et al., 2004]), suggesting that, if not farmers themselves, the occupants of the site at least had access to domesticated grains. Recent excavations at PPNA sites in the Jordan Valley indicate that these sites had extensive storage granaries, and that use of domesticated or pre-domesticated plant foods intensified during this period (Kuijt and Finlayson, 2009). Several non-native shell and bone ornaments were also discovered at the site, indicating the presence of regional or supra-regional trade networks. It is possible that different sites existed with various specialties (e.g., farming, hunting, bead-making, etc.), and that goods were traded on a regular basis. Regardless of the nature of the trade network, it is clear that a variety of interconnected permanent or semi-permanent Natufian/PPNA settlements existed throughout the hilly regions of the eastern flank of the Jordan Valley, including in Wadi Ziqlâb.

Microwear evidence from PPNA sickle-elements (identified by morphology and presence of silica sheen) recovered from sites in the Middle-Euphrates river valley indicates that PPNA sickles were compound tools constructed in a manner broadly similar to the compound projectile points common in earlier periods (Ibáñez et al., 2007), which indicates that the focus of technological innovation had shifted from hunting tools to farming tools by this period. The sickles' shafts were apparently straight (i.e., PPNA sickles were not actually "sickle-shaped"), however, and so the way PPNA peoples must have harvested

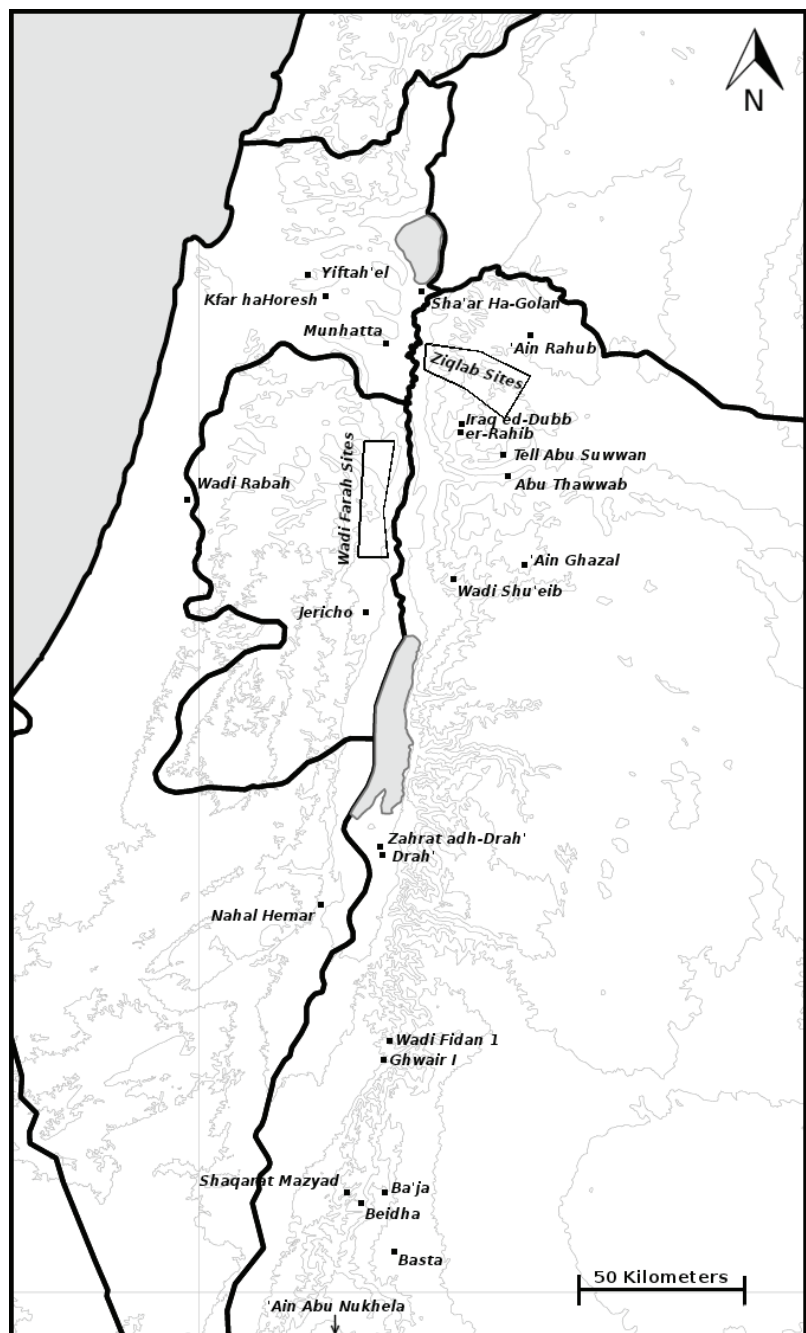


Fig. 2.2. Map of Neolithic sites mentioned in the text.

cereals—by gathering bunches of grass in one hand, and slicing the stalks with the sickle held in the other—was quite laborious and inefficient (Ibáñez et al., 2007). These findings indicate that although the technology of farming was becoming centrally important to PPNA peoples, they had yet to innovate technological solutions that would allow increased harvesting efficiency.

2.2.2. Early PPNB

Like the Natufian and PPNA, there is very little evidence for the Early PPNB period anywhere in the Ziqlab region, but it is less clear, however, if this absence of evidence is also due to preservation biases. It seems that most of the PPNA sites in the Jordan Rift Valley were abandoned at the end of the PPNA (and there is no evidence for any EPPNB sites in the Valley), and it may be that the Northern Jordanian Highlands were also depopulated at this time (Kuijt and Goring-Morris, 2002). The only possible EPPNB site in the Northern Highlands region—the site of er-Rahib—is, interestingly, also located in the Wadi el-Yabis. Only very minimal excavations were carried out at the site, however, and the site may actually primarily date to the early MPPNB (Kuijt and Goring-Morris, 2002). The EPPNB is thus best known from sites in the Northern Levant (e.g., from Syria and Anatolia [Twiss, 2007]), but recently, EPPNB remains were discovered directly overlaying PPNA layers at Zahrat adh-Drah` in southern Jordan, suggesting a cultural continuity at that site (Edwards et al., 2004). Although very few EPPNB sites have been excavated, there is a trend towards the adoption of rectilinear house-shapes in the northern areas (occurring first in the West and then later east of the Jordan) during this period, although not in the southern desert areas (Simmons, 2007).

2.2.3. Middle PPNB

The Middle PPNB period is best known from sites in the south, such as Beidah (Byrd, 1994) Shaqarat Mazyad (Kaliszan et al., 2002), and ‘Ain Abu Nukhela (Henry et al., 2003), or from west of the Jordan at sites such as Jericho (Gebel, 2004), Kfar haHoresh (Goring-Morris et al., 1998), Nahal Hemar (Bar-Yosef, 1985; Bar-Yosef and Alon, 1988), Yiftahel (Garfinkel, 1987), and others (see Twiss [2007]). There are only three sites in the highlands of northern Jordan with known MPPNB occupations: ‘Ain Ghazâl (Rollefson et al., 1992), Wadi Shu’eb (Simmons et al., 2001), and Tell Abu Suwan (Al-Nahar, 2010). The MPPNB layers at these three sites are modest compared

to the substantial LPPNB layers that overlay them, but apparently these northern MPPNB sites are larger than those in the south and west (Kuijt and Goring-Morris, 2002). Furthermore, the Northern Highlands sites all seem to have been newly established town sites, whereas many of the southern and western sites show marked continuity from earlier periods (Edwards et al., 2004; Gebel, 2004). Of the three northern sites, the MPPNB layers at ‘Ain Ghazâl provide the largest and best sample of northern MPPNB remains.

One pattern that occurs in the MPPNB layers of ‘Ain Ghazâl, and which is of particular interest to the current research, is that the diameter of structural wooden posts decreased throughout the MPPNB at ‘Ain Ghazâl³, suggesting the gradual depletion of mature forests in the surrounding region (Rollefson et al., 1992). Room size also decreased over time, in part due to remodeling of interior spaces during (the many) renovations of houses, but also possibly due to the aforementioned lack of large beams (Banning and Byrd, 1987; Rollefson et al., 1992). The typical house-form (called “pier houses”) consists of a single rectilinear room, subdivided by stone (or sometimes wooden) “piers”, creating a series of chambers along the side. Houses were all about the same size (20-30 m²), and most domestic activities appeared to have occurred outside the dwelling (e.g., on the roof) (Banning, 2003; Twiss, 2007). Banning (2003) suggests that the layout and uniformity of these houses indicates inhabitation by nuclear families, in control of their own food storage, but not in competition with each other.

Faunal and botanical evidence shows an increased reliance on goats at the expense of gazelle in the MPPNB, especially at ‘Ain Ghazâl (Twiss, 2007; Wasse, 2002). Although, morphometrically, it remains unclear if these goats were fully domesticated, there is an abundance of circumstantial evidence that suggests they were: 1) paleoenvironmental data suggests ‘Ain Ghazâl was not within an ancestral range of the wild goat progenitor population, 2) goats make up 64%

³ Post hole diameters reduced from 50-60cm in the earliest phases of the MPPNB, to only 15-20cm in the later phases.

of the faunal assemblage, which is much larger than is known from hunter-gatherer sites, and 3) mortality profiles suggest that animals were culled from a kept herd, and not a wild population (Wasse, 2002). There is a great deal of difficulty in interpreting culling patterns (Marom and Bar-Oz, 2009), and the survivorship curves from the MPPNB layers at ‘Ain Ghazâl and Yiftah’el (Horwitz and Lernau, 2003) do not seem to match well with any published ethnoarchaeologically derived survivorship curves. Marom and Bar-Oz (2009) suggest that survivorship data can be more easily interpreted if binned into “immature”, “subadult”, and “adult”. Doing so does “level” the differences between the two sites, as survivorship at MPPNB ‘Ain Ghazâl bins to 7.3%, 48.5%, and 44.1% in the three age groups respectively, and survivorship at Yiftah’el bins to 3%, 53%, and 44% respectively. Nevertheless, these data do not neatly fit into any of the three heuristic categories provided by Marom and Bar-Oz (2009) for “meat-only”, “milk”, or “wool” herds. They might, however, fit between the “meat-only” and “wool” categories. This would indicate that while meat and wool production were very important for MPPNB pastoralism, milk was yet to be included in the suite of pastoral products. There also is a wide range of body sizes in MPPNB herds at ‘Ain Ghazâl, suggesting that the animals were in the initial stages of domestication, thus exhibiting both wild and domestic morphological traits within the same herd (Wasse, 2002). Although wild game continue to be an important source of food, it appears, then, that MPPNB people had begun to rely on animal husbandry to provide a regular source of protein, lipids, and micronutrients⁴. It should be noted, however, that goats (domestic or otherwise) are not present in the faunal assemblages of all MPPNB sites (Kuijt and Goring-Morris, 2002), so clearly MPPNB people were still in the initial stages of incorporating pastoral production into their subsistence economies.

In a recent summary of the botanical evidence, Asouti and Fuller (2012) and Fuller et al. (2012) describe a highly variable spread of crop types

present at different sites, which calls the idea of a regional agricultural system (i.e., the “Neolithic Package”) into question. Not only does this new view show that the process of domestication proceeded at different rates in different places, but it seems that, while agricultural products certainly provided the bulk of MPPNB diets, MPPNB people were still actively experimenting with various combinations of cultivar species and land-races. The main species recovered from MPPNB sites include varieties of wheat (*Triticum aestivum*, *T. monococcum*, and *T. dicoccum*), barley (*Hordeum spontaneum*, *H. vulgare*, and *H. sativum*), pulses and legumes (*Lens culinaris*, *Pisum sativum*, *Vicia faba*, *V. ervilia*, and *Cicer arietinum*), and various other domesticates (*Ficus*, *Cucumis*, etc.), and frequency analysis of these botanicals suggest that cereals and legumes were the staple crop-types at MPPNB sites in the Mediterranean zone (Banning, 1998; Fuller et al., 2012). The presence of open-field weeds in the botanical record at MPPNB sites indicates that farmed fields were left fallow from time to time, perhaps according to planned crop rotation schemes (swiddening or extensive agriculture) (Banning, 1998). Sickle technology had improved by the MPPNB, and sickle shafts were now “curved” (i.e., actually “sickle shaped”), potentially doubling harvesting efficiency (i.e., over that in the PPNA) because the tool itself could now both gather the grass blades together and cut them in one stroke (Ibáñez et al., 2007).

Several researchers have suggested that the MPPNB was period of major social change in the Neolithic world, and that the Jordanian highlands were “colonized” during this period by groups emigrating from several of the earlier-established sites west of the Jordan (e.g., Jericho) (Edwards et al., 2004; e.g., Gebel, 2004). Bienert et al. (2004) (and others) point to the fact that all the known Northern Highlands MPPNB sites were founded in this period on virgin soil, and many of the Southern Highlands MPPNB sites, though mostly not founded anew, show significant changes in architectural style and size (i.e., the MPPNB “pier house” form, [Banning, 2003]). Bienert et al. (2004) go so far as to suggest that the completion of the switch to rectilinear houses that began in

⁴ See Vigne (2011) for an excellent recent discussion of how this process may have occurred.

the EPPNB (and continued through the MPPNB) was caused by the introduction of a new cultural paradigm brought by migrants to the highlands from west of the Jordan. If that is the case, then sites in the southern desert areas (such as ‘Ain Abu Nukhela, Shaqarat Mazyad, and Beidha) must have maintained their autonomy, as they continued to use circular or ovate house-forms throughout those periods⁵. Bar-Yosef (2002, 2001), on the other hand, interprets this phenomenon as evidence for the existence of a series of regional “PPNB cultures”, each representing a particular set of socio-economic traits (e.g., “farmer-herders”, “herder-hunters”, “foragers”). The unique characteristics of the MPPNB sites in the Jordanian Highlands, in his view, are the result of interaction between the settled, agricultural PPNB “core” west of the Jordan, and a periphery filled with mobile foragers in the eastern and southern deserts. In this scheme the Jordanian Highlands are the “interaction zone” between the two areas, and the unique characteristics of sites in this region derive from this duality of cultural and economic influences. Whatever the reason, it is clear that the MPPNB was a time of change throughout the Jordanian Highlands, and that divergent social (or socio-ecological) processes were occurring in each of the different sub-regions.

2.2.4. Late PPNB

The Late PPNB period is widely considered to be the florescence of PPN culture (Simmons, 2007). At the start of the LPPNB, most of the known MPPNB sites west of the Jordan were abandoned, and accelerated site growth and foundation of new sites occurs in the Jordanian Highlands and the desert regions. Several of these sites grew to sizes exceeding 10 ha and encompassing several hundred households (perhaps up to 3000 people or more) (Kuijt, 2000b; Kuijt and Goring-Morris, 2002; Rollefson and Kafafi, 2007). Almost all

these so-called “Mega-sites” are found east of the Jordan—mainly concentrated in the Jordanian Highlands—and they all seem to have experienced the same dramatic site growth at the beginning of the LPPNB—presumably from a final influx of new immigrants from the recently abandoned towns west of the Jordan (Gebel, 2004; Kuijt and Goring-Morris, 2002; Rollefson and Kafafi, 2007). The LPPNB settlement system was multi-tiered, and not every LPPNB village grew to “megasite” proportions. In the Northern Highlands, there are only three known “Mega-sites”: ‘Ain Ghazâl (Rollefson et al., 1992), Wadi Shu’eib (Simmons et al., 2001), and Tell Abu Suwan (Al-Nahar, 2010)⁶. Interestingly, unlike the southern “Mega-sites” which appear to all have been newly-founded, the three northern “Mega-sites” grew out of smaller, preexisting MPPNB settlements (Al-Nahar, 2010; Rollefson et al., 1992; Simmons et al., 2001). Not all LPPNB sites grew to “megasite” proportions, however, and the one known LPPNB site in Wadi Ziqlâb—Tell Rakkan I—was likely only about 1 ha in size (see Section 2.3.1 below).

LPPNB culture seems to have been slightly less heterogeneous than that of the MPPNB, and while some researchers argue for the presence of a number of regional sub-cultures (e.g., Gebel, 2004), most known LPPNB sites exhibit a common set of material cultural traits, including: 1) a highly standardized “naviform” blade-based stone tool technology, 2) advanced knowledge of plaster-making, 3) a similar style of multistory dwellings with many rooms known as “corridor buildings”, 4) a style of small clay animal figurines, and 5) mortuary practices that involved the secondary burial of skulls covered in plaster facial models (Banning, 1998; Kuijt, 2008a). This last practice (secondary skull burial) had been continually conducted throughout the Levant (and was not practiced in neighboring regions) since the Natufian (Rollefson et al., 1998), which indicates a reasonable degree of cultural continuity in the

⁵ Although there are many southern sites that did adopt rectilinear architecture (e.g., Baja, Basta, ‘Ain Jamam, Wadi Feinan 16, Wadi Fidan 1, es Sifiya, and Ghwair I), all of these sites are in the highland ecozone rather than the lowland desert ecozone.

⁶ The unexcavated LPPNB site of Kharaysin, also located in the northern highlands, may also be “megasite”, as surface finds extended for nearly 36 ha (Edwards and Thorpe, 1986). Until excavations can confirm the size of Kharaysin, its status as a “megasite” cannot be substantiated.

region up through the LPPNB. Finally, in some of the “Mega-sites”, such as ‘Ain Ghazâl, Baja, and Tell Abu Suwan, large statuary, painted plaster walls, and possible ritual or public space also occurred (Rollefson and Kafafi, 2007; Simmons, 2007).

At ‘Ain Ghazâl, sheep—virtually non-existent in the MPPNB—now join goats in almost equal numbers in the faunal record, in domestic herds, and the two species account for 69% of all faunal remains from this period (Wasse, 2002). A similar pattern holds true for other LPPNB sites in the region (Simmons et al., 2001). LPPNB survivorship profiles from ‘Ain Ghazâl show increased kill-off of younger animals compared to the MPPNB profile (Wasse, 2002). Although not exactly matching published ethnoarchaeologically determined kill-off patterns, the LPPNB patterns relatively closely approximate the ideal kill-off patterns proposed by Vigne and Helmer (2007) for “Type B meat”, “Type B milk”, or “wool” herds, as well as those proposed by Payne (1973) for “meat” or “wool” herds. The “binning” method espoused by Marom and Bar-Oz (2009) shows an LPPNB herd profile of 22% immature, 41.5% subadult, and 36.5% adult, which suggests that meat was the main pastoral resource, but does not rule out the idea that milk was becoming an important pastoral commodity at this time, especially if meat remained important and milk production in early domesticated ovicaprids was not as copious or continuous as it is in modern breeds. It is likely that cattle, too, had been brought under cultural control (if not completely domesticated) by this time, and although cattle are not over-abundant in the LPPNB faunal record of ‘Ain Ghazâl, they are prominent in the assemblages of other LPPNB sites in the Jordanian Highlands such as Wadi Fidan 1 (Twiss, 2007; Wasse, 2002; Zeder, 2008). The addition of sheep and cattle to the domestic mix added diversity to the suite of LPPNB pastoral economies and reaffirms the hypothesis that secondary products were becoming important⁷.

⁷ In addition to producing wool, sheep also produce more milk than goats, and most modern subsistence pastoralists utilize sheep mainly for these secondary products (Degen, 2007; Maltz and Shkolnik, 1980; Meged’ et al., 2008). Modern cattle pastoralists also extract most of their pastoral calories in the form of milk products (Smith,

The addition of sheep also changed the degree to which grazing by domestic herds may have impacted the local environment; sheep and goats have different dietary preferences (sheep prefer graze, while goats prefer browse), and combination herds can more efficiently (or more thoroughly) exploit the available fodder in grazing patches (Le Houérou, 1980; Ngwa et al., 2000; Stuth and Kamau, 1989). Combination grazing greatly suppresses the regrowth of woody vegetation, and if grazing pressures are high enough, this leads to an increase in the overall diversity of plant communities in frequently grazed areas, and potentially to an increased prevalence of open grasslands in regions that would otherwise have remained forested (Adler et al., 2001; Carmel and Kadmon, 1999; HilleRisLambers et al., 2001; Osem et al., 2002; Perevolotsky and Seligman, 1998). Finally, sheep are also well-matched with cereal agriculture, being more able than goats to take full advantage of field stubbles and straw (Thomson, 1987), suggesting that their addition may be related to the adoption of an integrated agropastoral subsistence system during this period.

A co-occurring intensified reliance on agricultural products, the fractionalization of the LPPNB agricultural system from one based on communally held plots or pooled labor to a set of independent autonomous household holdings, and an increase in risk in the LPPNB agricultural system is attested to via multiple lines of evidence. Firstly, the most commonly recovered LPPNB tools are highly-standardized sickle-elements made on naviform blades (a characteristic type of bi-directional blade core). The high level of standardization of LPPNB sickle elements decreased the time and effort to replace a worn element “in the field”, and also increased the efficiency of the harvest. Microwear analysis shows that sickle elements were now attached to the sickle-shaft in a manner so that each individual element protruded at an oblique angle to the shaft (i.e., like “teeth”), which was now even more curved than the sickle-shafts of the MPPNB (Ibáñez et al., 2007). This further increased the cutting efficiency of each stroke, allowing more grass stems to be

cut with the same amount of effort, and may also have increased the amount of grain that could be harvested in a given amount of time⁸, suggesting that, 1) limiting harvesting energy expenditure was important to LPPNB peoples (e.g., because daily energy budgets were becoming smaller, or caloric margins slimmer), 2) harvest time/labor requirements restricted the overall amount of grain that could be produced (especially if production had switched to the household level, as discussed below), and, 3) reduction of waste during harvest was increasingly important (i.e., that the margins for error between the amount planted, and the amount required to harvest was becoming smaller). Each of these three correlates point to increasing risk in the LPPNB agricultural system, but in any case, the level of technological investment directed toward this basic farming tool indicates that farming was an exceedingly important activity to LPPNB people. Secondly, the increase in dedicated storage features in LPPNB houses also attests to intensifying reliance on agricultural products (Gebel, 2004). These storage systems were likely both necessary to, and a consequence of, the larger populations of the LPPNB Mega-sites; that is, LPPNB agriculture was clearly capable of producing a surplus that could support a large population, but returns may have been quite variable from year to year, requiring long-term storage of grains for that population to make it through “lean” years (Goodale, 2009; Kuijt, 2009, 2008b; Spielmann et al., 2011). Thirdly, that LPPNB storage areas were

⁸ Although Simms and Russell (1997) report that experimental and ethnoarchaeological research among Bedouin groups who hand-harvest wheat and barley (i.e., they use no cutting implements) indicates that the study subjects were capable of reaping slightly more grain per hour with their hand-harvesting method than with an advanced lithic sickle, 1) the Bedouins they observed were not accustomed to using sickles but were very adept at hand-harvesting, 2) their observations were made on modern cultivars of wheat/barley in perfect growing conditions in sandy soils, and 3) they found that using sickles was still more energetically efficient than hand-harvesting. Furthermore, they point out that while advanced sickles may or may not offer advantages of higher harvest rates/efficiency, they do offer advantages of intensification, especially when it is necessary to utilize sub-optimal growing patches.

increasingly hidden from outside view suggests that agricultural labor had become concentrated at the household level (Kuijt and Finlayson, 2009), and that, 1) there was a need/wish to decrease the scope of “formal” food sharing (Enloe, 2003; Kent, 1993)⁹ and/or the extent of food sharing networks (e.g., by hiding surpluses from people you may be otherwise obligated to share with) (Halstead, 1999; Hitchcock, 1987), and/or, 2) that there existed variability in the agricultural returns taken by individual households but that social norms still dictated a general attitude of egalitarianism (i.e., that it was possible to have a larger surplus than your neighbors, but that it was socially advantageous not to flaunt this difference). Fourthly, food preparation areas (such as the location of milling slabs, ovens, and hearths), which were generally public in EPPNB and MPPNB houses, are now also located in private, secluded parts of LPPNB houses. This suggests that informal food sharing (the sharing of meals) with non-household members was also curtailed in this period (Wright, 2000), supporting the idea that households were growing more autonomous and inwardly focused. Taken together, the privatization of food storage, preparation, and consumption areas could also suggest that agricultural risk management networks—often connected to food sharing (Hegmon, 1991)—were now circumscribed by the boundaries of the household and/or the extended family, and that the basic unit of agricultural production—and therefore risk—was the nuclear family (Flannery, 1993).

Finally, rather than expand the settlement outward in response to population growth, LPPNB peoples chose to build inwards and upwards. For example, at ‘Ain Ghazâl, LPPNB houses were

⁹ I use the term “formal” in the sense proposed by Kent (1993), which relates to the sharing of raw or unprocessed foodstuffs typically through established or formalized systems of obligate sharing. Enloe (2003) further delineates this type of sharing into “primary” and “secondary” sharing by the exact type of social or merit conditions that obligate sharing, and which shape and define the character of the act of sharing. Formal food sharing is in opposition to “informal” (or what Enloe calls “primary”) sharing, which is typically the sharing of cooked foods with guests as a form of hospitality.

built closer together than during the MPPNB, were multi-storied, and exhibit a trend towards the increased compartmentalization of domestic space over time (Banning, 2003; Kuijt, 2000b). Thus, as the LPPNB progressed, villages begin to exhibit ever-increasing aggregation of dwellings, infilling of previously open space, reduction in domestic floor-space, and the innovation of multi-storied houses in LPPNB villages (Gebel, 2004). This suggests three concepts. 1) The need to conserve all available arable land around the site was of great importance to LPPNB villagers (Gebel, 2004). 2) The initial criteria for LPPNB site-founding did not include the potential for rapid growth (i.e., that the rapid population growth of LPPNB villages was neither predicted nor desired by the founding populations of LPPNB sites). 3) These factors forced people to live in closer proximity to their neighbors than they might otherwise prefer. If agricultural land was at a premium, and was owned or tenured at the level of the household or nuclear family, tensions between households may have increased due to competition for access to the most productive plots, and these tensions would have been exacerbated by the close living quarters of the LPPNB villages. Some scholars suggest that this increase in social stress fueled the increased need for privacy, secrecy, and the inward focus of households (Kuijt, 2000b). In addition to increased tensions related to differential access to agricultural land, the increased size of LPPNB towns may have led to other sources of social stress. For example, “scalar stress” associated with the increased number of interpersonal interactions accompanying larger settlement populations (Johnson, 1982) would have increased exponentially. Tacit cultural or subcultural differences may have sparked or fueled social conflicts arising between members of different clans or lineages now living close together in the LPPNB towns, especially if these social divisions derived from the amalgamation of different immigrant groups that came to the region during the preceding MPPNB period. At the largest LPPNB “Mega-sites” it was likely no longer possible to personally know every individual in the community, which would

potentially produce a general ethos of mistrust for all people outside of one’s immediate family or lineage, especially if effective mechanisms for mediation between individuals or corporate groups were not fully established (McIntosh, 1991). Rollefson and Kafafi (2007) suggest that the proliferation of non-residential spaces¹⁰ in the built environment of LPPNB villages indicates a social response to these stresses, and that these communal spaces were locations where community bonding events could occur to promote social healing. In any case, it is clear that size and density of many LPPNB villages would have presented their residents with hitherto unknown social problems that needed novel solutions.

2.2.5. PPNC/Final PPNB

In Northern Jordan, the PPNC is only known from the sites of ‘Ain Ghazâl and Wadi Shuieb¹¹. The PPNC period fills a “gap” that was previously postulated to have existed between the end of the PPN and the start of the LN, mostly based on the stratigraphy of Jericho (Kenyon, 1960). The length of this period is not well defined, nor does there exist general consensus that the PPNC should be considered as fundamentally “different” from the LPPNB. Indeed, several researchers suggest that “Final PPNB” is a better designation (see [Kuijt and Goring-Morris, 2002]).

Several important economic changes are identified with the PPNC. At ‘Ain Ghazâl, sheep now outnumber goats in the faunal assemblage by nearly 2 to 1. Sheep account for 48.3% of all faunal remains, and goats for 22%, and thus domesticated

10 Rollefson and Kafafi (2007) refer to these spaces as “religious/ritual space” or “cult buildings”, but I prefer to refer to them simply as “non-residential”, “communal”, or “community” spaces, because the case for religious, ritual, or cult activities occurring in these spaces is not conclusive.

11 There may be a PPNC layer at Tell Rakkan I, but the limited excavations at that site were unable to positively identify it. Outside of the Northern Highlands, PPNC layers have been tentatively identified at several other sites (See [Kuijt and Goring-Morris, 2002]), such as Yiftah’el west of the Jordan (Horwitz and Lernau, 2003) and Basta in the Southern Highlands (Rollefson, 1989). There may also be a PPNC layer at Tell Abu Sawwan.

ovicaprids account for 70.3% of all fauna (Wasse, 2002). The increased number of sheep in the faunal profile suggest 1) localized expansion of natural or artificial grasslands that increased the ratio of graze to browse in the site grazing-catchment¹², 2) tighter integration of the herding and agricultural economies so that herds needed to be capable of better advantage of field stubbles and fodder crops¹³, 3) increased importance of wool and meat¹⁴ in the pastoral economy, or 4) any combination of these factors. Binned according to the method espoused by Marom and Bar-Oz (2009), the transitional LPPNB/PPNC and PPNC herd survivorship patterns for ovicaprids at ‘Ain Ghazâl (19.8% immature, 42.7% subadult, 37.4% adult; and 25.5% immature, 36.6% subadult, 37.8% adult, respectively [Wasse, 2002]) are not significantly different than they were in the LPPNB (see section 2.2.4, above), but the ovicaprid survivorship curve from the PPNC layers at Yiftah’el (0% immature, 77% subadult, and 33% adult [Horwitz and Lernau, 2003]) are suggestive of a herd kept for milk—especially the “Type B” milk production strategy of Vigne and Helmer (2007). The difference in the faunal record between ‘Ain Ghazâl and Yiftah’el is interesting, as it suggests that a variety of pastoral strategies may have been practiced in the Mediterranean zone at this time. Wild game—mainly gazelles (11.8%) and pigs (11%)—continue to included in the diet in roughly the same proportions at ‘Ain Ghazâl as during the LPPNB. Interestingly, at nearby Wadi

12 Sheep have a preference for graze, and require more available graze in their diets than do goats (Bartolome et al., 1998; Rogosic et al., 2006). Too much browse can cause tooth loss and premature death of sheep, so successful sheep husbandry requires a diet composed mainly of graze (Nablusi et al., 1993).

13 Ethnographic research in Syria has shown that the yearly grazing cycle and needs of sheep can be successfully combined with cereal farming, especially if barley is grown mainly as a fodder crop (Thomson, 1987; Thomson and Bahady, 1983).

14 Comparative study of culled sheep and goats found sheep meat to be more calorie rich and to yield a larger amount of meat per animal (Gaili and Ali, 1985; Sen et al., 2004). In any case, among modern pastoral populations, the sheep to goat ratio increases when wool production or sale/consumption of meat becomes more important (Khazanov, 1994).

Shu’eib, sheep and goat comprise only 46.1% of the PPNC faunal assemblage, and pigs compose a much larger proportion of the fauna (15.4%) than do gazelle (0.5%) (Simmons et al., 2001). This may be due to Wadi Shu’eib’s location closer to the Jordan Valley, which was likely prime habitat for wild boar (Simmons et al., 2001), and further indicates that there was a wide degree of intra-regional variation in subsistence practices at this time. In all cases, however, herding is clearly the dominant focus of animal usage in this period.

Technological and cultural changes occur in the PPNC that show drastic departures from the fairly homogeneous and long-lived PPN cultural complex, and which also indicate a continuity with the subsequent Late Neolithic periods. For example, at ‘Ain Ghazâl and Wadi Shu’eib the ratio of flakes to blades in the lithic assemblages, which was close to 1:1 in the MPPNB and LPPNB, changes to about 2:1 in the PPNC (Rollefson, 1990; Rollefson and Köhler-Rollefson, 1993; Simmons et al., 2001), which is similar to the trend towards flakes in the LN (see section 2.2.6 below). The blades produced in the PPNC were also less regular, produced by plain percussion rather than indirect bunch percussion, and were more apt to bear significant amounts of cortex than in the PPNB, indicating a decrease both in standardization and in the level of technology invested in blade production, as in the Yarmoukian (Rollefson, 1990). Other components of the PPNC lithic tool kit exhibit broad similarity to the Yarmoukian, including adzes, axes, and knives (Rollefson, 1993). There was also a reduction in the quality and quantity of plaster floors, which are now made mostly of crushed marls than of lime plaster (Kuijt and Goring-Morris, 2002), and are similar to the types of “huwar” plaster being used in the Late Neolithic (Banning, 2010). PPNC contexts at ‘Ain Ghazâl also provide a small sampling of ceramics, indicating an early experimentation with a technology that becomes common in the Late Neolithic (Rollefson, 1993). Finally, it appears that the number of small fired-clay animal and human figurines declines in this period, and the (very) long-lived secondary-mortuary practice of skull removal

and re-burial is largely discontinued (Rollefson, 1993; Rollefson and Köhler-Rollefson, 1993).

There is evidence, however, to suggest some cultural continuity from the previous PPN periods. Cumulative frequency charts of burin geometry at ‘Ain Ghazâl and Wadi Shu’eib show a gradual and continual change throughout the entire Neolithic, from the MPPNB through the Yarmoukian (Rollefson, 1993; Simmons et al., 2001). The frequency of projectile points, while always quite low, also remains fairly constant across the transition at the two sites, although the size of the points decreases with time (Rollefson and Köhler-Rollefson, 1993; Simmons et al., 2001).

Still other pieces of evidence suggest that this was a period of rapid innovation and experimentation. For example, there is increase in the diversity of projectile point types during the PPNC at Wadi Shu’ieb, suggesting that this was a period of rapid experimentation and innovation in—at least—hunting technology (Simmons et al., 2001). At ‘Ain Ghazâl, the PPNC layers exhibit a diversity of house types with the two major types being rectilinear, semi-subterranean, corridor buildings, and square, single-room, above-ground dwellings, as opposed to the high level of dwelling standardization seen in the LPPNB (Rollefson and Köhler-Rollefson, 1993).

Absolute dates compiled from radiocarbon assays of the PPNC layers at ‘Ain Ghazâl and other Levantine sites suggest that the period lasted about 350 years, from about 8600 cal. BP to 8250 cal. BP (Kuijt and Goring-Morris, 2002). However, in a more recent analysis of the radiocarbon evidence using Bayesian methods and also including dates from Late Neolithic sites, Banning (2007a) places the boundary between the PPNC and the Yarmoukian at about 8450 cal. BP, suggesting that the PPNC or Final PPNB period only lasted about 100-150 years. Thus, if the PPNC/Final PPNB is looked at as a transition rather than discrete period, then the transition occurred fairly quickly—over the space of three to four generations¹⁵.

¹⁵ Recent cross-cultural research by Fenner (2005) into the generation intervals for developed nations, developing nations, and hunter-gatherers reveals a mean generation length of 29.1, 30.1, and 28.6 years respectively. It

2.2.6. Late Neolithic (Yarmoukian and Wadi Rabah)

The Late Neolithic period in the northern Jordanian highlands is known mainly from the sites in the Wadi Ziqlâb area, but also from the sites of Abu Thawwab (south of Jerash) (Kafafi, 1993; Kafafi, 1992), ‘Ain Rahub (north of Irbid) (Muheisen et al., 1988), ‘Ain Ghazâl (Rollefson, 1993), and Wadi Shu’eib (Simmons et al., 2001). The period itself has been mainly defined by the assemblages at larger sites in the Jordan Valley, such as Sha’ar Ha-Golan, Munhatta, and Jericho, and those on the coastal plain, such as Wadi Rabah. The Late Neolithic period is generally split into two sub-periods—the Yarmoukian period, and the Wadi Rabah period¹⁶. These two sub-periods were originally conceived of as synchronic culture-areas, based on the assemblages recovered from the two type sites (Sha’ar Ha-Golan and Wadi Rabah, respectively), but Bayesian analysis of the radiocarbon evidence at a regional scale

should be noted that demographic research by Eshed et al. (2004) indicates that the average age at death during the Neolithic was about 32 years, which is similar to the mean generation interval reported by Fenner. However, as Eshed points out herself in a later publication (Eshed et al., 2008), we are missing the remains of most of the PPN adult population due recovery biases, especially because most bodies seem to have been disposed of offsite in non-cemetery contexts. The adult skeletal matter that has been recovered has been subjected to significant postmortem manipulation of skeletal matter before secondary burial of only a few select individuals, and shows a distinct bias against the secondary burial of women. Furthermore, there is a large bias towards the recovery of infants and children at most PPN sites, as these age groups are the only ones that seem to have been regularly buried in primary contexts on site. It is therefore uncertain if it is even possible to adequately estimate the average human lifespan during the Neolithic from the extant demographic data. Finally, regardless of whether or not their estimates are representative, 22.4% of the sample population studied by Eshed et al. (2004) lived to be older than 40, and between 8.3% and 15.2% of the population at various Neolithic sites lived to be older than 50, which suggests that a generation interval estimate of 30 is not inappropriate.

¹⁶ Alternate designations do exist for the Late Neolithic, such as those based on the assemblages from Jericho, and/or for the southern desert sites (Banning, 2007b).

has shown these differences to be diachronic; the Yarmoukian period lasted from about 8450 (± 75) cal. BP to about 7875 (± 113) cal. BP, and, depending upon the particular Bayesian model used, the Wadi Rabah period began either directly at the end of the Yarmoukian (i.e., at around 7875 cal. BP), or, if one postulates a gap, at around 7760 (± 52) cal. BP and ended at about 7200 (± 85) cal. BP (Banning, 2007a, 2007a). Although there may be some interesting differences between the two sub-periods, for the purposes of this review, I examine the Late Neolithic period of the Northern Highlands as single entity, which exhibits some striking differences from the preceding periods, and the Late Neolithic in other parts of the Levant (Simmons, 2000). Firstly, pottery is now common, and it is the regional and diachronic variation in pottery styles, rather than in stone tools, that now provide the basis of the temporal and regional distinctions made by archaeologists. The pottery itself is of fairly coarse temper, and most recovered sherds are fairly utilitarian plainwares—although some incised, painted/slipped, and burnished decorations exist (Banning et al., 2011; Gibbs et al., 2006; Lovell et al., 2007). Secondly, domestic architecture is quite non-standardized. There is a remarkably wide diversity of house types seen at different LN sites, varying from circular or semi-circular to apsidal to rectilinear in shape, semi-subterranean to completely above-ground, single to multi-room, and with a wide variety of internal and external features such as hearths, benches, storage pits, patios, etc. (Banning, 2003; Kafafi, 1993). Architecture varies between sites in Wadi Ziqlâb itself, with reasonably well-built rectilinear single-room houses being the norm at Tabaqat al-Bûma, and small circular structures, and wall-less cobbled surfaces (perhaps tent-enclosed?) being the norm at al-Basatîn (Blackham, 1997; Gibbs et al., 2010). Thirdly, burial styles are dramatically different than the preceding period. The practice of secondary interment of skulls has now completely ceased, and is replaced with a wide variety of burial practices, including jar burial, communal burial, cist-burial, burial under tumuli, flexed burial, extended position burial, burial with and without grave goods, secondary and primary

burials, and burials with and without skull removal (Banning, 1998). Fourthly, the once common fired-clay animal figurine is largely replaced by “coffee-bean eyed” humanoid figurines (Kafafi, 1993). And finally, major changes in the lithic technology also occur in the LN. Cores are now single-platform or amorphous multi-platform types and are non-standardized (Kadowaki 2005). Blades, which used to be the most common formal lithic tools in the LPPNB, are now extremely rare (for example, making up only 5-7% of the lithic assemblages of the LN phases at Tabqat al-Bûma) (Kadowaki, 2007). The most common lithic tool types are non-formal flake tools, chipped and ground adzes, cortical scrapers, and highly retouched and denticulated sickle-elements, but the most common lithic artifact are unretouched flakes (making up 97% of the lithic assemblage at al-Basatîn, for example) (Gibbs et al., 2010). Although projectile points have been recovered from Abu Thawwab, Wadi Shu'eib and ‘Ain Ghazâl (Kafafi, 1993; Rollefson, 1993; Simmons et al., 2001), the Ziqlâb sites have almost no projectile points at all (Banning et al., 2011).

There are several types of basalt and limestone grinding/pounding implements at LN sites, including large querns, pestles, loaf-shaped handstones, and shallow grinding basins (Banning and Siggers, 1997; Gibbs et al., 2010). There is no local source of basalt in Wadi Ziqlâb—the nearest source is over 6.5 km to the north, and the next nearest source is almost 20 km to the east—so the presence of large basalt grinding implements at Ziqlâb sites suggests either a fairly high degree of residential mobility, regular logistical forays for raw materials acquisition, or participation in a regional trade network. The sickle-elements, heretofore the pinnacle of LPPNB technological innovation, are still more standardized than any other type of stone tool used in the LN, but are now made from a variety of blank types (blades or flakes), and exhibit quite a bit more variety in size and shape than do PPNB sickle-elements. Nevertheless, LN sickle-elements remain fairly standardized, especially in relation to the rest of the LN lithic tool kit (Banning and Siggers, 1997). The sickles are typically truncated at each

short edge, steeply retouched along one long edge, and may be denticulated along the other (Kadowaki, 2005). This standardization indicates that farming was still very important to Late Neolithic people. The presence of several types of grinding implements on imported materials at Late Neolithic sites supports this assertion.

Late Neolithic sites in northern Jordan are rather dispersed, and vary widely in size and complexity. While a few LN sites were as big or bigger than the largest LPPNB “Mega-sites” (e.g., Sha’ar ha-Golan at ~20 ha), and some the size of more modest LPPNB villages (e.g., Abu Thawwab at 6 ha) most known LN sites are quite a bit smaller than any of the known LPPNB villages. Many LN sites, including those in Wadi Ziqlâb, are only 500 m² or less, and so are better described as farmsteads than villages (Banning, 2003, 2001, 1998; Kafafi, 1992; Twiss, 2007). Some sites—such as ‘Ain Ghazâl, Wadi Shu’eib, and Tell Rakkan I—exhibit continuity between the LPPNB/PPNC and the LN, but most are founded on virgin soil at the beginning of this period (Banning, 2001; Banning et al. 2015, Kafafi, 1992).

There is also a fairly wide array of settlement patterns in this period. Abu Thawwab, for example, seems to have been the nucleus for a constellation of smaller sites that surrounded it (Kafafi, 1992). Excavations have not been conducted at any of these satellite sites, so it is unclear if they are perfectly contemporaneous with Abu Thawwab¹⁷, but if they are, then they may represent special-purpose sites (e.g., field-houses or herding stations), they may be part of a system of seasonal “pulsatory” transhumance (*sensu* Johnson [1969]), or they may be part of a true two-level site hierarchy¹⁸. This type of two-level site hierarchy has been considered as the typical settlement pattern of the Late Neolithic of

17 The sites were identified by Gordon and Knauf (1987) during the Er-Rumman Survey in 1985, and were dated to the LN based on the types of surface finds recovered.

18 If the smaller sites are not perfectly contemporaneous with Abu Thawwab, then the Abu Thawwab region would represent an interesting case of dispersal (or contraction) of settlement density that occurred during the Late Neolithic.

the southern Levant, and that the larger sites served as a focus of ritual and/or community activities (Banning, 2001). But it seems that a different settlement system existed in Wadi Ziqlâb, which is typified by a series small hamlets or farmsteads of about 500-600 m² in size each¹⁹ linearly dispersed along a single drainage, and home to perhaps 1-3 households each (Banning, 2001, 1998; Gibbs, 2008; Kadowaki et al., 2008). Four such small farmsteads—al Basatîn, al-Aqaba, Tabaqat al Bûma, and the upper levels of Tell Rakkan—have been discovered and at least partially excavated in the Wadi Ziqlâb drainage (Banning, 2001, 1995, 1992a; Banning and Najjar, 1999; Kadowaki et al., 2008). There are also several other as-yet undated sites in the Wadi that could also date to the Late Neolithic, so it is quite possible that the dispersed LN system of farmsteads in Ziqlâb consisted of perhaps 5-10 farmsteads (Kadowaki et al., 2008). Recent discovery of similar LN sites in Wadis Tayiba and Qusieba to the north of Ziqlâb (see section 2.3.5 below) suggests that the Wadi Ziqlâb pattern may be repeated throughout the tributary wadis of the eastern flank of the Jordan Valley. Furthermore, a similar pattern of small Late Neolithic settlements has been recently noted in the vicinity of Wadi Far’ah, west of the Jordan (Bar and Rosenberg, 2011). The Wadi Far’ah sites are in a geo-ecological context very similar to that of the Ziqlâb sites, as they are dendritically dispersed along wadi-systems draining the eastern flanks of the Samarran Hills into the Jordan Valley.

The Ziqlâb farmsteads are within easy walking distance of each other (the sites are

19 It should be noted that Tabaqat al-Bûma is the only LN site in Wadi Ziqlâb for which we can be absolutely certain of site size. Excavations exposed about 350 m² of the site (Banning et al. 2011), which was probably about 600 m² all together. It was not possible to fully explore the LN component of Tell Rakkan (Banning and Najjar, 1999), so it is unclear how large the LN occupation might have been. Al Aqaba is a highly disturbed site, making it difficult to determine the size of the original site, but its location and the similarity in artifact types suggest that it was likely similar in size to Tabaqat al-Bûma (Kadowaki et al., 2008). Al Basatîn could be slightly larger Tabaqat al-Bûma, but we tested a reasonably large proportion of the terrace during excavations at the site, so it is unlikely to be much bigger than 600 m², and certainly not bigger than 1000 m².

spaced within a 7 km transect), and radiocarbon and stratigraphic evidence suggests that they were occupied roughly contemporaneously (Banning, 2007a, 2001; Kadowaki, 2005; Kadowaki et al., 2008). Banning (2001, p.153) even suggests that “the inhabitants of many such small settlements in one wadi system may have thought of themselves as a single community”. A study of the stylistic and functional attributes and construction sequence of sickle-elements from two of the farmsteads (Tabaqat al-Bûma and al-Basatîn), Kadowaki (2005) shows that there are more similarities in construction between sickle elements found at the two sites than there are between these sites and Late Neolithic sites in other parts of the region. Kadowaki suggests that this may indicate a large degree of social cohesion between the sites. That the occupants of the two sites constructed and used sickles similarly also suggests that they likely pooled labor during the harvest period, and thus perhaps did so for other subsistence tasks (field-clearance, planting, herding) as well. In comparing the style, function, and construction of pottery recovered from Tabaqat al-Bûma, al-Aqaba, and al-Basatîn, Gibbs (2008) finds broad similarity in pottery construction and function between the three farmsteads, suggesting a high level of social relation between the sites, but also discovered crucial stylistic differences that suggest subtle or tacit cultural boundaries existed and that the individual farmsteads maintained at least partially unique identities. Thus, although the individual communities likely worked together to accomplish difficult or risky subsistence activities, it is likely that ownership and basic subsistence decision-making resided at the level of the individual hamlet.

Botanical evidence is extremely scarce at the Ziqlâb sites, and although specific charred grains have yet to be identified from LN deposits, the presence of sickle-elements clearly indicates the farming of cereal grains, and it is highly likely that pulses and legumes were also farmed (Banning, 2001; Banning et al., 1994). Interestingly, botanical evidence is also very scarce at ‘Ain Ghazâl and Wadi Shu’eib, where no grains could be identified in the many flotation samples taken from these sites (Rollefson, 1993; Simmons et al., 2001). Luckily,

botanical remains *have* been recovered from the sites of Abu Thawwab and ‘Ain Rahub. Emmer wheat (*Triticum dicoccum*), barley (*Hordeum distichum*), field pea (*Pisum sativum*), lentils (*Lens culinaris*), pistachio, and almond were recovered from Abu Thawwab (Zeidan Kafafi, 1992), and Emmer wheat (*Triticum dicoccum*), Einkorn wheat (*Triticum monococcum*), and flax (*Linum usitatissimum*) were recovered from ‘Ain Rahub (Muheisen et al., 1988).

Faunal preservation at the Ziqlâb sites is also unremarkable, and although finely detailed species differentiation or mortality profile analysis is not possible, preliminary faunal analyses have nevertheless revealed some interesting intersite variability (Kadowaki et al., 2008). The recovered faunal assemblage at Tabaqat al-Bûma is strangely dominated by the remains of cervid and canines (accounting for 57.8% of the analyzed sample). The remainder of the Tabaqat assemblage consists of cattle (4.4%), pigs (3.8%) and ovicaprids (34%). The faunal assemblage at al-Basatîn, on the other hand, is overwhelmingly dominated by ovicaprids (68.3%), but also has significantly more pigs (13.3%) and far fewer deer and canine bones (together only accounting for 2.9% of the analyzed sample). There is also a relatively higher proportion of cattle at al-Basatîn, accounting for 11.8% of the faunal assemblage. Only about half of those (5.6% of the total assemblage) were positively identified as likely to have been domestic, and while it is unclear if the remainder were domesticated, cattle are clearly more important at al-Basatîn than at Tabaqat al-Bûma. Although the poor preservation of ageable features on the recovered bones make for a tenuous assessment of ovicaprid herd mortality curves, those data that do exist suggest that management practices were not significantly different from preceding periods. At al-Basatîn, 17.2% of ageable remains were immature, 44.8% were subadult, and 37.9% were adult, which, according to the heuristic framework provided by Marom and Bar Oz (2009), is suggestive of a herd kept for meat, and also perhaps for wool, but not for dairy. Isotopic analysis of potsherds recovered from al-Basatîn can neither confirm nor deny the processing of milk, but do confirm that the site’s

inhabitants regularly cooked and ate the meat and/or marrow of goats/sheep and pigs (Gregg et al., 2009). The ovicaprid herding-species composition data suggests a sheep-dominated herding ratio of about 3:1, ostensibly supporting the case for wool production, but the sample size of species-identifiable ovicaprid bones is so small as to make these results virtually meaningless (only about 10% of the ovicaprid remains could be identified to the species-level). Herd mortality, ovicaprid speciation, and pot sherd isotopic data are not yet available for Tabaqat al-Bûma, but based on the overall differences in the faunal assemblages between the two sites, it would not be surprising if these data are shown to differ between the sites as well. In any case, it seems apparent that the inhabitants of al-Basatîn specialized in the herding of ovicaprids, and possibly cattle, and also focused on the hunting of wild boar, while the inhabitants of Tabaqat al-Bûma focused on the hunting of deer and the herding of ovicaprids, but the latter to a lesser degree than at al-Basatîn.

The faunal evidence from the Ziqlâb sites is in general alignment with that of other LN sites in the area. At Abu Thawwab, abundant remains (68% of the total faunal assemblage) of domesticated goat and sheep, moderately abundant remains of wild gazelle and cattle, and scant remains of wild boar and onager were recovered (Zeidan Kafafi, 1992). The Yarmoukian layers at ‘Ain Ghazâl, produced a faunal assemblage where sheep and goat make up 72.5% of the total LN faunal assemblage (Wasse, 2002), and Wadi Shu’eib, where sheep and goat make up 47.6% of the total LN faunal assemblage (Simmons et al., 2001). Of these sites, only faunal analysis detailed enough to differentiate sheep and goat remains comes from ‘Ain Ghazâl, where sheep compose 49.1% of the LN faunal assemblage and goats compose only 23.4% (Wasse, 2002). This also indicates a sheep-dominated herding ratio (in this case of 2:1), but it is again unclear if the reliance on sheep is common to all LN sites. The binned LN herd survivorship data from ‘Ain Ghazâl are not significantly different from the PPNC and LPPNB curves (20.7% immature, 39% subadult, and 41.3% adult [Wasse, 2002]), and again, although this is indicative of meat production, it

does not rule out milk or wool production (wool in particular, considering the predominance of sheep in the LN faunal record at ‘Ain Ghazâl).

Taken as a whole, the faunal evidence recovered from LN sites in the Northern Highlands indicates that Late Neolithic people relied heavily on domestic flocks of sheep and goat, but occasionally supplemented their diets with animal proteins derived from potentially domesticated cattle and pig, and/or from wild game such as deer or wild boar. That the proportion of hunted wild game species differs between sites suggests that individual hamlets may have been purposefully located to take advantage of specific game species. For example, the larger amount of pig bones at al-Basatîn may relate to the site’s location near the main perennial springs and the more deeply entrenched portions of the Wadi, which today are filled with thick riparian vegetation that provides excellent habitat for an abundance of wild boar, whereas the larger proportion of deer bones at Tabaqat al-Bûma may relate to its closer proximity to the wooded uplands, which were presumably excellent deer habitat in the Late Neolithic. Economic specialization may have extended beyond the realm of hunting, however, as the much larger proportion of ovicaprid bones at al-Basatîn, combined with the more ephemeral style of the architecture discovered there, suggest that its occupants might have specialized in pastoralism, perhaps centered around the production of dairy and other secondary products. Tabaqat al-Bûma (and perhaps al-Aqaba), on the other hand, may have specialized more in cereal production, especially considering the numerous fertile alluvial terraces in close proximity to the site. Thus, each small hamlet may have been a semi-specialized “node” in an economically integrated sub-regional network of sites, spaced out along each major Wadi system so as to take better advantage of localized variation in wild resource availability and suitability for agriculture and herding. This idea is in congruence with the material cultural evidence discussed above suggesting subregional cultural cohesion with subtle, but distinct, cultural boundaries between sites.

2.2.7. The End of the Late Neolithic

The end of the Late Neolithic period is still unclear in the Northern Highlands. In Wadi Ziqlâb, there is evidence for some minor upheaval at Tabaqat al-Bûma prior to another social, economic, and settlement reorganization at the beginning of the Chalcolithic. One of the major trends in material culture at Tabaqat al-Bûma was a gradual reinvestment in complex blade-based sickle technology over the Late Neolithic suggesting that people were once again intensifying their agricultural strategies (Banning et al., 2011). The brief abandonment before the relatively short final reoccupation of the site (Blackham, 1997) at the very end of the Late Neolithic period suggests that people were once again experimenting new settlement strategies. The specific motivation for this experimentation is currently unclear, but in any case, it seems that two totally new settlements were founded at the start of the Chalcolithic, and, of all the Neolithic settlements, only Tell Rakkan

I remained occupied. The first new Chalcolithic site—located near the modern village of Tubna—was established high in the uplands, perched on a hill-top well above the upper reaches of Wadi Ziqlâb, and the second new Chalcolithic site—Tell Fendi—was established out in the Jordan Valley proper, near the confluence of the Ziqlâb stream with the Jordan River (Banning, 1999; Banning et al., 1998; Blackham et al., 1997). These sites were larger than the previous Late Neolithic sites, and their vastly different locations and different material cultures indicate the emergence of a new socio-economic system at this time.

2.3. NEOLITHIC SITES IN WADI ZIQLÂB

Banning (Banning, 1983, 1982; Banning and Fawcett, 1983) began the early stages of what was to become the long-lived Wadi Ziqlâb Project (WZP) with an archaeological survey in 1981 that culminated in his PhD dissertation work concerning ancient human land use in the region

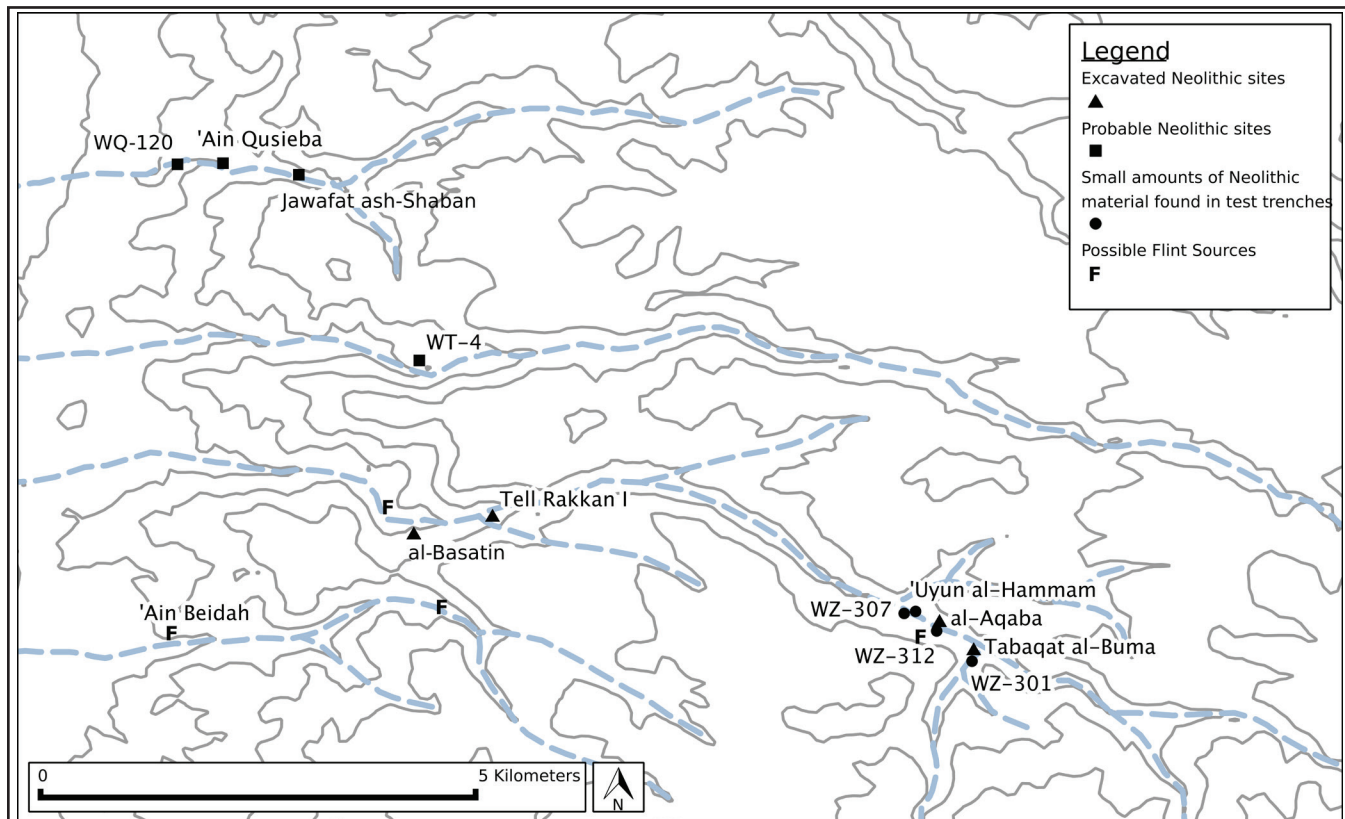


Fig. 2.3. Map showing the known Neolithic sites and potential flint sources in Wadi Ziqlâb and the neighboring Wadis.

(Banning, 1985). The Neolithic occupation of Wadi Ziqlâb has been a focus of the WZP since its inception, and continues to be so today. To date, four Neolithic sites have been positively identified and excavated by the WZP in Wadi Ziqlâb, three to four other locations have been identified in the Wadi where smaller amounts of Neolithic material have been recovered, and four more possible Neolithic sites have been tentatively identified during survey in the neighboring wadis. In this section, I provide a brief overview of the main details of these sites.

2.3.1. Tell Rakkan I

Tell Rakkan I (originally referred to as ‘Ain Jahjah) is a stratified PPNB through Chalcolithic site (see Figure 2.1) located on a small terraced promontory in the lower western section of Wadi Ziqlâb, adjacent to the second knick point (and waterfall) and the perennial artesian spring ‘Ain Jahjah (Figures 2.3 and 2.4). Paleoenvironmental modeling (see Chapter 5) suggests that the site was located bordering the Mediterranean Woodland and Savannoid (grassland) ecozones in their configuration during the LPPNB period. The site was first investigated in 1995 by surface survey, which noted several stratified deposits, numerous PPNB artifacts, plastered surfaces, and stone walls eroding from a 100 meter-long bulldozer cut made in the mid 1980’s when

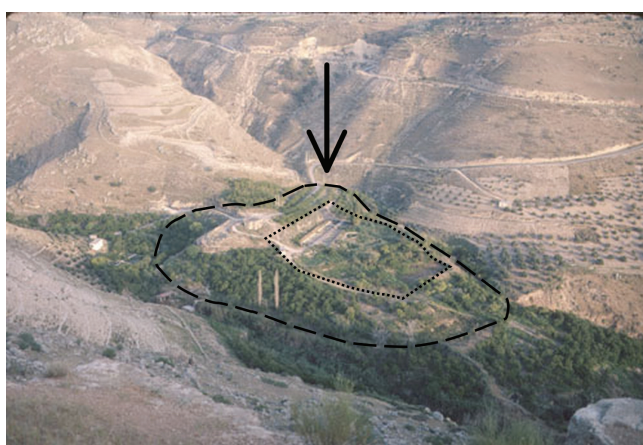


Fig. 2.4. Overview of Tell Rakkan I. Dotted line denotes the area of bulldozer disturbance, dashed line denotes the probable border of the Neolithic village.

some concrete fish ponds were installed on the site (Figure 2.4). Excavations were carried out in 1999, and consisted of four step trenches along the edges of the site near the dozer cut, which yielded Chalcolithic, LN, and PPNB/C artifacts (Banning, 1999; Banning and Najjar, 1999).

Two radiocarbon dates taken on charcoal associated with the lowest plaster floors in the exposed dozer cut yielded calibrated dates of 9427 (± 122) cal. BP and 9040 (± 250) cal. BP (Banning, 2001; Banning and Najjar, 1999). These plaster floors directly overlaid sterile subsoil (tufaceous earths), and so the earliest documented occupation of the site is likely not earlier than the mid 10th millennium BP (i.e., the latter part of the MPPNB). The lower contexts yielded characteristic LPPNB artifacts such as Naviform sickle blades, crested blades, Amuq and Byblos points, and plaster “white ware” vessels, as well as characteristic LPPNB architectural features such as fine plastered floors and double-leaf stone walls (Banning and Najjar, 1999).

The LN layers at Tell Rakkan directly overlay the LPPNB layers, suggesting that the site may be one of the few in the region displaying continuity over the PPN/LN transition. Although no architecture (except for the possibility of a single wall) was found in the LN layers, and no absolute dates have been processed for these layers, Banning (2001) estimates the main period of occupation to be from about 9300-7000 cal. BP (i.e., from the start of the LPPNB through the end of the LN5 phase of Tabaqat al-Bûma, see Figure 2.1). Several characteristic LN artifacts were found in the upper layers of the site, including sherds exhibiting characteristic Yarmoukian “herring bone” incised decoration, red slipped pottery, and pottery of friable fabric similar to that recovered at Tabaqat al-Bûma and al-Aqaba (although not with the same cross-hatched/combing incised decoration) (Banning and Najjar, 1999).

Determining the size of the site itself is complicated by the level of disturbance to the main deposits (Figure 2.4). The two tiered terrace upon which the site is situated is about 4 ha, and the upper tier upon which the site is directly located is about 3 ha. The original excavators estimated

the size of the LPPNB occupation of the site to have been between 0.75 and 1.5 ha²⁰, meaning that it could have housed no more than about 300 people (likely less)²¹. The LN occupation was poorly represented in the excavation units, which were located towards the periphery of the LPPNB occupation area, suggesting that the LN occupation of the site was on a smaller scale than the PPN occupation. It is therefore quite likely that the LN occupation of the site was as a small hamlet similar in size to Tabaqat al-Bûma or al-Basatîn.

2.3.2. LN Tabaqat al-Bûma

The site of Tabaqat al-Bûma is located on a small alluvial terrace near the active channel of the Wadi Ziqlâb drainage in the upper portion of the middle Ziqlâb near the confluence of two major tributaries (Figures 2.3 and 2.5). Paleoenvironmental modeling (Chapter 5) suggests that the site was located firmly within the Mediterranean Woodland ecozone during the Neolithic period. The site shows evidence of episodic occupation from as early as the Epipaleolithic through modern times, with the most intensive period of use during the Late Neolithic. The site was discovered in 1987 using a systematic subsurface testing strategy (Banning, 1996), and excavations continued at the site until 1992. The site has been subject of many publications (Banning, 1992a, 1992b; Banning et al., 1996, 1992, 1989; Blackham, 1997; Dodds, 1987; Ullah, 2012, 2009), and is currently the best-documented Late Neolithic hamlet in Northern Jordan.

²⁰ Banning and Najjar (1999) report the site to be between 1 and 1.5 ha, but Banning (2001) reports it to be between 0.75 and 1 ha. I have chosen to use the outside intervals of these two sources because my own efforts to judge the size of the site (including two site visits) showed it to be difficult to estimate due to modern disturbances (particularly by the construction of the fish ponds and terracing for pomegranate orchards).

²¹ Population estimates are derived by using the technique first published by Schacht (1981) where population is estimated by regression against site size [$P = 85 + (107.55 \times A)$, where A is the area in hectares]. Internal MedLanD research has updated the original regression with additional ethnographic data so that the estimates provided here derive from the following equation: $P = 83 + (159 \times A)$

The architecture at the site is characterized by free-standing stone masonry structures with a variety of floor substrates, including low-quality plaster, cobbled surfaces, and packed earth surfaces (Blackham, 1997). The houses themselves are of a variety of sizes and shapes, but they are all geometric (non-circular) four-walled structures, and the majority are square or rectilinear (Kadowaki, 2007). A total of ten structures were discovered at the site, with between two and three houses in use in any occupational phase (although some structures seem to have been reused as storage areas, refuse disposal areas, or animal pens in subsequent phases) (Blackham, 1997). There are a variety of internal features in the houses, including plastered and stone hearths, basalt and limestone grinding querns, possible storage platforms, floor-level door or entryways, and possibly windows (Kadowaki, 2007; Ullah, 2012). The pottery recovered from the site shares some general traits with Wadi Rabah and Yarmoukian types, but is also unique enough to defy absolute correlation with established pottery “cultures” of the region (Banning et al., 2011). The lithic assemblage is also consistent with Wadi Rabah assemblages, although the proportion of sickle-element types is different at Tabaqat al-Bûma than at “typical” Wadi Rabah sites (Banning et al., 2011). Interestingly, it appears that sickles



Fig. 2.5. Overview of Tabaqat al-Bûma. The site plan has been overlaid at approximately the correct scale and orientation. The arrow in the background points to the location of the nearby site of al-Aqaba.

not only become more common over time at the site, but they also become more technologically sophisticated, indicating a temporal trend of increased importance of sickles with specific morphological traits (Banning et al., 2011).

The Late Neolithic occupation at Tabaqat al-Bûma occurred in five distinct architectural phases (designated LN1-5) from ca. 8600 to 6200 cal. BP (Figure 2.1) (Banning et al., 2011; Blackham, 1997; Kadowaki, 2007). The site was apparently not abandoned between each phase, with the possible exception of an abandonment between phases LN4 and LN5 (Banning, 2007a). The first Neolithic usage of the site (phase LN1) was as a cemetery, and two slab-covered and rock-lined cist tombs, dug into the Epipaleolithic paleosol, were encountered in the excavation units (Banning et al., 2011). No domestic artifacts or architecture were recovered from this phase, indicating the special-purpose usage of the site as a cemetery in this phase. Only two of the four radiocarbon dates that exist from this phase are reliable, and Bayesian analysis constraining the start of this phase to the end of the PPNC suggests that it lasted from about 8625 (± 61) cal. BP to about 8104 (± 202) cal. BP (Banning et al., 2011). Very little of the second phase was captured in the excavation units, but it seems that this phase marked the beginning of domestic occupation at the site, as evidenced by the mainly destroyed remains of two to three houses. No radiocarbon dates exist for this phase, but if constrained by the dates from the previous and subsequent phases, it would have lasted from around 8000 cal. BP to 7600 cal. BP (Banning et al., 2011). The LN3 is the first well represented occupational phase, and the site seems to have been a small farmstead with two clusters of domestic buildings housing perhaps two to three families (Banning et al., 2011). Kadowaki (2007) finds the spatial patterning of artifacts from this phase to be suggestive of a small cooperative unit, with shared outdoor workspaces and common areas where communal food preparation possibly occurred. Microrefuse analysis of one of the house floors from this phase suggests that food processing and meal preparation took place indoors, however, which would indicate that the occupants were

attempting to reduce informal sharing of cooked foods (Ullah, 2012). Bayesian analysis of the radiocarbon dates from this phase indicates that it began at about 7624 (± 82) cal. BP and ended at about 7357 (± 70) cal. BP (Banning et al., 2011). The LN4 phase is marked by the construction of one new structure, and the abandonment and collapse of two of the structures from the previous phase, with the other structures being reused (Banning et al., 2011). While Kadowaki (2007) sees evidence for more constricted use of space in the architecture, and less communality of food preparation in the spatial patterning of the larger artifacts, suggesting that the occupants of the site were less cooperative than in the previous phase. Microrefuse analysis of one of the domestic structures, however, suggests that food preparation no longer took place indoors, indicating an increase in the informal sharing of cooked foods, which is contra to the expectations of decreasing communality of resources (Ullah, 2012). Bayesian analysis of the radiocarbon dates from this phase, with a small abandonment gap postulated before the reoccupation of the site in phase LN5 and constrained by the earliest dates from the nearby Chalcolithic site of Tubna, estimates this phase to have lasted from about 7357 (± 70) cal. BP to 7174 (± 102) cal. BP (Banning et al., 2011)²². The final phase seems to have been a reoccupation of the site after a brief hiatus, and is marked by the construction of two new structures. Kadowaki (2007) interprets the architectural and artifact patterning as once again indicative of a small cooperative farmstead of two-three families who shared communal open-space and food preparation activities. Domestic microrefuse data is currently unavailable from this phase, but it will be interesting to see if the contrasting patterns of the previous two phases continues in this one. Bayesian analysis provides a very rough estimate of the length of this occupation, and suggests that it lasted from about 7100 cal. BP to about 7000 cal. BP.

2.3.3. LN al-Basatîn

The site of al-Basatîn is a Late Neolithic and

²² Banning et al. (2011) admit that this probably underestimates the date for the end of the LN4.

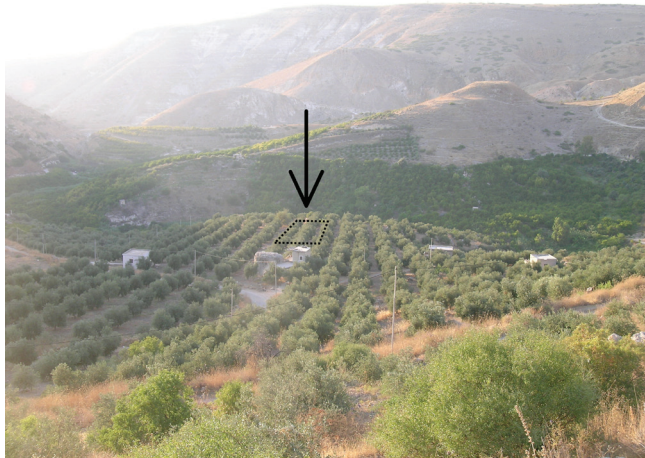


Fig. 2.6. Overview of the al-Basatîn terrace. The dotted line shows the approximate extent of the main excavation grid.

Early Bronze Age site located about a kilometer downstream from Tell Rakkan I on a large bench terrace elevated above the current course of the Wadi by about 100 meters (Figures 2.3 and 2.6). Paleoenvironmental modeling (Chapter 5) suggests that the site would have been firmly within the Mediterranean Savannoid (grassland) ecozone during the Neolithic. The site was initially discovered during geoarchaeological testing in 2000, test excavations in 2002 located the main subsurface deposits, and large scale excavations were undertaken in 2004, 2008, and 2009 (Banning et al., 2004; Gibbs et al., 2010, 2006; Kadowaki et al., 2008; Maher and Banning, 2001). Abundant Late Neolithic material has been recovered. There is insufficient evidence for the determination of distinct phases of occupation at al-Basatîn, but radiocarbon dates taken from the LN layers of the site suggest an occupation from between 7700 to 7300 cal. BP (Figure 2.1) (Kadowaki et al., 2008). These dates place the site roughly contemporaneous to the LN3/4 occupation layers at Tabaqat al-Bûma, or during the Wadi Rabah cultural phase of the regional chronology (see Figure 2.1). However, it should be noted that stratigraphic analysis of the site is not complete, so it is unclear if these dates reflect the entirety of the occupational period at the site. Given the large degree of culture affinity between the two sites (see below), it is highly likely that the founding

and abandonment of al-Basatîn would coincide with the timing of phase changes at Tabaqat al-Bûma. Therefore, until definitively proven otherwise, we should consider the main period of occupation at al-Basatîn to coincide with the LN2 and LN3 phases of Tabaqat al-Bûma, which would mean an occupation that began around 7900 cal. BP, and ended around 7200 cal. BP.

Lithic and pottery styles at al-Basatîn and Tabaqat al-Bûma share more similarities with each other than they do with other LN sites in the southern Levant, suggesting a close cultural affinity (Gibbs, 2008; Kadowaki, 2005). Al-Basatîn differs from Tabaqat al-Bûma in some significant ways, however, including some of the specifics of pottery and lithics manufacture and style (Gibbs, 2008; Kadowaki, 2005). But there are some differences that are more striking. For example, in contrast to the abundance of domestic structures and indoor areas discovered at Tabaqat al-Bûma, mostly outdoor surfaces with flat-lying debris have been discovered at al-Basatîn. Also, aside from a few short alignments of stones, no rectilinear structures have been discovered at al-Basatîn either. In fact, only two features have been discovered that could be interpreted as “houses” in the traditional sense of the word, and they are both circular structures of around 2 to 3 meters in diameter. The interpretation of these buildings as domestic derives mainly from the discovery of an ashy feature in the interior portion of one of the structures that was likely a hearth. Future analysis of detailed microarchaeological samples taken from these structures will aid in their final interpretation. By far the most common architectural feature at the site is cobbled surfaces of varying quality and geometry that are not associated with any walls. To date, at least five, and perhaps six (one may be a natural cobble layer) of these surfaces have been discovered. The best constructed of these surfaces is also the most geometric, being a perfect circle of about 2 meters in diameter. The largest cobbled surface is about 4 meters along its longest dimension, and was likely rectilinear in shape, although only one corner of it appeared in the excavation unit. These surfaces were mainly devoid of artifacts,

indicating that they were likely cleaned on a regular basis. A cache of refittable flint flakes, a stone axe, and a paired handstone and pestle were, however, discovered *in situ* on the largest of the surfaces, and preliminary analysis of flotation samples recovered from this surface revealed the presences of charcoal, olive pit fragments, and unidentifiable seeds (Kadowaki et al., 2008). Future analysis of detailed microarchaeological samples taken from these surfaces will aid in the interpretation of their use, but currently it is hypothesized that they were either used in relation to the processing and storage of agricultural products and tools (Kadowaki et al., 2008), or that they may have been the floors for tents (Gibbs et al., 2010). Three stone-filled storage pits were also discovered at the site, and a large basalt grinding slab was discovered in the bottom of one of these.

2.3.4. Al-Aqaba

Al-Aqaba (first referred to by its site number, WZ 310) is a highly eroded LN site located about 600 meters downstream and on the opposite bank from Tabaqat al-Bûma (Figures 2.3, 2.5, and 2.7). Al-Aqaba was discovered with the same systematic trenching strategy that revealed Tabaqat al-Bûma (Banning, 1996), and minor excavations at al-Aqaba were conducted concurrently with the excavations at Tabaqat al-Bûma. The pottery,

sickle elements, and other artifacts recovered from al-Aqaba are of identical style to those recovered from Tabaqat al-Bûma, suggesting a strong relationship between the two sites. The exact nature of this relationship is unclear, but at the very least, the occupants of the two sites were in very close and very frequent cultural contact with each other. Although no radiocarbon dates exist for the site, it is clearly contemporaneous with at least part of the occupation at Tabaqat al-Bûma (Figure 2.1) (Banning, 1999).

Very little architecture was discovered at the site, and most artifacts were found to be in secondary colluvial contexts, originating from further up the slope, and now overlaying later deposits (Bronze Age pits). No *in situ* material was found on the upper slopes, however, leading the excavators to believe that the original site has been totally destroyed, perhaps due to a land-slide or other mass wasting processes (Banning, 1999). It is thus very difficult to determine the original size and exact nature of the site, but it seems likely that it was also a small farmstead of one to three households.

2.3.5. Other Locations in Wadi Ziqlâb with Neolithic Material

Between the years of 1986 and 1992, eighteen trenches were dug into fifteen of the small alluvial terraces of the middle and upper Ziqlâb drainage



Fig. 2.7. The al-Aqaba terrace. The arrow indicates the approximate location of the original excavation trench.



Fig. 2.8. Site WZ-301, one of the terraces where small amounts of Neolithic material were recovered in test trenches.

(Banning, 1996). Aside from the discovery of the sites of Tabaqat al-Bûma and al-Aqaba by two of the test trenches (as discussed above), the subsurface testing recovered small amounts of Neolithic or probable Neolithic materials from four of the other sampled terraces (Figure 2.3 and 2.8). Although significant locational sampling biases may be present in the dataset (only one or two trenches were dug per terrace), the very low density of the recovered Neolithic material, and the close proximity of the terraces to either Tabaqat al-Bûma or al-Aqaba, suggest that they were utilized for agriculture rather than habitation (Banning, 1996). One of these locations—WZ-312—is also significant because it appears that flint nodules may have been quarried from an outcrop directly upslope from the terrace, and it seems that the raw nodules were at least partially processed on location (Banning, 2001, 1996). Another flint source has been identified in the lower reaches of the Wadi (see Figure 2.3), which may have been a potential source of tool stone for the inhabitants of al-Basatîn and Tell Rakkan I (Kadowaki et al., 2008).

Small amounts of Late Neolithic material have also been recovered at the site of ‘Uyun al-Hammam, which is located a few hundred meters downstream from Al-Aqaba and Tabaqat al-Bûma (see Figure 2.3). ‘Uyun al-Hammam is also important for the abundant Epi-Paleolithic

remains that are preserved in an ancient paleosol below the colluvial layers (Maher, 2011, 2007; Maher et al., 2002). The most interesting potential Neolithic feature at ‘Uyun al-Hammam is a bundle burial in stone-lined rubble-filled pit (Maher, 2007). Although no absolute dates yet exist for this feature or burial, and despite the fact that no diagnostic grave goods were recovered, the presence of a few LN potsherds recovered in the upper layers of the rubble fill, the general style of the burial (similar to the LN cist-tombs), and the previously documented presence of LN dug into the Epi-Paleolithic layers at nearby Tabaqat al-Bûma are all indicative that this burial dates from the Late Neolithic. In any case, the pit itself appears to have been first used as a storage feature (also similar to some of the burials from Tabaqat al-Bûma), and considering that ‘Uyun al-Hammam is located on what was once a broad alluvial terrace very near to a perennial spring (Maher, 2011), it is quite likely that the terrace was farmed, and perhaps even occupied during the Late Neolithic.

Finally, in addition to these locales, 18 other “unremarkable” surface lithic scatters were detected in the original survey of the Wadi in 1981 (Banning, 2001, 1983; Banning and Fawcett, 1983). The “unremarkable” aspects of these scatters related to the lack of diagnostic lithics, and it is quite possible that some or all of these scatters date



Fig. 2.9. Overview of the WT-4 terrace, showing the long bulldozer cut that bisects the site. The main portion of the Neolithic site is indicated by the arrow.

from the Late Neolithic, which as I have discussed above, is characterized by a fairly “unremarkable” lithic assemblage. Without excavation, the function of these sites are unknown, and although it is possible that at least some of them may be related to other small Neolithic hamlets, they may also be related extensive farming, pastoral, or hunting activities in the Wadi (Banning, 2001).

2.3.6. Neolithic Sites in Neighboring Wadis

The multicomponent site of WT-4, discovered during geoarchaeological survey in Wadi Tayiba (Figure 2.3) in 2000 and 2001 (Maher et al., 2002; Maher and Banning, 2001), seems to have had a substantial PPNB occupation (although it is not possible to determine if it is LPPNB). Based on an investigation of a large bulldozer cut that bisects the site (Figure 2.9) and the spatial extent of surface finds collected during two brief site visits in 2006 and 2008, I believe the PPNB occupation at WT-4 was probably very similar to that of Tell Rakkan and that it was likely a small village of not more than 1-2 ha in size. WT-4 may also have a Late Neolithic component but without excavation it is unclear exactly how large the LN occupation at WT-4 may have been.

A recently completed survey of Wadi Qusieba (to the immediate north of Wadi Tayiba) has discovered at least two Late Neolithic sites in that Wadi as well (Figure 2.3.) Test excavations at sites WQ-117, also known as ‘Ain Quseiba, and at WQ-335, known as Jawafat Shaban, show evidence of Yarmoukian and Wadi Rabah occupation, respectively (Banning et al., 2014, 2015). A third site, WQ-120, has a heavily blade-dominated lithic assemblage, which is typical of the PPNB, but so far no definitive PPNB-style blades have been found. Both ‘Ain Quseiba and WQ-120 are located in the highly incised lower stretch of Wadi Quseiba, below the first knickpoint in the Wadi Quseiba drainage system. ‘Ain Quseiba revealed the remains of at least two stone-lined semi-subterranean housepits, filled with ashy grey soil and abundant Yarmoukian pottery. A typical Yarmoukian stone figurine was recovered from one of these house-pits. Interestingly, the main faunal

remains recovered from the initial test excavations indicated a heavy reliance on aquatic resources, and relatively scarce evidence for farming or herding at the site (other than some basalt grinding stones).

Jawafat Shaban is located above the second knickpoint of the Wadi Quseiba system, on a small, low alluvial terrace adjacent to a small tributary wadi (Banning, et al. 2015). The site covers an area of around about 500 m², and although test excavations showed the site to be damaged, it was likely composed of a few stone buildings and associated outside areas. Faunal remains include goat, sheep, and cattle in addition to some wild taxa. Ground stone and sickle elements attest to the processing of cereals at the site, and abundant Wadi Rabah pottery date it to this period. Pottery and lithics from Jawafat Shaban are similar to assemblages from the Wadi Ziqlâb sites. The site therefore seems to have been a small farming hamlet generally contemporaneous with, and roughly analogous to, Tabaqat-al Bûma.

As of yet, and despite fairly intensive formal and informal survey, no Neolithic sites have been discovered in Wadi Abu Ziad. However, there are two sources of high quality flint in Wadi Abu Ziad (see Figure 2.3) which may have been the quarry for much of the stone used to construct tools in Wadi Ziqlâb (Kadowaki et al., 2008). Although no comprehensive sourcing analysis has been undertaken, there is abundant evidence that this flint was quarried in antiquity, including the likely remnants of extensive quarries at the Bronze Age site of ‘Ain Beidah near the outlet of the Wadi.

2.4. CHAPTER SUMMARY

In this chapter, I have provided a basic archaeological narrative model of course of the Neolithic period in the Northern Highlands of Jordan, with specific emphasis on the view of this trajectory from Wadi Ziqlâb. The basic picture is one of continual intensification and reliance on domesticated plants and animals and a general increase in material cultural, social, and settlement complexity from the advent of domestication economies in the PPNA until the culmination of “Pre-Pottery Neolithic Culture” in the LPPNB.

In the following Late Neolithic period, we see a drastic reorganization in all of these aspects of the Neolithic lifeway. At some sites, researchers see a phase of reorganization connecting these periods, which has been labeled variously the PPNC or the Terminal PPNB (and could just as easily be labeled the Early Late Neolithic). In many parts of Northern Jordan, this period is evidenced by the slow abandonment of the so-called PPNB “Mega-sites”, which are eventually only used on a seasonal or intermittent basis in the following Late Neolithic.

In Wadi Ziqlâb, while the nature of the transitional period itself is less clear, the picture of what was transitioned to is much clearer. Even though the one definitively known LPPNB site in the Wadi is much smaller than any of the Mega-sites, it nevertheless seems that, as with these better-known large PPNB villages, around 8500 years ago, the PPNB people of Wadi Ziqlâb largely abandoned the village they had inhabited for many hundreds of years. Whereas it remains unclear exactly where the people of the Mega-sites went to after leaving their ancestral villages, in Wadi Ziqlâb, it seems pretty clear that they dispersed into a series of smaller hamlets in the vicinity of the PPNB village of their ancestors. Thus, across the PPNB/LN transition, settlement changed from a single point of focus on the border of the Mediterranean Woodland and Savannoid ecozones, to a dispersed system of related smaller habitations spread throughout both ecozones. In

the LPPNB, Tell Rakkan I would have served as a “central place” from which logistical forays to either ecozone for wild game, pasture, and other resources would have been launched. It is unclear if these activities would have been undertaken communally, but there is evidence from other LPPNB sites that suggests not (i.e., that subsistence activities took place at the level of the nuclear family or household). In the Late Neolithic, however, each hamlet likely specialized in the gathering or production of those particular resources most available in, or most suitable for production in, its own ecozone. This specialization was not all-encompassing, however, and in addition to semi-regular trading or sharing of excess “specialized” resources between hamlets, each hamlet also seemed to have engaged in all types of subsistence activities to greater or lesser degrees. Thus, it seems that each hamlet could be considered as a single unit of production/consumption in a larger system; one semi-autonomous node in a wider net of interconnected hamlets.

Finally, the reader will have no doubt noticed that, although I have stated in Chapter 1 that this monograph investigates the *cause* of this reorganization, I have not discussed possible causes in this chapter. There is a history of archaeological thought concerning the PPN/LN transition to which I wish to add my own thoughts. These will be the sole focus of the next chapter.

CHAPTER 3

THEORETICAL APPROACHES TO THE PPN-LN TRANSITION

3.1. CHAPTER INTRODUCTION

In this chapter, I examine five leading explanations for the instigation of the PPN-LN transition. I critically review each idea, and discuss the current state of research. I then introduce a new approach to understanding the PPN-LN transition, which draws on Complex Adaptive Systems (CAS) theory and Resilience Theory (RT). I describe the salient portions of each theory, discuss how they can be applied to archaeological phenomena, and provide empirical evidence for the existence of complex adaptive phenomena within human subsistence economies. Finally, I sum up a narrative model of how complex phenomena may have led to the PPN-LN transition, present new CAS and RT-informed hypotheses for the PPN-LN transition, and examine their test implications.

3.2. EXISTING HYPOTHESES ABOUT THE PPN-LN TRANSITION

There are five leading schools of thought regarding the terminal PPNB/C to LN transition, which I have labeled: 1) the “Climatic-Forcing Hypothesis”, 2) the “Anthropogenic Catastrophe Hypothesis”, 3) the “Epidemiological Hypothesis”, 4) the “Social Breakdown Hypothesis”, and 5) the “Settlement Reorganization Hypothesis”. In this section, I summarize the main arguments of each hypothesis and examine their critiques.

3.2.1. The Climatic-Forcing Hypothesis

A basic tenet of the Climate-Forcing Hypothesis is that rapid or radical climate-change was the main driver of the social change seen at the end of the PPN. The theory’s earliest proponents were Davis and Simmons¹ (J. Davis

et al., 1990) and the idea was subsequently taken up by Bar-Yosef (Bar-Yosef, 2001; Bar-Yosef and Meadow, 1995) and Belfer-Cohen and Goring-Morris (Belfer-Cohen and Goring-Morris, 1997). All see the abandonment of the PPNB “Mega-sites” as corresponding with general climatic changes occurring in the region at that time. Both Bar-Yosef and Davis and Simmons referenced the results of the Cooperative Holocene Mapping Project’s (COHMAP) GCM climate-modeling results, published in a 1988 article in the journal *Science* (Anderson et al., 1988), while Belfer-Cohen and Goring-Morris referenced proxy records (pollen and speleothems) from the Levant. In the COHMAP model, both the Indian monsoon and winter storms coming from the Mediterranean penetrated far enough inland to bring summer storms to the Southern Levant in the first part of the Holocene. According to the model, the monsoon started to retreat to its current extent around 9000 BP, returning the Southern Levant to a classic Mediterranean climate and coinciding with the depopulation of the Mega-sites. Bar-Yosef connects this climate-change event with the contraction of summer grazing areas, which would have put pressure on the pastoral component of the PPNB economy. Simmons, on the other hand, sees this event connected with increased erosion rates on harvested fields that would have occurred during the PPNB summer monsoons. Rather than the recession of the monsoon, in Simmons’ model it is the cumulative effects of the monsoonal erosion on arable land throughout the PPNB that eventually leads to the abandonment of the Mega-sites, and the reorganization of the population to areas previously forested where the soil has been conserved. Simmons connects this with the so-

the main driver of the PPN-LN transition but instead now supports a combination of social pressures and environmental change (see section 3.2.4., below).

¹ Simmons no longer supports climatic forcing as

called “Neolithic cobble layers” that have been found interspersed between the PPN and LN occupation layers at ‘Ain Ghazál, Wadi Shu’eib, and other sites². Belfer-Cohen and Goring-Morris also see accumulating environmental degradation in-part due to human land-use but suggest that it was a brief climatic reversal (which they see occurring at 7900 BP) that pushed the already-weakened PPNB food-system over the brink of collapse. It is important to note that none of these early proponents of the Climate-Forcing Hypothesis promote climate-change as the *only* factor of the abandonment; all authors indicate that the natural effects of climate-change were amplified by human action. For example, Bar-Yosef postulates that the effect of reduction in natural summer grazing could have been amplified by a general increase in grazing pressure and woodcutting by PPNB peoples. All three sets of authors, however, implicitly or explicitly suggest that the major cultural and social transformation that occurred across the PPN-LN transition were somehow directly related to climate change.

A new wave of Climate-Forcing Hypothesis papers have been published in the last several years (Berger and Guilaine, 2009; Lee Clare, 2010; Migowski et al., 2006; Pross et al., 2009; e.g., Staubwasser and Weiss, 2006; Weninger et al., 2009, 2006). These writers, referencing newer climate reconstructions, point to a “global climate event” occurring around 8200 BP. This event was a change in the thermohaline current system brought on by an influx of meltwater from the retreating Laurentide icesheet (Abrantes et al., 2012). Proponents of the Climate-Forcing Hypothesis believe it was the trigger that led to a reduction in the range of the Indian Monsoon, in addition to a rapid drying of the Eastern Mediterranean. These researchers postulate the drying to have precipitated a massive change to terrestrial ecosystems of the Eastern Mediterranean and that these ecological changes would have, in turn, massively affected Neolithic cultures of the time³.

² It is worth noting that the exact nature of these cobble layers remains contentious.

³ For example, Clare (2010) goes so far as to postulate that the climatic deterioration would have caused

In their view, this was not only the instigation for the terminal PPNB societal transformation in the Levant, it also spurred the first waves of Neolithic migration into mainland Europe.

Perhaps the biggest critique that can be leveled against the Climate-Forcing Hypothesis is not that climate-change *could not* have been a factor in the abandonment of the PPNB Megasites, but rather that it is *the causal factor* for the change. The main issue for the Climate-Forcing Hypothesis is that, while the date of the 8200 BP event is well established⁴, the exact timing of the PPNB-LN transition remains unclear. The timing and effect of the event in northern Jordan is confirmed by recent sedimentological and radiocarbon analysis of Dead Sea cores, which show a dramatic drop in lake-level beginning at 8200 BP—likely caused by a rapid decrease in the amount of precipitation falling in the Sea’s catchment (e.g., the Jordanian Highlands)—and lasting until about 7800 BP (Migowski et al., 2006). Weninger et al. (2006) attempt to show a positive correlation between the 8200 BP event and major changes in the occupational sequence of several sites in Eastern Mediterranean but can only do so if the radiocarbon chronologies are stretched to fit the model through vague justification about the possibility of “dates from old wood” or “time lag” between trigger and abandonment. The most current analysis of the radiocarbon evidence from Northern Jordan suggests that the PPN-LN transition occurred around 8500 years ago (see Chapter 2), which is 300 years *before* the 8200 BP event and thus clearly too early to have been caused by it (Maher et al., 2011).

Interestingly, the “8200 BP event” is not well expressed in the AMCM climate model used in this research (see Chapter 5, Section 5.4.2, and Figures 5.40 to 5.42)⁵. Minimal precipitation

wide-spread warfare and the rise of chiefs or “big-men”.

⁴ There is evidence for the “8200 BP event” in ice cores taken from the Greenland ice sheets, sediment cores taken from the Red, Dead, and Mediterranean Seas, and in pollen cores from various locations in southern Europe and North Africa.

⁵ The AMCM instead shows the largest drop in annual precipitation to have occurred between 9500-9200 BP—near the end of the MPPNB.

impact of the 8200 BP event in the southeastern portion of the Mediterranean basin is corroborated by other GCM paleoclimatic reconstructions (e.g., Brayshaw et al., 2011), and it has been suggested that the impacts of the 8200 BP event were not globally uniform. Furthermore, both the AMCM and the model of Brayshaw et al. (2011) indicate that the early Holocene climate of the southeastern Mediterranean was never affected by the Indian Monsoon. If the major impact of the 8200 BP event was to the strength of summer rainfall, it follows that the event would have had a minimal impact in areas with minimal summer rainfall. Thus, this event was unlikely to have adversely affected people living in the Eastern Mediterranean in any case.

3.2.2. The Anthropogenic Catastrophe Hypothesis

The main premise of the Anthropogenic Catastrophe Hypothesis is that human-caused deterioration of the environment around PPNB sites was the main driving factor of the social transformation occurring at the PPN-LN transition. The hypothesis was first described in two publications in the late 1980's by Köhler-Rollefson (1988) and Rollefson and Köhler-Rollefson (1989), and elaborated in later publications by the same authors (Ilse Kohler-Rollefson, 1992; Ilse Kohler-Rollefson and Rollefson, 1990; Rollefson, 1997; Rollefson and Ilse Kohler-Rollefson, 1992). Their hypothesis derives mainly from evidence recovered during their excavation of 'Ain Ghazâl. One of the key pieces of data that inform their hypothesis is the diachronic pattern of the utilization of wood resources at 'Ain Ghazâl. Calculation of the amount of domestic fuel-wood, architectural wood, and the fuel-wood needed for plaster production yielded very high numbers that seemed to Rollefson and Kohler-Rollefson to have been completely unsustainable in the long-term. The evidence they uncovered from the PPNC layers at 'Ain Ghazâl seemed to support this idea; the wood used for architectural components was becoming scarcer, and posts, beams, etc. were becoming smaller, the quality of plaster was declining, and there was evidence for the increased use of

small brush and dung as fuel in domestic hearths.

Kohler-Rollefson and Rollefson also saw evidence for localized environmental deterioration in the economic data recovered from 'Ain Ghazâl. Their interpretation of the faunal evidence (reduction in the amount of woodland species over time) suggested that the local hunting catchment was becoming increasingly deforested. The rapid increase in the proportion of domestic ovicaprids relative to wild species suggested the local pastoral catchment was under increasing pressure, and was likely become overgrazed. Citing the prevalence of pasture on slopes greater than 4% in the direct vicinity of 'Ain Ghazâl, they suggest that local denudation by ovicaprids would have led to widespread erosion of these slopes, which eventually bled over into the adjacent agricultural lands. Furthermore, they postulated that these early domestic herds were originally kept in a site-tethered pastoral system (animals return to the site every day or every few days), which, as herd sizes increased, created increasingly difficult-to-solve scheduling conflicts between pastoral and agricultural activities at the site.

In their view, these Anthropogenic pressures led to two significant outcomes: First, overgrazing—mainly by goats—led to a general suppression of woody vegetation that caused increased erosion and ineffective fallowing of farm fields, and thus eventual fertility-decline and reduced cereal-yields. Second, scheduling conflicts between agriculture and pastoralism—exacerbated by declining yields—eventually led to the need for long-distance seasonal pastoral movement, which in turn led to the development of a specialized pastoral component of PPNB society. In their model, the accrual of deleterious impacts to the local environment eventually made life in the PPNB towns untenable. More and more people left the towns to engage in specialized pastoralism in the steppe and desert regions eventually only using 'Ain Ghazâl as a temporarily occupied way station in their series of seasonal migrations. The Anthropogenic Catastrophe Hypothesis suggests that it is this lifestyle change that also accounts for the radical change in material culture and settlement pattern across the transition.

A major critique of the Anthropogenic Catastrophe Hypothesis has been the lack of targeted geoarchaeological assays of the extent of early Holocene erosion and soil fertility decline in and around the vicinity of the large PPNC sites; the only geological evidence presented in the original articles was anecdotal (e.g., references to “Neolithic cobble layers”. See Section 3.2.1, above.). Recent detailed analysis of depositional sequences in Wadi al-Hasa in central Jordan by Schuldenrein (2007) has confirmed that the Early and Middle Holocene was characterized by increased rates of erosion but Schuldenrein considers this erosion to be driven by tectonic changes in the Dead Sea rift and exacerbated by the overall wetter climate of that period rather than anthropogenic in nature. Furthermore, in a review of the archaeological evidence for landscape degradation at ‘Ain Ghazâl, Campbell (2010) questions Rollefson and Kohler-Rollefson’s assertions on the basis of a numerical model based on ethnographic data about subsistence farming practices. The results of Campbells’ model suggest that Neolithic subsistence could not have been intensive enough to cause serious degradation around the site. Finally, researchers such as Perevelotsky and Seligman (1998) and Barton et al. (2010b) have begun to rethink the idea of degradation itself. What has traditionally been seen as only a negative (e.g., overgrazing leads to vegetation deterioration, hillslope denudation leads to erosion of soils, etc.), can also be looked at as a positive (i.e., heavy grazing increases biodiversity in the ecosystem, erosion from hillslopes replenishes soils in valleys and plains, etc.). Thus, it is unclear if the environmental impacts of Neolithic agropastoralism would actually have been deleterious to the Neolithic subsistence system at all.

In response to these critiques, Rollefson and colleagues recently returned to ‘Ain Ghazâl and undertook a detailed sedimentological study of the stratigraphy in four the original test trenches, as well as limited geoarchaeological survey in the vicinity of the site and LiDAR surface modeling of the site itself (Zielh et al., 2012). Together, the four studied stratigraphic columns span from the MPPNC through the Chalcolithic (but missing the

Yarmoukian) occupation of the site and include instances of a “rubble layer” in three of the profiles. In order to differentiate between anthropogenic, alluvial, and colluvial depositional processes between the layers of the studied stratigraphic columns, a variety of analyses were conducted on samples taken from each layer including granulometry, lithology, magnetic susceptibility, carbonate content, pH level, total organic carbon content, and radiometric dating assays of carbonized materials. The rubble layers were found to consist of *ex situ*, but of local origin, fist-sized (4-6 cm diameter) stones, of overwhelmingly limestone lithology (limestone:flint ratio of 6:1), which differ significantly from other layers (which have a limestone:flint ratio closer to 1:1, and a greater variety of clast sizes). The clasts are not sorted, or imbricated, and they are surrounded by a matrix of fine silt, with little sand or clay. Local geoarchaeological survey could not discover any “rubble layers” in non-site contexts, even in topographically lower areas, and LiDAR surface modeling revealed no geomorphological evidence for substantial past gullying, landsliding, or mass wasting that could be responsible for the rubble layers. Interestingly, there is also some evidence for occupational surfaces (compaction, etc.) existing within the rubble layers, although there is no evidence for substantial architecture or other evidence of sustained human occupation (accumulations of artifacts or midden deposits) from these layers despite their thickness⁶.

These data suggest to Rollefson and colleagues that the rubble-layers are actually anthropogenic features, contradicting earlier assessments postulating deposition by natural process exacerbated by either or both of climatic change and human alteration of vegetation on nearby slopes (e.g., Rollefson, 2009; Weninger et al., 2009). Rollefson and colleagues cannot definitively characterize the exact anthropogenic process by which the layers were deposited, but they do rule out the possibility that they were caused by the collapse of abandoned buildings.

⁶ The PPNC rubble layer was found to be nearly 3 m thick, while the Chalcolithic rubble layer was found to be several meters thick.

It is my own supposition that these are likely to be deposits of fire-cracked rocks used for cooking in basketry in these pre-pottery towns, but this would need to be confirmed through detailed analysis of thermal alteration in these cobbles. In any case, Rollefson and colleague's reanalysis has also led to a new understanding of the chronology of these features. Radiocarbon assays and stratigraphic analysis showed there to be two chronologically separate rubble layers: Of the three studied rubble-layers, two date near the end of the LPPNB⁷ (one radiocarbon date of 8800 cal. BP), and the third dates from the beginning of the Chalcolithic (several radiocarbon dates between 7300 and 6400 cal. BP⁸). The dates contradict earlier suppositions that these layers dated to the Yarmoukian period (e.g., Rollefson, 2009). This idea was based on the discovery of abundant Yarmoukian potsherds in some of these rubble-layers at the site but the new analysis finds these sherds to have been secondarily deposited in the now-dated "Chalcolithic" rubble layer.

Two other interesting stratigraphic discoveries were also made during Rollefson and colleagues' re-analysis of the site's stratigraphy. Firstly, the team discovered evidence of localized slope erosion during the PPNB (evidenced by filled rills and colluviation) but of decreased erosion and relative soil stability *during and after* the PPNC (evidenced by increased rates of pedogenesis). This suggests that erosion actually *decreased* through the PPNB/C, which directly contradicts the central test implication of the Anthropogenic Catastrophe Hypothesis (i.e., increased erosion over time due to human impacts). The final new stratigraphic find was the discovery of a previously-unknown erosional unconformity underlying the Chalcolithic deposits. This suggests another period of erosion at the end of the Yarmoukian/LN occupation of the site, and indicates that erosion rates at the site fluctuated over time. Interestingly, none of the rubble features

⁷ Rollefson and colleagues interpret this date to be in the PPNC, but they are only using the sequence of dates from 'Ain Ghazâl, and not the regional chronology.

⁸ It is interesting to note that these dates place the third "Chalcolithic" rubble layer roughly contemporaneous to the last phases of occupation at Tabaqat al Bûma.

or erosional episodes at the site align with periods of climatic drying (e.g., the 8200 BP event), but instead seem to align with periods of relative wetness (as determined from the Dead Sea lake level record). Although the PPNB/C and PPNC/LN transition of the site do not line up with the largest dessication event (i.e., the 8200 BP event), Rollefson and colleagues suggest that they do align with smaller periods of aridity and so now support a climatic driver for these cultural phase-changes.

3.2.3. The Epidemiological Hypothesis

The Epidemiological Hypothesis is a relatively new hypothesis for the PPN-LN transition put forth by Goring-Morris and Belfer-Cohen (2010), who previously championed a climatic cause of the transition (see Section 3.2.1, above). The main premise of this hypothesis is that the new, densely populated, larger villages of the LPPNB combined with a closer association of humans and animals than ever before in human history to create an ideal environment for the rapid evolution and spread of disease. Goring-Morris and Belfer-Cohen also point to the decreased nutrition/increased labor requirements inherent to the new Neolithic lifeway and suggest that the LPPNB population was also more susceptible to infection by these new pandemic diseases. They suggest that LPPNB people, previously unfamiliar with pandemic disease, had not yet developed appropriate mechanisms for maintaining public hygiene in their villages and that accumulated trash middens, polluted water-sources, and general uncleanliness would have exacerbated the situation even more. They see some evidence for increased awareness of hygiene in the LPPNB (e.g., the presence of wells at Atlit-Yam, the frequent re-plastering of floors at LPPNB sites) but suggest that eventually these initial steps were inadequate to stem the spread of disease. The only option was to disperse from these densely populated LPPNB towns and to live in widely-separated hamlets and small villages.

A major critique of this hypothesis is that, while perfectly plausible, Goring-Morris and Belfer-Cohen provide no genetic or other paleopathological evidence that would confirm

the presences of early pandemic diseases in PPNB villages. They cite increased rates of multiple burials at some LPPNB sites as evidence for epidemic outbreaks but this is circumstantial at best. Until solid genetic and paleopathological evidence is found, the Epidemiological Hypothesis remains an interesting, but unprovable, hypothesis for the changes that occurred over the PPN-LN transition.

3.2.4. The Social Breakdown Hypothesis

Kuijt (2000b) provides a third alternative scenario of the PPN-LN transition. Others researchers have endorsed this idea (e.g., Simmons, 2007, 2000; Verhoeven, 2002) and have expanded upon it. In the Social Breakdown Hypothesis, a new social paradigm emerged in the PPNB: the kin-based networks of earlier times were gradually replaced or expanded by social networks. These were grounded in other types of social bonds, economic ties, or by mortuary and other rituals. However, the Social Breakdown Hypothesis suggests that the organizational changes necessary to promote total group solidarity within the village did not occur concomitantly. Thus, there was insufficient means for governing the new social stresses that would inevitably stem from these nascent social relationships, as well as from things like population crowding, reduction in privacy, and loss of autonomous control of living spaces. In this scenario, these stresses eventually led to serious fragmentations in the social life of large LPPNB villages, that in turn led to a disintegration of late PPNB/C social structures and ritual beliefs. Proponents of the Social Breakdown Hypothesis do not dismiss environmental degradation (or climate change); they, in fact, embrace the idea. In the Social Breakdown Hypothesis, it is the *combination* of the new social stresses (and lack of social stress-relief) with increasing resource stress caused by mounting human-caused environmental degradation that led to the disintegration of the PPNB/C culture. The fragmentation of social bonds made it easier for individual families to leave the large villages (i.e., the social consequences of leaving were greatly reduced), and that as resource stress increased,

more and more families found it advantageous to move to smaller sites and to return to a more egalitarian, kin-based social organization system.

Proponents of the Social Breakdown Hypothesis point to the diminishing size and increasing fragmentation of interior domestic spaces, the in-filling of outdoor spaces at PPNB sites, changes in mortuary practices, and evidence of environmental deterioration (e.g., as in the Anthropogenic Catastrophe Hypothesis) to support this hypothesis. However, there is currently little evidence for the emergence of social inequality, hierarchy, or interpersonal violence that would likely have accompanied these suggested social changes and strifes. This lack has led some proponents of the Social Breakdown Hypothesis (e.g., Simmons, 2007) to place more emphasis on the environmental component of the argument, but all proponents of the Social Breakdown Hypothesis believe that the novel social stresses of life in the first large farming villages must have played some role in their eventual abandonment. While this scenario is indeed plausible, there is no clear reason why a reversion to a simpler lifestyle was the preferred choice at this time, rather than an escalation in social complexity as occurs at the end of LN/Chalcolithic.

3.2.5. The Settlement Reorganization Hypothesis

Finally, Banning (2001) provides a fundamentally different hypothesis for the impetus of the PPN-LN transition. Banning believes that shifting to a dispersed settlement system gave the people of the Late Neolithic many social, ecological, and economic benefits including less competition for, and easier access to, agricultural fields and pastures. Banning suggests that the shift would have spread agricultural risk over many ecotones and reduced conflict between agricultural and pastoral land-use—all without the need for fundamental impact to social and ritual institutions or drastic environmental degradation in the preceding period. If the first four hypotheses focus on internal or external “push” factors that could have *actively induced* change in the

LPPNB social or economic systems (i.e., *pushing* them towards a new way of doing things), then Banning's hypothesis focuses on a potent factor that could have *passively attracted* these same changes (i.e., *pulling* them towards a new way of doing things). Banning does not completely ignore push factors, however; he suggests that access to suitable grazing and farming land around the large PPNB sites became more constricted over time and that this likely led to scheduling problems between the agricultural and the pastoral components of the PPNB food production system. In many ways, Banning's narrative model of the PPN-LN transition can be looked at as an extension of the Social Breakdown Hypothesis, but one that emphasizes the potential benefits of settlement reorganization over the difficulties of life in LPPNB villages. Again, the main critique of this is that it is currently difficult to explain why dispersal was a better choice for LPPNB peoples than would have been intensification.

3.2.6. Summary and Critique of Existing Hypotheses

The preceding discussion has summarized the basic arguments for several of the leading hypotheses about the instigation of the PPN-LN transition, and it has provided some critiques of each. All are plausible to greater or less degree, but none are satisfactory. The most recriminatory critiques range from an over-emphasis on monocausal drivers to a basic lack of supporting archaeological evidence. The best of the existing ideas tie together multiple factors (e.g., environmental degradation *and* social stress) and take a long-term view (i.e., that these problems escalated over time). The implicit message is that there were some critical thresholds in social-strife or environmental-effects that the LPPNB socio-economic system eventually surpassed, but they all lack a basic theory that explains rapid change in a dynamic and recursive socio-natural system. Such theory exists, however, and the remainder of this chapter provides a discussion of how this theory can be applied to instances of rapid change in coupled human-natural systems in

general and to the PPN-LN transition in specific.

3.3. THE DYNAMICAL SYSTEMS APPROACH

Dynamical Systems Theory (DST) is a body of theory that has evolved out the work of researchers across a variety of disciplines (but particularly physicists, ecologists, and computer scientists) who, in the latter half of the 20th century, began to rethink previously accepted notions about the linear nature of natural phenomena (Kohler, 2012). They challenged the idea that the outcome of a series of stimulus events on natural systems could be accurately predicted, if only the “correct” equation were found. In other words, researchers began to question the validity of the quest for unified causal explanations. A reexamination of the linkages between stimuli and results, largely informed by the advent of computer-based simulation modeling, led to the idea of feedback loops and uncertainty; “predictability” was replaced by “emergent properties” as the epitomizing factor of natural systems (Lansing, 2003).

Complex Adaptive Systems (CAS) are a special subset of dynamical systems. The CAS concept is, in essence, a framework for investigating how the independent decisions and actions of individual components of a system, 1) self organize, 2) are dynamic and change over time, 3) interact to derive novel, unpredictable, emergent properties of the system, and 4) may adapt to work in the interest of the system as a whole (Miller and Page, 2007; Mitchell, 2009). The focus of CAS research has been to use alternative methods of analysis—particularly simulation with agent-based models—to understand these properties in a variety of complex systems, including human social systems, in a way that reductionism cannot achieve.

The type of CAS that are of most interest to archaeologists are “Socio-Ecological Systems” (SES)². SES are defined by Glaser et al. (2012:4) as “complex, adaptive system[s] consisting of a bio-physical unit and its associated social actors and institutions. The spatial or functional boundaries of the system delimit a particular ecosystem and its problem context.” Importantly, this means

that SES are “real,” tangible things, that exist in the physical world with distinct boundaries in time and space, and so can be observed and studied empirically. Thus, SES can be studied as regionally distinct analytical units (Bourgeron et al., 2009). This property is particularly helpful for archaeologists, who are accustomed to conducting research at regional scales.

Considerable debate exists about whether DST is truly an integrative or unified paradigm (Byrne and Callaghan, 2014; Manson, 2001, 2003; Miller and Page, 2007; Mitchell, 2009; Reitsma, 2003). This is, in large part, a consequence of the widely varying nomenclature employed by DST researchers. In addition to “Complexity Theory”, “CAS”, and “SES”, there is also “Resilience Theory” (RT), conceived by C.S. Holling (first described in Holling, 1973), popularized by two edited volumes (Gunderson et al., 2010; Gunderson and Holling, 2002), and which is frequently considered as intellectually distinct from DST. The RT approach may not be very well integrated with the CAS/SES approaches, but there is much methodological and conceptual overlap between them because both derive from similar early DST roots. More importantly to the research presented here, both are useful sources of ideas for a dynamical systems view of change in Human systems. In particular I use: 1) the interrelated ideas of the adaptive cycle, resilience, and “panarchy” (Folke, 2006; Gotts, 2007; Gunderson et al., 2010; Gunderson and Holling, 2002; Redman, 2005; Redman et al., 2009; Walker et al., 2006), and 2) the parallel ideas of critical transitions, catastrophic regime shifts, “tipping points”, “basins of attractions”, and alternative stable states (Abel et al., 2006; Folke et al., 2004; Kinzig et al., 2006; Lamberson and Page, 2012; Lansing, 2003; Scheffer, 2009; Scheffer and Carpenter, 2003). I use these, and other concepts in my discussion of change in non-linear systems in the following section.

3.3.1. Change in Non-Linear Systems

Because of their non-linearity, cause-and-effect logic is difficult to apply towards

understanding change in dynamical systems. There currently exists no integrative theory of change in these types of systems. There have been, however, some useful approaches to understanding how complex systems change over time. The RT idea of the “adaptive cycle” is one of these. Originally envisioned as a 2-D diagram (Figure 3.1a), it has since been expanded into 3 dimensions (Figure 3.1b) (Gunderson and Holling, 2002). It is a heuristic diagram for temporal change, with axes corresponding to system potential, system connectedness, and system resilience. The potential of a system is a measure of its capacity (customarily measured in terms of accumulated resources), the connectedness of a system is a measure of the amount of integration present in the system (typically viewed as the tightness of the coupling between elements of the system), and the resilience of a system is a measure of its ability to adapt to new conditions (generally understood as its flexibility or adaptability, and measured in terms of things like degree of specialization, etc.). The “figure 8” diagram of the adaptive cycle is formed as the state of the system proceeds through time in the 3-dimensional space of potential, connectedness, and resilience. Although there is an extensive literature about the adaptive cycle and its four phases, the most important concept is that system resilience fluctuates over time in roughly inverse proportionality to its potential and connectedness. RT suggests that systems can undergo rapid change when resilience is reduced and potential and connectedness are high. The system may then either re-emerge into a totally new niche¹, or remain in the same niche, but returned to its initial, less complex state (i.e., the system exhibits “boom/bust” temporal dynamics). This repeats over time, as the cycle stays in motion because, “there is a fundamental trade-off between being adaptive and being efficient” (Scheffer 2009:78). In other words, increased resilience can only be had at the expense of decreased potential.

Holling and colleagues have envisioned a system of interconnection between adaptive cycles at different scales, which they term “Panarchy” (Gunderson and Holling, 2002). The panarchy concept is a way of understanding the emergence

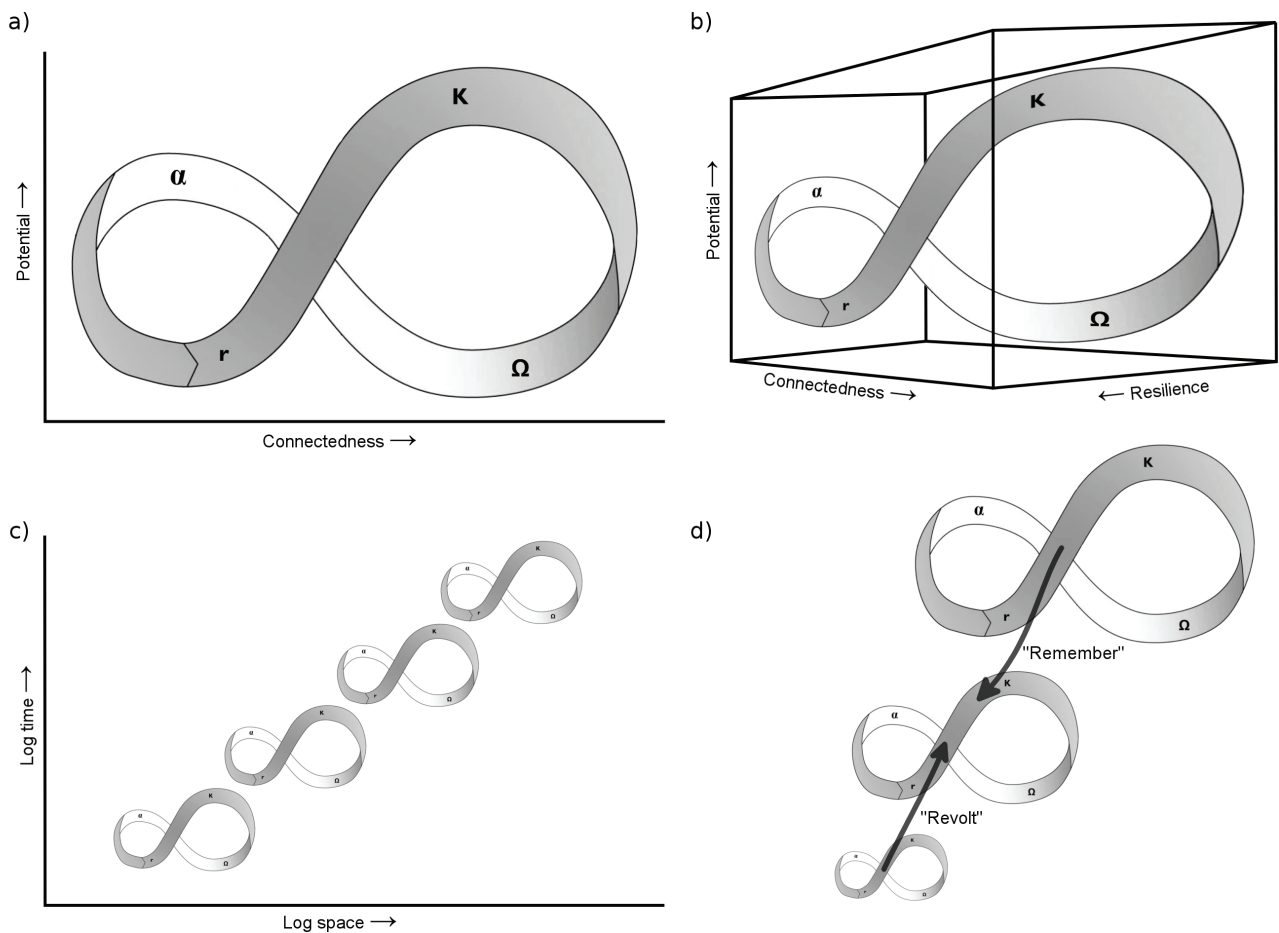


Fig. 3.1. Representations of adaptive cycles. A) 2-D representation of the adaptive cycle showing the four phases of Exploitation, Conservation, Release, and Reorganization. B) A 3-D representation of the adaptive cycle showing the relationship between potential, connectedness, and resilience during the different phases of the cycle. C) An illustration showing how different adaptive cycles can exist at different scales. D) An illustration of the concept “Panarchy” showing the connection (Remember, Revolt) between different scales of adaptive systems. This figure is a composite exemplifying concepts originally published by Gunderson and Holling (2001).

and feedback of hierarchically arranged systems from heterarchical processes. A main idea of the panarchy is that system components scale logarithmically as a function of time and space so that smaller adaptive phenomena (e.g., an individual or family group) exist as independent cycles within larger adaptive phenomena (e.g., a society) (Figure 3.1c). Each scale of adaptive phenomenon will have an areal footprint and a “cycle width” (length of time between boom/bust dynamics). There are two types of possible

feedback connections between adjacent scales, termed “Remember” and “Revolt” (Figure 3.1d). The important thing is that the panarchy hypothesis predicts a negative feedback (Remember) from larger, slower adaptive cycles to faster, smaller adaptive cycles, and a positive feedback (Revolt) from faster, smaller adaptive cycles to larger, slower adaptive cycles. These two forces are terms in a balancing equation that determines the stability state of the entire panarchy. Although conceptually simple, complexity is achieved as a function of the

differences in the cycle width of all the different scales of adaptive phenomena in the panarchy, and the relative alignment of the adaptive states of the adaptive phenomena at each scale. Thus, small-scale stability or growth can be maintained via large-scale “remember” feedback, even if local conditions should seem to require release and reorganization (e.g., individual families may maintain a subsistence lifeway out of tradition or greater social pressure). Conversely, larger scale system structures can change (in a potentially punctuated way) via an amalgamation of small-scale “revolt” negative feedback events in the subsystem (e.g., an accumulation of individuals/families making subsistence transitions), even if the larger-scale cycles were nominally stable.

To see how these ideas can be used to form an applied understanding of change over time in real systems, we can plot our expectations for change in system potential, connectedness, or resilience as a time-series (Figure 3.2) This plot can be used to help analyze/explain patterning in real time-series plots of various proxies for potential (e.g., population, number of farmed plots, crop yields, capital, infrastructure, etc.), connectedness (e.g., number of households in a community, heterogeneity of vegetation), and resilience (similar proxies as those for connectedness, but reversed metrics) over time.

Figure 3.3 shows a heuristic time-series graph of system potential over several sequential “boom/bust” cycles of an adaptive system. Starting from time t_1 , the overall amount of system potential can increase, decrease, or remain constant over time, depending upon the current balance of negative to positive feedback forces. If positive feedback outbalances negative feedback, then the system experiences net growth of potential and connectedness over time (though at the expense of resilience), resulting in a pattern of compounding success. If negative feedback outbalances positive feedback, then the system experiences net reduction of potential and connectedness over time (but regains resilience), resulting in a pattern of cascading failure. If the positive and negative feedback forces are well balanced between the various levels of the system (a phenomenon I suggest be called “Remain”), then the panarchy experiences

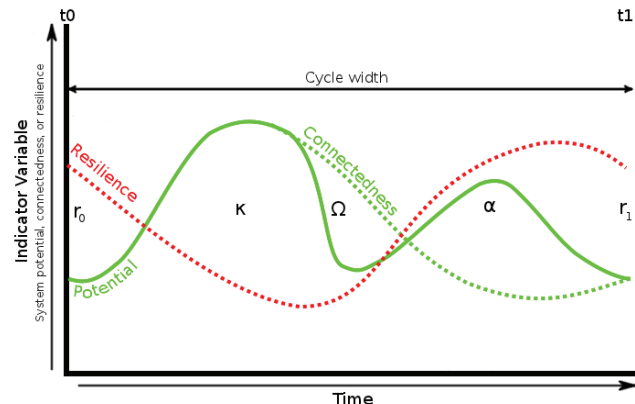


Fig. 3.2. The adaptive cycle plotted as a time series graph. The x-axis is time, and the y-axis is an indicator variable for system potential, connectedness, or resilience. The solid green line shows the expected pattern for system potential, the dashed green line shows the expected pattern for system connectedness over time, the dashed red line shows the expected pattern for resilience over time.

no (or insignificant) net change over time, resulting in a pattern of long-term stability⁹. It is important to note that at any time t , a new cycle begins, and the balance of the system can change. Thus, the trajectory from the system state at time t_1 to any of the possible system states at time t_4 is neither linear nor predictable, and it is impossible to predict which particular system state will be achieved at time t_4 . That is, given any set of initial conditions, there are multiple pathways to each possible system state at any later time, which is what makes the system “complex”. Furthermore, the contingencies of history matter in this scheme, in that the earlier pathways taken serve to limit the number and character of available future pathways. In other words, the probability of a particular system state being achieved at time t_4 varies greatly depending upon the pathways taken at times t_1-t_3 .

Feedback processes also can lead to punctuated change. Scheffer and colleagues (Folke et al., 2004; Janssen et al., 2003; Janssen and Scheffer, 2004; Scheffer, 2010, 2009; Scheffer et al., 2012, 2009; Scheffer and Carpenter, 2003; van

⁹ This is similar to the concept of “metastable” equilibrium in traditional systems theory (e.g., Butzer, 1982.)

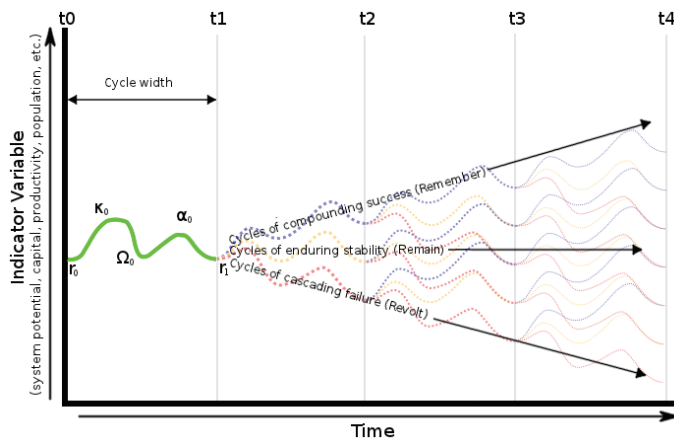


Fig. 3.3. Diagram of potential trajectories of an adaptive system over time. At any time t , a new cycle begins. Arrows indicate steady-state trajectories for continual Remember, Revolt, or Remain, but note that multiple pathways (combinations of Remember, Revolt, or Remain between any time t) could have been taken to achieve any of the potential system states at time t_4 .

Nes and Scheffer, 2005) center a DST approach to rapid system change – “critical transitions” around the idea of alternative stable states. Figure 3.4 shows three different patterns of system state change to major indexing variables. Figure 3.4a shows steady-state change where there is a linear relationship between the system state (y-axis) and some critical variable (x-axis). Figure 3.4b shows a more complex relationship between the system state and the critical variable, where change is more rapid over some subsection of variable values, and less rapid in others. In this figure, the steeper zone of the curve is less stable than the flatter portions, but there is still a fixed relationship between the critical variable and the state of the system (i.e., if one is known, the other can be predicted). Figure 3.4c shows yet another relationship between the system state where there is a “zone of vulnerability” where two alternative systems states are possible for the same value of the critical variable. Scheffer and colleagues label this type of curve a “catastrophe curve”. The dashed portion of the curve cannot be traveled smoothly, so at critical points F_1 and F_2 , the system state jumps from one portion of the curve to the other (Figure 3.4d). An

important aspect of this type of curve is that even if the critical variable returns to its value from before the critical transition (e.g., point F_2), the system remains in the alternative system state, and will remain there until the other critical threshold is surpassed (e.g., point F_1). In fact, it is possible for the system to enter into a cyclical recurrence between these two stable states as the critical resource varies between the two critical thresholds, which is called “hysteresis” (Scheffer, 2009).

Scheffer and colleagues use another heuristic – the “stability landscape” – to provide more detail on this phenomenon (Figure 3.5). A stability landscape is a graph where the slope of the line represents the rate of change (Scheffer, 2009). Thus, if the slope

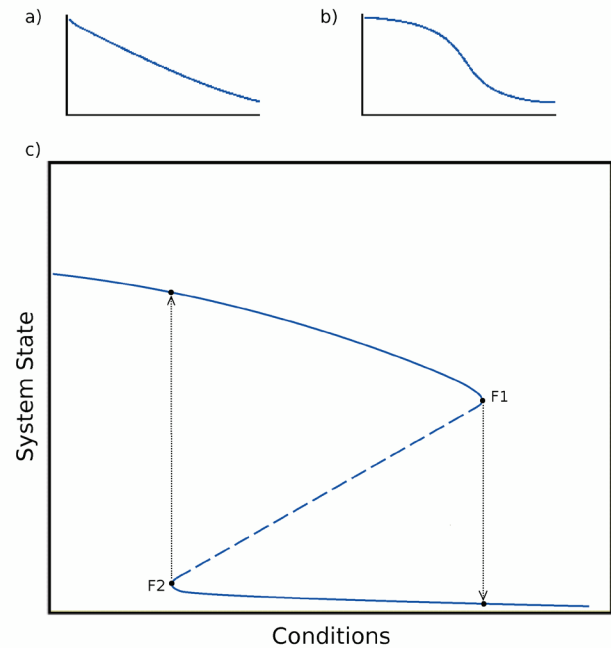


Fig. 3.4. Diagram of different types of system state change. The line in (a) represents linear steady-state change over time. The line in (b) represents a more complex pattern of change, where change occurs more rapidly under certain ranges of conditions. The line in (c) represents a system with a “critical transition”, and (d) shows an example of this type of transition in an SES. Modified from Jensen and Scheffer (2004) with permission.

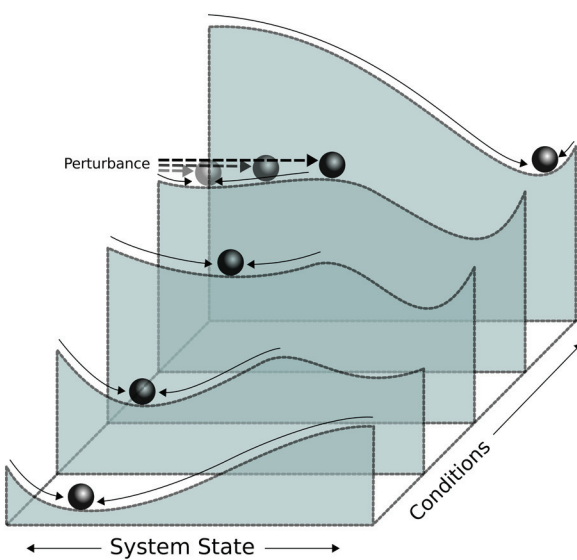


Fig. 3.5. A time series of “stability” landscapes crossing over a critical transition point.

Note that initially there is only one attractor (stable state), but as the system is stressed, another attractor develops. When the system is stressed past the critical threshold (F_2), it is pulled to the second attractor, and a new stable state is achieved. The depth of the “basin of attraction” indicates amount of system resilience. Reproduced from Scheffer and Carpenter (2003) with permission.

is zero, the rate of change is zero. Scheffer uses the analogy of a “ball in a cup,” such that if the stability landscape is concave, the ball will always fall to the bottom of the “trough.” Such troughs can thus be thought of as “basins of attraction,” or, more formally “attractors.” Attractors are essentially the stable state of the system under a specific set of conditions (i.e., the conditions that set the current stability landscape). Where the stability landscape is convex, the ball will always fall away from the “peak.” Such peaks can thus be thought of as “repellors.” If conditions are such that there is only one stable system state, there will be only one attractor (or none at all) on the stability landscape. In the case of two (or more) possible stable system states, then there will be two (or more) attractors, separated by a repellor. Thus, if the perturbation is large enough to overcome the force of the separating repellor, it is possible for the system state

(the “ball”) to fall into one or the other attractor. It is this dual attraction and repulsion that results in the rapid pace of change across critical transitions.

Furthermore, the width and depth of the “basins of attraction” can be thought of as measures of the system resilience under the given conditions (Figures 3.5 and 3.6). Thus, a deep, wide attractor is highly resilient, and even large perturbations will not “knock the ball out of the cup” (Figure 3.6a). However, a shallow, narrow attractor is highly vulnerable to change, and a relatively minor perturbation may be sufficient to induce system state change (Figure 3.6b). This is exemplified in Figure 3.5, which shows a series of stability landscapes for different positions on a “catastrophe curve”: as the system nears the critical transition point (F_2), the resilience of the original attractor reduces, and the amount of perturbation required to switch to the alternate attractor lessens. Related to this, systems that are vulnerable to critical transitions are also characterized by higher degrees of subsystem homogeneity and connectivity (Scheffer et al., 2012) (Figure 3.7). Ironically, these homogeneous and highly

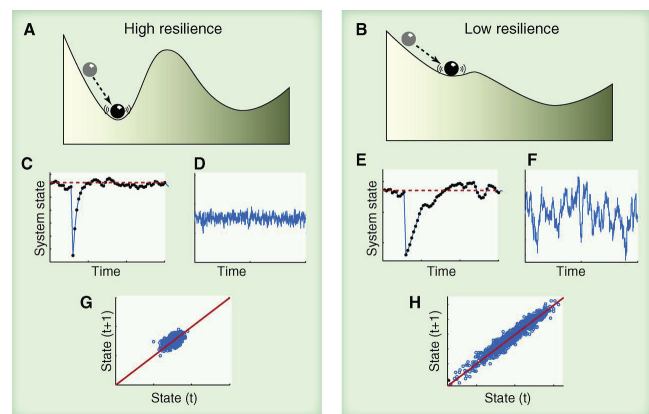


Fig. 3.6. Heuristic graphs showing the time-series indicators for a “stable” system (a) and for a system that is approaching a critical transition (b). The unstable system is characterized by a loss of resilience (“shallowing” of the basin of attraction), which is visible in the time-series graph as a larger degree of variation and stochasticity over time. Reproduced from Scheffer (2012) with permission.

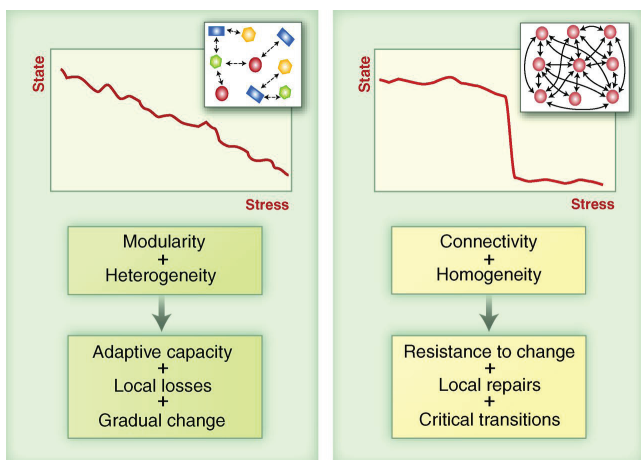


Fig. 3.7. The differences in system connectivity and heterogeneity between steady-state change (continual revolt, remember, or remain) and rapid change (critical transitions). Reproduced from Scheffer (2012) with permission.

connected systems are actually more stable in the short-term, as they continually act to resist change until the critical threshold is surpassed.

Scheffer and colleagues have recently begun to examine what they call “early warning signs” that indicate that a system is approaching a critical transition (Scheffer, 2010; Scheffer et al., 2012, 2009), and some of these warning signs these are of particular interest for analyzing archaeological data and model output. Firstly, systems that are at risk for a critical transition will exhibit slower recovery after a minor perturbation than will highly resilient systems. This will be observable on a time-series plot of system state (e.g., system potential) as difference in the slope of “recovery lines” after a reduction in system potential (Figure 3.6, c and d). Resilient systems will have very steep recovery lines (Figure 3.6c), and systems at risk for critical transitions will have less steep recovery lines (Figure 3.6d). Secondly, the system state of highly resilient systems will be less variable over time than will systems at risk for a critical transition. This is also observable on time-series plots of system potential (Figure 3.6, e and f), where the variation in system potential in resilient systems will have higher amplitude and be more stochastic (Figure 3.6e), and the variation in system potential in at-risk systems will be more regular and have lower peak amplitudes. Finally,

related to the idea that at-risk systems have higher connectivity and homogeneity, at-risk systems should appear to “resist” adaptation in the face of changing socio-environmental conditions. Thus, at-risk systems should show a disparity between the pattern of change on a time-series plot of system potential compared to the pattern of change on a times-series plot of key environmental variables (Figure 3.6h), while the patterns should be correlated in highly resilient systems (Figure 3.6f).

3.3.2. Are There Alternative Stable States of Human Subsistence?

Before using these to draw insights into the PPN-LN transition, a more fundamental question must be answered: Can CAS theory actually explain the variability in human subsistence strategies? The tendency in anthropology in recent decades is to view human variation in terms of continua or unsegmented fields of variation (e.g., Binford, 1980; Feinman and Neitzel, 1984; Kelly, 1995, 1983). But, if viewed from a DST perspective, we would expect that the unique socio-natural conditions of particular subsistence activities would tend to push societies engaging in them into similar adaptive milieus. That is to say, there would be multiple stable and non-overlapping human socio-economic “system states”.

Together with colleagues, I recently undertook an analysis of world-wide ethnographic data (Ullah et al. 2015) in order to see if this test implication holds true. In the analysis, we saw interesting clustering of societies highly suggestive of the attractor/repellor phenomena. We also saw that the clustering was largely controlled by a small number of highly important variables, such as resource density, mobility, and population size. When we parsed the dataset along gradients in some of these variables, we noticed that the clustering changed in interesting ways. We discovered that changes in these variables brought some attractors closer together, created new ones, or eliminated others. That showed us that even though the general possibilities for human subsistence is largely governed by a small number of highly important variables, moving from one subsistence

attractor to another is more possible under some socio-environmental conditions than others.

This analysis suggests that discrete subsistence strategies *do* exist in human subsistence behaviors, meeting the expectations of DST for the existence of multiple stable states centered on attractors and separated by repellors, and validating the idea that a series of discrete subsistence behaviors should be modeled (rather than a continuum). Furthermore, it shows that subsistence phenomena pattern at multiple scales, aligning with the idea of Panarchy, and suggesting that panarchical relationships may exist across multiple scales and types of SES. At a macro-scale, societies focusing on hunting and gathering are distinctly separated from those engaged in herding or agriculture, and these latter two are also separate from each other. At a finer scale, there are adaptive milieus related to specific types of agriculture and herding (and also likely for different types of hunting/gathering too). Each of these identified clusters is defined by a unique suite of subsistence behaviors, which vary only within a small range of options. While individual behaviors might be present in more than one cluster, the total combination of behaviors that define a cluster are unique and do not overlap. In other words, although each individual basin encompasses a zone of variability *within* each subsistence strategy, there is no “continuum” of subsistence variability *between* each strategy.

The attributes of the particular resource-type that a society focuses on appears to place limits on the variability of its subsistence endeavors to a particular sphere of behavioral choices. These spheres thus do appear to act as “attractors” (*sensu* Scheffer [2009]), drawing in and holding groups within them, and a major change in the system state is necessary for a group to escape from its current sphere. Such change can come from many sources including external influence, technological advancement, social change, evolutionary change, environmental change, climate change, or any combination of these. “Escaped” groups cannot exist in the space between spheres for very long, however, as these “in between” spaces constitute zones of highly unstable behavioral suites, which act as “repellors”. Thus, groups that exit a

particular basin of attraction due to perturbation will tend to be very quickly pulled back into one of the “attractors” in a classic “critical transition”.

3.4. A DYNAMICAL SYSTEMS HYPOTHESIS FOR THE PPN-LN TRANSITION

If human societies are, indeed, Complex Adaptive Systems, then we ought to be able to use DST theory to derive test implications for when human systems ought to undergo change, and in this section, I will do so. I start with a narrative sketch of Neolithic farming communities as components of panarchical regional SES. This sketch will help to narrow down the particular test implications that are relevant to understanding the nature and causes of major transformational events such as the PPN-LN transition. Furthermore, the narrative will also help us better understand the scale complexity of the issue, and inform our choice of analytical techniques for a more quantitative analysis of the PPN-LN transition.

3.4.1. A Narrative DST Model of PPN Regional Social-Ecological Systems

Theoretically, the finest meaningful panarchical scale of the Neolithic SES (or any SES for that matter) is logically that of individual agents (which would include individual humans, animals, and plants). However, considering the resolution of archaeological and paleoecological data, the minimum analytical unit must be individual human households and landscape patches. Fortunately, this scale match much of the information known about Neolithic socio-economic organization, which likely took place at the level of the household in most places (see Chapter 2). There are a number of connections in place at this smallest scale of the Neolithic Panarchy. Each household is connected to a finite number of landscape patches, which are chosen according to a variety of preferences and needs related to subsistence tasks, and which have their own unique and dynamic properties. Thus, the household and its landholdings can be seen as a small-scale

autonomous “regional” SES in its own right, with a definable regional footprint (i.e., a “catchment”), and an observable adaptive “cycle-width.”

Households are connected laterally to each other, however, through social and lineage bonds, economic ties, and labor pooling. Likewise, landscape patches are connected to each other hydrologically through their positions in the drainage network of the region, and biologically as parts of a contiguous series of vegetated ecotones. Each patch or household will have a unique life-history, and a unique configuration of component properties, which can be the source of interesting consequences when amplified through these interconnections. The total intra-scale variability of households or landscape patches will, however, be limited by larger scale phenomena, such as regional cultural norms, level of technology, climate regime, species composition, or geological parent material. Some of these larger-scale phenomena may be in large part exogenous (e.g., volcanic eruptions, Milankovitch cycles, and invading armies), but many will arise internally as novel products of the heterarchical interaction of the smaller-scale system subcomponents.

However, novel variations exist within the range of variability that emerges from cross-scale interaction. For example, the exact temporal cycle-width and spatial scale at which each household operates will be determined by the size of each household (number of people), the basic needs of each person (e.g., per capita food requirements), the social and economic structure of the household (e.g., the subsistence system), and the state of the local environment (e.g., localized abundance or depletion of critical resources). Thus, similarly-sized households engaged in similar socio-economic practices would cycle through their adaptive life-cycles at similar paces, and act within similar spatial scales.

Each household SES is subsumed under the larger adaptive phenomenon of the “village” to which it belongs (and where its inhabitants physically reside). The combined land-use of all households in the village defines the spatial scale at which the village SES operates and interacts with the landscape (i.e., the village’s catchment).

The village cycles through the phases of its own adaptive life-cycle, which has a longer cycle-width than any of the individual households¹⁰. Thus, the cycle-width and spatial scale of the village is in part determined by the sum of all the system-states of its households, but the village can also be thought of as an autonomous regional SES in that the fate of the village is independent from any particular household (i.e., the total is greater than the sum of the parts).

Finally, it is possible to envision another, larger, scale of this panarchy, where multiple villages are connected into a regional network (e.g., tied by trade, pooled labor, marriage, ritual). This regional network is another autonomous SES, moving at an even slower cycle-width, and operating on an even larger scale, and is composed of all the villages of the network and their catchments. Again, the cycle-width and spatial scale of this largest-scale of the Neolithic panarchy is in part determined by the sum of its constituent villages, but it is independent of the fate of any one village.

3.4.2. Gradual and Punctuated Change in PPN Regional Social-ecological Systems

What are the cross-scale relationships that exist within this sketched Neolithic panarchy, and how do they relate to an understanding of the possibilities for change and stability in a Neolithic regional SES¹⁰? It is useful to begin by examining the timing of adaptive cycling in the different levels of the Neolithic panarchy. Starting at the household level, in a highly unconnected, resilient SES, there would initially be no uniformity of adaptive “cycle-width” between households, and households would not be synchronized in any particular adaptive phase. Thus, as long as higher-order structures do not emerge, the resilience of this SES remains high, the life-cycle of households would remain unsynchronized, and the success or failure of any one household would have little effect on the others or on the village as a whole. Material correlates of high resilience will be heterogeneity

¹⁰ Although I focus on the relationship between households in villages in this discussion, the relationship between villages and a regional network is analogous.

in household form (e.g., population size, house forms) and subsistence practices, and evidence of independence of households in terms of basic subsistence tasks or goods¹¹ (i.e., connectedness between households will be low). In particular, the household-level land-use strategies of this resilient village SES would be arranged in such a way that changes to the landscape patches used by an individual household would not greatly affect the productivity of patches used by other households. This could be due to specific land-management strategies (such as tenuring or extensive land-use), or due to inherited landscape characteristics (such as patchiness or high diversity). In this loosely connected village SES of unsynchronized households and unconnected landscape patches, the disruptive force of “revolt” from each autonomous household (and their associated bits of landscape) continually prevents the village from coalescing into a static identity, and it remains a flexible, highly adaptive SES. If the resilience of this SES decreases, however, the conservative force of “remember” will emerge at the level of the village (or regional culture-system), and will begin to act as a syncing mechanism, holding and extending the conservation phase of each household’s cycle so that they eventually appear to remain in phase with each other over the short-term (i.e., increasing overall synchronization in the panarchy). Here, “remember” may be a purely social force (e.g., an inherited set of beliefs about the “right” way to live), or may be a socio-natural force (e.g., an inherited state of environmental productivity, inherited resource surplus, inherited livelihood options, etc.¹²). In any case, one of the main ways that this conservative force is operationalized is by reducing the number of choices available to households, thereby increasing subsystem homogeneity (e.g., less variety in household form and subsistence practices), and increasing connectedness (e.g., households will begin to rely on pooled labor

11 It is important to note that this does not imply that pooled labor or sharing will not exist. It only implies that households will not need to rely on these things for basic survival.

12 This is equivalent to the idea of “ecological inheritance” used in Niche Construction Theory (Day et al. 2003; Laland et al. 2001, 1999; Odling-Smee et al. 2003).

or sharing). The force of “remember” from the village will increase if the village itself is in a conservation phase of its own adaptive cycle.

These relationships are “scale-free,” in the sense that they occur at every level of the panarchy. This means that a similar scenario exists between the scale of the village and of the regional village network. In a resilient village network, villages will be largely independent, and will not rely heavily on inter-village trade or regional labor pools. Villages will maintain relatively independent identities, perhaps reflected in local variation of artifact and building styles, ritual or mortuary practices, and economic practices. Farming and grazing catchments will not overlap (in space or time), and environmental impacts in one catchment will not (greatly) affect the productivity of others. Each village will have its own life-cycle-width, and the villages will not be in phase with each other as they proceed through the adaptive cycle. This loosely connected regional network remains highly adaptable, and the autonomy of each village prevents the regional network from solidifying into an overarching political framework (i.e., through the disruptive force of “revolt” from each of the villages). However, if village autonomy decreases, and the villages come to rely on each other in a more tightly connected system of trade or labor pooling, or if individual village catchments cannot remain independent, then the force of “remember” from the regional system can begin to act to align and synchronize them. Further, the strength of “remember” will increase if multiple tiers of the panarchy are aligned; if the regional network of villages is in a conservation phase, and a village is itself in a conservation phase, then the strength of “remember” acting upon an individual household in that village will be even stronger.

How might the balance of these cross-scale interactions change over time? The simplest and most basic way – and one that is common to all complex systems – is through the effects of stochasticity in the system. That is, there is always a chance that cycle-widths between and among the various scales of adaptive phenomena in the Neolithic SES may align simply due to random chance. If so the balance of “revolt” and

a “remember” might shift simplt due to chance occurrences. Stochastically-induced change would be largely unpredictable, and would be characterized by increase in system connectedness, coupled with a decrease in resilience. But, because the source of change is random, these could occur without an accompanying increase in system potential.

Another way to change the balance of the SES is through the interference of an external event. Examples of external events include climate change or an extreme weather event, an influx of migrants, an invasion by hostile groups, large-scale wildfires, introduction of exotic pests or species, or a volcanic eruption. The event would affect all households to a similar degree, which might work to “reset the adaptive clock” simultaneously for all of them. This would “artificially” induce a high-degree of intra-scale synchronization. The event need not be drastic or even extremely rapid to have this effect (especially if the SES was already developing reduced resilience), and there may even be significant lag-time between the onset of the event and its consequences. Further, the induced synchronization may not last over the long term, and the system may recover resilience as households and landscape patches reattain heterogeneity. Thus, in cases of external influence, there would be a fairly rapid transition to a more connected, less-resilient system following shortly after evidence of an exogenous event or regime change, and there need not be an accompanying increase in system potential.

However, a more interesting pathway to a shift in the balance of cross-scale dynamics could stem from the self-organizing nature of the system itself. In this scenario, the effect of history within the system acts to increasingly limit the subsistence choices available to households so that it becomes more and more probable that households will be doing the same types of things, at the same scales, in the same places, and at the same time¹³. What types of historical factors could so act to limit the choices available to people in the system? The scope of possible subsistence choices in an SES is largely

determined by the combination of social/cultural, technological, and ecological characteristics of the SES. Some of these are relatively constant factors (e.g., the amount of labor a person can exert, the amount of food needed for good nutrition, the dietary requirements of herd animals), some are dynamic and change over time (birth and death rates, climate, soil fertility and depth, cereal yields, fodder availability), and some could be variably constant or dynamic (e.g., factors that largely depend on human agency, such as cultural proscriptions on certain behaviors, systems of land tenure, ideas about work-ethic, ideas about sharing or wasting, etc.). The interplay between the dynamic and static variables—especially the interplay between ecological and social factors—can work to limit decision possibilities over time. For example, a newly-founded Neolithic SES in a pristine environment would likely have more choices available for the location of subsistence activities than one existing in an environment that has been used for a number of years and so has fewer “good” locations for subsistence due to depletions of soil fertility, erosion of topsoils, and reductions to fodder availability that have accrued over time. Thus, any human-caused environmental “degradation” need not be severe to have an effect on the resiliency of the system. Choices would be limited further if social or cultural conditions also were such that specific activities were not allowed or were socially unfeasible. In any case affected by such historical contingency, there would be a gradual increase in system connectedness over time, coupled with a general decrease in resilience and an increase in system potential.

These examples have shown three mechanisms for both gradual and rapid change in a regional Neolithic SES. But how might we know whether or not a system was at risk for change? First, it is important to realize that gradual or rapid transitions can happen at any time, at any scale, and to any individual component of the panarchy, but in a highly resilient system, they do so without affecting or being influenced by other components of the panarchy. Conversely, a vulnerable system is so connected that a critical transition in any of the system’s subcomponents

¹³ This aligns with the concept of “Path Dependence” as originally laid out by David (2007, 2001, 1993, 1988).

may cascade throughout the system.

It is this idea—synchronized change occurring at a regional level—that is of most interest for our DST approach to understanding the vulnerabilities of Neolithic agropastoral SES. How might this occur? Remembering that the disruptive force of “revolt” from lower scales of the panarchy affects the stability of the entire panarchy, we can imagine that as synchronization of the adaptive cycles of households increases, the disruptive force of “revolt” on the village—enacted as a household enters into a less-stable phase of its adaptive cycle—increases. If a sufficient number of households enter into an unstable phase in relatively rapid succession (which is more likely if household cycles are synchronized and connected), the concurrent disruptive force of all these “revolts” could be large enough to pull the village into an unstable state of its own. If other levels of the panarchy are also synchronized and highly connected, then this type of event could result in a “cascade” of rapid instability throughout the panarchy, both downwards from the village to other previously unaffected households, but also upwards to larger-scale adaptive phenomena in the panarchy such as the regional trade network (and perhaps even beyond). It is thus possible to imagine a lengthy period of apparent synchronization and stability within our fictive Neolithic panarchy, but where system resilience is greatly reduced, and so the entire system is at high risk for rapid and lasting change.

On the other hand, a highly synchronized system is also more vulnerable to outside disturbance. Thus, even if internal “revolts” fail to happen, a system that has become overly-connected and less resilient may be more easily “pushed” into a critical transition by an external event. If that event is very rapid and intense (e.g., rapid climate change, an invading army, an influx of refugees, etc.), then the chances that the system will cascade into a critical transition are increased.

What about resilient systems? If households and landscape patches remain unsynchronized (and thus less connected and more heterogeneous), then the disruptive force of any individual “revolts” are spread over a larger period of

time, and can be absorbed at the village level. In this case, individual households and villages in the regional network can succeed or fail independently depending upon the conditions of each subcomponent as an autonomous SES, and the risk of failure at the village level is not increased if some of its households have failed (i.e., because individual system components are not highly connected). If conditions are such that failures of subcomponents (e.g., households) begin to occur at an increased rate, the staggered timing of these failures means that the potential of the entire system simply reduces with each failure. Resilient systems are more resistant to external pressures as well. Each component of a loosely connected resilient system is free to adapt to new conditions in its own way, so there is less chance that even a relatively drastic external event would trigger simultaneous failure of all system components. Thus, a highly synchronized, tightly interconnected regional SES is at much higher risk for a large-scale critical transition than a non-synchronized, loosely connected one.

3.5. CHAPTER SUMMARY

In this chapter, I have shown how DST theory can provide a general theory for change in human subsistence systems. I then used DST to update, consolidate, and reformulate the existing ideas about the instigating factors for the PPN-LN transition into a new model, which showcases the multiple avenues for change in the Neolithic socio-ecological system. The model shows how stochasticity, external events, and internal historical contingency can act – together or separately – to change the balance of cross-scale dynamics in the regional Neolithic SES, and lead to a less resilient, more connected system that is at risk for major transformation. The transition could have been instigated by the internal socio-natural dynamics of the PPN SES itself, through a series of simultaneous “revolts” that resulted in cascading failure of the entire system¹⁴. The model

¹⁴ This scenario thus subsumes the “anthropogenic catastrophe”, “social breakdown”, and “settlement reorganization” hypotheses.

also shows how an external event could have “pushed” a relatively stable PPN SES into a critical transition that might not have otherwise occurred¹⁵. These two scenarios are not mutually exclusive, as an external event could have pushed an already-unstable PPN SES into a critical transition that was likely to happen anyway. It should also be noted that the magnitude of the external event in this third possibility could be much smaller than that needed in the second. Finally, the model also shows how the PPN-LN transition may not have been a true critical transition at all, but instead could have been the response of a resilient system to internal or external pressures that resulted in a relatively rapid decrease in system potential and connectedness over several decades (but in a way that was *not* a critical transition).

Which of these scenarios is most plausible for the PPN-LN transition in northern Jordan? The review of the archaeological record of the region in Chapter 2 and of the specific pieces of evidence supporting and contesting existing hypotheses in Section 3.2 (above) have provided only tantalizing snippets of evidence. The fragmented archaeological record is sufficient for a general reconstruction of possible Neolithic lifeways but has yet proven generally insufficient as a detailed source of information about past land

15 This scenario thus subsumes the “epidemiological” and the “climate forcing” hypotheses.

use dynamics, system resilience, synchronization, and homogeneity, or the exactitudes of regional chronologies and their connections with climate change events. Those snippets of evidence that do exist¹⁶ can be construed to support the idea that the resilience and scope of subsistence choices within the PPNB system were reducing over time, while its homogeneity, connectedness, and potential were increasing, but it is very difficult to understand how these characteristics pattern over time and space. The dynamics of ancient SES are not preserved, and so not only is it unclear exactly how vulnerable the PPN SES was to a critical transition by the end of the PPNB/C, we are also lacking an understanding of the processes and interactions that could have led to vulnerability or to resilience—to continuing long-term success or to a catastrophic failure and reorganization. The best method to use to facilitate and understanding of these issues is simulation modeling, which is the focus of the next chapter.

16 For example, the increased reliance on domesticates (and reduced use of wild resources), the technological effort spent increasing efficiency of harvest, and the increased standardization of tools suggests that system potential and homogeneity were increasing, but also indicates a restriction of subsistence choice, and therefore a reduction in overall system resilience. Also, the reduced variability of house forms, the infilling of open space in villages, the potential existence of community-bonding ritual activities suggest increased connectedness (although the proliferation of private storage facilities is somewhat contradictory to this).

CHAPTER 4

MODELING SOCIAL AND NATURAL PROCESSES

4.1. MODELING SOCIAL AND NATURAL PROCESSES

A first tenet of the simulation modeling approach in archaeology is that it should not attempt to “digitally reconstruct the past.” That is, instead of building a model of the Neolithic socio-natural system of Wadi Ziqlâb, a simulation approach should instead scientifically examine dynamics within a variety of *potential* PPN social-ecological systems. This is accomplished by creating a robust set of interconnected, but simplified, social and natural process models that reasonably simulate the way these processes behave in the real world. The modeling approach then dynamically and recursively interconnects them in a framework of a more complex “system” model. The resulting platform is a kind of modeling laboratory within which to run a series of simulation experiments about past socio-natural systems. The “modeling laboratory” used in this research was developed under the MedLand project, and so is known as the MedLand Modeling Laboratory, or MML (Barton et al., 2015, 2016).

A laboratory such as the MML cannot, and should not, encompass *everything* in the system it is meant to study, but rather should focus around a *minimal set* of components and connections that may be responsible for driving the major dynamics of the system (Kohler and van der Leeuw, 2007; Walker et al., 2006). In the case of the MML, this goal is the motivations for, and consequences of, Neolithic subsistence land-use over the long term. This section provides a brief overview of the scope of the MML, and a general outline of its workings. The remainder of this chapter will describe the inner workings of the model in greater detail.

4.1.1. Overview of the Mediterranean Modeling Laboratory

The MML is a combination of a DEVS-Suite (Kim et al., 2009) agent-based model of subsistence agropastoralism (“AP-SiM”) with a GRASS GIS (GRASS Development Team, 2016) Landscape Dynamics Model (“LandDyn”), connected by a third overarching custom software architecture, referred to as the Knowledge Interchange Broker (“KIB”) (Sarjoughian et al., 2015). The MML simulates non-irrigated subsistence cereal farming and site-tethered pastoralism and its connection to surface process dynamics (i.e., erosion and deposition, vegetation growth, and soil fertility) at a regional spatial extent and at an annual temporal scale (Barton et al., 2015). The KIB acts as both an interpreter and a messenger between the social and natural halves of the MML and also serves as a manager for the coupled agent/landscape simulations by explicitly modeling the interactions between AP-Sim and LandDyn. Using the KIB to model interactions within a hybrid model also provides the researcher with the ability to manage a number of disparities between the agent and environment subsystem models that are inherent to this kind of coupled modeling platform, including disparities of timing, structure, scale, and resolution (Mayer and Sarjoughian, 2007).

The agent-based component of the hybrid model (i.e., AP-Sim) is based on ethnographic data for village-based subsistence agropastoralism in the Mediterranean region (Al-Jaloudy, 2006; Corbeels et al., 2000; Gibbon, 1981; Hirata et al., 1998; Kamp, 2000; Kamp, 1987; Khresat et al., 2008; Khresat et al., 1998a; Kramer, 1980; Kramer, 1982; Nablusi et al., 1993; Nordblom et al., 1995; Shoup, 1990; Thomson et al., 1986; Thomson, 1987; Thomson and Bahhady, 1983;

Watson, 1979). It consists of two agent types: villages and households. Villages represent a collection of households and are responsible for sending information received from the KIB to the appropriate households. Household agents represent a family of agropastoralists acting as a cohesive unit. Household agents farm wheat and barley and raise sheep and goats to acquire food, which they require for survival and growth. The number of people represented by a household strongly influences what it can do. The maximum amount of land that can be planted and subsequently harvested is based on the percentage of each household that is available to do work. The desired amount of farmed land is also based on population, since the number of plots to be farmed by a household in a given year is based on the kilocalorie needs of that household and yield expectations based on the average yield of the previous year. The amount of grazed land is dependent on the number of sheep and goats possessed by a household. Households consume most of the farmed wheat and barley directly and use the rest as supplemental fodder for the goats and sheep. Sheep and goats also need to graze wild vegetation to round out their diet, and they provide households with additional kilocalories derived from meat and milk products. The yearly consumed kilocalorie need of each household is thus translated to a yearly gross farming kilocalorie need as the sum of wheat and barley kilocalories that will be directly consumed with those that will be used as supplemental fodder. Household birth and death rates change based on household need/kilocalorie yield ratios. If a household fails to meet its energy requirements, the probability increases that a household member will die and the probability of a new household member being born decreases. Likewise, if a household exceeds its energy needs, death rates decrease and birth rates increase.

The KIB is responsible for all data interchange between the DEVS-Suite-based AP-Sim and GRASS-based LandDyn. When a household agent requires information about a landscape patch, it sends a coordinate to the KIB, which then caches all such information requests from agents about each specific coordinate. The output from those

queries is processed and sent to the requesting household agent. After agents have formalized their subsistence plans, the KIB then relays these decisions as impacts at specific locations, and executes LandDyn scripts that appropriately modify land cover and soil fertility values and calculate the amount of erosion and deposition. This information is then used to update the digital topographic map as well as the map of soil depths. The newly updated maps of soil fertility, soil depth, land-cover, and topography are all then used by the agents to make new subsistence plans for the next year, creating a dynamic simulation of the consequences of yearly household-based subsistence decisions in a low-level Mediterranean agropastoral socio-natural system.

4.1.2 Comparison to Other Land-use Simulation Models

The MML belongs to a broad category of simulation modeling systems commonly referred to as Land-Use/Cover Change (LUCC) models. It is useful to examine the scope and goals of the MML in comparison to some of these other LUCC modeling systems. There are three essential components to any LUCC platform: a social process modeling engine, a natural process modeling engine, and a method of connecting the two.

An increasingly common social modeling engine used in LUCC is Agent-Based Modeling (ABM), and this is what the MML employs. ABM is a general modeling framework (or “mindset”, *sensu* Bonabeau [2002]) that allows for multiple independent entities that operate according to sets of decision-making logic in response to stimuli. ABM allows for “emergent properties” – phenomena that develop within the system over time and which could not be predicted at the start of the model run based solely on its input components – in the simulation, which cannot be included in other types of simulation modeling. For example, equation-based approaches often seek to simulate the general trends of systems via a single overarching numerical model. These models can and do produce emergent properties, but are limited in the *complexity* of

the kinds of emergent phenomena they can model (Bonabeau, 2002; Van Dyke Parunak et al., 1998).

The scale of ABM model complexity differs greatly between the various ABM LUCC systems, however. Many of the most socially-complex LUCC's (e.g., the "ENKIMDU" project (M. Altawee, 2008; John H Christiansen and M. R. Altawee, 2005; Wilkinson et al., 2007), and the "MASON Afriland" and "MASON Central Asia" projects [(Cioffi-Revilla et al., 2010, 2008, 2007; J Daniel Rogers et al., 2012)) explicitly track such things as life history (birth, growth, maturity, aging, and death), cultural biases (individual preferences), personal relationships (marriages, father or motherhood, membership in social groups), movements, and life requirements of individual human (and also sometimes animal) agents. These projects are focused on understanding the influence of social dynamics as opposed natural dynamics, and so have heavily parameterized their social modeling engines. Other LUCC platforms do focus on the natural dynamics, and so opt for extremely simplified social ABM implementations (e.g. the very rudimentary social aspects of artifact deposition in "CHILD" project (Clevis et al., 2006; N. M. Gasparini et al., 2006; Tucker et al., 2001) and the slightly more complex social interactions in the "CybErosion" project [Wainwright, 2008]). Still other LUCC's have attempted to create both complex social models and complex natural models (e.g. the "Village Ecodynamics" project (Kohler et al., 2007; Kohler and Varien, 2012; Varien et al., 2007). In all of these cases computational complexity comes at a price; all of these models are computationally intensive, take weeks or months to complete a single modeling cycle, and produce complicated results that are often difficult to interpret. A few LUCC projects have struck a middle balance, however, opting for a moderate level of both social and natural complexity (e.g., the LUCITA model [Lim et al., 2002], and the "Midwest LUCC" project [Evans and Kelley, 2004]), and the MML takes this route as well. This balance allows for reasonably complex LUCC simulation on standard desktop computers.

ABM model complexity is also related to the specific ABM modeling platform used. Several

of the most socially complex simulations use advanced ABM platforms like MASS (Ivanyi et al., 2007) (e.g., ENKIMDU), and MASON (Luke et al., 2005) (e.g., MASON Afriland and Central Asia) to achieve their complexity, while simpler LUCC platforms opt for simpler ABM engines like Swarm (Swarm Development Group, 1999) (e.g., LUCITA). Using an extant ABM platform offers several advantages, mainly in the reduction of programming efforts, a broad base of existing code, and a wider community of developers and researchers. An existing platform may not provide all the behavior desired or software extensibility required for the particular modeling goals of a LUCC project, however, so several LUCC projects have taken the step of coding their own ABM systems from scratch (e.g., Village Ecodynamics, Midwest LUCC, CybErosion). The MML takes a third route by incorporating an ABM system that is fully open-source and easily modifiable (DEVS-Suite [Kim et al., 2009]). This has allowed the development of custom agent behavior and software connections without the need to program an ABM from scratch.

Another difference between LUCC platforms is the scale of social agency. Some LUCC platforms model land-use decision-making at the level of the individual (e.g., ENKIMDU and CybErosion), allowing individuals to perform actions specific to their age, gender, role in society, or other proclivities. However, most platforms model decision-making at the level of the household, and the MML takes this route as well. This is because the household is the minimal economic unit in subsistence agropastoral economies, and most land-use decisions, labor pooling, and consumption occurs at this level (Barlett, 1980; Wilk and Rathje, 1982). Most platforms, including the MML, are also hierarchical, however, in that there are multiple levels of agency (e.g., households and villages) and certain decisions are only made at one level (e.g., the household) while others can only be made at a higher level (e.g., the village). For example, while basic subsistence motivations and decision-making may occur at the household-level, actual allocation of land, mediation of property disputes, and other higher-

level decisions are made at the village level.

Not all LUCC simulations are spatially explicit (e.g., HilleRisLambers et al., 2001), but land-use is by its very nature a spatially explicit phenomenon, and so a spatially-explicit modeling platform offers key advantages for LUCC. Most ABM frameworks are inherently spatial (e.g., Argonne National Laboratory, 2012; Wilensky, 1999), but typically only include rudimentary spatial processing capabilities, and so are not suitable for simulating spatial processes at the scale or accuracy needed for robust LUCC. Many agent-based LUCC systems incorporate ABM for the social aspects of the system (i.e., decision-making), but use a cellular model (CM. e.g., the use of raster data containers, “map algebra”, and cellular automata) for the physical aspects (i.e., “natural” process) of the system (Parker et al., 2003). CM are spatially explicit by their very nature, so are far better and more efficient simulators of spatially explicit processes than are ABM’s. The MML takes this “hybrid” approach, using an ABM for the social component of the modeling laboratory and a CM for the physical aspects of the modeling laboratory. Typically, such “hybrid” LUCC platforms incorporate custom-built CM spatial modeling engines (e.g., all of the aforementioned projects have built custom spatial modeling engines¹). Thus, many LUCC projects have had to limit the scope of their spatial engines, mainly due to the complexity of coding a geographical modeling platform from scratch. This takes the form of decreased spatial resolution in some platforms (e.g., the “Village Ecodynamics” project, which models the landscape at 200m resolution [Kohler et al., 2007]), whereas other platforms are limited in terms of complexity (e.g., allowing only a few layers of spatial data)². The MML, on the other hand, was developed to utilize

¹ Note, however, that the ENKIMDU model incorporated an existing agricultural landscape process model: the USDA’s “Soil and Water Assessment Tool”, or SWAT (Wilkinson et al., 2007).

² A special case is that of the CHILD project which has developed a custom spatial data model based on evolving triangulated networks that allow for both very high and very low spatial resolution to coexist in the same data model.

the powerful open-source GIS software platform GRASS (GRASS Development Team, 2016; Neteler and Mitasova, 2007a) as its spatial engine. Because GRASS has been optimized to efficiently handle massive amounts of cellular data, the MML can operate at much higher spatial resolutions³ and can include many layers of spatially mapped environmental information. This makes for more complex and rich physical modeling than would otherwise be possible on a basic desktop computer.

In order to properly simulate land-use “dynamics” (inter-system feedback over time) LUCC platforms require a means to connect their social modeling engine with their natural process modeling engine. In other words, the two systems must be bound together so that changes in one are “sensed” by the other. There are three ways to achieve this connection: “loose coupling”, “close coupling”, or “full integration” (*sensu* Goodchild et al., 1992). “Loose coupling” implies manual transmission of data from one module to the next. This is the typical workflow of most un-scripted GIS procedures, for example, and is not suitable for simulating processes that must be repeated many times. “Close coupling” means that individual modules are programmed such that the ending of one triggers the start of the other feeding its output to it directly and so on in a cyclical manner. “Fully integrated” implies that the entire system is programmed into a single software system. Although full integration typically results in faster model run-times and a more seamless user experience, due to the programming effort needed for full integration, most LUCC platforms are closely coupled modular systems⁴ where each part of the model is an independent software entity. While the MML is technically a “closely coupled” system, it employs a third, overarching software “wrapper” that controls module timing and execution, and thus obtains some of the aspects and benefits of a “fully integrated” experience from a modular set of software pieces (e.g., an easy-to-use GUI

³ Theoretically, sub-meter resolution is possible in the MML, but for most projects, 5-15 meter resolution provides the best compromise of accuracy to run-time.

⁴ But the “Village Ecodynamics” model is a fully integrated system.

interface, standardized I/O protocols, integrated command architecture, faster running speeds, etc.).

A final difference between the various LUCC platforms is the temporal scale at which they operate. Some LUCC simulations operate as true “discrete event” simulators, so that both social and natural processes occur at the times and temporal interval that is most natural for them (e.g., the ENKIMDU model), but most use a fixed “base” temporal interval. The specific interval differs between projects; some simulate land-use on a daily basis (e.g., CybErosion), while others simulate on a monthly or seasonal basis (e.g., LUCITA), and still others on a yearly basis (e.g. Village Ecodynamics). Such “fixed temporal base” LUCC platforms use different methods to resolve the effects of the simulated social and natural processes to the base temporal interval. Some amalgamate several “discrete events” that are internally simulated at higher temporal resolution (e.g., Village Ecodynamics), while others calculate the effects of modeled social and natural phenomena as averages or as a single equation parameterized to a certain temporal resolution (e.g., LUCITA). The MML uses an annual “base interval”, and uses a combination of both “discrete event” amalgamation (e.g., for individual farming and grazing plot choices, and for population growth) and time-averaged process equations (e.g., for landscape evolution, and for land-cover change) to achieve that resolution.

4.2. MODELING AGROPASTORAL SUBSISTENCE PLANNING IN THE MML

At the beginning of each simulation year, households must decide upon a subsistence plan consisting of the total amount of farming and grazing plots that they will need as well as the total amount of firewood they will need to gather throughout the year.

4.2.1. Choosing the Number of Farmed Plots

To determine the number of wheat plots (N_w) needed in the coming year, households use the following decision rules:

$$\text{Eq. 4.1. } N_w = \frac{(P_h \cdot F_w) + (P_h \cdot F_w \cdot p_s)}{\mu_w \cdot E}$$

Where, P_h is the current population of the household, F_w is the total amount of wheat needed for subsistence purposes [kg/pers.] (i.e., the “food wheat” needed per person), p_s is the “seeding proportion” needed for reseeding the next years’ crop [percentage of crop], μ_w is the average amount [kg/ha] of wheat that was grown on the plots owned by the household in the previous year, and E is unit-less “expectation” scalar that determines how conservative farmers are when predicting the amount of land they will need (as the value of E increases, farmers will try to plant more and more above the minimum needed to survive). Thus, the number of wheat plots is determined as the total amount of wheat needed by the household plus the extra wheat needed as seed crop, all divided by the amount of wheat expected to be produced from a typical plot.

In the model, barley is used only as supplemental fodder for ovicaprids. To determine the number of barley plots (N_b) needed in the coming year, households use the decision rules in Eq. 4.2. where, P_h is the current population of the household, P_{oc} is the number of ovicaprids per person (determined by the modeler, this should be based on the importance of pastoral products in the diet), DM_{tot} is the total amount [kg] of digestible matter needed by the average animal in the herd (the actual amount will vary based on the goat/sheep ratio, breed characteristics, and herd profile, as entered by the modeler), p_b is

$$\text{Eq. 4.2. } N_b = \frac{(P_h \cdot P_{oc} \cdot DM_{tot} \cdot p_b) + (P_h \cdot P_{oc} \cdot DM_{tot} \cdot p_b \cdot p_s)}{\mu_b \cdot E}$$

the proportion of the total diet of a herd animal that will be provided by supplemental barley foddering [percentage], p_s is the same “seeding proportion” used in Equation 4.1, μ_b is the average amount [kg] of barley that was grown on the plots owned by the household in the previous year, and E is the same “expectation” scalar used in Equation 4.1. Thus, the number of barley plots is determined as the total amount of barley needed as supplemental fodder by the herd owned by the household plus the extra barley needed as seed crop, all divided by the amount of barley expected to be produced from a typical plot.

4.2.2. Choosing the Amount of Grazing Land

To determine the number of grazing patches (N_g) needed in the coming year, households use the following decision rules:

$$\text{Eq. 4.3. } N_g = \frac{(P_h \cdot P_{oc} \cdot DM_{tot}) - (DM_{stub} + (P_h \cdot P_{oc} \cdot DM_{tot} \cdot p_b))}{\mu_g}$$

Where, P_h , P_{oc} , DM_{tot} and p_b are as in Equation 4.2 above, DM_{stub} is the amount of digestible matter [kg] provided by grazing the stubble of the wheat and barley fields owned by the household, and μ_g is the average amount [kg] of digestible matter that was grazed from all the patches exploited by the household in the previous year. Thus, the number of grazing patches is determined as the total amount of digestible matter needed by the herd minus the amounts of digestible matter obtained from stubble-grazing on wheat/barley fields and that obtained as supplemental barley fodder, all divided by the amount of digestible matter expected to be produced from a typical grazing patch.

4.2.3. Choosing the Amount of Firewood Gathering Patches

The number of firewood gathering plots (N_{fw}) needed in a given year is determined by the following algorithm:

$$\text{Eq. 4.4. } N_{fw} = \frac{(P_h \cdot F_{tot}) - F_{clear}}{W_i \cdot RC_m}$$

Where, P_h is the current population of the household, F_{tot} is the total amount [kg] of firewood needed per person per year, F_{clear} is the amount of firewood obtained during any new agricultural field clearances that occurred that year [kg], W_i is the intensity at which people gather wood [kg/m²], and RC_m is the number of raster cells per square meter (i.e., a conversion factor to scale the impacts to the current raster resolution). Thus, the number of firewood gathering patches is determined as the total amount of firewood needed by the household minus the amount they obtained during field clearances, all divided by the amount of firewood that will be gathered from each firewood gathering patch. It is important to note that firewood gathering differs from other activities in that there is no “average return” from the cells, but instead a “gathering intensity” that is determined by the modeler.

4.2.4. Simulating Farmer/Herder Knowledge Biases

It is important to note that in real life, farmers and herders would not have perfect knowledge of mean return rates from their farming and grazing plots. Memory biases (Koriat et al., 2000]; e.g., transience, absentmindedness, blocking, misattribution, suggestibility, bias, persistence, etc. [Schacter, 1999], and biases of estimation (e.g., errors of representativeness and availability, insensitivity to sample size and predictability, misconceptions of chance, biases due to retrievability of instances, imaginability, etc. [Tversky and Kahneman, 1974]), are always acting to prevent such perfect knowledge, and the model simulates this by randomly perturbing the actual values of μ_w , μ_b , and μ_g according to a

Gaussian function before sending them to the agents to be used in the decision algorithms.

4.3. MODELING THE LOCATION OF AGROPASTORAL SUBSISTENCE ACTIVITIES IN THE MML

Once each household has developed its subsistence plan for the year (consisting of the number of plots/patches for each type of subsistence behavior), they then must choose the locations of each of these patches. The model has a very simple “negotiation” algorithm, which sets the order in which land patches are chosen by each house and village. This essentially occurs in a “round-robin” system which loops through the list of households in each village, allowing each household to pick one patch in turn until all households have fulfilled their land requirements. The order of the households is randomized

each year, so that one particular household is not always getting the first choice of land patches. This system ensures every household has at least some high-ranked land cells in their possession in any given year⁵. In the case of multiple villages, each the households in each village choose separately from each other, and the household’s choices are constrained by the choices of households in villages that chose land prior to them. Like the order of households within villages, the order of villages is also randomized each year so that one village does not always get to choose first.

Land patches are chosen based on their “value” to the households. In general, households seek to minimize walking costs while maximizing

⁵ This is the default behavior of the model. The modeler can choose not to randomize the order of households each time, and to allow each household to pick all their land patches in one go (not round-robin). Doing so would assume some sort of social hierarchy (chiefly authority, for example) where households of “high status” get to pick first, and so may be appropriate in some modeling scenarios. Neolithic society is widely assumed to be egalitarian (Simmons, 2007), however, so I use the default randomization and round-robin routine in all the models presented in this research.

subsistence returns when deciding upon the locations of plots, and do so using a land valuation equation specific to a particular subsistence task. Thus in any given year, agent movement is governed by the balance of a unique series cost minimization and benefit maximization decisions, which provides a dynamic and constantly changing pattern of movement over time.

4.3.1. Choosing the Location of Farm Plots

For farming plots, households want relatively level land that has deep fertile soil, but which is not too far away from the village. Thus, farming value (FV) of potential plots are evaluated using the following equation:

Eq. 4.5.

$$FV = SV \cdot \left(\frac{(F+F_w) \cdot (SD + SD_w)}{F_w + SD_w} \right) - \left(\left(D_w \cdot \frac{D}{D_{max}} \right) + LC_{dval} \right)$$

Here, SV is a slope modification value (0° - 10° , $SV=1$; 11° - 20° , $SV=0.75$; 21° - 60° , $SV=0.25$; 60° - 90° , $SV=0$) that makes lower slopes more valuable than higher ones, F is the current soil fertility value [percentage] (scaled 0-1), F_w is a weighting factor for soil fertility in the decision algorithm, SD is the current soil depth [m] (scaled 0-1), and SD_w is a weighting factor for soil depth in the decision algorithm. The maximum soil depth needed for full yields is 1m (Carter et al., 1985; Christensen and McElyea, 1988; Rhoton and Lindbo, 1997; Sadras and Calvino, 2001; Wong and Asseng, 2007), so for depths greater than 1m, SD is set to 1. D is the least-cost distance of the current cell from the center of the village, D_w is the least cost distance weight in the decision algorithm, and D_{max} is the maximum calculated least cost distance value on the least cost map. Finally, LC_{dval} is a land-cover “devaluation” coefficient such that the degree of devaluation of vegetation other than wheat/barley grassland is set according to a “graphing function” (a sequential series of boolean-separated linear regressions that approximate the results of a more complex regression function) parameterized by

breakpoints entered by the modeler. Adjusting LC_{dval} preferences farm plots with certain land-cover values essentially sets the fallow-cycle of the system (e.g., forest-fallow, bush-fallow, short-fallow, intensive agriculture, *sensu* Boserup [1965]). Thus, the left side of the equations estimates the general suitability of a plot of land for farming, and the right side estimates the costs to the agent if they were to farm that plot, and the equation balances to an estimate of the total “value” of a particular plot of land to agents from a particular village. This equation selects for deep fertile plots, but it scales the attractiveness of such plots based on their slope and reduces their value based on their distance from the village along the least-cost route and the amount of vegetation currently on the plot. It is also important to note that in the current simulations, agricultural plots are not tenured. Every year, agents simply farm the “best” (according to Equation 4.3) land parcels available to them, and thus, agents are free to drop a parcel of previously farmed land if they perceive that another parcel of land is better.

4.3.2 Choosing Grazing Patches

Once all of the households have chosen agricultural plots, they must decide on locations for grazing. For pastoralism, slope and soil attributes are unimportant when deciding upon grazing locations. However households do prefer grazing patches that have abundant fodder but which are not too far from the village (Oba, 2012). Thus, the grazing value (GV) of potential grazing patches is evaluated according to the following equation:

Eq. 4.6.

$$GV = \frac{(LC_w \cdot LC) + \left(D_w \cdot \left(1 - \frac{D}{D_{max}} \right) \right)}{LC_w + D_w}$$

Here, LC is current the land-cover value of a particular patch, which is proxy for the amount of available digestible matter (fodder) available in the patch, and LC_w is the weight of the land-cover

value in the decision algorithm. D is the least-cost distance of the current cell from the village [sec], D_w is the least cost distance weight in the decision algorithm, and D_{max} is the maximum calculated least cost distance value on the least cost map. In Mediterranean environments, slightly immature grassy open oak and pine woodland produces the largest amount of digestible matter, and digestible matter actually decreases as these woodlands mature into denser oak forests (Al-Jaloudy, 2006). To account for this, any LC value above 40 (which corresponds to these open grassy woodlands) are rescaled by a boolean function in descending order (e.g., 41 is changed to 39, 42 to 38, etc.) before being rescaled from 0-1 and entered into the equation. This equation favors patches of land with high fodder production but scales their attractiveness according to their distance from the village along the route of least accumulated costs. Thus grazing patches that have large amounts of edible vegetation, but which are very far from the village, are less attractive to agents than are grazing patches that have less edible vegetation but which are very close to the village. The actual number of cells chosen depends upon the total number of ovicaprids being herded and the stocking rates of these animals on the landscape. In our models, the total number of ovicaprids herded is linked to the village population by a ratio of animals to people determined *a priori* by the modeler at the start of each model run. This ratio stays constant during each simulation. Stocking rates are also determined by the modeler at the start of each model run, as is the ratio of goats to sheep (which determine the amount of fodder needed and the total kilocalorie output from the herd, based on its size in any given year).

4.3.3 Choosing Firewood Gathering Patches

Finally, households must meet their requirement for firewood. If households clear a plot of land for farming, they acquire an amount of wood equal to a proportion of the standing biomass of the plot, determined from the land-cover value of that plot at the time of clearance. Any additional firewood needed by the

household must be gathered from other parts of the landscape. The wood value (WV) of landscape patches is calculated by the following equation:

Eq. 4.7.

$$WV = \frac{LC + \left(D_w \cdot \left(1 - \frac{D}{D_{max}} \right) \right)}{1 + D_w}$$

Here, LC is the land-cover of a particular patch, D is the least-cost distance of the current cell from the village [sec], D_w is the least cost distance weight in the decision algorithm, and D_{max} is the maximum calculated least cost distance value on the least cost map [sec]. Land-cover values between 9 and 50 are rescaled from 0-1 before being input into the equation. Land-cover values below 9 (which equate to grasses and non-woody shrubs) are deemed to not produce large enough pieces of woody material to make firewood gathering efficient, and so are set to 0. Typically, D_w should be set higher than 1 ($D_w = 3$ by default) because ethnographic research shows that distance is the primary concern when gathering firewood (Tabuti et al., 2003). Thus, the equation favors firewood gathering on those patches with the greatest amount of woody material suitable for firewood and that are also closest to the village. The amount of wood actually gathered depends on two things: the total amount of wood need per person, and the intensity of wood gathering.

4.4. MODELING AGROPASTORAL SUBSISTENCE RETURNS IN THE MML

The returns of subsistence activities will depend on the type of activity, the particular characteristics of how the activity is performed,

and the conditions of the plot that the activity is performed on. Each activity is parameterized at the start of the modeling run, and the MML calculates the returns of each type of subsistence activity at each cell based on these parameters and the conditions at the cell in a given year. These conditions are formed by both the location of the plot in the natural system (soil depth, erosion rates, and climax vegetation type) as well as previous human usages of the plot (reduction of vegetation, reduction of soil fertility).

4.4.1. Calculating Farming Returns

Wheat and barley returns (WR and BR , respectively) are measured in terms of kilograms of harvested grain, and are calculated according to the following equations:

Eq. 4.8. $WR = \frac{(PR_w \cdot SV \cdot Max_w)}{RC_{ha}}$

Eq. 4.9. $BR = \frac{(PR_b \cdot SV \cdot Max_b)}{RC_{ha}}$

Where PR_w and PR_b are the potential wheat and barley production rates of a particular plot (scaled from 0 to 1), Max_w and Max_b are the maximum wheat and barley yields possible under ideal conditions [kg/ha], SV is the slope modification value (as used in Equation 4.5), and RC_{ha} is the number of raster cells per hectare (in the model, the size for an individual farm plot is the same as the starting raster cell resolution). As suggested by Rhoton and Lindbo (1997) and Christensen and McElyea (1988), PR_w and PR_b are calculated as the average of three regressions against precipitation, soil depth, and

Eq 4.10. $PR_w = \frac{((0.51 \cdot \ln(P)) + 1.03) \cdot ((0.28 \cdot \ln(SD)) + 0.87) \cdot ((0.19 \cdot \ln(F)) + 1)}{3}$

Eq 4.11. $PR_b = \frac{((0.48 \cdot \ln(P)) + 1.51) \cdot ((0.34 \cdot \ln(SD)) + 1.09) \cdot ((0.18 \cdot \ln(F)) + 0.98)}{3}$

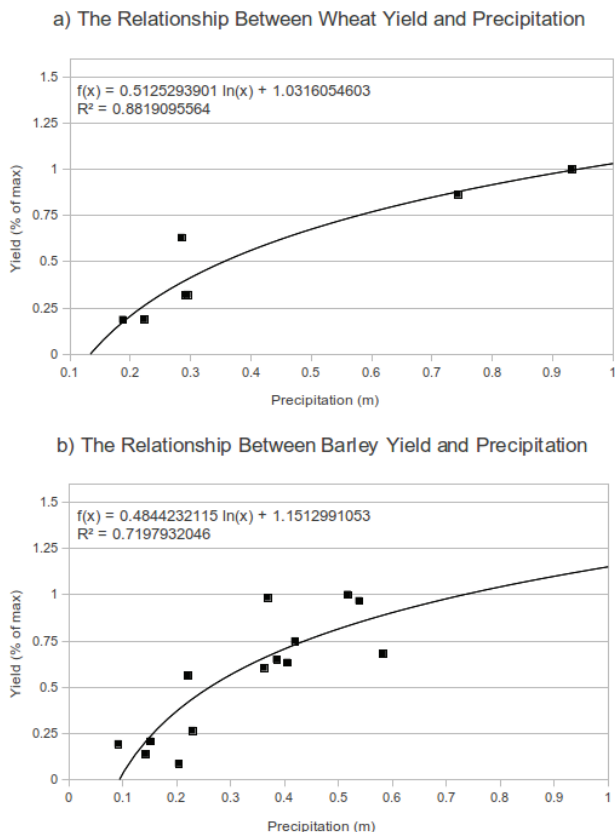


Fig. 4.1. The regressive relationship between precipitation and a) wheat yield, and b) barley yield. Data for these plots comes from Araus et al. (1997a, 1997b), Pswarayi (2008), and Merah et al. (2000).

soil fertility (Eq. 4.10. and Eq. 4.11., respectively)

Where P is the amount of annual precipitation (in meters), F is the current soil fertility value [percentage] (scaled 0-1), SD is the current soil depth [m] (as in Equation 4.5). The particular regression coefficients in Equations 4.10 and 4.11 derive from data presented by various authors. The regressive relationship between wheat/barley yield and precipitation was determined from data presented by Araus et al. (1997a), (1997b b), Pswarayi (2008), and Merah et al. (2000) (Figure 4.1). The regressive relationship between wheat/barley yields and soil depth was determined from data presented by Wong and Asseng (2007) and Carter et al. (1985) (Figure 4.2), and the relationship derived from these data also generally agrees with those presented by Sadras and Calvino (2001) (although these latter

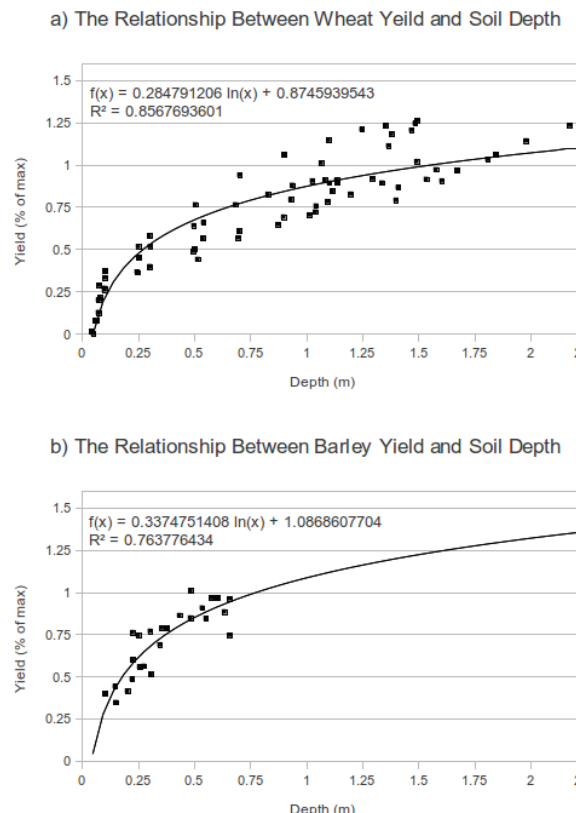


Fig. 4.2. The regressive relationship between soil depth and a) wheat yields, and b) barley yields. The data for these regressions comes from Wong and Asseng (2007) for wheat, and Carter et al. (1985) for barley.

data were not used to determine the regression). And finally, the regressive relationship between wheat/barley yield and soil fertility was determined from data presented by Barzegar et al. (2002) and Quiroga et al. (2006) (Figure 4.3).

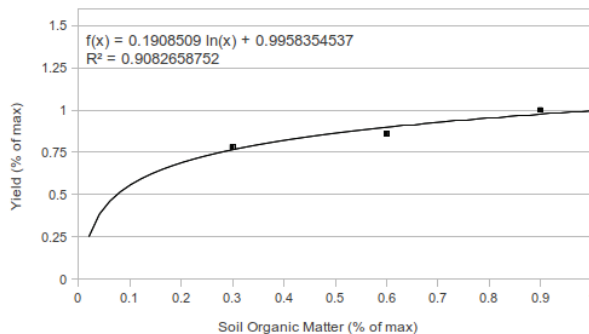
4.4.2. Calculating Grazing Returns

Grazing returns (GR) are measured in kilograms of digestible matter and are calculated according to a different logic than wheat and barley returns:

$$\text{Eq. 4.12.} \quad GR = \left(\frac{DM}{RC_{ha}} \right) \cdot G_i$$

Where DM is the amount of sustainably available “digestible matter” (edible biomass) in a

a) The Relationship Between Wheat Yield to Soil Organic Matter



b) The Relationship Between Barley Yield and Soil Organic Matter

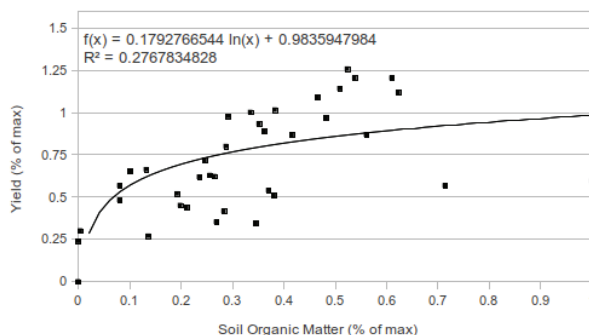


Fig. 4.3. The regressive relationship between soil organic matter (fertility) and a) wheat yield, and b) barley yield. The data for these regressions comes from Barzegar et al. (2002) for wheat and Quiroga et al. (2006) for barley.

patch [kg/ha], RC_{ha} is the number of raster cells per hectare (again, grazing patches are constrained to be the size of the current raster resolution), and G_i is a “grazing impact factor” (unit-less multiplier, allowing for “unsustainable” grazing practices). The value of DM for each cell is calculated by a “graphing function” (a sequential series of boolean-separated linear regressions that approximate the results of a more complex regression function):

Eq. 4.13.

```

if: 50 ≥ LC ≥ 40, DM = 800 - (10 · LC),
elif: 40 > LC ≥ 27, DM = (27.27 · LC) - 663.64,
elif: 27 > LC ≥ 4, DM = (2.27 · LC) + 38.64,
elif: 4 > LC ≥ 1, DM = (12.5 · LC),
else: DM = 0

```

Where, LC is the land-cover value in the 50-year succession regime of the model (coded 0-50).

4.4.3. Calculating Woodgathering Returns

Because wood is typically gathered at a set density at each patch (Karanth et al., 2006), firewood gathering returns (FR) are measured in kilograms of wood, and will be the same at each patch:

$$\text{Eq. 4.14. } FR = W_i \cdot RC_m$$

Where W_i is the intensity at which people gather wood [kg/m^2], and RC_m is the number of raster cells per square meter (i.e., a conversion factor to scale the impacts to the current raster resolution).

4.5. SIMULATING SOIL FERTILITY AND VEGETATION DYNAMICS, AND THE DIRECT IMPACTS OF SUBSISTENCE ACTIVITIES IN THE MML

Subsistence activities have both direct and indirect impacts on the land cells upon which they occur. Although there are many types of direct impacts that occur in the real world (e.g., terrace construction, pit digging, etc.), subsistence activities in the MML can only directly impact land-cover (vegetation) and/or soil fertility.

4.5.1. Modeling Soil Fertility Impacts and Dynamics

Soil fertility is tracked in the MML as percentage values, and fertility impacts and the fertility regain rate are both measured in percentage reduction to fertility. All soils start off in each model run at 100% fertility (see Chapter 5, Section 5.3.3), the rates of reduction and regain are set as constants at the start of the model, and the parameterization of the farming system will then dictate the pattern of fertility dynamics over time.

Farming⁶ a plot disrupts the natural connections between vegetation, soil, and nutrient flow that occur in natural vegetative communities, and so decreases the amount of nutrients (fertility) available in the soil by an amount that greatly depends upon the particular environment and the type of agriculture being conducted (Khresat et al., 1998a). Although any amount of annual fertility decrease *could* be modeled, experimental research on historical fields suggests that Mediterranean dry wheat/barely farming reduces the fertility of a plot by 0.5-1% each year (Bonet, 2004; Bonet and Pausas, 2004; Bonet and Pausas, 2007; Khresat et al., 2008; Khresat et al., 1998a).

The percentage of remaining soil fertility in a patch affects the farming returns from that patch (see Section 4.4, above), thus incorporating the feedback effects of soil-fertility change as a kind of indirect human impact. This system is purposefully kept simple in the MML, and thus, by adjusting the depletion and regain percentages, it is possible to model the net effect of many different systems of fertility conservation or depletion that would be too complex to model more specifically.

4.5.2. Modeling Vegetation Impacts and Dynamics

The successive regrowth of vegetation on cleared or grazed plots is a complex process influenced by several variables, including climate, topography, geology, phytogeography, and human and animal land-use, and not least, the nature and after-effects of the initial disturbance (Bazzaz, 1979; Huston and Smith, 1987; Turner et al., 1998). There are many existing succession simulation models (e.g., Keane et al., 2004; Usher, 1981), but most of the existing vegetation

⁶ At this point grazing has no directly modeled effect on soil fertility in the MML. Although it is conceivable that grazing may have some negative effect on soil fertility, these would likely be very small and indirect. Grazing likely does have positive effects on soil fertility, especially from the addition of organic matter and nitrates from dung whilst stubble grazing, and on water infiltration (Savory, 2013). These additions can in part be modeled in the MML by a change in the overall fertility regain rate on farmed or fallowed fields.

succession simulation engines attempt to address this complexity through a corresponding increase in complexity of model code (Gustafson et al., 2000; e.g., Pausas, 1999a). The vegetation succession dynamics engine in the MML, on the other hand, is a simple linear succession scheme – sometimes referred to as a “gap” model (Pausas, 1999b) – that allows disturbed patches to regrow through a series of successive stages of vegetation communities. Although Pausas (1999b) argues that gap models are overly simple for long-term vegetation dynamics simulation, the connection of the MML succession model to the human land-use surface process models adds much of the complexity Pausas argues for, without requiring it to be embedded within the vegetation model itself. The MML gap model is parameterized to the rates and form of vegetation regrowth noted on cleared fields in the Mediterranean region. Under ideal conditions, a completely cleared patch will regrow to mature oak woodland after fifty years (Bonet, 2004; Bonet and Pausas, 2004; Bonet and Pausas, 2007), and the rate of change from one plant community to the next is faster in the earlier stages than at the latter (i.e., a power law) (Casado et al., 1986; Debussche et al., 1996). Thus, the model has 50 successive stages⁷ organized so that the rate of successive vegetation community change slows over time (Table 4.1).

The actual rate of regrowth (V_r) in a patch (and thus the actual timing of the succession) depends upon the soil depth and fertility of that patch, and is calculated by taking the average of two power regressions via the formula in Eq. 4.15, where F is the current soil fertility [percentage fertility] of the patch and SD is the current soil depth [m] of the patch. The resulting regrowth rate scales between 0 and 1 according to a power law so that regrowth slows exponentially as the average of soil depth and fertility approach 0⁸. The

⁷ But note that not all parts of the landscape are capable of supporting climax Mediterranean forest (value “50” in the 50-year succession scheme). There is a “base” paleovegetation map (see Chapter 5, Section 5.5) that provides the “maximum succession” value for each patch, and the vegetation in that patch can never exceed that limit.

⁸ The maximum effective soil depth in the regression is 1m, and all deeper soils are truncated thusly for

Table 4.1. Table of vegetation succession stages in the MML vegetation dynamics model, and their corresponding vegetation communities.

Land-cover Type	Succession Stage (yrs)	Land-cover Type	Succession Stage (yrs)
Bare land	0	Moderately dense maquis and small trees	26
Very sparse grassland	1	Maquis and small trees	27
Sparse grassland	2	Sparse young woodland and maquis	28
Moderately sparse grassland	3	Moderately sparse young woodland and maquis	29
Moderate grassland	4	Young woodland and maquis	30
Grassland	5	Young open woodland and sparse maquis	31
Grassland with very sparse shrubs	6	Mostly young open woodland and very sparse maquis	32
Grass and sparse shrubs	7	Mostly young open woodland	33
Grass and moderately sparse shrubs	8	Young open woodland	34
Grass and shrubs	9	Young open woodland	35
Shrubs and grass	10	Young open woodland	36
Shrubs and moderately sparse grass	11	Moderate open woodland	37
Shrubs and sparse grass	12	Moderate open woodland	38
Shrubs and very sparse grass	13	Moderate open woodland	39
Shrubs	14	Maturing and moderate open woodland	40
Shrubs and developing maquis	15	Maturing and moderate open woodland	41
Developing maquis	16	Maturing and moderate open woodland	42
Developing maquis	17	Maturing open woodland	43
Maquis	18	Maturing open woodland	44
Maquis	19	Maturing open woodland	45
Moderately dense maquis	20	Maturing open woodland	46
Moderately dense maquis	21	Maturing open woodland	47
Dense maquis	22	Maturing open woodland	48
Dense maquis	23	Maturing open woodland	49
Dense maquis and sparse small trees	24	Fully matured woodland	50
Dense maquis and small trees	25		

$$\text{Eq 4.15.} \quad V_r = \frac{\left((-0.000118528 \cdot F^2) + (0.0215056 \cdot F) + 0.0237987 \right) + \left((-0.000118528 \cdot SD^2) + (0.0215056 \cdot SD) + 0.0237987 \right)}{2}$$

actual rate of regrowth (V_r) is in units of “ideal yearly succession change”, so that values of V_r less than one mean that vegetation recuperates at some fraction of the maximum possible yearly rate.

Grazing and wood gathering impacts act as a slow attrition of vegetative cover over time. As the returns of grazing are measured in kilograms of vegetation, it is easiest to assess their impact

these calculations.

in these same units (i.e., in kilograms of biomass removed). The rate of vegetation reduction by grazing in a patch varies according the value of G_i in Equation 4.12. In essence, G_i sets the “stocking rate” for the grazing catchment; higher stocking rates mean larger amounts of fodder are extracted from each grazing patch in any given year. All else being equal, this translates to a lower total number of needed patches each year, but also means that the

Table 4.2. Table of equivalences showing between MML vegetation community/succession value and above-ground biomass (kg/m^2). These equivalent values are used as breakpoints in the graphing function that converts between the two. Biomass values are determined from the averages of values reported by three independent studies in the Mediterranean region: De Jong et al. (2003), Rapp et al. (1999), and Terradas (1992).

Land-cover Type	Succession Stage (yrs)	Biomass Value (kg/m^2)		
		De Jong et al. 2003	Rapp et al. 1999	Terradas 1992
Grass with sparse shrubs	7	0.095	*	0.1
Maquis	18	0.729	*	0.6
Young Open Woodland	35	0.67	0.75	0.8
Mature Woodland	50	1.689	1.66	2.5

land-cover of grazed patches is reduced by a larger amount each time it is grazed. Firewood collection reduces each patch simply by the value of $W_i \cdot RC_m$ (Section 4.4.3 above), which is already in units of kilograms of biomass per square meter, and, unlike grazing, is the same for every patch in every year.

Agents can both graze a patch and gather firewood on that same patch in the same year, so the impact of the two activities is cumulative. Once the total amount of reduction to biomass from grazing and wood gathering is calculated, the impacts must be converted from units of biomass [kg/m^2] to an amount of reduction in units of “succession amount per year”, (i.e., the same units as V_r from Equation 4.15). This is done according to a graphing function, with equivalency breakpoints parameterized by data on average amounts of above-ground biomass for various vegetation communities in Mediterranean environments (as reported in Table 4.2).

Once the vegetation regrowth rate (V_r) at a particular patch is established, and the actual amount of biomass that was grazed away by ovicaprids and/or removed by wood gathering on the patch has been converted to succession units (V_i), the net change to the vegetation in the patch in that year (V_{net}) can be calculated according to the following formula:

$$\text{Eq. 4.16} \quad V_{net} = V_i + V_r$$

The next year’s land-cover map is created by

adding the map of V_{net} to the previous year’s land-cover map. If human impacts outpace regrowth, then V_{net} will be negative and land-cover will be reduced by V_{net} amount. If the human impacts in a patch are less than the regrowth/regain rate, however, V_{net} will be positive and vegetation will regrow by V_{net} amount until the maximum succession value for the patch is reached.

Farming, on the other hand, directly replaces native vegetation with “artificial” vegetation. In the case of the MML, the planted crops are wheat or barley both of which are annual grasses. Thus, the impact of farming a plot is simulated in the MML by directly changing the vegetation succession value of the plot to that of a pure, dense, grassland, which is “5”. Actively farmed plots are inaccessible for grazing or wood gathering⁹, but newly released farming plots become available to these activities again, and vegetation dynamics return to the governance of Equations 4.15 and 4.16.

The direct impacts of human land-use also have unintended consequences (indirect impacts), and so a series of feedback connections is built into the MML to account for these. Changes to land-cover will affect the amount of soil erosion or deposition that occurs. These changes to soil depths will, in turn, affect the rate at which vegetation regrows and the way agents value and choose parcels. Land-cover affects both the local conditions of soil detachment in a particular patch and the way water that flows through the watershed.

⁹ But note that the fodder gained from stubble-grazing and the wood gained from plot clearance is accounted for in the overall subsistence plan (see Section 4.2, above).

In order to connect the local “soil detachment protectiveness” of land-cover to the surface process equations (Section 4.7, below), an intermediate measure is required. In the case of hillslope processes, this measure is the “C-factor” of the RUSLE/USPED equations (Equation 4.18, below). C-factor is a unit-less measure of the capabilities of a vegetation community to protect from soil dislodgement and transport; specifically, it is the ratio of observed soil loss under a specific vegetative regime versus that under clean-tilled continuous fallow with all other variables held constant (Wischmeier and Smith, 1978). Thus, “real” local values of C-factor must be determined through empirical field experiments which is outside the scope of the current research. Fortunately, Wischmeier and Smith (1978), have documented C-factor for a wide variety of land-cover communities under a variety of specific local conditions, and it is possible to estimate a series of C-factor values for specific vegetation communities in the MML vegetation succession model (Table 4.3). These specific equivalences (i.e., the series of match succession values and C-factors) can then be used as breakpoints in a graphing function to estimate values of C for other succession stages.

The C-factor map thus created is entered directly into the hillslope surface process equation (Equation 4.18, below), and the value of C in a particular cell directly affects the amount of erosion or deposition calculated for that cell. C is not a variable in the other surface process equations (soil diffusion or streams), however, so the effects of vegetation must be accounted for in different ways. In the soil diffusion equation

Table 4.3. Table of equivalences between MML vegetation community types/succession stages and C-factor values.

Land-cover Description	Succession Stage (yrs)	C-Factor Value
Bare land	0	0.1
Sparse grassland	2	0.08
Grass with sparse shrubs	7	0.05
Shrubs and sparse grass	12	0.03
Maquis	18	0.01
Moderately open woodland	37	0.008
Fully matured woodland	50	0.005

(Equation 4.17), the effect of vegetation is encapsulated in the local environmental modifier term κ . There is no specific environmental term in the stream equation (Equations 4.19 and 4.20), however, and any local aquatic vegetation must be accounted for by the substrate erodibility term K_t .

Vegetation also affects the way water flows through the system by slowing water’s flow and thus affecting local infiltration and outflow rates. Because the process equations used in the MML were originally developed as 2-D models for use in predicting erosion/deposition on discrete landscape patches or stream-power over linear stream segments, they require the water influx rate to be calculated externally. Most hydrological models integrate the effects of vegetation on runoff by using cover-specific coefficients that account for vegetation’s ability to slow the force of flowing water (e.g., Krysanova et al., 2005). The most suitable measure of this that is used in the MML is the C-factor coefficient, but it cannot be directly translated. Instead, a map of “flow hindrance” is created from the map of C-factor by making a linear regression of C-factor to the percentage of water that will leave the cell. The regression is parameterized to so that a C-factor value of 0.005 (mature woodland) will only allow 10% of the water to exit the cell, whereas a C-factor of 0.1 (bare land) will allow 98% of the water to leave the cell. Then, the average amount of precipitation (see Chapter 5, Section 5.4), is multiplied by “flow hindrance” to create a map of “net flow contribution”¹⁰. The MML leverages the hydrological modeling capabilities of the GRASS module “r.watershed”¹¹, which accepts the map of “net flow contribution” to control the amount of runoff each cell contributes to the overall runoff map. It is this final runoff map that affects both the hillslope process

10 “Flow contribution” can also be thought of as “rainfall excess”, which is the hydrological term for the amount of rainfall that flows into the hydrological system (i.e., precipitation minus infiltration).

11 The “r.watershed” module also uses a “multiple flow direction” algorithm that produces much smoother and more realistic patterns of flow convergence and divergence than does a simpler “single flow direction” (also known as a “D-8”) algorithm (Wilson, 2012).

equation (value A in Equation 4.18) and the stream equation (value A in Equation A.1, which is used to estimate the value R in Equation 4.20).

4.6. MODELING POPULATION DYNAMICS IN THE MML

Although the MML does not track the life histories of specific individuals, it nevertheless includes a realistic simulation engine of demographic change. The base level of agency is at the household, and so this is also the base demographic unit. Thus, while the MML does not know if specific individuals have been born or died in a household, it does know how many people are alive in each household in each year. Household population changes according to a probabilistic function that balances the chances of a birth or a death in each year. These rates are determined by the ability of a household to feed all its inhabitants, so all subsistence yields from household farming and grazing must be tallied and compared to the total caloric need of the household's inhabitants. Yields must be converted to kilocalories for this comparison. Wheat is converted by multiplying the total kilograms produced on all plots farmed by the household by its caloric yield per kilogram. Calculating the caloric yield for pastoralism is more complicated. First, the fodder barley yield, the amount of fodder gained from stubble-grazing wheat and barley straw, and the amount of wild fodder grazed must be summed. The total amount of fodder then determines the actual number of animals that were fed (as opposed to the number of animals that the household *planned* to feed), by dividing it by the fodder need per average animal in herd (which is in turn determined by the herd composition ratio and the fodder requirements for each type of herd animal). Finally, the total number of animals fed is multiplied by the average caloric yield per herd animal to determine the total amount of kilocalories gained from pastoral products¹².

12 The caloric need per person, the caloric yield per kilogram of wheat, the fodder requirements of herd animals, and the caloric yield per herd animal type are all defined by the modeler at the start of the model run. See Chapter 6 for how these values are determined for Neolithic farmers and their domesticates.

Each household in the village starts the simulation with the same "average" birth and death "percentage probabilities"¹³, but then may begin to diverge from each other depending upon the recent history of subsistence success or failure of each household. If the subsistence plan of the household falls short of the household's needs (i.e., below a predetermined "buffer" of the total "by the numbers" household caloric need), the probability of a birth occurrence declines and that of death occurrence increases. If the subsistence plan meets or exceeds the household's needs, then the opposite occurs. The amount of increased or decreased birth or death probability depends upon the degree of over- or under-production, and the maximal rate of probability change allowed per year. Up to 15% over- or under-production induces an increase or decrease of half the allowable amount, 15-25% over- or under-production induces an increase or decrease of two thirds the allowable amount, and greater than 25% over- or under-production induces an increase or decrease of the full allowable amount, and birth and death probabilities can increase or decrease up to a predetermined maximum and minimum amount¹⁴. If the subsistence plan of the household provides just-adequate sustenance in a given year (i.e., *within* the "buffer" of the household caloric need), then the probability of a death or birth occurrence slowly returns to the initial "average".

An actual birth or death only occurs in a given year as a series of "random chance" operations. The total number of "random chances" is equal to the total number of people currently alive within the household. For each "random chance", a stochastically generated percentage value is compared to the household's current "percentage probability" for births or deaths respectively. If the random "percentage value" is less than or equal to the current birth or death "percentage probability", then a birth or death "occurs". The total number of "births" and "deaths" is then balanced, yielding the

13 See Chapter 6 for more information about Neolithic birth and death rates.

14 The maximum allowed yearly change to birth and death probabilities, and the total maximum and minimum birth and death probabilities are set by the modeler at the start of the simulation.

actual household population change for that year.

4.7. MODELING LANDSCAPE EVOLUTION IN THE MML

The landscape evolution component of the MML is executed by a single add-on script for GRASS, called “r.landscape.evol”¹⁵. The operation carried out by the script estimates the amount of elevation change due to erosion or deposition that would occur at each point on a landscape in a given year (i.e., a unique set of climatic, physical, and environmental conditions at an annual scale), and iteratively enacts these elevation changes over time (Mitasova et al., 2013). The script uses different process equations for different landforms and implements them in a manner that optimizes the ratio of model run-time to accuracy of erosion/deposition calculations.

4.7.1. Estimating Elevation Changes Due to Soil Creep

The module implements a diffusion equation for areas near drainage divides, a three-dimensional transport-capacity limited implementation of USPED for hillslopes and gully heads, and a transport-capacity limited reach-average shear stress function for channels.

The diffusion equation used by the MML is well-known and simulates “soil creep” – the movement of soil downslope due to the effect of gravity and particle movement from rainsplash, bioturbation, and other local factors – on portions of the landscape where there is not enough accumulated runoff for overland flow (Culling, 1965, 1963, 1960; Heimsath et al., 2002). The diffusion equation estimates the change in elevation (dz) directly:

$$\text{Eq. 4.17} \quad dz = \kappa \cdot \sin(\beta)$$

Where, κ [m/1000yr] is the diffusion coefficient

– an empirically-derived constant estimating the base-line soil-creep rate for different climate/vegetation regimes (Mitasova et al., 2015)), and β is the topographic slope [deg]. Thus, the value of dz is determined as a localized adjustment of κ , as scaled by the steepness of the local topography.

4.7.2. Estimating Transport-Capacity on Hillslopes

Sheetwash and rilling/gullying are both hillslope processes, and erosion/deposition deriving from these processes in the MML are estimated using the Unit Stream Powered Erosion Deposition equation (USPED), derived from concepts described by Kirkby (1971), adapted for two dimensional landscapes by Moore and Burch (1986), and operationalized in a GIS environment by Mitasova et al. (1996a). It is an adaptation of the (Revised) Universal Soil Loss Equation (USLE/RUSLE) to scales larger than a farm field, and for an increased suite of overland flow processes¹⁶ (Degani et al., 1979; Flanagan et al., 2003; Mitasova et al., 2001, 1996b; Renard et al., 1991; Renard et al., 1997; Singh and Phadke, 2006; Warren et al., 2005; Wischmeier et al., 1971; Wischmeier, 1976; Wischmeier and Smith, 1978). Although Moore and Burch (1986) referred to this approach as Unit Stream Power Erosion/Deposition, this name is somewhat misleading in the context implemented here, as the algorithm focuses on hillslopes, small watersheds, and

¹⁶ The USLE/RUSLE equation was developed as a tool for agricultural scientists to estimate the amount of erosion that would occur on a particular farm plot, given certain input conditions (Renard et al., 1991; Renard et al., 1997; Wischmeier, 1976; Wischmeier et al., 1971; Wischmeier and Smith, 1978). The *LS* factor of the USLE/RUSLE equation is essentially a way to estimate the erosive power (velocity) of running water across the farmplot, and is a combination of the ratio of the actual field length to the USLE experimental plot length (a constant) and a polynomial regression of the average slope across the entire plot. Although it is frequently used at landscape-scales, *LS* becomes increasingly meaningless as the scale of analysis increases. Substituting upslope accumulated area per contour width times the sine of slope for *LS* provides a valid way to include information about the erosive power of flowing water at these larger scales.

¹⁵ The r.landscape.evol GRASS addon script can also be used independently of the other components in the MML.

small channels (i.e., rills and gullies), rather than streams and is, in fact, *less* applicable to larger streams and rivers (Warren et al., 2005).

The USPED equation estimates the transport capacity (q_s) of flowing water at the cell, which is implemented in the MML as:

$$\text{Eq. 4.18} \quad q_s = R K C A^m \sin(\beta)^n$$

Where R is the rainfall intensity factor for the region [(MJ·mm)/(ha·hr·yr)] and is computed by an equation that combines monthly precipitation amounts (Renard and Freimund, 1994; Renard et al., 1997). Values of R vary from 0 with no theoretical upper limit (although a practical upper range could be said to be between 20 and 30 with values much above 30 highly unlikely under terrestrial conditions). K is a soil erosion resistance factor [(ton·ha·hr)/(ha·MJ·mm)] based on the percent of sand, silt, clay, and organic matter in the soil. K is scaled from 0 to 1 (i.e., “not erodible” to “highly erodible”). C is a unit-less vegetation erosion protection factor based on the overall ability of different vegetation to hinder raindrops and surface flow and to bind soil in place. C , like K , is also scaled from 0 to 1¹⁷. A is the upslope contributing area (flow accumulation per unit cell resolution) and β is again the topographic slope of the cell. The exponents m and n are empirically derived and vary depending upon the process being modeled¹⁸.

Implementing the USPED algorithm in a GRASS script combines GIS modules for calculating slope, aspect, and upslope accumulated

¹⁷ R , K , and C in Equation 4.18 are the K-factor, C-factor, and R-factor of the USLE/RUSLE, which have been calculated empirically for a variety of settings in the Mediterranean (Boellstorff and Benito, 2005; Essa, 2004; Hammad et al., 2004; Martínez-Casasnovas and Sánchez-Bosch, 2000; Renard and Freimund, 1994; Renard et al., 1997; Wischmeier and Smith, 1978). See Section 4.5.2, above, for more information about how C-factor is derived.

¹⁸ For sheetwash (flow accumulation large enough for diffuse laminar flow of water), $m = n = 1$, whereas for rill/gully flow (flow accumulation large enough for concentrated turbulent flow of water), $m = 1.6$ and $n = 1.3$ (Mitasova et al., 2001).

area using map algebra. Input data for the script includes a raster DEM of initial surface topography, soil erodibility (K-factor as a constant for uniform soil or a raster map for variable soil), vegetation cover (C-factor as a constant or raster map), and rainfall intensity (R-factor as a constant only). An underlying bedrock topography DEM is also input to provide a limit on the total depth of unconsolidated sediment that can be eroded¹⁹.

4.7.3. Estimating Transport-Capacity in Streams

For flow in channels, the MML estimates transport capacity as a function of shear stress acting upon the channel bottom (G. R. Foster et al., 1972; Howard and Kerby, 1983):

$$\text{Eq. 4.19} \quad q_s = S_e K_t (\tau)^\alpha$$

Where S_e is the annual number of storm events, K_t is a unitless transport capacity coefficient relating to the typical size of clasts in the channel (ranging from 0.001 to 0.000001, but typically 0.00001 for gravelly, sandy-bottom streams), τ is the shear stress [Pa = kg/m²], and α is an empirically derived exponent related to the type of transport in the channel (typically 1.5 for bedload, and 2.5 for suspended load).

Shear-stress is calculated according to the standard “reach-average” formula:

$$\text{Eq. 4.20} \quad \tau = g_w \cdot \tan(\beta) \cdot R$$

Where g_w is the hydrostatic pressure of water equal to $g \cdot p_w$ (g is the gravitational acceleration constant [9.81 m/s²], and p_w is the density of water

¹⁹ Bedrock topography is created by the r.soildepth.py script, which implements soil-depth modeling as described in Chapter 5, Section 5.3.1. In r.landscape.evol.py, when bedrock is reached, it is assumed that no discernible erosion will occur in the time spans being modeled. Therefore soil erodibility is set to zero.

[10000 kg/m^3]), β is the topographic slope [deg], and R [m] is the hydraulic radius of the channel. In a GIS with perfectly square cells, R is best estimated simply as the channel depth (h) [m] (See Appendix A, Section A.1 for the method of calculating h).

4.7.4. Estimating Erosion/Deposition Potential from Transport-Capacity

Both USPED and the reach-average shear stress equation only estimate the transport-capacity (q_s) of flowing water at each cell. In order to determine the net elevation change (dz) predicted by these methods, the MML first must compute erosion/deposition potential (ED_p) at each cell. To do so, it assumes that the system is operating at full transport capacity, and the divergence of q_s across the cells of a DEM in the downstream direction provides ED_p directly. In a GIS, this is done by finding the divergence in both the x and y directions (i.e., the two cardinal grid directions of a rectangular raster gridding system), and summing to find the divergence in the most downstream direction (Mitasova et al., 1996a, 1996b; Warren et al., 2005):

$$\text{Eq. 4.21} \quad ED_p = \frac{\partial q_s \cdot \cos(\alpha)}{\partial x} + \frac{\partial q_s \cdot \sin(\alpha)}{\partial y}$$

Where q_s is the transport capacity as calculated by USPED or the reach-average shear stress equation, and α [deg] is the topographic aspect of a cell.

4.7.5. Converting Erosion/Deposition Potential to Net Elevation Change

Transport capacity, and thus ED_p , is calculated in units of weight per unit area per year ([T/ha.yr] for USPED, and [$\text{kg}/\text{m}^2.\text{yr}$] for the reach-average shear stress equation). However, in order to iteratively model erosion and deposition across a landscape over time, the calculated values of erosion and deposition must be re-expressed as depth of sediment per cell [m]. This is done by multiplying ED_p by its areal units (hectares for USPED, square meters per cell for reach-average shear-stress

equation), and dividing by the unit density of the soil (p) [m^3] times the cell resolution (res) [m^2]:

$$\text{Eq. 4.22} \quad dz = \frac{ED_p \cdot u_a}{p \cdot r}$$

Soil density is approximated using the method outlined by Rawls (1983) combining the percentages of sand, silt, clay and organic matter. Like K-factor, soil density can be entered as a single value or a map of spatially varying values²⁰.

4.7.6. Implementing Landscape Evolution

Landscape evolution is change in topography over time. The MML uses the estimated net elevation change (dz) in each year to represent these changes. But before implementing them, we must know which process equation should be used to model net elevation change for each cell of the DEM. In other words, we must know which surface processes govern landscape evolution on each of the different landforms of the input landscape. Processes are not discrete, however, and there is a natural progression from diffusive soil creep (governed by raindrop force and gravity) to hillslope processes such as overland flow and rilling/gullying (governed by the strength of accumulated flow) to stream processes (governed by the strength of accumulated flow and turbulence). It is important to choose the optimal locations on the terrain for the transition between surface process models to ensure smooth transition in estimated net elevation change from one landform to the next. Although transition points vary with overall watershed geometry, area, and topographic relief, and also change during the course of a hydrologic event (e.g., as a function of rainfall intensity and duration during a storm), their general

²⁰ Although `r.landscape.evol` has been programmed to accept a spatially varying soil density map, and such data is available for the Ziqlab Region (e.g., the SOTER soils data, see Chapter 5), the interface module of the MML has been programmed to only accept a single numerical value. Thus, I use a single soil density value of 1.2184, generated from empirical data for Terra Rossa soils reported by Onori et. al (2006).

locations can be estimated in a GIS on the basis of upslope accumulated area (A) and topographic slope curvature (see Appendix A, Section A.2).

Once the location of flow process transition boundaries is determined, it is possible to use this geometry to paste together the dz maps produced by each process equation in a geomorphologically appropriate “global dz ” map²¹. Although the process outlined in Section 4.7.2 above ensures that the MML uses realistic transition points between the different process equations, when the final “global dz ” map is assembled, small linear aberrations in dz will be present across process transitions because it is still a “hard” boundary. Furthermore, larger aberrations in dz can occur at other points in the landscape when a process equation receives input conditions outside its underlying assumptions or input numerical data which exceed its mathematical limits. While careful tuning of the equations and smoothing of the input DEM help to reduce the frequency and severity of such aberrations, they nevertheless still occur occasionally due to the abstraction required in the creation of digital topographic models. This is combated by an adaptive “soft-knee” limiter (a type of low-pass smoothing algorithm), that is calibrated to remove abnormal spikes or linear artifacts in the “global dz ” map, while minimally affecting other areas (see Appendix A, Section A.3). The smoothed “global dz ” map is then can be added to (for deposition) or subtracted from (for erosion) the initial DEM, to create a new DEM after a cycle

²¹ It is important to note that this procedure must occur after the output of all the process equations are standardized to the same units of elevation change (dz) [m]. It would be extremely problematic to calculate the divergence of qs across process boundaries because 1) each equation produces very different value of qs for the same input conditions, 2) this is especially difficult across very large flow thresholds, such as between channels and adjacent slopes because of very high differentials between qs as calculated down the slope bordering a channel and qs calculated in the downstream direction within a channel, and 3) USPED and the reach-average shear-stress equation create output in different measurement units, so standardization would have to occur before calculation of flow divergence anyway, and 4) the diffusion equation produces dz directly. Therefore this could not be included in the patched qs map before calculation of divergence anyway.

of land-use and landscape change. This process is iterated at each cycle of the MML to simulate decades to millennia of landscape evolution.

4.8. CHAPTER SUMMARY

This chapter has described the general scope and has detailed certain aspects of the inner workings of the Mediterranean Modeling Laboratory. The MML has been designed to study the types of agropastoral socio-natural systems that existed during the Neolithic period in the Mediterranean region, and thus the MML provides a virtual space within which to conduct an empiric and replicable set of modeling experiments into the long-term effect of potential Neolithic subsistence systems. The character of the social and natural process equations described in this chapter reflect that purpose. Furthermore, the MML is designed specifically to study the long term consequences of subsistence land-use decision-making within this type of socio-natural system. Therefore, the social modeling engine of the MML focuses on this aspect of Neolithic social systems, and it purposefully chooses not to focus on other social aspects. This is also reflected in the scale of the social model (households versus individuals), which better reflects the social level at which most land-use decisions are made. The natural models are also designed with human land-use in mind, and the MML focuses on those aspects of the natural system that would be affected by and would, in turn, affect human land-use decisions. Finally, the MML has been designed with multiple interconnections between social and natural phenomena, so that all events have repercussions and these repercussions can drive the evolution of emergent socio-natural phenomena that could not be studied in any other way.

CHAPTER 5

PALEOENVIRONMENTAL RECONSTRUCTION

5.1. CHAPTER INTRODUCTION

The modern environment is a product of thousands of years of complex human-environmental interaction under changing climatic regimes. Thus, it is inappropriate to use modern conditions as a direct analog for the environment in which Neolithic people lived. However, uniformitarian principles suggest that it is possible to create realistic models of past environments based on an understanding of similar process in the modern world. This procedure requires both purely inductive techniques (e.g., direct interpolation from proxy records), purely deductive techniques (e.g., modeled reconstructions based only on an understanding of environmental processes), and techniques that are both inductive and deductive (e.g., model-based reconstructions that also require some empirical input).

In the broadest sense, “environment” can be construed to be everything external to a human agent. Even narrowed to encompass only external environmental conditions, this vague notion is still unhelpful for most kinds of socio-natural research questions. I therefore constrain the concept of “environment” only to those external variables that may have important feedbacks within typical socio-natural systems. In the simulation approach used in this study, I constrain the environment to: 1) topography (the physical shape of the surface of the earth), 2) soils (their depth, resistivity to erosion, and their fertility), 3) climate (macropatterning of temperature and precipitation), and 4) vegetation (the spatial and temporal patterning of plant communities).

Each of these variables needs to be reconstructed before dynamic simulation of Neolithic socio-natural systems is possible. It should be noted that the resulting reconstructions are “snapshots” – reconstructions of the landscape

at specific points in time – and are thus static interpretations based the available proxy data and processual models I have chosen to use. However, these reconstructions serve as the starting point and backdrop for dynamic simulation and, thus, will have a large impact on the simulation results. This chapter details the processes I use to reconstruct these environmental variables as they might have been during the LPPNB/PPNC and the Late Neolithic and provides an assessment of the reliability of the final reconstructions.

5.2. RECONSTRUCTION OF ANCIENT TOPOGRAPHY

The forces of erosion, deposition, and even tectonism can act on timescales short enough to have caused significant alteration of the physical geometry of the landscape over the Holocene. Thus, the topographic relief of region today is often quite different than it was in the past. A reconstruction of the Neolithic topography is therefore a vital first step in a LUCC model of Neolithic land-use because it is important that the agents base their land-use decision on Neolithic topography, and not on the anthropogenic topography of today. Without a time-machine, it is impossible to recreate large areas of the Neolithic topography exactly; we can, however, identify remnants of Neolithic topography and areas that have changed since the Neolithic and use this information to approximate the lay of the land as it was during the Neolithic period.

5.2.1. Landscape Evolution Research in Wadi Ziqlâb

The construction of an explicit GIS-based reconstruction of an ancient landscape must be grounded in intimate knowledge of the landscape

history of the region being reconstructed. Wadi Ziqlâb is an ideal location for this, as the region has been the focus of several geoarchaeological research projects over the last several decades including new research conducted by the author. The following subsections summarize the findings of previous and new geoarchaeological research, and provide a synthesis of Late Quaternary landscape evolution in the region.

5.2.1.1 Previous Landscape Evolution Studies in Wadi Ziqlâb

In 1986-87, The Wadi Ziqlâb Project began a systematic series of subsurface testing of alluvial terraces in the main Ziqlâb drainage system (see Chapter 2). The LN sites of Tabaqat al-Bûma and al-Aqaba were discovered during this trenching procedure, and it was discovered that both sites were almost completely obscured from the surface by thick layers of overlaying colluvial deposits. Following the discovery of the two sites, Field and Banning began geoarchaeological research into the interplay between geomorphology and archaeology in Wadi Ziqlâb (Field, 1994; Field and Banning, 1998). The thrust of their research was to better understand the colluvial forces that buried Tabaqat al-Bûma and al-Aqaba, with an eye towards predictive modeling of buried Neolithic site locations. Their research thus focused on classifying the types of mass-wasting occurring in the Wadi, understanding the frequency and locations of wasting events, and interpreting the effects of colluvial processes on preserved archaeological material in the Wadi. In addition to examination of remnants of historic and ancient mass-wasting events, they were also able to study 290 new mass-wasting events that occurred in the Wadi during the winter of 1992 – an especially wet year.

Field and Banning's research concludes that translational earth flows and rotational earth slumps are the main forms of mass-wasting in the Wadi, and that the frequency and severity of these events increases dramatically during especially wet winters—an observation corroborated by Farhan (1986) and El-Naqa (2001). They found that slumps tend to occur high on Wadi slopes near

their rims and the Terra Rossa soils of the plateau. Some slumps do, however, also form in “hollows” (incipient gully heads) where surface flow becomes concentrated. The slumps remain largely intact as they move rotationally along an arced surface of detachment, creating a characteristic crescent shaped “terrace” at their tops. The slumps also retain the internal bedding and sedimentary features of the original landforms from which they detached.

They found that earth flows, on the other hand, are mainly located in “hollows” or on the steeper mid-portions of the Wadi’s slopes. Some 60% of these flows did not reach the Wadi bottom, and the 40% that did were the most fluid (i.e., had the highest internal water contents). The flows often carried displaced material 300 m or more, but were not particularly high-energy events. Flows had different levels of bedding and clast inclusions, which related to variations in flow turbidity, viscosity, and parent material, but many were so fine-grained that they resembled annual slope wash deposits. According to Field and Banning, it therefore appears like that it is these intermittent earth flows, rather than annual slope wash (or rotational slumping), that are the main depositional process responsible for burying the Neolithic sites located on remnant Wadi terraces. This is particularly important because it is likely that Neolithic sites were located preferentially on these terraces close to the valley slopes, and so tend to be covered more deeply than one would expect if only alluvial processes were at work (Banning et al., 1994).

Another team of researchers from Yarmouk University carried out a geoarchaeological study in Wadi Abu Ziad (the next drainage south of Wadi Ziqlâb) during the storm events of 1992 (Al-Shreideh, 1992). This study mapped the relationship between hydrographic features and archaeological sites in the Wadi. Although the study mainly focuses on the changes in outflow of the perennial springs in the Wadi during storm events, it also describes the effects of flooding in the Wadi’s washes and documents bank erosion of some of the lower fluvial terraces in the Wadi. The study is important because it provides evidence that fluvial erosion is, and has been, a

very important factor in reshaping the morphology of the wadi-bottoms in the Ziqlâb region.

In the early 2000's, Maher (2011, 2005, 2000; Maher and Banning, 2001) conducted new geoarchaeological work in the region, including a broad geoarchaeological survey of Wadi Ziqlâb, Wadi Tayyiba, and Wadi Abu Ziad, and a detailed stratigraphic study of Wadi Ziqlâb. Maher's work, although mainly focused on the Epipaleolithic occupation of wadis, was formulated to better understand landscape change in the region, and so it is a particularly helpful source of information for paleotopographical modeling in the region. Among the most helpful resources created during her work are geomorphological maps of the main Ziqlâb drainage channel, geological cross sections of the Wadi at various points, stream-profiles diagrams of the main channel and major tributaries, and a collection of detailed stratigraphic drawings for several locations along the Wadi. This work also helped to define the relationship of the modern and ancient springs (identified from tufa deposits), the location and severity of headward incision of the channel during the Holocene, the location and general chronology of the major fluvial and colluvial terraces, and also discovered several new archaeological sites from different periods. She identifies three major ancient river terraces, which, although not continuous, are found along the entire length of the Wadi: 1) a highly eroded, but generally contiguous upper terrace generally occurring 10-30 m above the Wadi channel, 2) a broad, flat, variably-eroded middle terrace that is 5-10 m above the Wadi channel and, and 3) a lower terrace that is only 1-3 m above the modern Wadi channel. Although Maher was not able to map the terraces over the whole region or to directly date their formation (e.g., by OSL), she was able to define a series of associations between archaeological sites from different periods and each of the terraces. The oldest materials recovered from the upper terrace are Middle Paleolithic¹, the oldest materials in the middle terrace date to the Epipaleolithic²,

and the lower terraces contain only secondarily-deposited Roman/Byzantine and modern artifacts.

Maher identifies four "knick points" in the main and tributary channels of Wadi Ziqlâb where headward erosion has created steep drop-offs³. These knick points are very important for paleotopographic reconstruction in the region as they mark points of change in the relationship (and distance) between the Wadi channel and the remnant terraces. The highest knick point is found on only one of the two tributary forks of the Wadi at 750-800 masl, and is well within the upland region in the East. The second-highest knick point is found on both of the major forks at around 200-450 masl. It marks the boundary between the gentle valley profile of the uplands and the more incised profile of the lowlands. The final two knick points occur close together in the lower western end of the Wadi – very near two of the Neolithic sites – at 50-100 and 50-125 masl. These knick points likely correlate to the well-known series of four knick points that are found in many of tributary wadis of the Jordan Valley (on both its eastern and western flanks), which are known to occur at more or less the same elevation above sea level as those identified by Maher (Horowitz, 2001). Horowitz believes the knick points formed during interpluvial periods that, though generally drier, were times when most of the precipitation fell in short thunderstorm bursts. This caused massive runoff and flooding thereby drastically increasing the rates of erosion. The sequence of knick points exists due to the interaction of the timing of these interpluvial periods and the rate of tectonic uplift of the highlands. The oldest two knick points (the two at that occur at the highest current elevations) formed around 2.31 mya and 1.75 mya respectively, and thus are quite ancient geomorphological features in the region. The lower two knick points date to 280 kya and 40 kya respectively, and thus were also already present during the Neolithic. Based on

red paleosol that is always truncated by an erosional unconformity, and almost always overlain by Neolithic or Late Neolithic material in colluvial deposits.

3 These knickpoints are so steep that they form waterfalls in the portions of the Wadi that have perennial stream flow.

¹ These were surface-finds recovered during pedestrian survey.

² The Epipaleolithic material is found in a buried

the difference in elevation between wadi outlets and the lower knick point, Horowitz calculates a current uplift rate of 450 mm per thousand years, suggesting that these lower knick points have been very active over the Holocene and remain so today (see also Section 5.2.1.2, below).

Maher studied 15 exposed profiles in the Wadi to better understand its depositional history. The Terminal Pleistocene was apparently a period of fluvial terrace aggradation with stable surfaces evidenced by advanced pedogenesis. Most of the Epipaleolithic sites discovered in the Wadi are found in this paleosol, which is strongly correlated with the basal layers of the middle terrace. The following period was one of intense erosion, perhaps related to the dryer and more seasonally variable conditions of the Younger Dryas. A post-Epipaleolithic unconformity, present most prominently on the middle terraces, most likely dates to this period. As there are no remains of Natufian through PPNA sites preserved in the Wadi, this erosional period likely lasted until the last phases of the PPNA or the earliest phases of the EPPNB. The unconformity is overlain in some places by a thinner layer of alluvium, characterized by smaller clast sizes than the earlier alluvial layers of the Terminal Pleistocene deposits. This thin layer is likely the only Early Holocene deposit in the Wadi and consists of reworked material eroded from upstream terraces. In other areas, the unconformity is directly overlain by a massive grey colluvial layer. The earliest PPNA material in the Wadi – the basal levels at PPNA Tell Rakkan – rests directly upon the unconformity, and dates to the late MPPNB (see Chapter 2). All *in situ* PPNA and LN material in the Wadi is found fully within the grey colluvium, or in intrusive pits dug into the red paleosol. Thus, it is likely that the colluviation described by Field and Banning (1998) began in the MPPNB, and the Neolithic was a period of net colluvial aggradation on the middle terraces (although it seems that there were at least a few periods of alluvial erosion in the channel). The remainder of the Holocene saw alternating cycles of minor erosion and deposition and witnessed the formation of the lower terrace in the current Wadi-bottom. Finally, although she did not conduct

in-depth stratigraphic study of outcrops in Wadi Tayyiba or in Wadi Abu Ziad, Maher reports that due to differences in morphology, catchment size, and the history of human occupation, the depositional sequences in the three wadis are not the same. Thus the sequence of events documented in Wadi Ziqlâb is not necessarily mirrored in the other two wadis.

5.2.1.2. New Geomorphological Fieldwork

In 2006, 2008 and 2009, I carried out additional geoarchaeological and geomorphological fieldwork in the Wadis Ziqlâb, Tayyiba, and Abu Ziad (Figure 5.1). The purpose of the new field work was to build on the foundational work reported in Section 5.2.1.1, above, and to better understand landscape formation in Wadi Tayyiba and Wadi Abu Ziad, as compared to the better known sequences in Wadi Ziqlâb. My goals were to identify, document, and date strata from different landforms in all three wadis, to better understand the scale and morphology of remnant Neolithic landforms (see Figure 5.1 and 5.2, below), to better understand the patterning of soils and soil-depth in the region (see Section 2.3, below), and to obtain GPS ground control points with which to incorporate this data into a GIS (see Figure 5.2, below). Fieldwork focused on the middle and western portions of the Wadis in the regions that would have been utilized by the Neolithic inhabitants of the region but portions of the upper (eastern) portion of Wadi Ziqlâb were also studied. Three types of research were carried out: 1) systematic pedestrian and vehicular survey of portions of the wadi bottoms, hillslopes, and terraces (and GPS data collection), 2) targeted survey/mapping and GPS data collection at specific locations and landforms, and 3) stratigraphic analysis and ^{14}C sample collection at known and new sedimentary profiles in each Wadi. Fieldwork was accompanied and expanded by intensive stereoscopic analysis of high-resolution (10–25 cm) declassified CORONA satellite imagery from the 1960's⁴. Higher resolution aerial

⁴ CORONA imagery served as the main remotely-sourced imagery source because it documented the area before many of the modern human alterations (e.g., road-

photographs from the 1970's and 1980's and GeoEye imagery from the 2000's supplemented the CORONA imagery where available.

Detailed results of this work are presented in Appendix B, but the most important data gained from this new research concern the extent of middle terrace remnants and soil depths on remnant landforms in all three wadis. A detailed map of middle terrace remnants was produced by digitization over high resolution imagery informed by field data collected during survey (Figure 5.2).

5.2.2. Considerations for Paleotopographic Reconstruction in Wadi Ziqlâb

The method of paleotopographic reconstruction to be used in the Ziqlâb region must be able to deal with several issues pertaining to the scope of this project. The first is the overall scale of the reconstruction. Although all the Neolithic sites are fairly tightly clustered in the middle and lower portions of the Wadi, the surface process model of

building, agricultural terrace bulldozing) occurred.

the MML (see Chapter 4) requires the boundaries of the input DEM to be delineated by real drainage divides. Hydrological analysis in a GIS shows that Wadi Ziqlâb stretches over 30 km from its headwaters to its confluence with the Jordan River in the West, narrowing from almost 7 km to less than 2 km in width along this traverse, and drains an area of almost 110 km². Adjacent to the north is Wadi Tayyiba, which is nearly as long as Ziqlâb, but considerably narrower along its entire length. Tayyiba tapers from slightly more than 3 km in its eastern headwaters to less than 1 km near its outlet into the Jordan Valley, and drains an area of only 56 km². To the south of Ziqlâb, Wadi Abu Ziad is smaller still. At about 13 km in length, it is much shorter than both the other wadis and quickly tapers from a width of about 3.5 km in the upper reaches of its catchment to a width of less than 1 km at its outlet, draining an area slightly larger than 28 km². Preliminary site-catchment analysis using least-cost modeling shows that it is highly likely that Neolithic herders would have used grazing land in all three wadis (Ullah, 2011). Together,

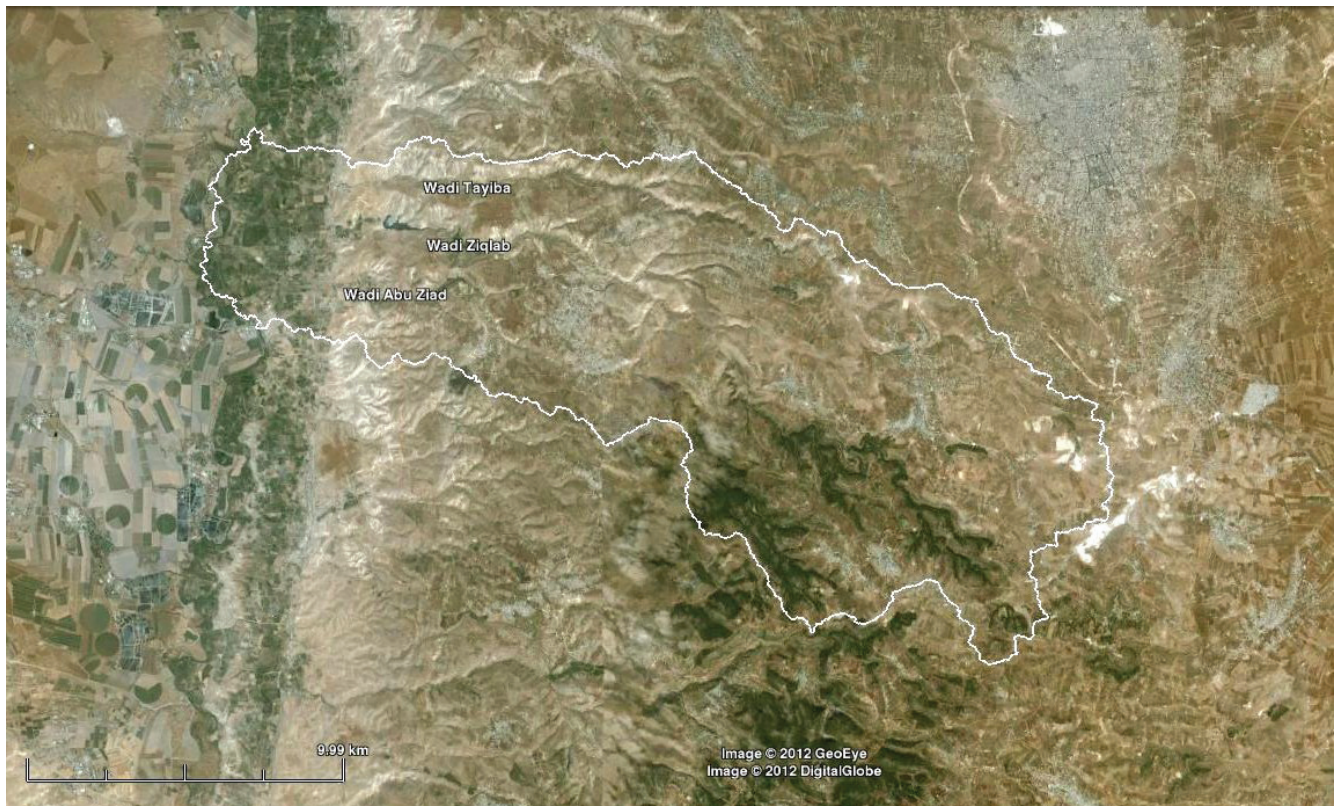


Fig. 5.1. Outline of the project area on GeoEye imagery.

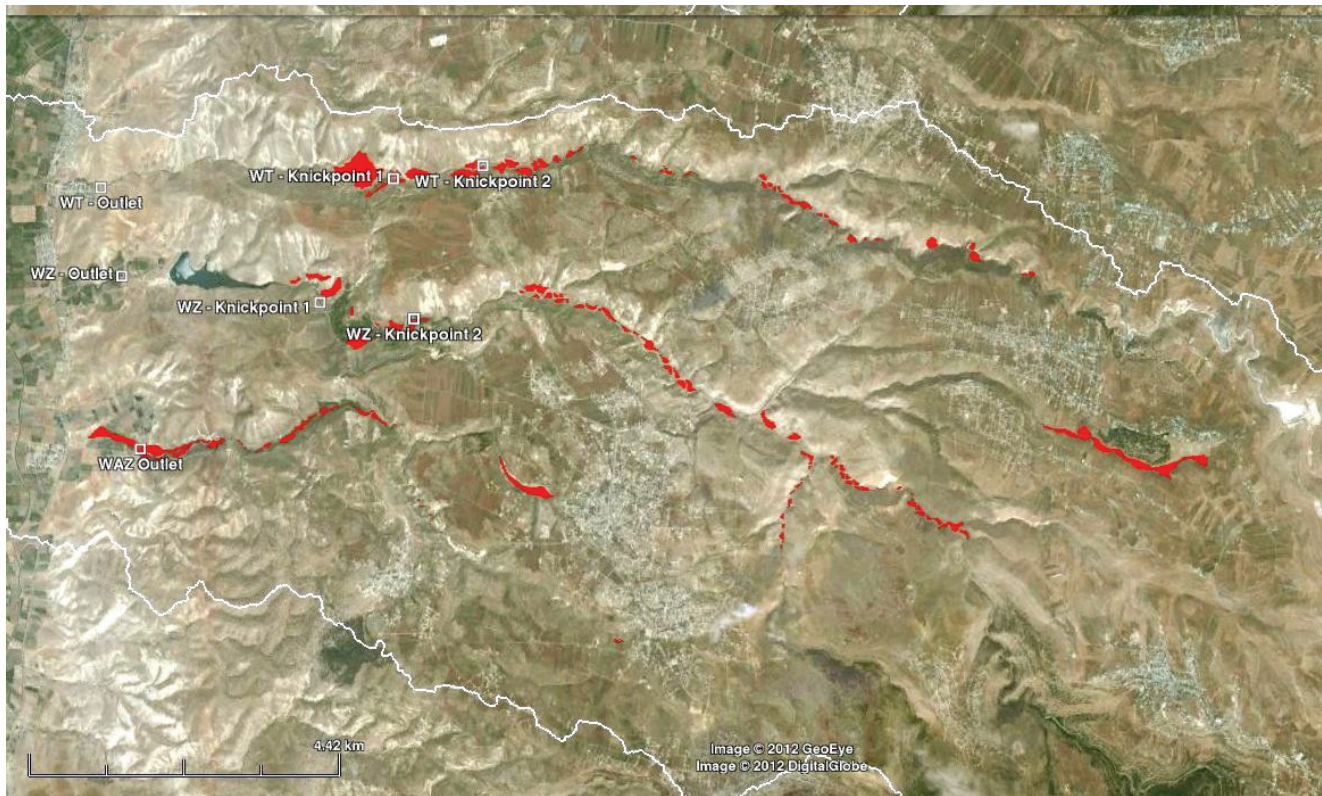


Fig. 5.2. GeoEye imagery of the project areas with the knick points and wadi outlets marked, and the middle terrace remnants outlined in red.

these three catchments drain an area of nearly 218 km² (Figure 5.1), and the Neolithic topography must be reconstructed across this entire area.

The second issue pertains to the degree of post-Neolithic landscape evolution that has occurred in the region. Fieldwork confirms that the landform most positively identified with the Neolithic occupation of Wadi Ziqlâb is the middle terrace, but the main topographic changes that have occurred since the Neolithic are extensive bank erosion of this terrace and mass-wasting of slope sediments onto it (see Sections 5.2.1.1 and 5.2.1.2, above). GIS-aided mapping of the extent of the middle terrace in all three Wadis shows that large stretches exist where the middle terrace is entirely absent (Figure 5.2). This is due to channel incision and lateral erosion, localized rilling on the terraces themselves, gully intrusion from adjacent hillslopes, and the expansion of tributary wadis in all parts of the drainage system. Furthermore, the surface topography of the remaining terraces remnants has been significantly steepened by Late Holocene colluviation, which

has completely covered and obscured any smaller terrace remnants located at the foot of slopes. The method of paleotopographic reconstruction should be able to account for these types of landscape changes and should also be adaptable enough to accommodate changes in the relationship between the current channel and the middle terraces over the entire length of the each of the wadis.

The third issue is the relationship of the scale of remnant landforms in the region with the scale of the digital terrain data used in this project. High-resolution topographic data (1m or greater), such as LIDAR or DEM extraction from high-resolution stereo imagery such as Quickbird or IKONOS, are desirable for detailed digitization of remnant landform geometry, but are unsuitable for use as a base for paleotopographic reconstruction for several reasons. Firstly, many of these data sources are prohibitively expensive, secondly, their extreme detail means that many modern alterations to the landscape (such as agricultural terraces and road cuts) and other artifacts (such as buildings and trees) obscure the

basic topographic trends, and finally, such data are typically of restricted spatial extent. At the time of the analysis, the best source of freely available, wide coverage digital elevation data for Wadi Ziqlâb region was the 30 m-resolution ASTER GDEM2⁵. This lower resolution is actually *better* for paleotopographic modeling, because many of the modern alterations and artifacts (such as trees and buildings) visible in the high-resolution data are absent or reduced in the GDEM2 due to spatial averaging. The GDEM2 has relatively low inherent spatial error⁶ and is created from atmospherically corrected and calibrated stereo ASTER imagery with wide spatial coverage appropriate for watershed-scale paleotopographic reconstruction.

5.2.3. Existing Methods of Paleotopographic Reconstruction

There are three existing approaches to paleotopographic approximation. The most common technique is simple stratigraphic correlation using either basic analytical techniques like the type-fossil approach or simple sedimentary analysis. Graphic or logical techniques such as the Harris Matrix are also commonly used, or even more advanced techniques such as absolute dating via OSL, C13 or other methods. This technique has the benefit of relative simplicity, but it produces only a heuristic picture of ancient landscapes – typically in the form of graphical correlation of stratigraphic units.

Another method extends the level of detail and the usefulness of the basic stratigraphic correlation technique for use in spatial studies via interpolation methods in a GIS. Interpolation is a predictive technique that uses one of a suite of mathematical functions to approximate the value of unknown points based on the values of known nearby data

⁵ Note that as of the time of the final editing in 2016, 1 arc-second SRTM DEM's are now available with global coverage. These could potentially be more accurate than the ASTER GDEM2 at similar native resolution.

⁶ The average vertical RMS error of the GDEM2 is 8.36 m, and the average horizontal RMS error is 0.104 arc-seconds (~ 3.21 m) in the EW direction and -0.175 arc-seconds (~ -5.40 m) in the NS direction (Tachikawa et al., 2011).

points. When employed in a GIS framework, it is possible to use interpolation to “fill the gaps” between observed stratigraphic sections, thereby creating a continuous “trend surface” DEM of the “top” of the buried layer from a series of spatially segregated stratigraphic sections. Interpolation benefits from an abundance of known data points, so the most successful reconstructions derive from many sources of stratigraphic data, including natural sections, excavation units, geophysical survey, and augers (H. Chapman et al., 2009; Contreras, 2009; García Puchol et al., 2008; e.g., Lilburne et al., 1998; Prochnow et al., 2007). The technique can produce very detailed renderings of buried, missing, or otherwise obscured strata or paleosurfaces, but it is important to note that most studies that use this technique are focused on predicting the lay of buried surfaces or soil horizons on a single landform (or at most, a small collection of related landforms) in depositional contexts. Another drawback of this technique is that it is designed for the reconstruction of buried remnant patches of ancient surfaces, and thus is best suited for use in depositional environments, such as river valleys, deltas, and alluvial fans. As the spatial scale of interest increases—and in more erosive contexts—it becomes increasingly difficult to accumulate a sufficient quantity of stratigraphic observations of a particular buried stratigraphic layer (or correlated layers) to make good quality interpolation feasible.

A third technique uses interpolation in a broader, less constricted manner, and relies less on detailed stratigraphy and more on basic geomorphology. As outlined by Arrowsmith et al. (2006), the method requires detailed geomorphological mapping of the study region so that landforms can be coded according to a chronosequence of depositional and erosive events which are correlated to the archaeological sequence in the study area. Mapping can be accomplished via a combination of fieldwork and stereoscopic analysis of high-resolution aerial photographs or other remotely sensed data (e.g., LIDAR, Quickbird, SPOT, ASTER), and the map should delineate the major landforms at the highest resolution possible. The geomorphological chronosequence

can be correlated to the archaeological time-line of the region via a combination of absolute dating methods (e.g., direct OSL or radiometric dating of sedimentary layers) and relative dating methods (e.g., the “type fossil” and other stratigraphic correlation techniques). The goals are to identify all landforms that have not experienced significant change since a particular archaeological period and differentiate them from those parts of the landscape that have changed in the intervening millennia. These delineations are then digitized in a GIS and used to extract the elevation data of the relatively unchanged portions of the landscape from a DEM of the modern surface. That information is then used to interpolate an approximation of the topography in the other areas. Because of its reliance on interpolation from portions of the current land surface, this technique is better suited for those regions that have experienced net erosion in the millennia succeeding the study period – such as downcutting alluvial systems or hillslopes that have experienced mass-wasting – where many remnant landforms remain unburied or at least relatively unaffected by subsequent deposition.

5.2.4. A New Method for Reconstructing Paleotopography

Each of three existing methods of paleotopographic conditions satisfy some of the necessary conditions and requirements for landscape reconstruction in this project, but none of them satisfy all. Thus, I have developed a new method that borrows appropriate techniques from each of the existing methods, but introduces some new techniques to fully satisfy the requirements of paleotopographic reconstruction in the project area.

The first step in the new process is to use high-resolution stereoscopic imagery (CORONA, aerials, Geo Eye) to create a digitized map of remnant portions of the middle terrace and the locations of knick points, narrows, and other flow-regime changes. These higher resolution data may not align absolutely with the GDEM2 data, however, so direct translation of the digitized area is not possible. This is because the median size of middle terrace remnants in the Tayyiba,

Ziqlâb, and Abu Ziad drainages is about 7, 5, and 2 GDEM2 raster cells, respectively (Table 5.1 and Figure 5.2). This small number of raster cells means that the geometry of many of the remnant terraces will be poorly delineated at the native 30m GDEM2 resolution, and small translational errors in terrace digitization could lead to the inclusion of GDEM2 cells not belonging to the landforms digitized from higher resolution imagery. Therefore, the digitized terrace outlines are only used as a “guide” for an automated identification of the area below the terrace edges which are then removed and interpolated over, as in the third procedure in Section 5.2.3 above. The automated procedure thus relies solely on the GDEM2 topographic data and so avoids the introduction of translational errors between data-sources or resolution-induced sampling errors.

Resolution errors are further combated by decreasing raster cell size with a Regularized Spline-Tension (RST) interpolation from the native 30 m of the input GDEM2 to a 10 m resolution in the output raster⁷. RST interpolation connects input data points with all other points via “spline” functions, which can be “tuned” by manipulation of “smoothing” and “tension” parameters (Mitasova and Mitas, 1993; Neteler and Mitasova, 2007b). The smoothing parameter affects how closely the splines must pass by data points, whereas the tension parameter affects the overall “stiffness” of the splines themselves. Reducing the raster cell size during the interpolation allows for smoother, more detailed, topographic modeling than is possible at its native 30 meter resolution, but it is important to remember that such interpolation cannot “add”

⁷ A resolution of 10m was chosen as a compromise between precision and model run-time. Although it is important to have a raster resolution that is high enough to reasonably replicate the scale at which most fluvial process occur (i.e., the width of gullies or streams), increasing resolution exponentially increases the number of cells, and thus the number of calculations that must be done every simulation cycle. A 10m cell resolution allows for a reasonable increase in the resolution of modeled fluvial process, while only increasing the size of the base DEM to about 5 million raster cells. This translates to a 3-4 minute run-time per simulation cycle – an acceptable compromise. RST interpolation is implemented in GRASS via the v.surf.rst module.

Table 5.1. Areal (ha) statistics for middle terrace remnants in all three of the Wadis of the project area.

Statistic	Wadi Tayyiba	Wadi Ziqlab	Wadi Abu Ziad
<i>n</i>	35	65	27
Mean	1.28	0.85	1.04
Median	0.6	0.43	0.2
Mode	0.22	0.18	0.06
Std Dev	2.72	1.59	2.14
Min	0.1	0.05	0.01
1st Quartile	0.28	0.22	0.1
3rd Quartile	1.15	0.89	0.95
Max	16.23	11.85	10.02

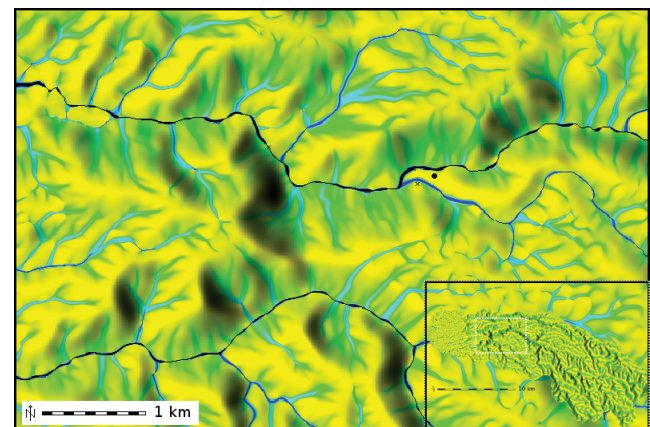


Fig. 5.3. Detail of the flow accumulation map near Tell Rakkan. Inset shows the whole project area.

data not collected at the original resolution; that is, the extra detail added by interpolation is only a model, informed by the data that was originally collected by the sensor at its native resolution and carried out according to the parameters of the RST run (i.e., the “tension” and “smoothing” values) (Mitasova and Mitas, 1993). The approximating properties of RST interpolation are actually beneficial for certain aspects of paleotopographic approximation, and so RST is an integral component of the reconstruction in its own right. For example, by setting the tension and smoothing parameters to increase spline stiffness and decrease the influence of individual points in the local neighborhood in the RST interpolation results in a new DEM of the project region that has gentler slopes and softer topographic breaks, which better approximates the original geometry of the wadi slopes and remnant alluvial terraces before the increased colluvial activity of the Late Holocene.

The remainder of the automated procedure involves a combination of hydrological modeling and cost-surface approximation techniques to delineate areas of the landscape that are most likely to be related to recent/current fluvial activity, or which are likely to be newer than the time-period in question. The first step is to understand current fluvial activity in the wadi system and is accomplished via GIS-based hydrological modeling. I advocate for a hydrological modeling engine that uses a multidirectional flow-routing

algorithm (MFD) to estimate the flow of water across the landscape⁸ (Neteler and Mitasova, 2007b). MFD routes a proportion of the outflow from a cell to all downslope cells – scaled according to the degree of elevation difference – and thus produces more accurate/realistic modeling of flow lines than does a simpler “D-8” algorithm that can only route flow to the single-most downslope cell. MFD results in a realistic map of the accumulated flow in all parts of the landscape (Figure 5.3).

The main regions of current or recent fluvial activity are typically 1) gullies and washes, 2) the active channels of small tributary wadis, 3) the active channel and active floodplain/terraces of the main wadi itself. In most of these landforms the modeled flow patterns produced by the MFD routine are typically diffuse; that is, these landforms are generally defined by the presence of active flow across their entire surfaces. Thus, the isopleth that delineates all flow accumulation values higher than a particular threshold for that landform⁹ also delineates the geometry of these landforms themselves, and so these landforms can be “automatically” digitized via a boolean map algebra statement. In the main wadi drainages, however, the nature of flowing water is to

⁸ Multidirectional flow routing is implemented in GRASS via the r.watershed module.

⁹ The different thresholds in modeled flow accumulation for each of the specific landforms must be determined by “trial and error” experimentation for a given area under a given type of environment and climate.

“concentrate” in the central channel, and this is reflected in the results of the MFD flow-modeling routine. In these areas, the focused flow means that the thresholding approach tends to only define the active channel itself and cannot define the boundaries of the active floodplain or any alluvial terraces that are newer than the period in question, so an additional step is required to “automatically” digitize these landforms. This “next step” takes the form of a cost-surface approximation procedure that is based on the topographic relationship of floodplains and terrace risers to the active channel. Floodplains are typically flat (or slightly “backwards” sloping), and are separated from the active channel by levies or risers. Relict alluvial terraces are typically remnants of such floodplains that are now left stranded above the current active plain by subsequent channel incision. Thus, assuming a locally uniform amount of incision, all correlated relict terraces and floodplains in a particular portion of the drainage network should be found at the same height above the active channel. Directly measuring height-above-channel in a GIS is difficult but can be approximated by the “accumulation” of slope over horizontal distance as one travels perpendicularly away from the active channel. This is achieved in a GIS by using the channel line as derived from the MFD hydrological model as a series of starting points for a “walking cost” approximation routine that calculates the cost of travel from the starting point(s) to all other points on the landscape along the route of least resistance. Costs are calculated from an input map of the cost it takes to traverse each cell. In this case, the “cost” of traversing a cell is the linear distance of the cell from the active channel, multiplied by the topographic slope of that same cell¹⁰. A threshold/cutoff determined on this output “cost-surface” map approximately delineates all cells below a certain height above the channel, and the isopleth thus formed can be extracted via a boolean map algebra equation.

¹⁰ Note that in future approximations, a better measure of cost for this application is the accumulated gain in elevation as each cell is traversed. A map of local elevation gain at each cell can be calculated as the cell-resolution times the tangent of slope. The new GRASS add-on module `r.stream.distance` can calculate this automatically.

Again, trial and error experimentation is required to obtain a reasonable result; the thresholding cost-value will be different for different drainages in different environments and climates and will also change according to the position of the particular wadi segment in the drainage network.

5.2.5. Neolithic Paleotopographic Reconstruction of the Ziqlab Area

Using the techniques described in section 5.2.4 above, and knowledge of the locations of various narrows, widenings, knick points, wadi confluences, the outlet points for the three wadis (see Appendix B), and those terraces that have known Neolithic material from Section 5.2.1 (Figure 5.2), I was able to delineate those portions of each wadi that are likely newer than the Neolithic (Figure 5.4). Once these areas were identified, digitized, and removed from the base GDEM2, RST interpolation was used to create a new “paleoDEM” (Figure 5.5).

It is useful to compare the original GDEM2 topography with the simulated paleotopography. Figure 5.5 shows side-by-side 3-D views of the original GDEM2 and the interpolated “PaleoDEM”. The first thing of note is that the interpolation routine smoothed the topography in the plateau region and in the wadi bottoms. Much of the “roughness” in the GDEM2 likely stems from trees and human structures, so the smoothing affect likely helps to remove these types of modern artifacts from being included in the digital topography. Some of the GDEM2 roughness may also be due to erosion scars in these landforms which tend to cause “lumpy” terrain. Again, the interpolation routine removes these features which is appropriate for the purposes of the reconstruction. It is also clear that the interpolation flattened the bottom of the Wadi significantly, and the incision below the Tell Rakkan knickpoint is less intense than on the GDEM2. Figure 5.6 shows another set of 3-D views of the PaleoDEM, this time colored by the amount of elevation change from the GDEM2. This is a useful heuristic to help confirm the nature of the paleotopographic reconstruction on the different landforms in the project region.

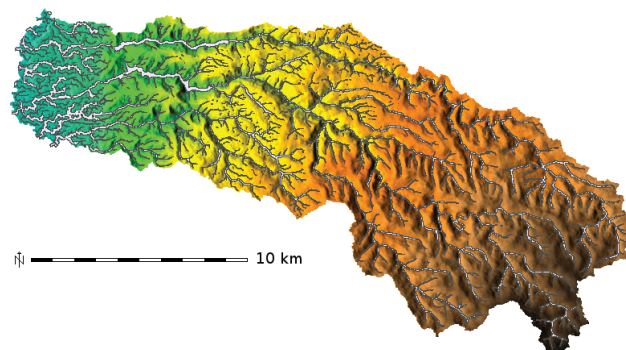


Fig. 5.4. Map of the portions of the project area detected by the automated detection routine. The elevation data within the boundaries defined by the routine is ignored during the interpolation of the “PaleoDEM”.

Using this heuristic image, we can confirm that the wadi-bottoms have indeed been filled in, and that the sections below the knickpoints have been filled in more (up to about 30 m in some places) than those above the knickpoints. The general smoothing effect in the plateau region seems to be from both the flattening of “lumps” as well as the filling in of “pits”. There also seems to be a small degree of spatial patterning in the location of these artifacts, with “lumps” being located preferentially in the interior of the plateaus, and “pits” being located preferentially near gully incisions. This patterning lends credence to the assertion that the “lumps” are likely houses, trees, or other protrusive human-made features, and that the “pits” are likely erosion scars.

We can also see that the interpolation has extensively reshaped the slopes as well. The colluvial deposits of the later Holocene have been removed at the foot of slopes, returning them to morphologies more similar to

those of Neolithic landscapes. The upper slopes have also been modified, and material has been removed from the plateau edges. While the removal of material in these areas seems counter to our goal of paleotopographic reconstruction (i.e., we ought to be *adding* material in these areas, rather than removing it), this procedure does shape the morphology of these features in a way that is similar to their supposed Neolithic form before substantial removal of material by colluviation and mass-wasting (i.e., softer slope breaks at the edges of the plateau, and gentler slopes overall).

5.3. RECONSTRUCTING ANCIENT SOILS

There are three properties of soils that are important in the MML: 1) their depths, 2) their resistivity to erosion, and, 3) their fertility. Because all three of these properties may have changed considerably over time, it is imperative to the success of the modeling endeavors undertaken in this research that the conditions of these soil properties be reconstructed as they might have been at the start of the LPPNB.

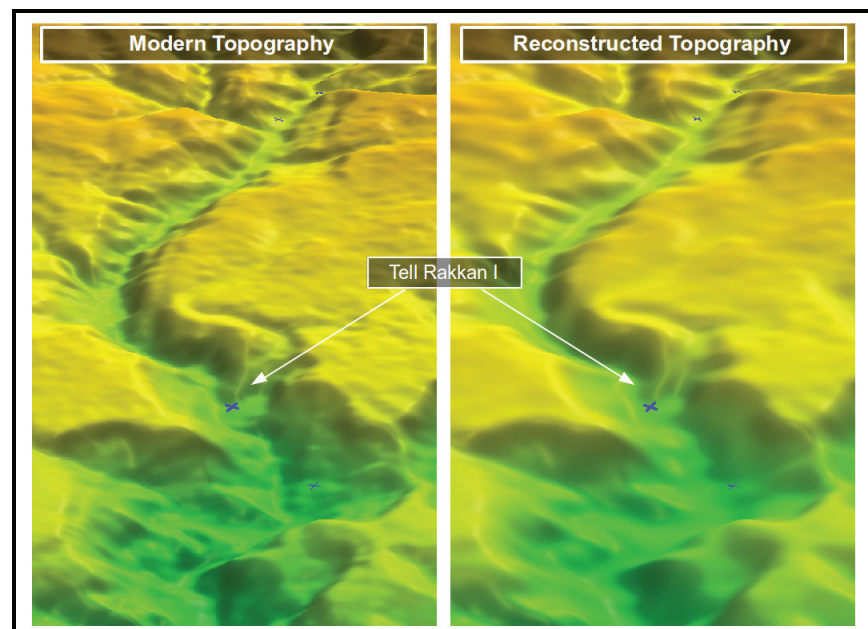


Fig. 5.5. 3-D perspective views of the modern DEM (left) and the interpolated “PaleoDEM” (right). The large blue X marks the location of Tell Rakkan, and the smaller blue X’s mark the location of the other LN sites.

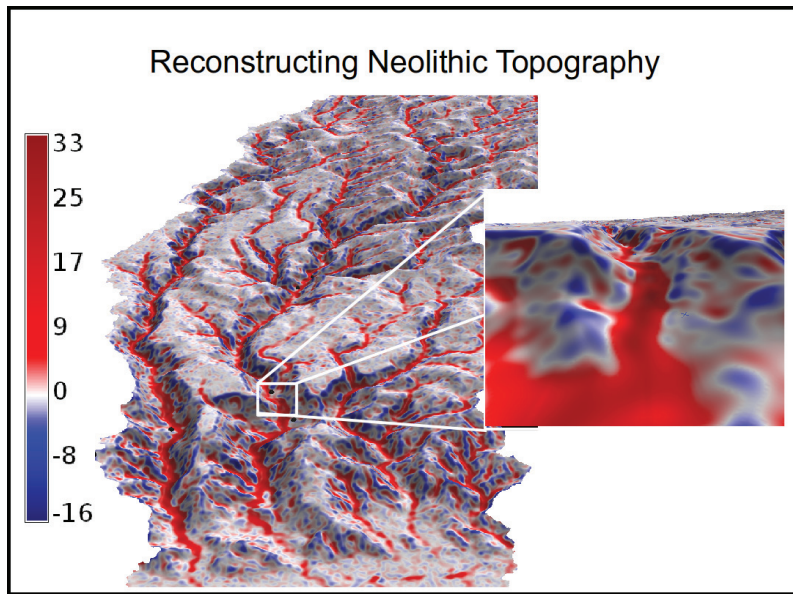


Fig. 5.6. 3-D perspective view of the project area, colored by the difference in elevation between the Modern DEM and the “PaleoDEM”. Red indicates areas of raised elevation in the interpolated “PaleoDEM”, and blue indicates areas of lowered elevation. Inset shows a close up of the pattern near Tell Rakkan.

5.3.1. Sources of Soil Data in the Region

The earliest soils research carried out in Wadi Ziqlâb was a rough summary of soil and bedrock types in the Wadi carried out in the late 1960's by Fisher et al. (1966), and was based largely on aerial photographic data with minimal ground truthing. This research produced the only high-resolution soil (Figure 5.7) and bedrock (Figure 5.8) maps currently available, but unfortunately they only cover the main Ziqlâb drainage itself. The highest resolution full-coverage geological map of the region is a 1:200,000 map from the Israeli Geological Survey (Sneh et al., 1998), and the highest resolution full-coverage soils map of the region is the 1:500,000 revised Soils and Terrain (SOTER) map from the International Soil Reference and Information Centre (Batjes et al., 2003). Although these maps are admittedly coarse, they nevertheless remain the only source of digitized full-coverage spatial soils and bedrock data available for the project region, and so, supplemented by field work conducted

by Maher (2011, 2005) and by the author (see Section 5.2.1, above), form the starting point for the GIS-based paleosoil reconstructions described in this section.

5.3.2. Modeling the Depth of Soils Across the Landscape

Due to extensive soil loss in many areas, and the accumulation of colluvial sediment minimally affected by pedogenesis in others, modern soil depths bear little resemblance to those of the early or middle Holocene. Modeling the depth of soils (i.e., depth from surface to bedrock) on the landscape is important both for surface-process simulation and for simulating agricultural output and vegetation regrowth. Many factors affect the depth of sediment in any given time, such as climatic conditions, vegetative cover, the position of the landform in the landscape, and the overall age of the landform/landscape in general. The two main processes that change soil depth are sediment transport (erosion/deposition) and regolith production (subsurface weathering). Despite a significant amount of research into the relationship of environment, surface processes, and bedrock weathering rates (Braun et al., 2001; Burke et al., 2007; Dietrich et al., 2003; Heimsath et al., 2000; Heimsath et al., 2002, 2001, 1999, 1997; McBratney et al., 2003; Minasny and McBratney, 2006, 1999), there exists no clear consensus for a single algorithm or procedure for predicting soil thicknesses across an entire landscape. The situation is further complicated by the fact that soil depths are the product of many interacting physical, chemical, and biological processes, and so the depth profile of each landscape is sure to be different, if not completely unique. Regardless of these complexities, a variety of approaches have been taken: from simulated landscape evolution over thousands of years (Minasny and McBratney, 2006) to basic extrapolation from existing soil

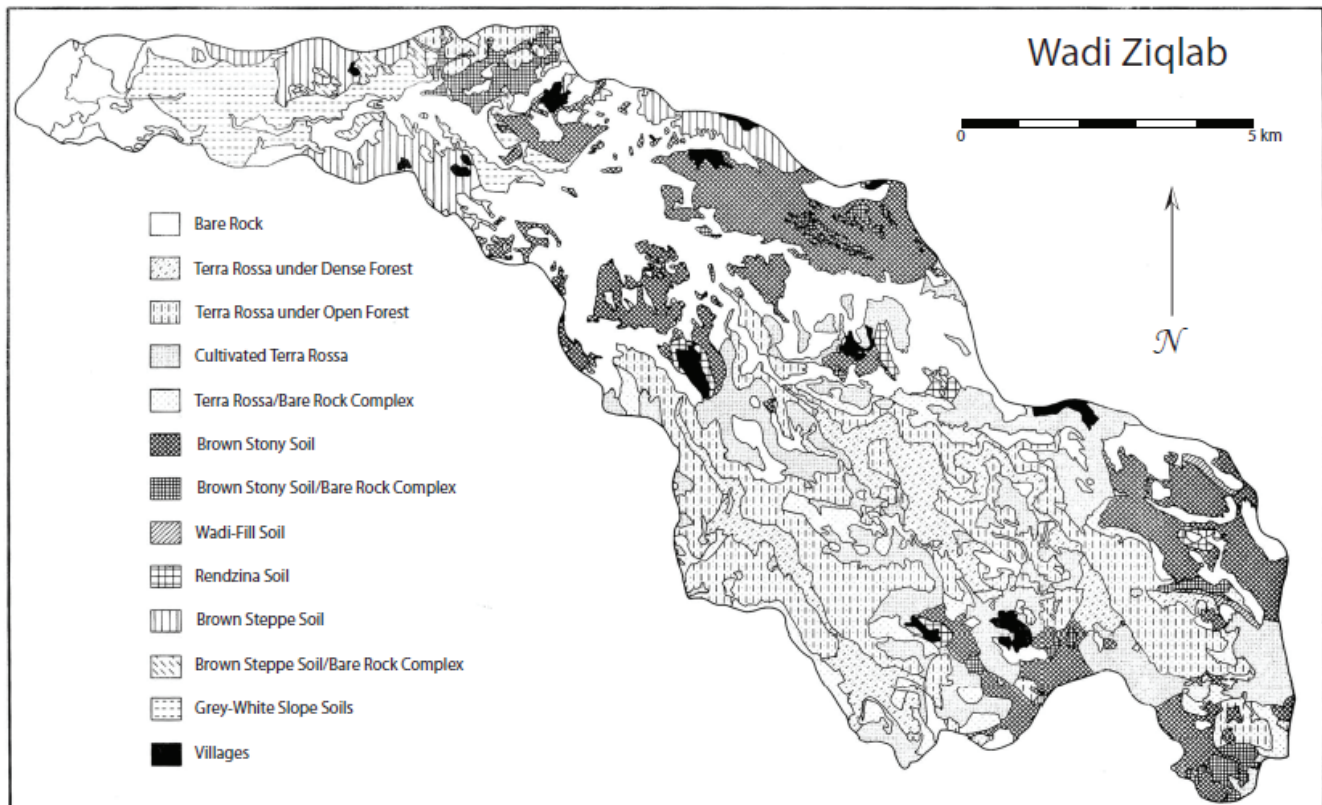


Fig. 5.7. The Fisher et al. (1964) soils map of Wadi Ziqlâb.

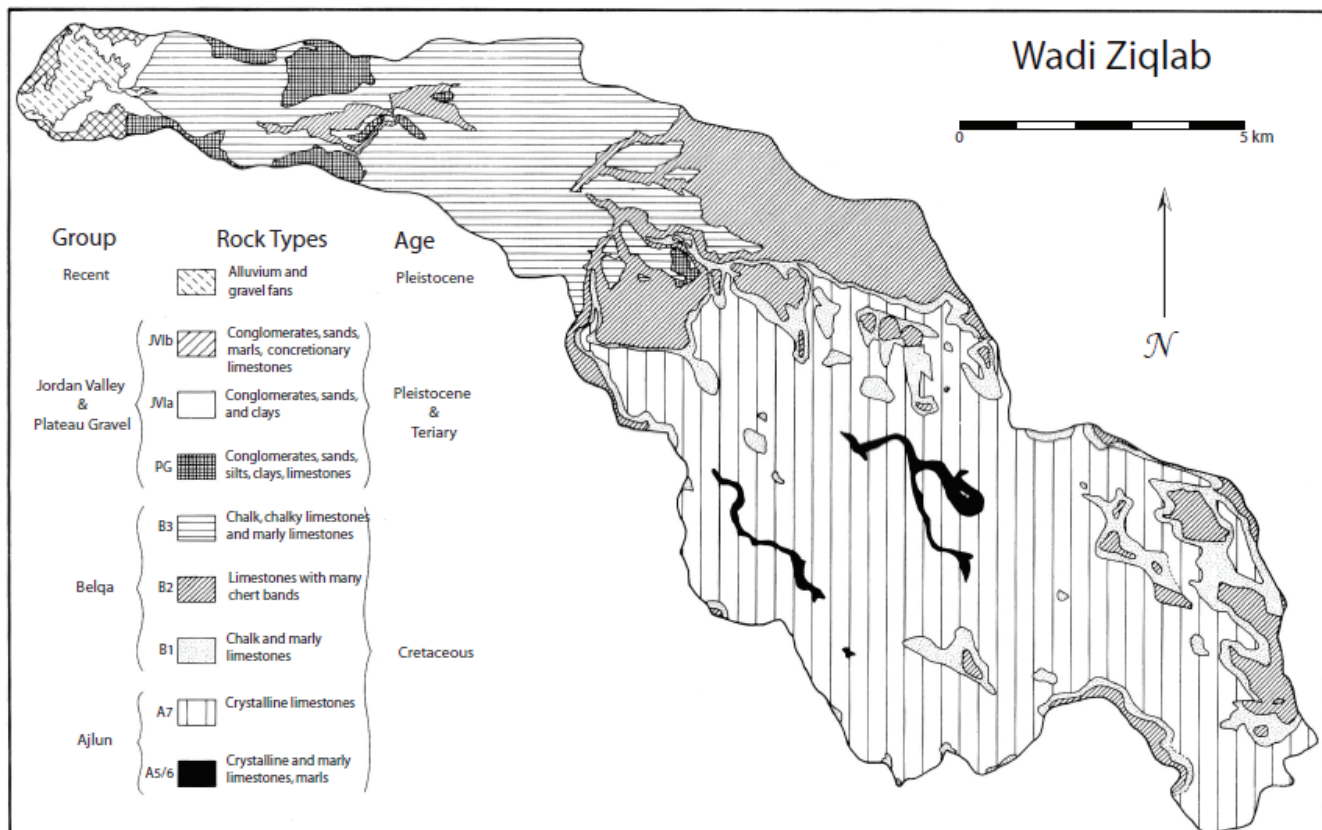


Fig. 5.8. The Fisher et al. (1964) bedrock geology map of Wadi Ziqlâb.

profiles (Förster and Wunderlich, 2009). I employ a technique that is intermediate between these two extremes—implemented in a script for GRASS (“r.soildepth”)—to create “soil depth” maps across varying topography. The method encapsulated in the script takes advantage of the known relationship between various derivatives of topography (slope and curvature) and local soil depths. The basic relationship is non-linear (Heimsath et al., 2002), but can be simplified to the following general rules¹¹: 1) All else being equal, soils tend to be shallower in areas of high slope, and deeper in areas of low slope, and 2) all else being equal, soil depths tend to be shallower in areas of high topographic convexity, and deeper in areas of high topographic concavity. The method I have developed uses these topographic rules to first construct a map of idealized soil depth “rates” across the landscape, which is then rescaled according to the known minimum and maximum soil depths in the study region (See Appendix A, Section A.4 for how soil depth “rates” are calculated).

5.3.2.1. Modeling Soil Depths in Wadi Ziqlâb

During the geoarchaeological fieldwork described in section 5.2.1.2 above, I examined remnants of undisturbed Terra Rossa soils in the uplands of the Ziqlâb catchment near the hilltop town of Tubna, reworked Terra Rossa soils on the agricultural plateau below the town of Dayr Abu Said, and several soils on the terraces in Wadi Ziqlâb itself. The best intact Terra Rossa soils are found only in the upland areas under forested conditions. Mild to moderately reworked Terra Rossas are found in most other areas of the uplands and the lower plateau, where agriculture, forest clearance, and intensive grazing have significantly altered the land cover. Soils on these remnant landforms were observed to be between 0 and ~20 m in depth. The modeled Neolithic paleotopography (created as described in Section 5.2, above) served

¹¹ It should be noted that these rules, and this method of soil-depth estimation, are meant for landscapes dominated by fluvial and/or colluvial processes. This method is not appropriate for use in landscapes dominated by other processes (e.g., arctic tundra, dunes, glaciated slopes).

as the base input to the soil depth estimation function. Without access to any real empirical information on the particular baseline relationships between slope, curvature, and soil depths of all parts of Neolithic Wadi Ziqlâb, I calibrated the soil-depth approximation function to those remnant landforms I observed during fieldwork.

Figure 5.9 shows the resulting Neolithic soil depth map derived from these initial conditions. We can see that the deepest soils are in the Wadi-bottoms and flat plateau region, and the shallowest soils on the hillslopes. This pattern aligns with our understanding of the soil depth patterns across the landscape, and provides a reasonable soil-base for the start of the LPPNB. The one abnormal pattern present in the model is that Wadi-bottoms and the flat plateau areas appear to have similar depth profiles. This is due to the inability for the soil-depth estimations routine to differentiate between flat areas at the bottom of a basin (e.g. the Wadi-bottoms) that would receive a large amount of sediment input, and those in elevated locations (e.g., up on the plateaus) that wouldn’t receive much sediment input at all. The presence of deeper-than-normal soils on the plateau region is not overly vexing, however, as these very flat areas are likely not very susceptible to erosion anyway, and clearly retain a significant proportion of their ancient Terra Rossa soils even to this day (Appendix B).

5.3.3. Modeling Soil Erodibility

Other than their depths, the other two soil properties having an effect in the models are resistivity to erosion and fertility. In the MML, soil resistivity to erosion is measured as the K-factor used in the well-known RUSLE equation, and it is measured in units of volume of erosion per unit erosive force (see Chapter 4). Measuring K-factor directly is difficult and costly, so it is usually estimated from measurable soil properties. The method most commonly used today is to use a lookup table, such as the one provided by Stewart et al. (1975), which is the method I use in this research. This method requires the soils to be first classified according to the USDA standard soil texture, which can be calculated by the USDA’s

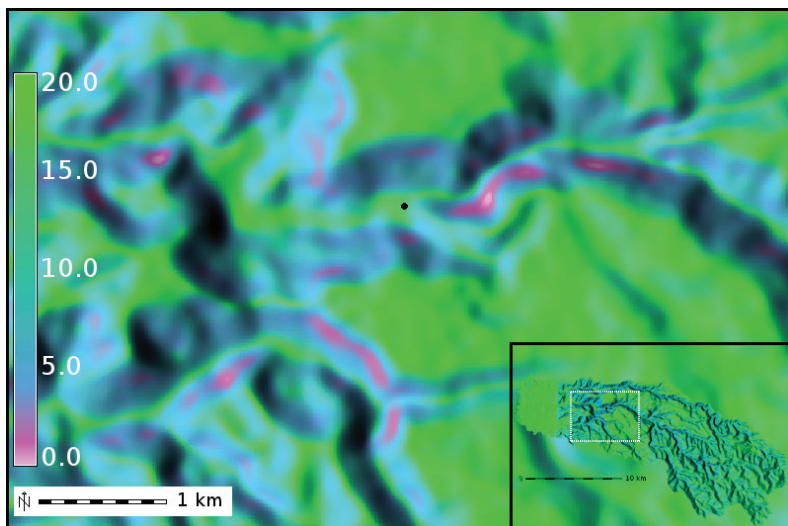


Fig. 5.9. Detail of the map of modeled soil depths in the vicinity of Tell Rakkan. Inset shows the entire project area.

online Soil Texture Calculator software (USDA, 2012) from standard soil-texture data (percent sand, silt, clay, and organic matter in the matrix).

Because soil texture and K-factor vary spatially, it is very important that the soil data be spatially explicit (i.e., GIS-compatible). The scale of the data is also important. Although very spatially detailed soil data with many subdivisions of soil types (e.g., Fisher et al., 1966) would seem to be preferable, it is counter-intuitively inappropriate to use these high-resolution data when modeling the spatial patterning of soils in the past. This is because the finer-scale patterning of soils likely has more to do with localized (and perhaps anthropogenic) erosion of ancient soils and subsequent formation of a variety of (often anthropogenic) younger soils on redeposited material over the intervening millennia¹². Many of the finer subdivisions of soil-types may thus be “artificial” in that they did not exist in the early Holocene, so using spatially coarser data with fewer subdivisions of types results in a more generalized K-factor map. This avoids the error of creating soil variations that did not exist in the past.

The SOTER soils geodatabase (Batjes et al., 2003) best meets these criteria, and so serves as the input soil data source used in the models

¹² Empirical research indicates that this seems to be true in northwest Jordan (Khresat et al., 1998b).

presented in this research. The SOTER soil data is encoded as discrete vector polygons, attached to a database with detailed soils information, including all the textural data needed to define the USDA soil texture category. I recoded the polygons according to K-factor value determined from the lookup table in Stewart et al. (1975), and then converted the map to raster format. Because of the way the original data were encoded, the boundaries between soil units are unrealistically sharp. This is problematic, as sharp boundaries will cause the landscape evolution equations (Chapter 4) to become unbalanced during calculation of flow divergence, which

tends to result in the calculation of unnaturally large amounts of erosion or deposition “spikes” in these areas. Furthermore, the coarseness of the input data (SOTER is 1:500,000) means that the geometry of these borders is also unrealistic, consisting of several long straight lines connected by sharp angles. Both of these issues can be ameliorated through a multi-stage smoothing process. First, several decreasing scales of modal moving-window filters are applied to the map, which smooths the sharp angles of the borders into gently arcing curves. The sharpness of the borders is then blurred by applying a moving-window mean-smoother with a large cell neighborhood. The resultant soil borders are unrealistically smooth with very simple geometries. In reality, soil borders are typically complex and are often convoluted or “fuzzy” (Burrough, 1989; Burrough et al., 1992). Realistic “fuzzy” border geometry is modeled by introducing stochastic “jittering” in the border regions¹³. The resulting borders are more complex and realistic than those

¹³ This is achieved by first temporarily transforming the raster soil to a vector points map with each raster cell assigned to a unique point. The geometry of this temporary vector points map is then “perturbed” by adding a Gaussian random value to the X and Y coordinates of each point (in this case with μ of 0 and θ of 80 m). The “perturbed” map is then translated back to raster format, and a medium-sized median moving-window filter is applied.

of the input data, allowing a more naturalistic transition between one soil unit and the next without inducing artificial “boundary effects” in the landscape evolution equations (Figure 5.10).

5.3.4. Modeling Soil Fertility

The fertility of agricultural soils has a large impact on agricultural yields (see Chapter 4). Thus, it is important to model the spatial patterning of variation in fertility of the soils present in the Ziqlâb region. The modern inhabitants of the Ziqlâb region exhibit clear preferences for doing agriculture on specific soils; they prefer to plant non-irrigated cereal crops on the reworked Terra Rossa soils of the western plateau, and on the brown stony soils of the lowest terraces in the wadi bottoms. But non-irrigated cereal crops are also planted on all other the soils in the region, including the colluvial soils and rendzinas of the limestone slopes. Unfortunately, it is unclear if these modern preferences relate only to the fertility of these soils, and not with their other characteristics such as ease of plowing, amount of field stones, or proximity to modern villages and roads. The SOTER data and the data collected by Fisher et al. (1966) suggest that modern soils in the Ziqlâb region do contain differing amounts organic carbon and nitrogen, the two hallmarks of soil fertility for plant growth. However, a study of different soils in Northern Jordan suggests that most modern soils actually contain a similar – and low – amount of organic matter, ranging between 0.5% and 1.1% (Khresat et al., 1998a, 1998b). Furthermore, a comparative study of soils in the Ajloun region (a few kilometers south-east of Wadi Ziqlâb) shows that soil organic material decreased by 30% after 50 years of continuous rainfed annual wheat and barley cultivation compared to a neighboring plot that retained the native pine/oak forest cover over the same period (Khresat et al., 2008). Although there was no significant difference in Potassium and Nitrogen content between the two soils, the farmed plot did show significant increases in soil bulk density and and soil pH, and significant decreases in cation exchange capacity. In general, the cultivated soils

were found to be significantly depleted of nutrients after 50 years of continuous cropping¹⁴. These contrasting reports further confuse the matter, but would seem to suggest that differences in soil fertility are largely anthropogenic. In any case, it is highly unlikely that modern patterns of farming soil fertility decline exactly match those that may have been induced by the Wadi’s Neolithic inhabitants, who lived in different locations, had vastly different farming technology than do today’s occupants, and who farmed very different varieties of grains and pulses. Furthermore, many of these modern soils were likely not present in the Wadi at all during the Neolithic, especially the colluvial soils that now cover much of the ancient river terraces where Neolithic farmers would likely have planted their crops.

Similar to modeling soil texture, modeling the spatial patterning of ancient soil fertility is complicated by the fact that modern patterns of soils—and thus fertility—are unlikely to be similar to those of the distant past. Thus we are faced with two complications: 1) high-resolution modern soil maps are inappropriate because many modern soils likely did not exist in the Neolithic, or had very different spatial patterning, and 2) modern soils likely have drastically lower amounts of organic carbon and nitrogen than did ancient soils. In light of these complications, the best solution is to assume that all soils in the Neolithic were at 100% of their respective fertility, and it is this approach used in the models presented in this research.

5.4. PALEOCLIMATE RECONSTRUCTION

Climate variables—especially temperature and precipitation—play an important role in both natural processes (affecting things such as erosion rates and vegetation growth rates) and social processes (affecting things such as farming returns and grazing patch rejuvenation). Climate is essentially a “moving average” of weather conditions that represents the “typical” weather of a

¹⁴ This is supported by an earlier study in the area around Irbid (also very close to Ziqlâb) by the same research team (Khresat et al., 1998a).

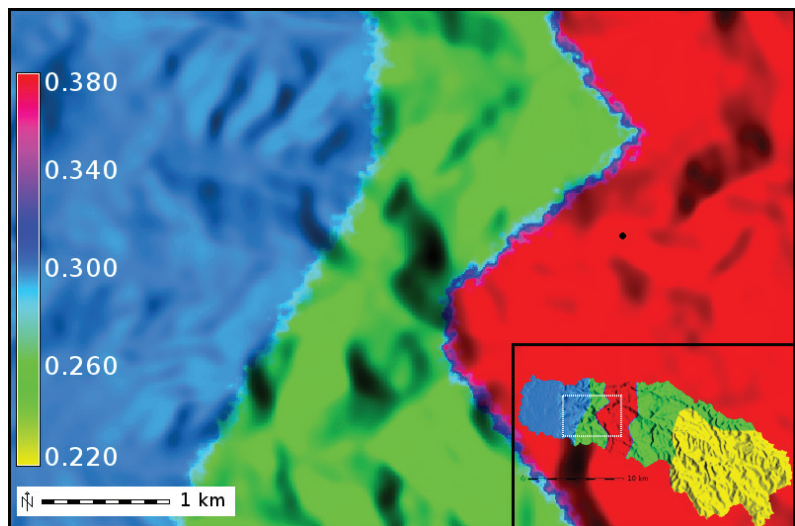


Fig. 5.10. Detail of the K-factor map in the vicinity of Tell Rakkan. Inset shows the entire project area.

region and its changes over time. It is important for the research presented here to reconstruct climatic conditions as they were during the Neolithic, rather than today, for use as input into the social and natural systems models used in the MML.

5.4.1. Methods of Paleoclimatological Modeling

There are several methods for estimating climatological conditions in the past, but they can be broken down into two general types (Bradley, 1999): 1) estimates derived from proxy records, and 2) estimates based on atmospheric physics. Proxy records include things such as pollen cores, ice cores, glacial varve records, cave speleothems, tree ring sequences, and deep-sea cores, all of which provide indirect evidence for past climatic conditions in their catchment zones (such as the composition of gases trapped in ice bubbles, the thickness and chemical composition of tree-rings, and the species composition and abundance in pollen cores or diatomaceous sediment samples).

Proxy records are widely used to gain a general understanding of how climate changed in the past, but there are some problems with using them to reconstruct the climate of a particular location (Bradley, 1999; Campin et al., 1999; McShane, 2011; Wilson et al., 2005). Firstly, because many proxy records are composed of

material drawn from very large catchments (especially deep sea cores and pollen records), they are highly subject to problems of scale. That is, it becomes difficult to understand the meaning of particular changes in the proxy (e.g., species abundance), when the size of the catchment becomes very large. Secondly, proxy records suffer from locational biases. Such records are only preserved in very specific locations, where all the necessary conditions for the production and preservation of the record exist. For example, pollen records require a moist anoxic environment in order to be preserved, and so can only be

found in places like fens, bogs, and lakes. This locational bias means that most of the time, the nearest proxy record is at quite a distance from the location of a particular archaeological site or study area and so may not perfectly reflect the climatic conditions of that site. Thirdly, the temporal resolution and temporal accuracy of the resultant climate reconstruction depends on the temporal resolution and temporal accuracy of the proxy record. If the proxy record is coarse (such as pollen records recovered from disjointed layers or features at an archaeological site), or if the dating method used to chronologically order the data is coarse or contains high inherent error (such as radiocarbon for certain periods and materials), then the climate reconstruction based on these data will be correspondingly coarse or inaccurate as well. Fourthly, many proxy records, especially those based on plant or animal remains, can be affected by non-climatic processes, including human alteration of the environment (e.g., by intentional burning or clearance). Finally, although it is arguable that reference to multiple proxies should be used to provide a more robust and fine-grained picture of past climates, many of the existing records are incompatible due to methodological differences (e.g., in classification of species, in dating methods, in sampling strategy) and so cannot be combined or even directly compared in a meaningful way. These

issues make it quite difficult (but not impossible) to use proxy records directly in the type of socio-natural systems modeling of the MML. These proxy records nevertheless provide historical data that may be directly related to climatic conditions and therefore are useful to use as comparative “checks” on the accuracy of other methods of paleoclimatological estimation. Many of the extant proxy records in the Southern Levant relevant to this study can be found in Robinson et al. (2006).

Simulation modeling based on atmospheric physics is an alternative and widely accepted method for estimating past climatic conditions. There are several different specific methods of paleoclimatic simulation, however, and each has its own merits and difficulties. Most methods fall into a general category of models that are known as General Circulation Models (GCM’s), spatially explicit models that simulate the circulation of ocean and atmospheric currents in order to estimate global- or continental-scale past climate conditions¹⁵. One downside of GCM models is that their global or continental scope make them computationally very intensive, and so typically they are run at very coarse spatial and temporal scales. “Fine” resolution GCM climate models have cell-sizes of 10 km or more, which makes it difficult to estimate the climate in a particular location. While this particular issue does not in itself preclude the use of climatological values retrodicted (“hindcasted”) by a GCM paleoclimatological model in the MML, it is a symptom of another issue with GCM modeling that does have ramifications for its use in the MML. GCM models are based solely on an understanding of broad-scale climate, and so do not, and cannot, include local information,

¹⁵ Briefly, GCM modeling is based on a knowledge of global/regional/historic processes that influence climate, such as Milenkovitch Cycles (eccentricity, axial tilt, and precession of Earth’s orbit), major volcanic eruptions and meteor impacts, the concentration of greenhouse gases and airborne particular matter in the atmosphere over time, the spatial and temporal pattern of sea temperature and ocean levels, and the spatial and temporal patterning of major ocean and wind currents. See Donner and Schubert (2011) for an excellent and thorough review of the history of development of GCM modeling, and a complete description of how GCM modeling works.

even if there are well known localized variables that influence climatic conditions in that location (Otto-Bliesner and Schulz, 2009).

5.4.2. The Archaeoclimatology Macrophysical Climate Model

Fortunately, there is an approach to paleoclimatological modeling that does incorporate localized variables in addition to allowing truly fine-scale spatial and temporal paleoclimatological retrodiction. The method, known as the Archaeoclimatology Macrophysical Climate Model (AMCM) (Bryson and Bryson, 1996; Bryson and McEnaney-DeWall, 2007; Ruter et al., 2004), retrodicts climatic variables at the locations of modern weather stations that have the standard 30-year-average climate data¹⁶. The AMCM retrodicts climate by deriving the relationship between local 30-year-average weather conditions and a GCM model. The procedure creates a multiple regression equation between local weather variables (e.g., mean annual precipitation) and influential climate phenomena (e.g., the location of the jet stream) that can be fine-tuned by the modeler. The model then uses this regression to retrodict the past climate at the location of the weather history¹⁷. The AMCM can retrodict monthly rainfall totals, monthly mean, minimum, and maximum temperature, monthly number of rain days, monthly snow fall, monthly evaporation, monthly days below 0°C, and monthly days above 40°C at 100-year intervals to 40,000 years BP, as long as these variables are present in the input data for a particular weather station.

The data recorded by the two World Meteorological Organization weather stations in or near the Wadi Ziqlâb region are in the town

¹⁶ This is the period from 1961 to 1990, as recorded by the World Meteorological Organization (World Meteorological Organization and National Climatic Data Center (U.S.), 1998)

¹⁷ It is important to note that climate change in the modern era has been shown to be the product of both natural and social processes (Griggs and Noguer, 2002; Pachauri, 2007; Solomon, 2007), and AMCM also accounts for the human contribution to atmospheric dust and greenhouse gasses in the post-industrial period.

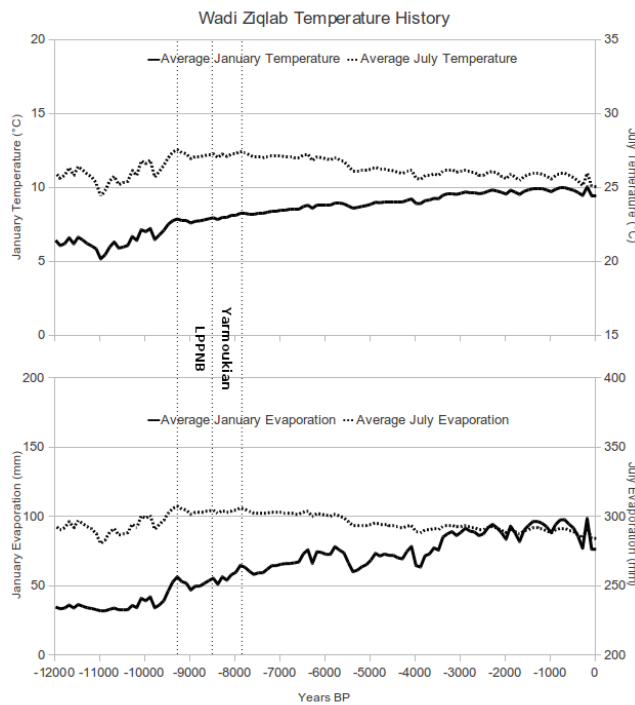


Fig. 5.11. Holocene temperature history for the Wadi Ziqlâb region, as modeled by the AMCM. All dates are in calendar years before present.

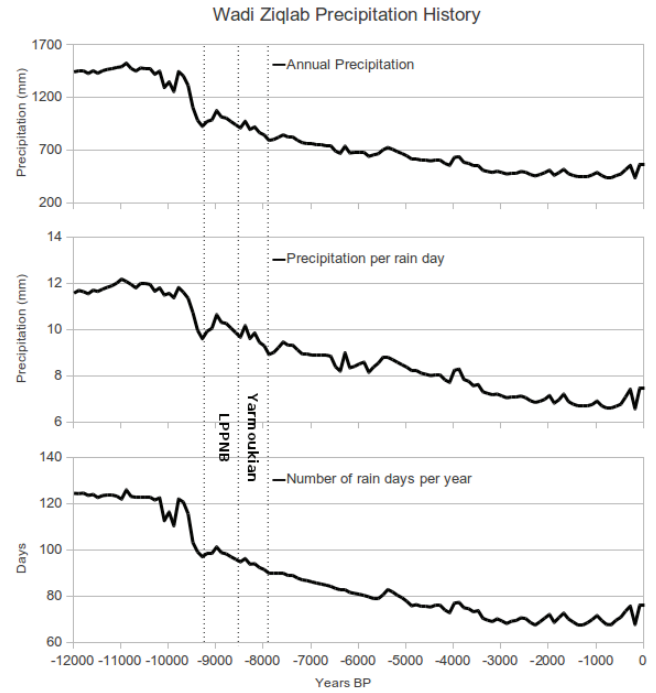


Fig. 5.12. Holocene precipitation history for the Wadi Ziqlâb region as modeled by the AMCM. All dates are in calendar years before present.

of At-Tayyiba, situated in the western plateau zone bordering the Jordan Valley, and at the Irbid nursery, in the eastern upland area. The climatic variables recorded by these two stations include monthly amount of precipitation, the monthly mean temperature, the number of rain days per month, the amount of evaporation per month, and the monthly days below 0° C or above 40° C, and so these are also the types of data output from the AMCM in the location of these two stations. Rather than choose the AMCM model output of only one of the weather-station locations to represent the entirety of the project area, I average the output for the two stations, and use the resulting mean values.

Figures 5.11 and 5.12 show the resulting temperature and precipitation histories as modeled for the Wadi Ziqlâb region over the Holocene with the LPPNB/PPNC and the Yarmoukian periods highlighted. Some interesting trends are noticeable in the model output: Summer temperatures and summer evaporation rates are actually slightly lower today than they were

in the Neolithic, but summer temperatures are not significantly different between the LPPNB/PPNC and the Yarmoukian. Winter temperatures (and evaporation rates) are significantly warmer today than they were in the Neolithic, and winters were slightly warmer in the Yarmoukian than in the LPPNB/PPNC. Precipitation amounts are likewise much lower today than they were in the Neolithic, and in general were slightly lower in the Yarmoukian than they were in the LPPNB/PPNC. Interestingly, it seems that this is because of both reduced storm frequency as well as reduced precipitation per storm event (a trend continuing until the modern day). The LPPNB/PPNC is characterized by a brief, but dramatic upswing in precipitation, which had decreased very rapidly at the end of the preceding MPPNB. By the end of the LPPNB/PPNC, precipitation amounts had dropped back to the same levels as the end of the MPPNB. The Yarmoukian is also characterized by a brief upswing in precipitation, albeit much smaller than that of the LPPNB, but precipitation

generally declined over the period and continued to do so until it stabilized in the late Holocene (with brief periods of stability in the Wadi Rabah/Early Chalcolithic, and at a few other times). The number of rain days per year also briefly surged in the LPPNB/PPNC (following a sharp decline in the MPPNB) but then generally declined over the Yarmoukian and subsequent periods.

It is also useful to understand how the seasonality of rainfall changed over time. One way to do so is to examine the average amount of precipitation that fell each month (Figure 5.13). It is interesting to note that the LPPNB/PPNC and Yarmoukian are characterized by *both* a general decrease in annual precipitation *and* significant fluctuation in the seasonality of rainfall. For example, one interesting trend is the rapid reduction of March rainfall that began in the middle of the MPPNB. Although declining, March remains the month with the heaviest rainfall throughout all phases of the Neolithic; but, by the Bronze Age, March rainfall is no more significant than that of January or February. As with the trend in annual precipitation, the LPPNB/PPNC is characterized by a brief, but dramatic upswing in March precipitation, which had decreased very rapidly at the end of the preceding MPPNB. This pattern is repeated in January rainfall to a somewhat lesser degree, and again in February to an even lesser degree. It becomes clear that the brief resurgence of higher annual precipitation in the middle of the Yarmoukian is due to an increase in March precipitation in those years, which is *not* mirrored by an increase in January and February rainfall. One other interesting pattern is the *increase* in May precipitation starting at the beginning of the LPPNB, and continuing through the Yarmoukian, Wadi Rabah/Early Chalcolithic, until eventually declining again in the middle of the Bronze Age. The precipitation rates in all other months remain relatively stable over the middle and late Holocene.

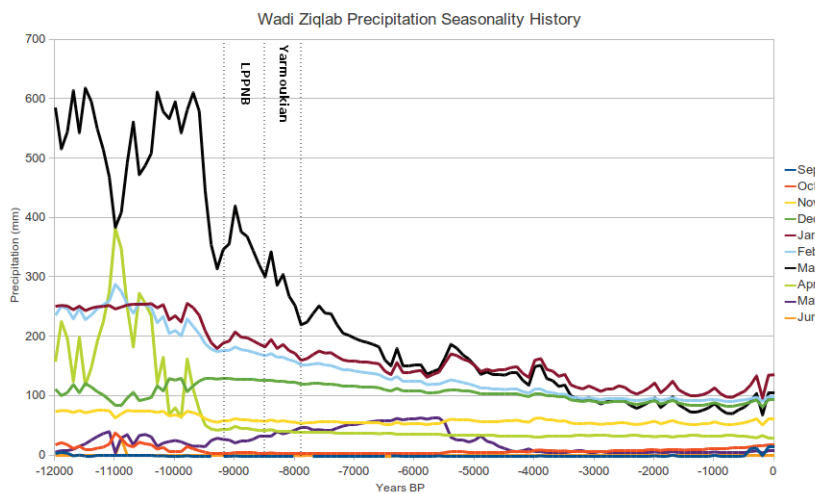


Fig. 5.13. Holocene precipitation variability history for the Wadi Ziqlâb region as modeled by the AMCM. All dates are in calendar years before present.

5.4.3. Conversion to MML Climatological Input

The particular climate variables that are required by the MML include the annual amount of precipitation, the number of storm events per year, the average length of a storm event, the average precipitation per storm event, and the R-factor (a measure of rainfall “intensiveness”). We must calculate these values from the AMCM output data: The amount of annual rainfall is simply the total of each month’s precipitation. If we assume that each rainy day equals one storm, we can use that number to estimate the annual number of storms. We can then estimate the amount of precipitation per storm by dividing the total annual precipitation by the annual number of storms. Estimating R-factor is more difficult because R-factor is actually a measure of raindrop force over time, which is information not collected by most weather stations (nor can it be directly retrodicted by the AMCM). R-factor can, however, be estimated from the AMCM output by first calculating the Modified Fournier Index (MFI, a measure of the temporal periodicity of rain events) from the monthly rainfall totals in a given year, and then deriving the R-factor

from the MFI value via a regression function developed by Renard and Friemund (1994).

Estimating the average length of a storm event is also problematic. Like R-factor, it is not recorded in the original climate data, and thus also not output by the AMCM. Unlike R-factor, however, it cannot be estimated from any of the other AMCM output. Research has shown that the average length of storms in northern Jordan in the modern era is about 8 hours with a standard deviation of about ± 4 hours (Hammad et al., 2006; Volohonsky et al., 1983). We cannot use these modern data directly, however, because it is clear that modern conditions do not match those in the past (see Section 5.4.2, above). This discrepancy not only stems from a higher number of storms (rainy days) during the Neolithic but also in a larger amount of rainfall per storm event, so it is highly likely that storms during the Neolithic were longer than those of today. In the absence of a more robust method for estimating the length of storms during the Neolithic period, I use the upper end of the 1σ confidence interval for modern storm-duration times which yields an estimate of 12 hours for the average length of Neolithic storms.

Although the MML is capable of accepting dynamic climatic variables (i.e., a list of different climatic variables for each model-year), I have chosen to use mean values for the time period being modeled (the LPPNB/PPNC). Although the climate was indeed variable within this period (as noted in Section 5.4.2, above), I have chosen to hold the climate as a constant in order to better understand the impacts of human component of the Neolithic socio-natural system. Although the specific patterning of *intra*-period climatic variability (e.g., yearly changes in climatic conditions from the beginning of the LPPNB to its end) might indeed have played a part in the instigation for the post-PPNB dispersal, it is likely that average *inter*-period variability (i.e., differences in the average climate between the LPPNB/PPNC and the Yarmoukian) will capture much of that motivation. Table 5.2 summarizes the input MML climate values for the LPPNB/PPNC and for the Yarmoukian as converted from the AMCM output.

5.4.4. Conversion to Full-coverage Climate Maps

The AMCM output from multiple weather stations can be converted to full-coverage raster maps of each climate variable using a method developed by Hill et al. (2008) that extrapolates the data from each weather station point to other points on the landscape via multiple regression against various topographic features (such as elevation, aspect, slope, distance to coast, etc.). The method must be calibrated to the climatic characteristics for the particular region, however, and so requires a fair amount of analyst expertise. Hill et al. (2008) perfected the process using the Southern Levant, however, and created maps for each AMCM output variables at 100-year intervals for the last 40,000 years at 90 meter resolution. Although these maps are not used directly by the MML, they are used to develop the paleovegetation maps that *are* used as input (see Section 5.5, below).

5.5. PALEOVEGETATION RECONSTRUCTION

Due to millennia of intensive human land-use and climate change, modern patterns of vegetation in the study region are very different from those of the past (Fall et al., 2002). It is therefore inappropriate to use modern vegetation patterns (such as those derived from classification of multispectral satellite imagery) as input into

Table 5.2. Climate variables as input to the MML for the LPPNB/PPNC and Yarmoukian periods. Values extrapolated from the averaged AMCM output for the Tayyiba and Irbid Nursery weather stations, and then time averaged across the length of each time period.

Climate Variable	LPPNB/PPNC Averages	Yarmoukian Averages
Storm length (h):	12	12
R-factor:	8.78	6.78
Precipitation per rain event (mm):	10.13	9.62
Number of rain days:	99	94
Annual Precipitation (mm):	995	895

MML simulations of Neolithic subsistence, and so we must turn to Predictive Vegetation Modeling (PVM, sometime also referred to as Species Distribution Modeling). The essence of PVM is to “decode” the complex interactions of many environmental, ecological, and geological (and sometimes also social) phenomena that interact to determine the spatial patterning of vegetation at local, regional, or even global scales.

5.5.1. Methods of Paleovegetation Modeling

The first attempts at large-scale PVM began in the late 19th century, with “snapshot” models that predicted the global spatial patterning of climax vegetation communities based on manual mathematical calculations that formalized early modeler’s assumptions about the dependence of vegetation on climatic variables (Miller et al., 2007). In the modern era, more complex PVM algorithms have been used. The most common method involves the creation of Generalized Linear Models (GLM’s), which are regression models between spatial patterning of vegetation and various predictor variables) (e.g., Davis and Goetz, 1990; Kupfer and Farris, 2007; Miller and Franklin, 2002). GLM models require many assumptions to be made about the linearity of the relationships between many independent variables and, therefore, most GLM vegetation models are provided with the caveat that they are very site-specific (i.e., not applicable to large regions) (F. Davis and Goetz, 1990). Several methods have been suggested for overcoming such site-specificity, but the most commonly used techniques boil down into two categories: more advanced “weighted regression” techniques, and decision-rule techniques¹⁸. Weighted regression models (such as Bayesian Estimators and Geographically Weighted Regression) essentially allow for the importance of specific predictor variables in the regression to change in different sub-regions based on prior knowledge (e.g., Kupfer and Farris, 2007). In contrast, rule-based methods (such as Classification Tree analysis)

are hierarchical, non-linear methods of predicting spatial variability that rank predictors and sort them according to the linkages of a boolean decision “tree”, ultimately predicting the type of vegetation in a patch by the final “branch” of the tree that is reached in that area (e.g., Miller and Franklin, 2002). Both methods result in significant improvement over the GLM methods (Kupfer and Farris, 2007; Miller and Franklin, 2002); but, in order to achieve this increased accuracy, both types of models must be highly parameterized with intimate knowledge of the many ecological relationships between the species being modeled and the predictor variables used in the modeling routine, making them quite complicated for use in paleovegetation reconstruction on a large scale.

Maximum Entropy (MAXENT) modeling – a type of unsupervised computer-learning technique – was adapted for use in PVM by Phillips et al. (2006) specifically as a way to overcome the need for prior intimate knowledge of the interrelationships needed by GWR and CT models¹⁹. The MAXENT method is conducted within a GIS-compatible open source software tool (MaxEnt 3.3 [Phillips et al., 2010]), and requires input of “presence only” data for different vegetation types at specific locations (such as that collected along vehicular or pedestrian transects during survey), and raster maps of environmental predictor variables. These predictor variables include geographic variables such as slope, aspect, elevation, soil type, and distance to nearest coastline, as well as climatic variables such as solar insolation, evapotranspiration rate, seasonal precipitation, and seasonal temperature. The MAXENT routine creates a unique set of rules governing the interaction of these variables at each input site for each known vegetation class then uses these rules to predict the probability of the existence of that vegetation class at all other points on the landscape. This automation makes MAXENT especially suited for retrodicting the spatial patterning of vegetation in the deep past because it can be used

¹⁸ See Soto-Berelov (2011) for a more exhaustive list of modern PVM techniques.

¹⁹ But it is not the only machine-learning method developed to do so. See Soto-Berelov (2011, table 5.1) for other machine-learning techniques that have been applied to PVM.

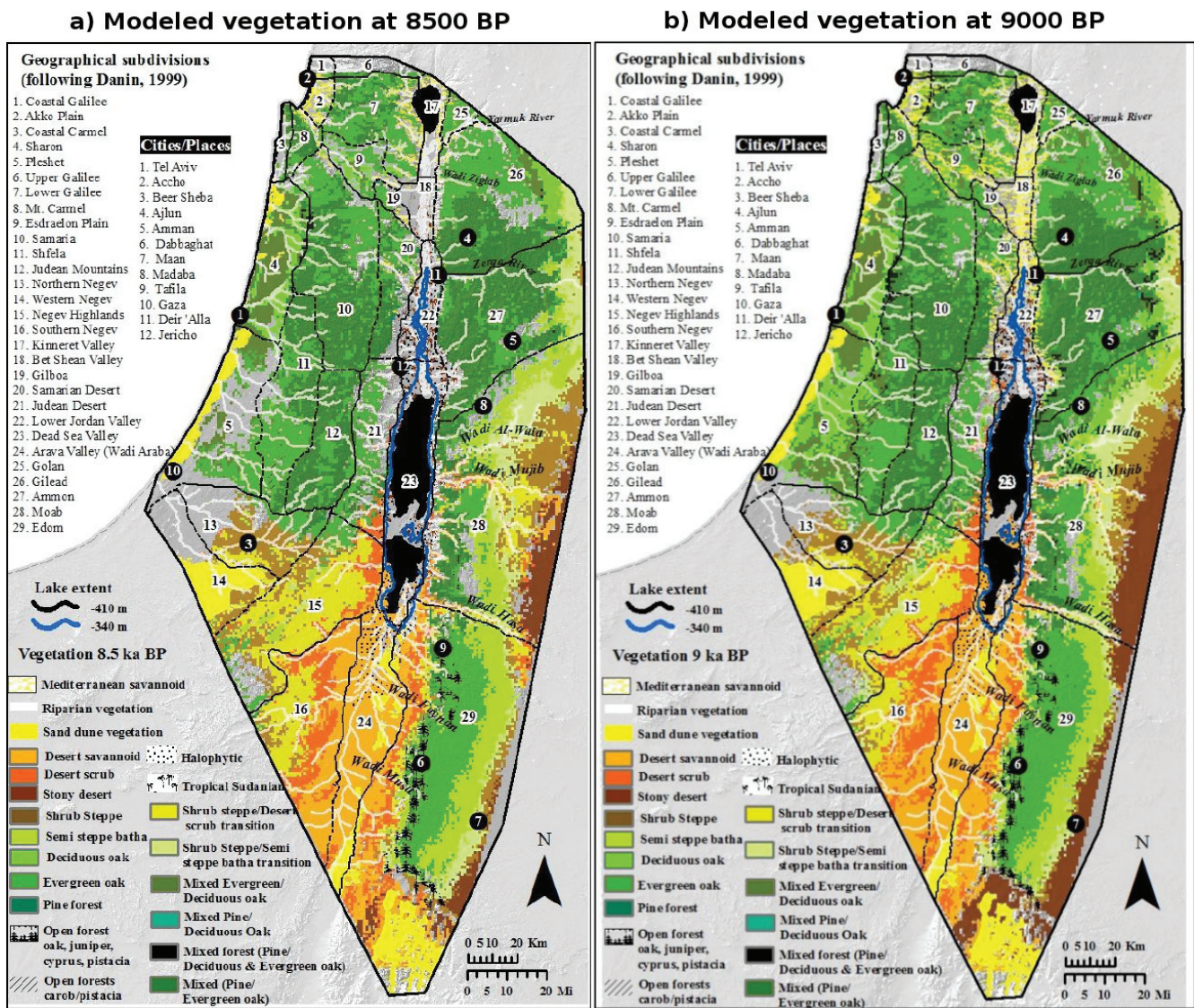


Fig. 5.14. Vegetation maps of the southern Levant as created by the MAXENT PVM for the year 8500 BP (left) and 7500 BP (right). After Soto-Berelov (2011).

directly with the climate raster map produced from the output of the AMCM model runs.

5.5.2. Paleovegetation Modeling in the Southern Levant

Soto-Berelov (2011) used this approach (i.e. MAXENT modeling with paleoclimate maps derived from AMCM data) to model the spatial patterning of vegetation over the Holocene for the entire southern Levant (Figure 5.14). She compiled an exhaustive database of historical vegetation transects across the length and breadth of Israel, Palestine, and Jordan, carefully verified

and extended by new field work, to serve as the vegetation presence input for a MAXENT PVM classification routine of the region. Furthermore, she refined the MAXENT classification by comparing its output under modern climatic conditions to those of other PVM techniques and with existing vegetation maps created from classified remotely-sensed imagery. Then, substituting the paleoclimate maps created by Hill et al. (2008), she was able to use the refined MAXENT classification rules to predict the spread of several types of climax vegetation communities at 1 km resolution at 500-year intervals from 12,000 BP to the present day. Soto-Berelov checked the

Table 5.3. Table of equivalences used to convert the MAXENT climax vegetation types to stages in the vegetation succession order used in the MML.

MAXENT Landcover Category (from Soto-Berelov, 2011)	MML Landcover Category
Evergreen oak maquis and forest, Transition deciduous - evergreen oak forest, Deciduous oak maquis and forest, Pine forest, Open forests of Juniper, Open forests of Pistacia atlantica, Open forests of carob and pistachio, open forests of juniper, oak, pistachio, Mediterranean non forest	Mature Woodlands (succession value 50)
Semi steppe batha, Transition Shrub steppe-semi steppe batha	Immature Woodlands (succession value 36)
Transition Shrub steppe-Desert vegetation, Transition Shrub steppe-Desert savannoid	Shrub Maquis (succession value 19)
Shrub steppe	Shrubs (succession value 14)
Mediterranean savannoid, Hydrophytic/Mediterranean savannoid	Grasslands (succession value 5)
Desert vegetation, Desert savannoid, Halophytic, Sand dune, Sudanian, Hydrophytic/Tropical Sudanian, Halophytic/Tropical Sudanian, Halophytic/Hydrophytic	Sparse Grassland (succession value 3)

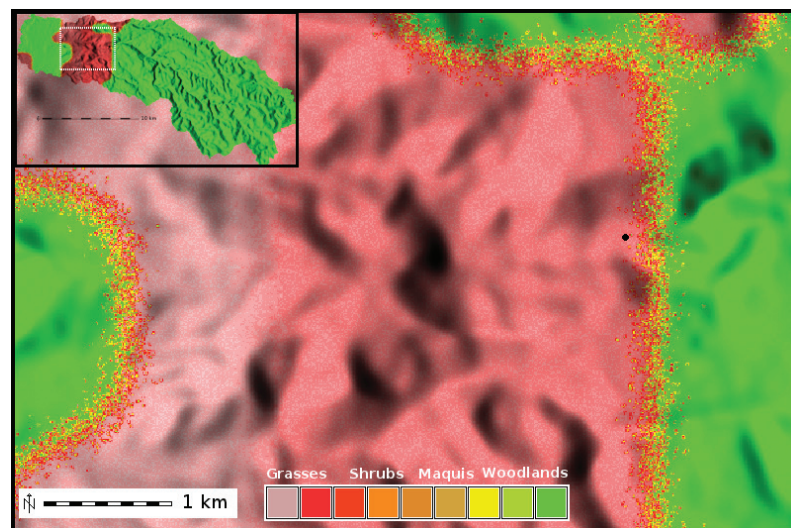


Fig. 5.15. Detail of the input LPPNB/PPNC vegetation map in the vicinity of Tell Rakkan. This map derives from the MAXENT PVM output for the year 8500 BP (Figure 5.11-a), and was converted to the MML input format according to the conversion rules defined in Table 5.3. Inset shows the entire project area.

accuracy of the produced PVM maps against available external proxy records, and by internal accuracy assessment using typical “training set”/“testing set” data separation techniques commonly applied to most types of classification analysis. It is important to note that her PVM maps predict the climax vegetation that would likely have been present at each 1 km cell *without* human interference (i.e., based solely on natural predictor variables). These climax models are ideal for use in MML modeling experiments, as they can serve both as “initial” conditions (i.e., the pattern of vegetation before intensification of Neolithic land-use at the beginning of the LPPNB) and as “boundary” conditions that constrain the upper-limit of the vegetation regrowth to the environmentally-appropriate succession level predicted by the MAXENT model for each cell at each time period. Thus, I use Soto-Berelov’s paleovegetation model for 9000 BP as the initial conditions for the LPPNB/PPNC MML simulations and as the basis for the climax vegetation conditions in throughout the period. Her paleovegetation model for 8500 BP (i.e., the Yarmoukian) is used to understand the extent of anthropogenic vegetation change after 700 simulated years of LPPNB/PPNC land-use (i.e., her 8500 BP model represents the pattern of vegetation that would have existed at the end of the LPPNB/PPNC had there been no human impacts).

5.5.3. Conversion to MML Vegetation Input

Soto-Berelov’s models cannot be used directly in the MML because she uses a different vegetation

classification scheme (i.e., she is interested in climax vegetation communities across many plant geographic zones, and not succession within one zone), and must be reclassified to fit the succession scheme used in the MML. Table 5.3 shows the equivalence rules used to complete this reclassification. Once the PVM maps are reclassified, they must be brought to the proper resolution (i.e., from 1 km to 10 m), their geometry must be refined to remove sharp angles, and the boundaries between plant communities must be softened to prevent destabilization of the landscape evolution routine in those areas. This is done in much the same way as with the SOTER soils data (Section 5.3.3, above), except that the final median-smoother window is not applied. This allows the perturbed border areas are allowed to remain “patchy”, which more realistically simulates the way vegetation transitions across ecozones (Figure 5.15).

5.6. CHAPTER SUMMARY

In this chapter, I have reviewed previous geoarchaeological work in the Wadi Ziqlâb region and have reported the results of the new work that I carried out for this project. This work makes clear the point that the Early/Middle Holocene environment of the Wadi was quite different than it is today, and underscores the need for explicit paleoenvironmental reconstruction before simulation modeling of Neolithic land-use is possible. Following this, I described the way in which the findings of the geoarchaeological fieldwork inform a GIS-based reconstruction of the physical environment during the Neolithic period. I discussed the methods I used to digitally model past environmental conditions and analyzed the resultant reconstructions of Neolithic topography, soils, climate, and vegetation. I also discussed the implications of specific details of the reconstructions, and how the reconstructions themselves will serve as input to the landscape/land-use simulations reported on in subsequent chapters.

CHAPTER 6

MODELING THE PPN-LN TRANSITION IN WADI ZIQLÂB

6.1 CHAPTER INTRODUCTION

This chapter describes the way I use the MML to better understand the conditions that led to the PPN/LN transition. First, I draw upon the archaeological data presented in Chapter 2 and the DST approach to the transition outlined in Chapter 3 to define three general types of subsistence systems that could have been in operation in PPNB Wadi Ziqlâb. I then flesh out these subsistence strategies by drawing upon the archaeological data from the PPNB (Chapter 2), and ethnographic data (introduced in this chapter). These data are used to parameterize the MML (as described in Chapter 4) for each of the three subsistence systems. Finally, I devise a series of modeling experiments to systematically vary a small number of key aspects of each potential PPNB subsistence system. This allows for a better understanding of the long-term dynamics of different aspects of subsistence and extended knowledge of the implications of subsistence choices on long-term resilience and vulnerability.

6.2. COMPOSING PPN LAND-USE MODELING EXPERIMENTS

The goal of the MML modeling experiments conducted in this research is to better understand the sequence of events that led to a major social transition visible in the archaeological record, but before any such experiments can be conducted, the economic and social aspects of the MML must be parameterized to reflect Neolithic lifeways¹. But what is the best way to do that? The fragmentary nature of the archaeological

record—especially that of Tell Rakkan I—precludes direct parameterization of the model from archaeological data alone. Furthermore, the current picture of life in Neolithic Levant suggests that there were a variety of agropastoral subsistence systems simultaneously in existence across the region and over time (Asouti, 2006; Asouti and Fuller, 2012; Conolly et al., 2011; Rollefson, 2004; Zeder, 2008), so we also cannot use a better preserved/studied PPN site in the region (such as ‘Ain Ghazâl) as a direct analog for the PPN lifeway of Tell Rakkan I. The same issue arises for ethnographic data; we cannot pick just one ethnographically known group to be used as an analog for PPN subsistence at Tell Rakkan I.

We must nevertheless use data from modern and ancient peoples who live(d) in similar environments to Wadi Ziqlâb and practice(d) a similar lifeway to that which we believe was practiced by Neolithic people in the Wadi. But how do we choose which values to use, and from which particular modern or ancient society and/or geographic area to choose them from, without falling into the trap of strict ethnographic analogy (i.e., as originally conceived of by Gould [1978] and others)? It is precisely this conundrum that the simulation modeling approach is designed to address. Since we cannot know “the” lifeway of the Neolithic inhabitants of Wadi Ziqlâb, several plausible scenarios for subsistence at Tell Rakkan I must be constructed, simulated, and compared to archaeological reality.

I generate such scenarios through the following process: 1) Basic numerical data on subsistence-based agropastoralism in Mediterranean environments are collected from as wide a variety of ethnographic datasets as possible, 2) these data are collated, and the spread and central tenancies of each parameter are tabulated and collected into a central database, and finally, 3) the aspects of the

¹ The environmental and physical aspects of the MML must also be parameterized to the natural conditions of the Neolithic period, but I have already discussed how this was accomplished in Chapter 5.

system that are most likely related to the cause of the PPN/LN transition are identified and a series of simulation experiments are designed in which these aspects are varied systematically across a reasonable parameter-sweep. It is important to note that although this process may utilize aspects of ethnographic data, it is nevertheless a scientific approach to the study of past lifeways, and not an analogical one (Wylie, 1985).

6.2.1. Parameterizing Neolithic Subsistence Behavior

Of the discrete subsistence systems identified in the analyses presented in Section 6.2, PPN economies in the Wadi Ziqlâb region are most likely to have been within the “subsistence pastoralism”, “mixed agropastoralism”, or “intensive agriculture” adaptive basins, so it is necessary to conduct modeling experiments for each of these three subsistence types. To do so, I have compiled a database of plausible values for the basic socio-economic/socio-ecological underpinnings Neolithic subsistence. These data derive from an extensive literature review of ethnographic, archaeological, and agronomic research relating to traditional small-scale subsistence systems based on sheep/goat pastoralism and wheat/barley agricultural with ancient or primitive/heirloom breeds/cultivars in Mediterranean environments. Although quite a bit of diversity exists within the database, I have chosen to hold the basic components of each of the three possible Neolithic subsistence systems (agriculture, agropastoralism, and pastoralism) constant, and only vary a few key components of the systems that relate directly to the amount of time people spend engaging in pastoralism versus farming. Thus, the three modeled subsistence systems differ only in the ratio of reliance on (and thus effort expended to produce) animal products versus cereal crops. “Agriculturalists” must obtain 80% of their diet from cereals and 20% from animal products, “agropastoralists” require a 50% mix of cereals and animal products, and “pastoralists” need to obtain 80% of their diet from animal products and only 20% from cereals. The

other components of the subsistence system do not change between models and are based on averages calculated from the compiled ethnographic database. They are reported in Table 6.1, and it is also important to note that individuals in all three subsistence systems are assumed to require an average of 2500 “agropastoral kilocalories” per day in order to remain healthy². Production in each of the three modeled subsistence strategies is therefore tuned to this goal.

These strategies are implemented in the MML by adjusting the yearly per capita kilocalorie goals for both agricultural and pastoral subsistence activities to match the ratios reported above. Poc (the number of ovicaprids per person) in equations 4.2 and 4.3 (Chapter 4), must also be adjusted to meet these goals (see Table 6.2). Both of these factors affect the yearly land-use plans created by the agents by changing the ratio of the amount of land planned for use growing wheat and barley versus that planned for grazing. They are set at the start of a model run and remain constant throughout the length of the run.

6.2.2. Parameterizing Neolithic Wood Gathering Behavior

Because the effects of firewood and structural timber gathering are important aspects of one of the hypotheses being tested, proper parametrization of this behavior is essential. Ethnographic data suggests that small scale subsistence agropastoralists consume 1600-4300 kg of firewood per person per annum (Bhatt and Sachan, 2004; Fleuret and Fleuret, 1978; Fox, 1984; Karanth et al., 2006; Naughton-Treves

² Greer and Thorbecke (1986) report a “food poverty line” of about 2250 daily calories for subsistence agropastoralists in Kenya. (Hartter and Boston 2008, 2007). They and Thomson et al. (1986) report a daily caloric intake of about 3500 calories for subsistence agropastoralists in Uganda and northwest Syria, respectively, and that these calories come almost completely from agropastoral products. The PPN inhabitants of Wadi Ziqlâb consumed a significant quantity of wild resources, and although the exact proportion of the PPN diet derived from agropastoral products is unknown, I assume a 70/30 split between agropastoral and wild resources, thus producing a 2500 daily agropastoral caloric need.

Table 6.1. Table of economic and ecological data used to parameterize the models of PPN subsistence systems.

Data type	Data		Source
<i>Pastoral product yields</i>	<i>Baladi Goat</i>	<i>Awassi Sheep</i>	
Milk output (kg/yr):	200	60	Degen, 2007
Milk energy (kcal/kg):	753.6	1005.6	Mavrogenis and Papachristoforou, 1988
Percent milk not suckled:	66%	66%	Nablusi et al., 1993; Epstein, 1982
Percent milch animals:	36%	20%	Nyerges, 1980
Milk yields (kcal/yr):	99475.2	39821.76	Calculated from the above
Meat output (kg/animal):	10.09	14.88	Sen et al., 2004
Meat energy (kcal/kg):	1090	2300	USDA, 2011
Percent meat animals:	25%	25%	Nyerges, 1980
Meat yields (kcal/yr):	10998.1	34224	Calculated from the above
Goat:Sheep Ratio:	2	1	Ullah, 2011
Average yield (kcal/yr/animal):	38560.597	16520.352	Calculated from the above
<i>Herd animal attributes</i>	<i>Baladi Goat</i>	<i>Awassi Sheep</i>	
Body weight (kg):	40	70	Wilson, 1982; Epstein 1982; Degen, 2007
Fodder requirement (kg/yr/head):	584	894.25	Stuth and Sheffield 1991
Percent diet from barley fodder:	10%	10%	Thomson et al., 1986
Wild fodder need (kg/yr/head):	525.6	804.825	Calculated from the above
Barley need (kg/yr/head):	42.05	71.54	Calculated from the above
<i>Agricultural Product Yields</i>	<i>Barley</i>	<i>Wheat</i>	
Energy yield (kcal/kg):	3000	3540	Smith, 2006; Fairbairn et al., 1999
Maximum possible yields (kg/ha):	2500	3500	Pswarayi et al., 2008; Araus et al., 1998, 2001
Seed reserve:	15%	15%	Hillman, 1973
Required labor (man days/ha/yr):	50	50	Dabasi-Scheng, 1978
<i>Wood gathering</i>			
Wood need (kg/person):	2000		Karanth, 2006
Gathering intensity (kg/m ²):	0.08		Karanth, 2006
<i>Labor and planning</i>			
Maximum farming distance (hrs):	3		Estimated from McCall 1985
Maximum grazing distance (hrs):	8		Ullah, 2011
Farm yield expectation scalar:	75%		Estimated from Grisley and Kellogg, 1983
Labor availability (man days/yr):	300		Estimated from McCall 1985
Wood gathering distance weight:	3		Estimated from Karanth, 2006; Hartter and Boston, 2007, 2008

et al., 2007; Reddy, 1981) and that they gather wood at an intensity of between 0.06 and 0.09 kg/m² (Karanth et al., 2006). The rates of use and gathering intensity depend upon the actual use and style of domestic hearths, cooking methods, winter temperatures and house types, and the general character of the vegetation in near the village. In the models presented here, I use a wood need of 2000 kg/pers. per year, and a gathering intensity of 0.08 kg/m², which is consistent

with the firewood needs of the inhabitants of an agricultural village like PPNB Tell Rakkan (e.g. domestic cooking and heating with occasional plaster-making [Asouti and Austin, 2005]).

6.2.3. Parameterizing Neolithic Population Dynamics

Based on an archaeological estimate of the size of Tell Rakkan I (Banning and Najjar, 1999;

Table 6.2. Table showing the values of the independent variables used to create the six modeling experiments.

	Good pastoralists	Good agropastoralists	Good agriculturalists
Agropastoral ratio:	20/80	50/50	80/20
Ovicaprids per person:	26	17	7
Herd stocking rate:	~0.15 animals/ha	~0.15 animals/ha	~0.15 animals/ha
Farming fertility decline:	1% per yr	1% per yr	1% per yr
	Greedy pastoralists	Greedy agropastoralists	Greedy agriculturalists
Agropastoral ratio:	20/80	50/50	80/20
Ovicaprids per person:	26	17	7
Herd stocking rate:	~0.3 animals/ha	~0.3 animals/ha	~0.3 animals/ha
Farming fertility decline:	2% per yr	2% per yr	2% per yr

Banning, 2001, and also see the discussion about Tell Rakkān I in Chapter 3), I chose to begin the simulation experiments with an initial population of 60 people evenly divided into 10 households³. Households will grow or die off over time according to the basic demographic model outlined in Chapter 4. Human population dynamics are extremely important drivers of change in socio-natural systems, however, so it is important to parameterize the demographic model to plausibly simulate Neolithic population dynamics. Archaeologists have estimated the total population growth rates of prehistoric agricultural groups to be between 0.05% and 0.1% (Bocquet-Appel, 2002).⁴ There is general agreement that subsistence-based agriculturalists have an average birth rate of 6.6% (Bentley, 2003), but little consensus has been

reached regarding death rates. In order to derive some estimate of plausible Neolithic death rates, a member of the MedLanD team conducted ABM experiments of demographic growth (Bergin et al., 2012). These experiments used the accepted birth rate as a given constant, and iteratively stepped through various death rates until the rate of overall population growth was within the limits of the archaeologically known rates. The research indicated that death rates of 5.2% and 5.7% represent the extremes of the accepted continuum of hypothetical prehistoric agricultural population rates (Cowgill, 1975), and these values are used as the “base” rates in the experiments discussed here.

6.2.4. Constructing Simulation Experiments for the PPN/LN Transition

3 I chose to start the simulation with an initial population that was well below the estimated maximum population that could have been housed at the site in order to allow the population to increase to meet any natural “equilibrium” that might exist and to avoid artificially large initial impacts derived from beginning with an impossibly large population. It should also be noted that while Byrd and Banning (1988) estimate PPNB houses to hold only 3-4 people, Banning (2003) also points out that “houses” do not necessarily equal “households” in the PPN. Therefore I chose to use an initial household size of 6 people, which derives from ethnographic data reported by Hillman (1973) and Kramer (1980; 1982).

4 Although research by Eshed et al. (2004) using skeletal material from the Levantine PPN suggest a higher population growth rate of 0.5% to 1% in that period, issues with the severe sample bias within the existing PPN skeletal collection raise serious doubts about the accuracy of this estimate.

I use the three hypotheses for the instigation of the PPN/LN transition laid out in Chapter 2 to devise a series of modeling experiments. To do this, I vary three key socio-ecological aspects of the plausible Neolithic subsistence system described in the previous sections. These variables are: 1) the ratio of farming to herding, 2) the density at which people stock herd animals in a grazing catchment, and, 3) the amount to which farming practices reduce soil fertility. I created three ratios of farming to herding to delineate three subsistence variants (Table 6.2): Agricultural, Agropastoral, and Pastoral. I then varied herd densities and soil fertility impacts to create two subsistence “mindsets” for these three subsistence

variants (Table 6.2). The “Good” subsistence mindset parameterizes agent land-use decisions to have a minimal impact on soil fertility under continuous usage (i.e., soil fertility is partially replenish with manure, compost, or other fertility-enhancing practices). A “Good” mindset also means that agents will try to achieve herding goals in a minimally invasive way by stocking herd animals at low densities (i.e., agents will attempt to use a larger grazing catchment for a particular number of herd animals). Thus, a “Good” mindset should lead to sustainable subsistence, but likely at the cost of slower growth. The “Greedy” mindset, on the other hand, parameterizes agent land-use in a manner that should yield faster returns, but which may have more severe and longer-lasting impacts. “Greedy” agents are less concerned about maintaining soil fertility and so undertake farming practices that can lead to a decline in fertility under continuous usage (i.e., they implement no proactive fertility conservation practices). “Greedy” agents will also attempt to extract more calories from their grazing lands by stocking herd animals at a higher density (i.e., they will use a smaller grazing catchment for the same number of animals). “Good” versus “Greedy” mindsets are implemented in the MML by changing the soil fertility impact value according to Table 6.2, adjusting the value of G_i (the “grazing impact factor”) in equation 4.12 (Chapter 4) to equal the stocking rates reported in Table 6.2.

6.2.5. Emergence and Experiment Repetition

Emergent phenomenon are an important aspect of complex systems, and the MML was designed to allow emergence (see discussion in Chapter 3). Therefore, even when starting from identical initial conditions, no two model-runs will evolve in exactly the same way. In fact, the degree to which the same initial conditions may result in vastly different outcomes is a meaningful and very important characteristic of human subsistence systems that relates to their resilience and vulnerability to change (see Chapter 3). All else being equal, a system that displays a high capacity for emergence over short to medium time-

spans is highly adaptable and resilient, but also potentially unpredictable at these time-spans as well. In contrast, non-resilient systems may appear to be relatively stable over short to medium time-spans, but may bifurcate catastrophically in some model runs (i.e., they may pass through a critical transition to an alternative stable state). This is also a kind of emergence, but one which occurs within longer time-scales. It is therefore essential to have a way to measure (or at least understand) the potential for emergence at different time-scales in each of the different simulated PPNB subsistence systems discussed above. The only way to achieve this is to repeat each of the individual simulation experiments multiple times and to visualize and measure the variability between each repeated run. That is the approach I have taken in this research⁵. Not all experiments result in significant variability between repeated runs (i.e., not all systems will have a high potential for emergence), however, and due to the amount of time and computer-power required to complete model-runs, I chose to focus my available computing power on experiments that seemed to have a high capacity for emergence after two consecutive runs⁶. Thus, while all experiments were repeated at least twice, experiments that showed divergence were repeated up to ten times. Although I believe this was a reasonable

⁵ Note that this reason is different from, but not necessarily contradictory to, the often-cited argument for repetition of model-runs in simulation studies, which is that aggregate statistics compiled across all repeated runs provide a confidence-interval on the general trend of a simulation run (i.e., aggregation controls for random model errors or stochastic variability) (see Galán et al., 2009). In the case of complex phenomena, aggregation will actually obscure the dynamics of the system and will not allow the identification of multiple stable states or other indicators of complexity.

⁶ Note that in the early version of the MML used in this research, there existed a memory bottleneck that exponentially slowed the run time of a simulation as the agent population increased. Therefore, the agricultural runs, which all achieved very high agent populations required run-times on the order of two or more weeks, limiting the number of repetitions that were feasible. In any case, none of the agricultural runs exhibited a tendency for extreme emergence over the 700-year time-span of this set of model runs. This bottleneck is fixed in the recently released public version 1.0 of the MML (Barton et al., 2015).

compromise for the current research, future research should follow a protocol of fewer experiment variants with more repetitions per variant.

6.3. CHAPTER SUMMARY

In this chapter, I have set up a series of experiments designed to help us better understand the dynamics of human subsistence system in the PPNB. I have set up and parameterized three different potential Neolithic subsistence

types: “agriculturalists”, “agropastoralists”, and “pastoralists.” The general character of these three modes of subsistence derive from the archaeological data from Wadi Ziqlâb and other PPNB sites in northern Jordan, and fleshed them out with data from research into modern groups engaging in similar subsistence activities. The series of modeling experiments will also test slight differences in subsistence mindsets, to better understand the potential for emergence, change, and catastrophe in potential Neolithic subsistence systems.

CHAPTER 7

RESULTS AND DISCUSSION

7.1 CHAPTER INTRODUCTION

In this chapter, I present the results of the modeling experiments described in Chapter 6 (Table 6.2). “Good” and “greedy” variants of agricultural, agropastoral, and pastoral subsistence were simulated, for a total of six sets of experiments. Each experiment was run for 700 annual cycles (i.e., the approximate length of the PPNB/C) with reconstructed PPNB/C climate, environment, and topography (see Chapter 5). The MML produces a prodigious amount of output data, including basic statistics for each modeled year about village and household population, yearly erosion/deposition, amount (area) of each vegetation type, soil fertility, and soil depth. These measures have been used in previous MML research to examine the effects of population, site location, and climate on the amount of human-caused environmental degradation, among other things (Barton et al., 2012, 2010a, 2010b; Ullah and Bergin, 2012). I use these and other statistics to compare the dynamics of subsistence in each of the different modeling experiments. I focus on diachronic trends in human population, landcover/vegetation, soil properties, and erosion and deposition rates. In particular, I will investigate how these experiments inform us about the potential for gradual and rapid change in Neolithic subsistence systems. I pay close attention to the evidence for potential “early-warning” indicators of rapid change or critical transition to an alternative system state (e.g., differences in resilience, multiple stable states, and stochasticity in time-series patterning, Chapter 3, Figures 3.6 and 3.7) (Scheffer, 2010; Scheffer et al., 2012, 2009). I also look for feedback relationships between scales/components of the different potential Neolithic SES (e.g., “Remember”, “Revolt”, “Disinterest”, Chapter 3, Figures 3.2 and 3.3). Finally, I frame

these findings in terms of the opportunities and limits afforded by each of the modeled subsistence strategies (agriculture, agropastoralism, and pastoralism) and mindsets (“good”, “greedy”).

7.2. POPULATION

The temporal dynamics of human population informs about the overall system-potential, system-stability, system-emergence potential, and system-resilience of a particular subsistence system. Furthermore, demographic data are relatively intuitive and familiar to archaeologists, and so may be a useful proxy measure to bridge simulation to archaeological cases. In this section, I examine the temporal patterning in village population over the 700 years of each model run.¹

7.2.1. Average Population Levels

I have aggregated the population data from all realizations of each experiment, and plot these as time-series in Figure 7.1. In these time series plots, I separate “good” mindsets from “greedy” ones, and plot each of the three subsistence variants separately for each mindset. The average population trendlines for all realizations of each experiment are shown as solid lines, and the range of variation across all realizations are shown as shaded areas around these trendlines. An initial observation of these time series data is that there is an initial “ramp up” period that occurs at the instantiation of every model-run when agents are loosed upon a “virgin” landscape². After this

¹ In this section, I am only examining the patterning of the total village population and not the populations of each individual household. Calculating household population over time in the version of the MML used in this research is very difficult. The newer version of the MML has been improved to facilitate this.

² This typically results in a dramatic initial increase in

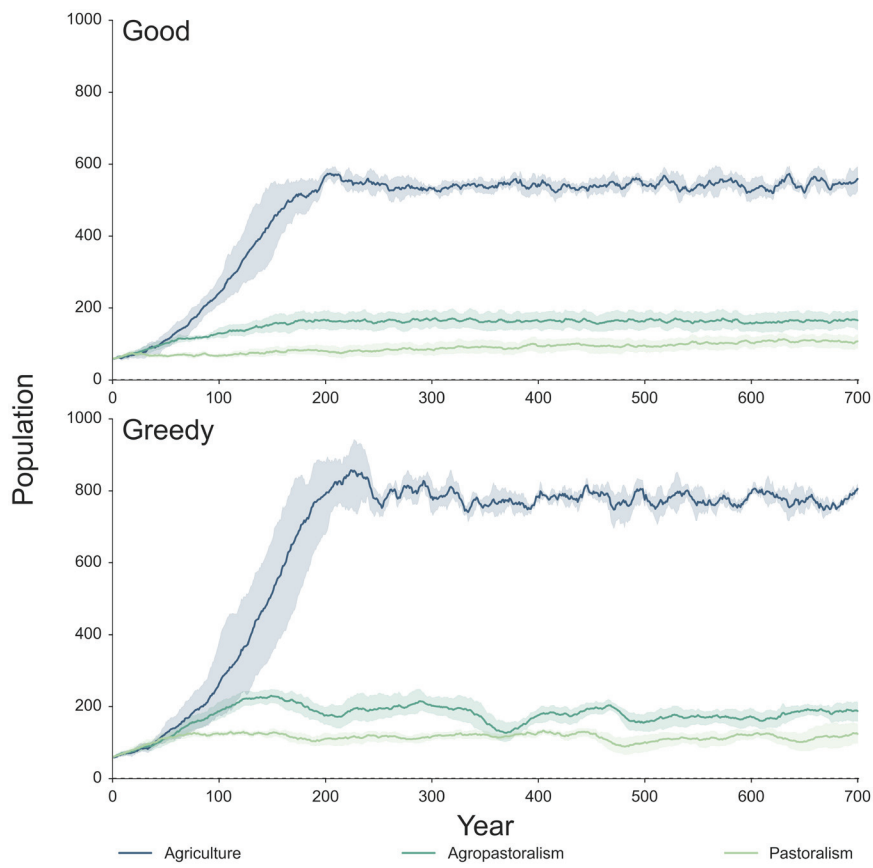


Fig. 7.1. Time-series plots show the trends in human population dynamics for Agriculturalists, Agropastoralists, and Pastoralists in each experiment. Solid lines show the mean of all realizations of each experiment. Shaded regions are the 99% confidence interval of these means. Top: “Good” model variants. Bottom: “Greedy” model variants. Agriculture results in much larger human population levels than pastoralism or agropastoralism. Greedy mindsets can result in greater short to medium-term unpredictability in population for all models.

initial rampup, each of the three subsistence strategies resolve to different population levels over time. Table 7.1 summarizes the maximum, minimum, and average³ “post ramp-up” populations achieved for each experiment. These values represent the rounded averages across all realizations.

Several interesting trends are visible in the data presented in Table 7.1. First, the three subsistence types result in markedly different

population, reaching a first “peak” before falling to some sort of equilibrium or to random or repeated fluctuation.

³ For models that had more than one stable state (see below), average population sizes were recorded for each state (indicated in Table 7.1 by a slash).

ranges of average population. Further, agropastoral and pastoral subsistence produce internally similar average populations, respectively, regardless of mindset. This is not true for the agricultural models, where realizations of the “good” subsistence variant resolved to much lower population levels than those of the “greedy” model variant. Finally, although there is a clear separation between subsistence strategies when looking only at the average population level, examining the maximum and minimum populations “post ramp up” populations shows some overlap between them. There is more significant overlap between all variants of pastoralism and agropastoralism, however, than there is between those of agriculture and agropastoralism.

7.2.2. Population Stability

While the summary statistics listed in Table 7.1 provide some interesting initial observations, they mask a great deal of temporal patterning and variability present in the raw time-series data. I looked at the raw population time-series for all individual realizations of all experiments to discern four general categories of temporal patterning: 1) “Metastable” trajectories that achieve a dynamic equilibrium around a single stable population state over time, 2) “Multi-stable” trajectories that have two or more periods of stability at different population levels 2) “Unstable” trajectories that more drastically fluctuate in population over time, and 4) trajectories that begin as “Metastable” or “Multi-stable”, but which trend to “Unstable” over time. While Figure 7.1 does not show the individual time-series traces for each realization of

Table 7.1. Table of population sizes and population stability measurements for each experiment.

Approximate “Equilibrium” Population Level(s)			
	Agriculturalists	Agropastoralists	Pastoralists
<i>Good</i>	550	200	70/125
<i>Greedy</i>	800	200/~300	70/130
Max and Min Population Levels (across all runs)			
	Agriculturalists	Agropastoralists	Pastoralists
<i>Good</i>	625, 490	235, 180	150, 40
<i>Greedy</i>	950, 700, 625	360, 280, 70	250, 160, 40, 25

Table 7.2. Summary of demographic stability patterns for all experiments.

Overall Population Stability (between all runs)			
	Agriculturalists	Agropastoralists	Pastoralists
<i>Good</i>	Metastable	Metastable	Multi-stable
<i>Greedy</i>	Metastable	Trending to Unstable, Unstable	Multi-stable, Trending to Unstable

each experiment, indications of these patterns are visible in the patterning of the across-realization experiment means and error envelopes that it does show. For example, the error envelope of the “greedy pastoralism experiment increases over time, which is an indication that many of the realizations trended towards instability over time. Another example is the “greedy agropastoralist” experiment, where the mean population trend line achieves different stable states over time. Table 7.2 summarizes the general population stability patterning for each of the modeling experiments. Interestingly, there is a clear association of “Metastability” with agriculture, and “Multi-Stability” with pastoralism. Agropastoralism, however, can lead to either “Metastability” or to instability, depending upon subsistence mindset. The presence of “Multi-Stable” population trajectories in the experiment results is especially interesting in relation to the idea of multiple stable states and hysteresis between them.

7.2.3. Population Cyclicity

The presence of hysteresis is important in

relation to the concept of critical transition, so a measure of cyclicity within modeled population trajectories is important. Looking again at the general population time-series diagrams in Figure 7.1, it is also apparent that several trajectories appear to be oscillating at regular intervals (i.e., they are hysteretic). Periodicity (or “Cycle Width”, to use the term coined in Chapter 3) in time-series data can be assessed through a procedure known as Lag-1 Autocorrelation, which can give an empirical assessment of the presence and character of hysteresis within model output. Lag-1 Autocorrelation works by calculating the correlation coefficient of two identical copies of a time-series as they are iteratively “lagged” against one another in single time-step increments. This produces a plot of correlation coefficient at different “lags”, or “cycle widths”, measured in years. I conducted Lag-1 Autocorrelation on the population time-series for all realizations of each of the experiments, and then plotted the across-realization mean trendline and error envelopes in Figure 7.2. These plots also show a 95% confidence interval produced by a lag-1 autocorrelation of a “white noise” (random) time-series of equal

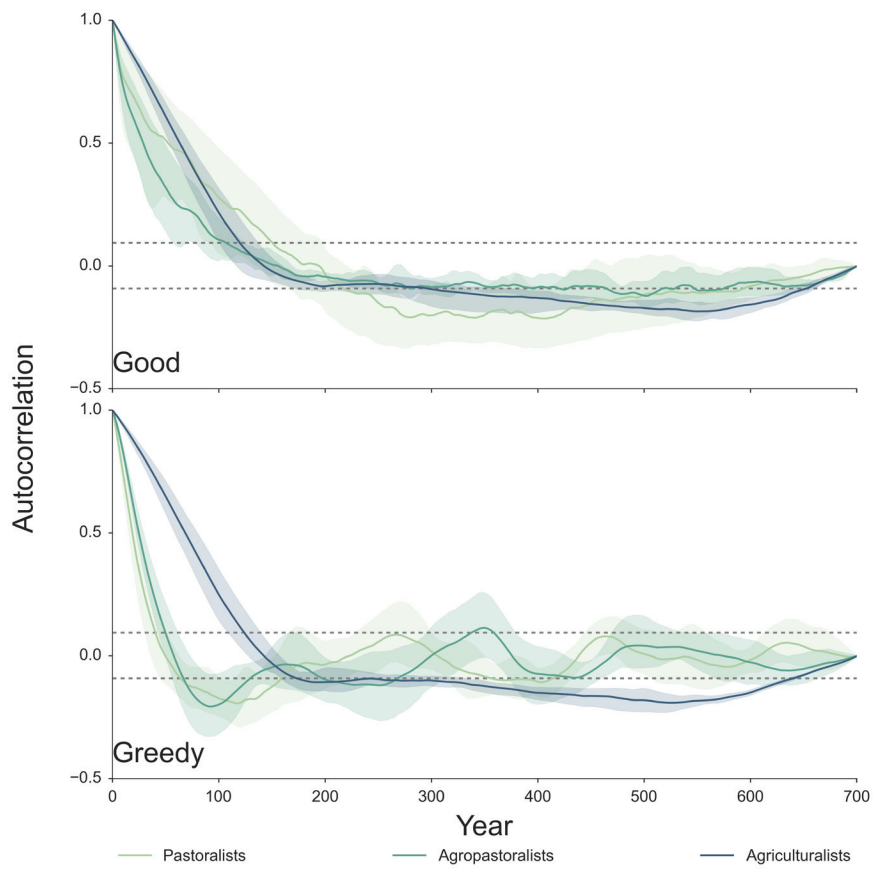


Fig. 7.2. Lag-1 autocorrelation plots of human population time-series shown in figure 7.1. Solid lines show the mean of all realizations of each experiment. Shaded regions are the 99% confidence interval of these means. The dashed lines are the 95% confidence limits of a montecarlo lag-1 autocorrelation simulation of a white noise data set. Lag-1 autocorrelation reveals cyclical patterns in time-series data. Autocorrelation values above or below the limits of those derived from the white noise data set are considered important. Here we see that the “Good” mindsets produce very little cyclical patterning in human populations, whereas “greedy” mindsets appear to produce population cycles every 250–350 years for pastoralists and agropastoralists, but not for agriculturalists.

length. If the correlation coefficient exceeds this confidence interval at a particular lag time, then that time period can be considered a significant scale of repeated oscillation in the time-series trajectory.

Several things are apparent from the results of this analysis. Firstly, all experiments were highly autocorrelated at very short lags (up to about 50 years), indicating the presence of very short-term oscillation in population in all subsistence variants. Secondly, all agricultural subsistence

variants and the “good” variants of pastoralism and agropastoralism remain highly autocorrelated up to medium time-scales (up to about 150 years). This is clearly related to the “Metastability” of these runs, where they achieve a relatively short-term oscillation around a stable dynamic equilibrium. The remaining “greedy” variants of agropastoralism and pastoralism exhibit a second strong scales of cyclicity at about 250 and 350 years, respectively. This is clearly related to the tendency of these subsistence variants to produce unstable population trajectories, which vary widely over time. It is interesting to note that this variation seems to be quite regular at small time-scales, and potentially also again at a larger time-scale. This may suggest that the variation is not random, and may be a sign of a cyclical set of feedbacks. In this sense, these “unstable” population trajectories might be better understood as “highly dynamic equilibria”. Finally, “good” pastoralism exhibited a wide variety of autocorrelation between repeated runs, as indicated by the large error envelope for this experiment in figure 7.2. Some

runs result in a very large, continuous range of significant autocorrelation (from 1 year up to about 300 years), other runs result in only short or very short-term periods (up to only about 30 years), and still other runs have medium-term autocorrelation (up to about 100 years). This is clearly related to the exact timing of hysteresis (“flipping”) between alternative stable states, which is not consistent between runs (i.e., the “flip” can occur at any point in a model run).

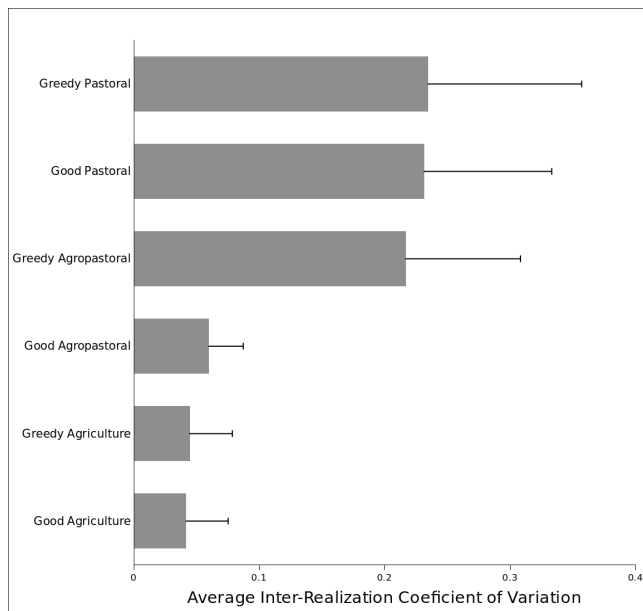


Fig. 7.3. Average inter-realization variability in human population across all 700 years for each of the experiments. Error bars show the standard deviation (in the positive direction only). Agriculture always results in low variability between each experiment realization, whereas pastoralism always results in higher inter-realization variability. Agropastoralism exhibits a phase change, where the “good” mindset results in low inter-realization variability, but the “Greedy” mindset” results in high inter-realization variability.

7.2.4. Inter-Run Variability in Population Trends

A relatively simple statistical method to assess inter-run variability is to calculate the coefficient of variation in absolute population between model runs at each model-year for each experiment and then to calculate the average and standard deviation of yearly coefficient of variation over all 700 years. These measures are summarized in Figure 7.3 as modified box-plots for each experiment. In this figure, low average coefficients of variation indicate minimal inter-run variation over time, whereas high coefficients of variation indicate large inter-run differences. Interestingly, pastoralism

always produced high inter-realization variability, regardless of the mindset given to the agents. Agriculture, on the other hand, always resulted in quite low inter-realization variability. Finally, and most interestingly, agropastoralism exhibits a clear phase change where the “good” variant resulted in low inter-realization variability, but the “greedy” mindset produced high variability. This phase change indicates that the landuse mindset of agents may only be important under certain combinations of subsistence activities, but that it can be quite significant when it does have an effect.

7.3. VEGETATION DYNAMICS

Vegetation is a good proxy for system potential (especially related to the grazing potential of the system) and for the amount of interconnection between the human and natural components of the SES. Vegetation is highly dynamic in both the spatial and temporal dimensions, so both dimensions must be analyzed.

7.3.1. Spatial Pattering of Vegetation

Figure 7.4 shows an example map of vegetation from each of the modeling experiments. These maps were selected from years of high population numbers, and so show the maximal impact of human activity on vegetation. Visually comparing the spatial patterning of vegetation types on these maps provides a basic understanding of the different sizes and spatial configurations of the catchment, or “zone of impact”, of the different modeled human subsistence activities around the site of Tell Rakkan I. The size of a subsistence catchment is related to both the overall population being supported and the general amount of land required for the type of subsistence being practiced (Ullah, 2012). Thus, it is unsurprising that agriculturalists clearly require the largest farming catchments (in fact, the “greedy” agricultural experiment required the entire watershed for human subsistence activities), pastoralists the smallest, and agropastoralists an intermediate-sized catchment. We would also expect “greedy” model variants require larger catchments than their

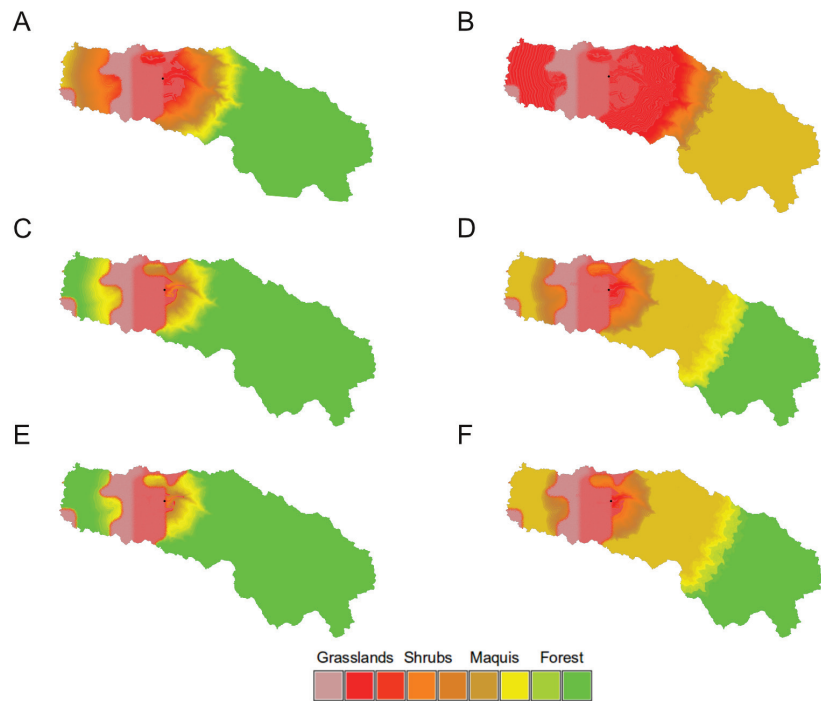


Fig. 7.4. Example “high population” landcover maps for all runs of all models. A: Good Agriculture, B: Greedy Agriculture, C: Good Agropastoralism, D: Greedy Agropastoralism, E: Good Pastoralism, F: Greedy Pastoralism. The agricultural subsistence variant has a much larger environmental footprint than do agropastoralism or pastoralism. Likewise, a “Greedy” mindset increase the size of the footprint and severity of the impact of each subsistence variant.

respective “good” variants – which we can also see clearly when comparing the maps. However, it is somewhat surprising that the vegetation patterns produced by “greedy” pastoralism and “greedy” agropastoralism are quite similar, and are *more* severe than that produced by “good” agriculture. This suggests, once again, that mindset can have a surprising affect on the dynamics of human landuse and consequent impacts on local environments.

Focusing on the spatial patterning of the different vegetation classes depicted on these maps shows differences in the spatial configuration of human landuse activities, and how these relate to landcover change. In all modeled subsistence strategies, there are areas of grassland in the immediate vicinity of the site. These are anthropogenic grasslands, which are

either cultivated or fallowed farm fields. Beyond these grasslands, there exists a transitional zone of shrubs and maquis. These are also anthropogenic, but are created by grazing over time. This transitional zone is much larger in the “greedy” model variants, as are the grasslands produced by farming.

7.3.2. Temporal Patterning of Vegetation

While visual assessment of the maps of peak-population landcover provide a good initial assessment of the maximum amount and location of vegetation impact each modeled subsistence strategy might produce, this approach does not reveal how these impacts accrued or changed over time. The MML outputs a landcover statistics file that records the amount of area given over to each of the 50 landcover classes in every year of a simulation run. These data can be analyzed in a variety of ways, but the simplest is to calculate

the coefficient of variation in the spatial extent of each landcover class over time (i.e., across all 700 years) for all simulation runs, which can then be averaged for each experiment and plotted together (Figure 7.7) so that the temporal variability of each landcover class for every experiment can be directly compared. Plots of this nature have been used in previous MedLanD research (Barton et al., 2012, 2010b; Ullah and Bergin, 2012), and the method of interpreting them has been described in depth in those publications. In general, gazing and woodgathering tend to produce plots that show increased variability of maquis and young woodlands than would have occurred in the absence of humans. This is due to the “top-down” impact of these activities, manifesting in a slow attrition to climax vegetation, which tends to

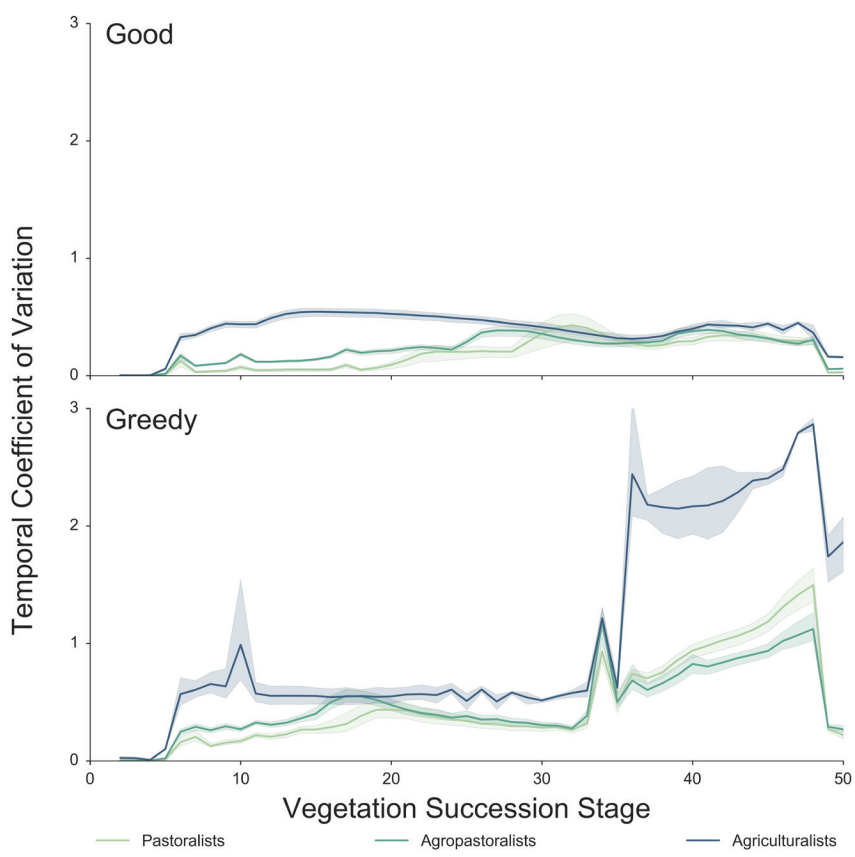


Fig. 7.5. The coefficient of variation in the spatial extent of each of the 50 landcover types over the entire 700 years for each of the modeled subsistence strategies shows which vegetation types are most affected by each subsistence variant. Solid lines show the mean of all realizations of each experiment. Shaded regions are the 99% confidence interval of these means. Bare and grasslands are on the left of the plots, whereas maquis and woodlands are on the right. The shape of the resultant “curves” show the types of vegetation that are most affected by human landuse. Pastoralism and agropastoralism are general skewed more to the right, whereas agriculture is generally left-skewed. A “greedy” mindset results in a greater impact to forests for all three subsistence variants, and increases the impact on shrubs and maquis in agropastoralism and pastoralism.

increase biodiversity in grazing catchments, as long as the catchments are not over-grazed (Barton et al., 2010b; Perevolotsky and Seligman, 1998). Farming, on the other hand, tends to produce plots that show massive increases in the amount of grasslands. This is due to the “bottom-up” impact of farming, which “instantaneously” changes the landcover of a patch to grassland, typically

leading to reduced biodiversity in agricultural catchments (Barton et al., 2010b). These “vegetation variability” plots thus can show the relative importance of farm-plot clearance, ovicaprid grazing, and firewood gathering in affecting land-cover change between the experiments. That is, the balance of “top down” to “bottom up” disturbances will create a unique curve in the plot of vegetation-type variability, and the form of this curve (size, shape, number and location of peaks) can be used to interpret the specific combination of disturbance types in a given subsistence model.

Looking at the variability plots for each of the twelve models (Figure 7.5), several patterns are apparent. First, “good” model variants produced the expected pattern that the agriculturalist models should produce a vegetation variability curve skewed to the left (i.e., “bottom up”), pastoralist models should produce a variability curve generally skewed to the right (i.e., “top down”), and that agropastoralists should have a non-skewed curve (i.e., “top down” and “bottom up” balancing to mainly disturb secondary succession

vegetation communities). Second, “greedy” model variants produced much more landcover variability in general than did “good” model variants. However, rather than a simple amplification of the variability patterns produced by “good” land-use, “greedy” land-use resulted in fundamentally different variability. Chiefly, being “greedy” resulted in a large increase in “top down” effects

for all models. Some of this is certainly due to the greater yearly impact to vegetation in grazed plots caused by a higher ovicaprid stocking rate, in addition to increased firewood gathering due to generally larger populations in these models. But in fact, it is the “greedy” agriculturalist models in which the largest increase in a right-skewness manifests. This is counterintuitive to the expectations that it is grazing and woodgathering that cause right-skewed curves, as these models were among those with the lowest amount of grazing. They did have the largest populations, so woodgathering was likely very intense. These subsistence regimes also resulted in very large farming catchments, so field clearance and regrowth dynamics on the edges of this catchment may also be driving much of this right-skewed variation. This last idea is supported by the additional observation that being “greedy” also seemed to add additional left-skew to all subsistence models. This is likely due to increased rotation in the fallow-cycle because of heavier yearly fertility loss in these models. Finally, although there were some minor differences between “lazy” and “hardworking” model variants, being “lazy” did not lead to markedly different variability patterns, which again runs counter to expectations.

Another way to look at vegetation variability over time is to calculate a measure of the diversity of vegetation types at each time step, and to construct a time-series plots of this biodiversity for each model run. I measured plant biodiversity using Simpson’s Index of Diversity

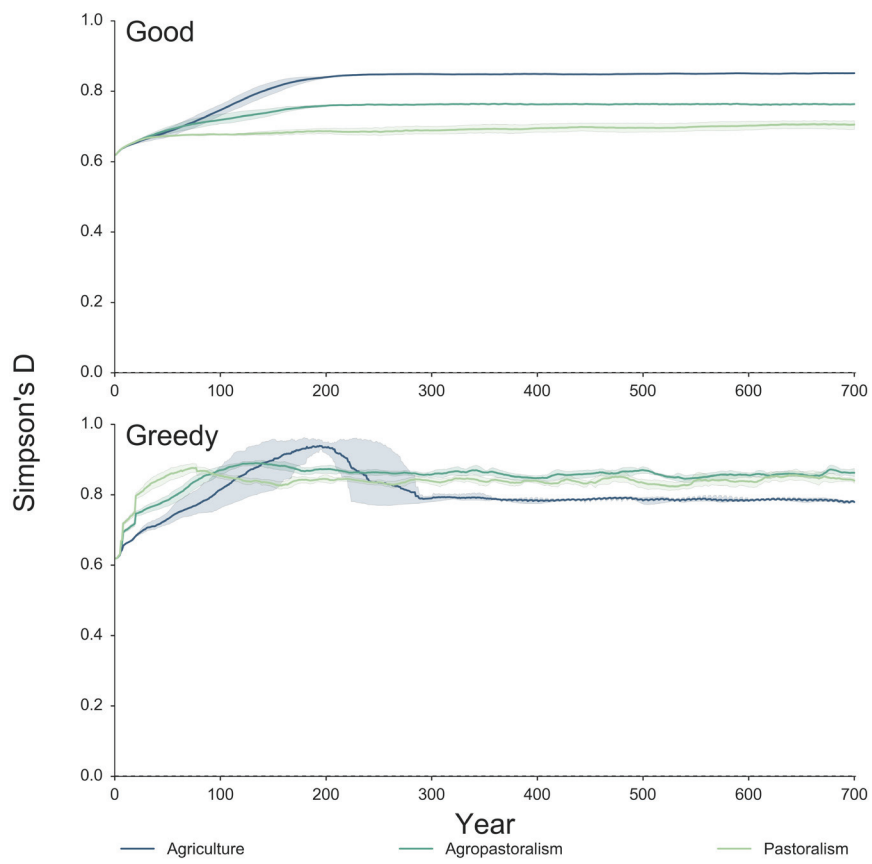


Fig. 7.6. Time series plots of the “Simpsons D” statistic derived from the maps of vegetation in every year show how plant biodiversity changes over time in each experiment. Solid lines show the mean of all realizations of each experiment. Shaded regions are the 99% confidence interval of these means. Human landuse increases biodiversity over time in every experiment. “Good” mindsets produce stabilized levels of biodiversity after an initial period of equilibration. “Greedy” mindsets produces less diverse plant ecologies, however, and biodiversity can vary over time.

(frequently referred to as “Simpson’s D”), which is a simple and widely-used measure of ecosystem diversity calculated as the proportion of each individual species in relation to the total number of species present in the ecosystem. Simpson’s D is measured on a scale of 0-1, where 0 is no diversity (all individuals in ecosystem are from one species), and 1 is maximum diversity (all species represented in equal quantities). In order to use this index, I considered each of the 50 plant succession stages as individual “species”, and used the areal coverage (square meters) of each

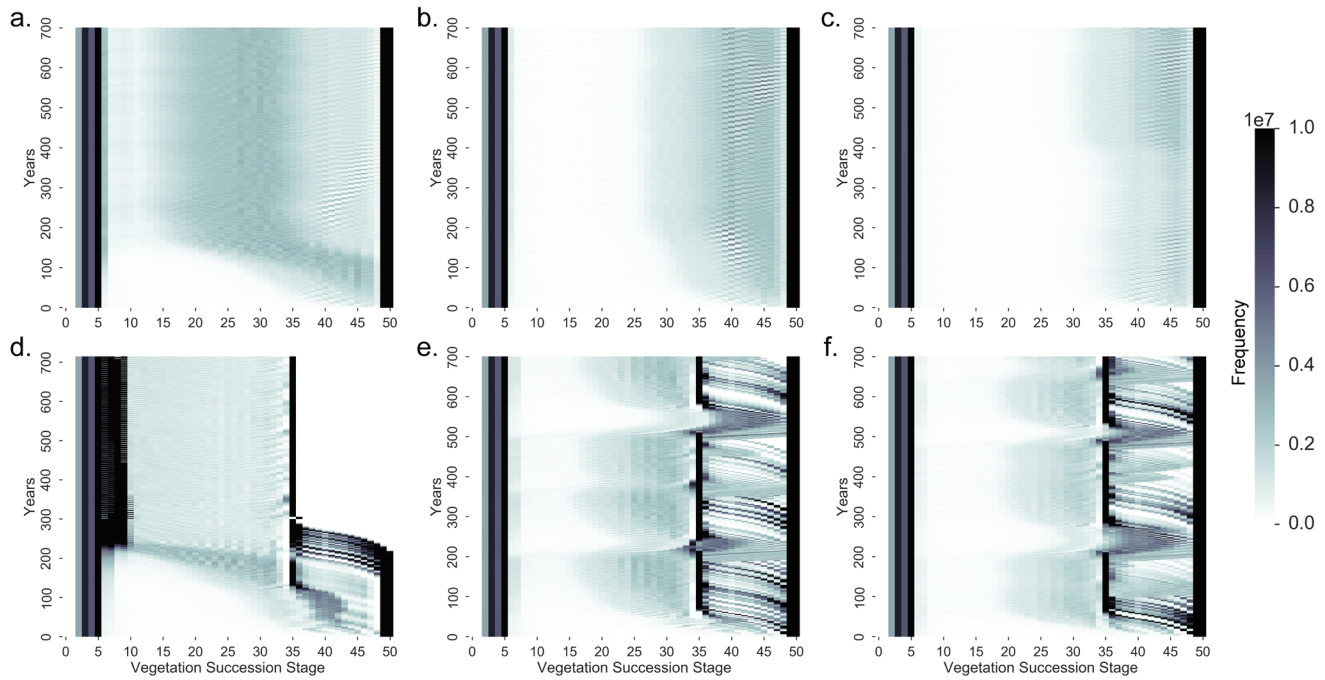


Fig. 7.7. “Heatmap” plots of the frequency of each vegetation type over time reveals temporal dynamics in vegetation impacts. Bare and grasslands are on the left of the plots, whereas maquis and woodlands are on the right. Each row shows the frequency of these vegetation types in a particular year. Darker colors are higher frequencies, and lighter colors are lower frequencies. A: Good Agriculture, B: Good Agropastoralism, C: Good Pastoralism, E: Greedy Agropastoralism, D: Greedy Agriculture, F: Greedy Pastoralism. “Good” mindsets produce fairly even temporal dynamics for all subsistence types. “Greedy” mindsets, however, produce cyclical impacts to maquis and woodlands for pastoralists and agropastoralists, and results in total deforestation for agriculture.

vegetation type in any given year as a measure of the “number of individuals” present in the ecosystem.

The resultant biodiversity time-series plots for all experiment runs are shown in Figure 7.6. Several interesting patterns are visible in these plots. Firstly, all types of human land-use resulted in *increased* biodiversity. This is counter to the commonly-held notion that human landuse tend to *reduce* the diversity of the natural components of ecosystems. Some land-use strategies had a larger affect on biodiversity than others, however. “Greedy” agropastoralists and pastoralists had similar amounts of temporal variability (stochasticity) in biodiversity and more variability than the other models. All pastoralist models, and the “greedy” agropastoral models had similarly elevated amounts of between-run variability (again, shown as the shaded areas

around each trendline). “Greedy” variants of the agropastoral and pastoral models produced similar patterns of biodiversity over time, and both produced generally higher amounts of biodiversity than their “good” counterparts. Interestingly, and opposite to the above trend, the “greedy” agriculturalists produced *less* biodiversity than their “good” counterparts over time. However, the “greedy” agriculturalist realizations produced an initial “spike” in biodiversity, in which the maximum possible biodiversity score was nearly achieved. This initial spike co-occurs with the timing of the initial population growth “ramp up” for that experiment seen on figure 7.1. Unlike the population ramp up, which flattens out, the spike in biodiversity rapidly declines to a much lower level. It seems clear that this initial surge and subsequent decline in biodiversity is related to

both the right-skewness of the temporal vegetation curves and the total eradication of forests by the end of the “greedy” agriculturalist experiment. Furthermore, that this “spike” occurred early in the simulation indicates that it may have been created by some sort of boundary condition (i.e., the population outgrew the available land). Biodiversity did eventually stabilize in these realizations, however, supporting the idea that once this boundary condition was met, some kind of carrying capacity had been reached. The time-series trendlines for all the experiments are slightly negatively sloped, however, indicating that biodiversity reduces over time in these anthropogenic landscapes, albeit very slowly.

Yet another visualization technique can help make more sense of the *dynamics* of vegetation change over time. This technique, known as a “heat map” or “wavelet plot”, is a rasterization of a statistical matrix in which numbers are replaced by a color ramp. In this case, the matrix was composed of the spatial extent (measured in number of cells) of each of the 50 vegetation classes at all years of the model. The x-dimension of the matrix represents each of the 50 landcover classes (with succession stage increasing to the right), and the y-dimension represents time (with time progressing “up” from the bottom). The resulting heat map diagram offers a simple visual

representation of the timing of change across all vegetation classes at once, and so is a powerful heuristic device for discovering subtle patterns not easily-noticeable with other techniques.

Example heat maps from individual runs of each of the six experiments are shown in Figure 7.7. Comparing these plots reveals interesting differences in the temporal patterning of vegetation change between the different experiments. First, a clear differentiation exists between “good” and “greedy” variants for all subsistence types. All “greedy” variants show a marked increase in variability of landcover class 36 (immature woodland) after the first 50 to 200 years of simulation. The “top-down” nature of grazing and wood gathering suggest that they are the human activities that most likely produced this effect. The specific landcover value of 36 like has to do with the agent decision algorithms for choosing grazing and wood gathering patches under the “greedy” mindset, as immature woodlands will produce the largest combined yield of fodder and firewood. It is likely, then, that there exists a boundary condition for all “greedy” subsistence, that results in a net increase of those forest types that support large flocks. What is especially interesting is the different way in which these models respond to this boundary condition. The “greedy” agricultural models result in total

Table 7.3. Summary of general trends in population dynamics for each experiment type as revealed by Lag-1 Autocorrelation (see Figure 7.2).

Autocorrelation Time Spans (all realizations)					
		Agriculturalists	Agropastoralists	Pastoralists	
Good	Short through medium time scales	Short and long time scales	Variable between runs		
	Short through medium time scales	Short and long time scales	Short and long time scales		
Greedy	Short through medium time scales	Short and long time scales	Short and long time scales		
	Strong	Strong, very weak	Strong or weak	Strong, strong or weak	
Autocorrelation Cycle Width Strength					
		Agriculturalists	Agropastoralists	Pastoralists	
Good	Strong	Strong, very weak	Strong or weak		
	Strong	Strong, strong or weak	Weak		
Greedy	Strong	Strong, strong or weak	Weak		
	Strong	Strong, strong or weak	Weak		

Table 7.4. Summary of inter-realization variation in population for each experiment.

Long-term Population Variability Trends (inter-realization)			
	Agriculturalists	Agropastoralists	Pastoralists
Good	Decrease	Decrease	Increase
Greedy	Decrease	Fluctuates	Increase

deforestation within the first few years of reaching the boundary condition, suggesting that it acts more like a “brick wall” for a highly agricultural subsistence base. The pastoral and agropastoral models experience temporary deforestation which then oscillates over time as the forest regrows and then is cleared again. Furthermore, for pastoralists, this oscillation appears fairly regular, but for agropastoralists, it is more random. In general, all of these “greedy” strategies lead to a reduction in the number of vegetation communities present on the landscape over time, in favor of those that are more productive for grazing and/or agriculture. As the number of landcover types decreases, humans must rely on a less diverse palette of vegetation for grazing and woodgathering which suggests that the level of connectedness of the pastoral-ecology component system increases as the number of vegetation communities decreases.

There is some equally interesting patterning among the heat map diagrams of the “good” subsistence strategies as well. First, there is a clear difference between the wavelet patterns of “good” agriculture and those for “good” agropastoralism and pastoralism. The main difference between these two groups is in the size of impact to the spatial extent of grasslands and shrubs: the latter group has a relatively small effect, while the former has a relatively large. This corresponds to expectations about the “top down” nature of grazing impacts versus the “bottom up” nature of farming impacts. Second, “good” pastoralism exhibits clearly visible oscillation in vegetation extent at fairly large timescales, suggesting some large-scale cyclicity in ecosystem change. Finally all “good” variants exhibit small-scale temporal oscillations in the woodland vegetation range (classes 35-50). These oscillations occur at slightly different intervals for each subsistence

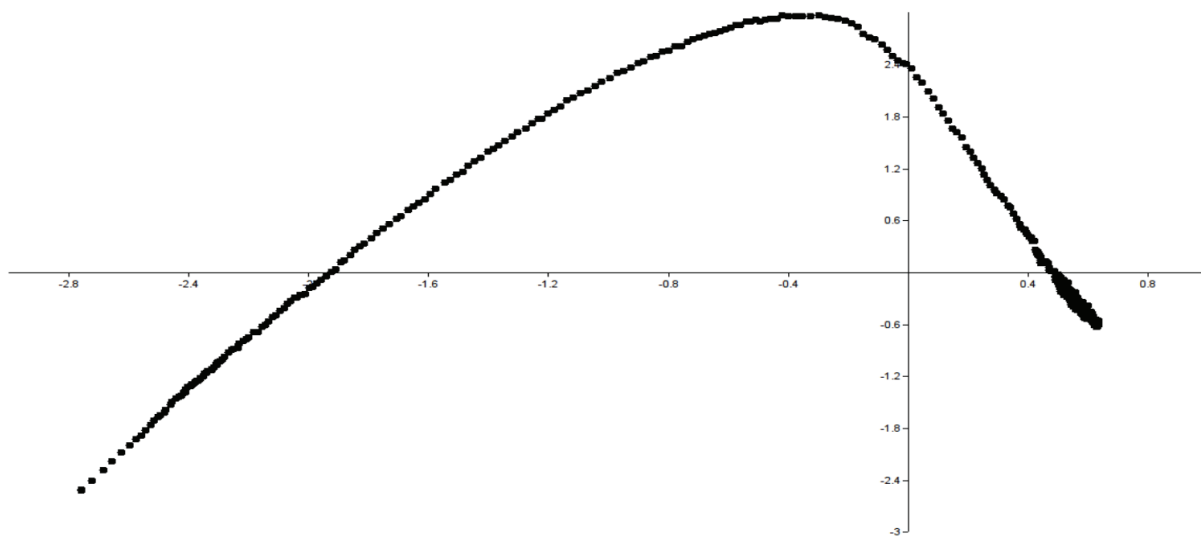
and their intensity seems to change repeatedly over time. It is unclear what is causing these, but they may indicate some finer-scale interactions or patterns related to the maximum succession values of vegetation communities in the different parts of the project region (i.e., the climate-induced caps on vegetation in different areas of the region).

7.3.3. Landcover Dynamics and Population Stability Patterns

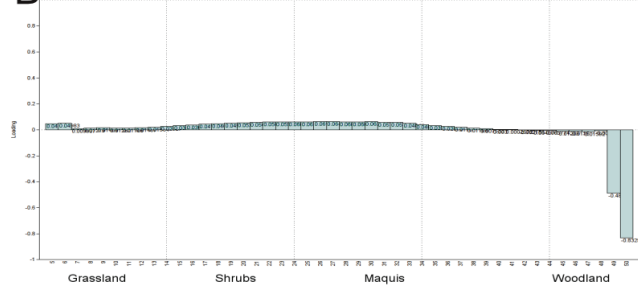
How do these temporal and spatial trends in land-cover relate to the four patterns of population identified in Section 7.2.2, above? To investigate this, I subjected the temporal vegetation matrices used to construct the vegetation heat map plots to Principle Components Analysis (PCA). PCA redistributes the variability present in the data set along a series of decreasingly important axes, or “components”. “Scree” plots, which show the percentage of the variability accounted for by each component, indicate that almost all the variability present in all input data sets lies within the first two components. Thus, the spatial patterning of the input cases (individual model-years in this analysis) in the 2-D space created by using the first two components as axes in a bivariate plot should accurately capture the patterning of temporal variability in vegetation. That is, years with similar vegetation profiles should plot close together on the PCA biplot, and years that have significantly different vegetation should plot far apart. Four distinct patterns appear in the resultant plots which match the population stability patterns summarized in Table 7.3: “Metastable”, “Multi-Stable”, “Unstable”, and “Metastable trending to Unstable”.

Figures 7.8 through 7.11 show example PCA biplots for “Metastable”, “Multi-stable”, “Unstable”, and “Metastable trending to

A



B



C

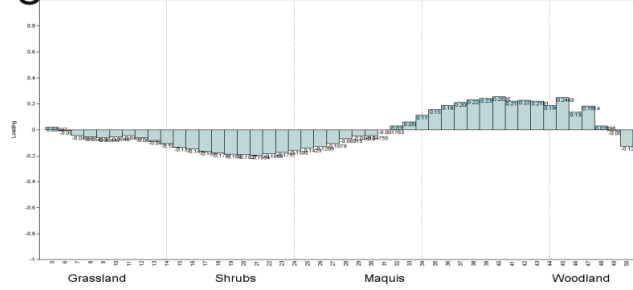


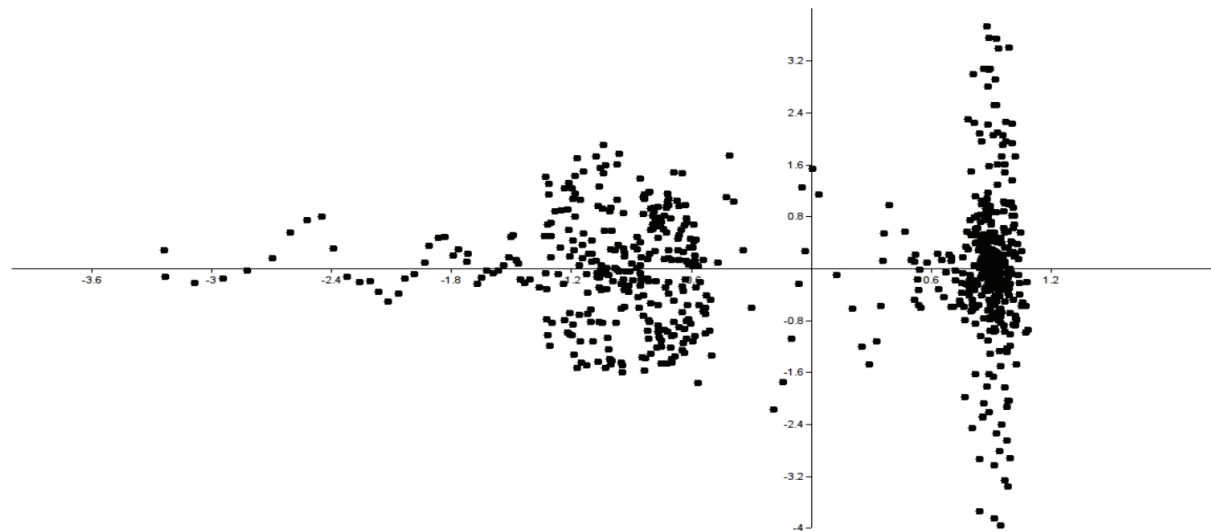
Fig. 7.8. A) A principle components analysis of the temporal patterning of vegetation variation for an example “metastable” experiment run shows how the vegetation adjusts over time to a relatively small region of stability. Each dot represents an individual year of the experiment. **B)** The loadings for each vegetation class along principle component 1 (y-axis in PC plot). **C)** The loadings for each vegetation class along principle component 2 (x-axis in PC plot).

“Unstable” experiment realizations. These plots show Component 1 along the y-axis, and Component 2 along the x-axis. The loadings for each vegetation classes across each axis are also shown in these figures which helps to explain the visual patterning. “Metastable” realizations (Figure 7.8) exhibit a “clump and tail” pattern on the PCA plots. The “tail” relates to the “ramp up” period where vegetation is being actively and directionally altered from year to year, and the “clump” relates to the stable vegetation state that is achieved once these models reach metastability around a dynamic equilibrium. It is notable that the “clumps” are highly spatially autocorrelated

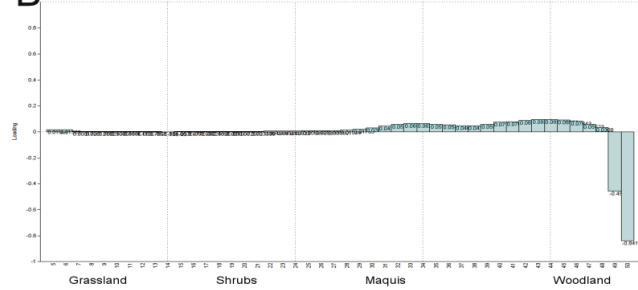
on the PCA plots indicating that once metastability is reached, vegetation only varies within a small range. The loadings plots indicate that most of the change occurring during the “ramp up” period is in the woodland vegetation classes, and that most change occurring once metastability is achieved is in the grassland through maquis vegetation range.

“Multistable” realizations (Figure 7.9) exhibit a “bimodal” pattern on the PCA plots, where most input years are collected into two distinct clusters. This clearly indicates that there are two alternative stable vegetation states in these models. There is also a “tail” that relates to the “ramp up” period in these models, but perhaps more interesting is

A



B



C

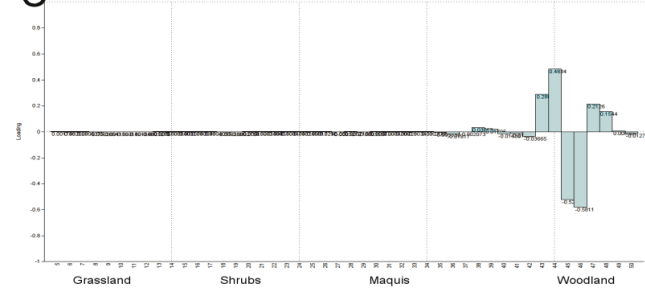


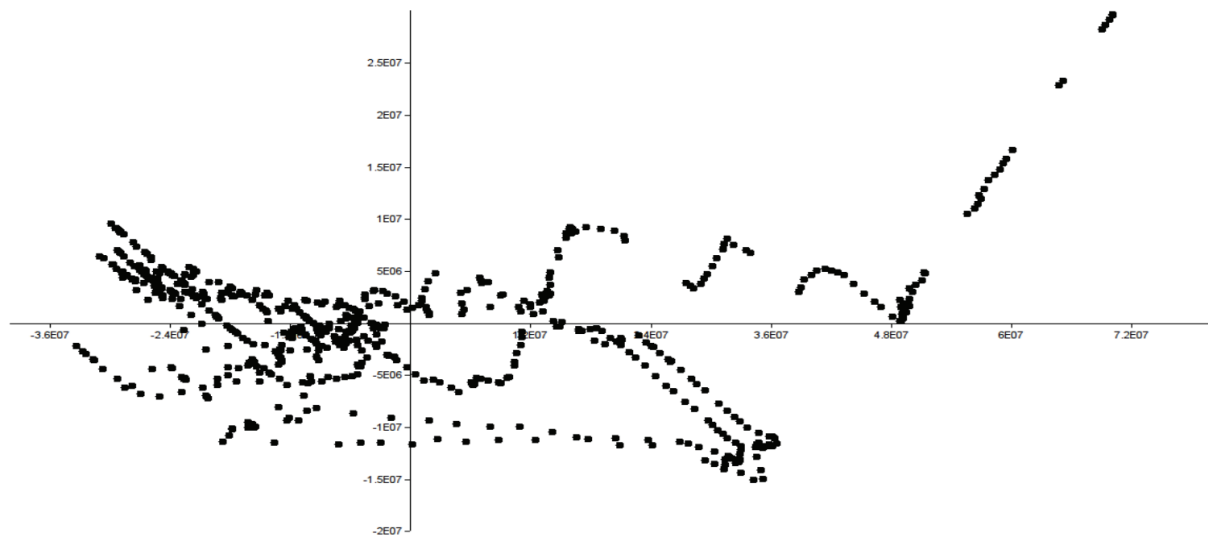
Fig. 7.9. A) A principle components analysis of the temporal patterning of vegetation variation for an example “multi-stable” experiment run shows two distinct configurations of vegetation. These zones represent alternative stable states of the model. Each dot represents an individual year of the experiment. B) The loadings for each vegetation class along principle component 1 (y-axis in PC plot). C) The loadings for each vegetation class along principle component 2 (x-axis in PC plot).

the presence a several “outlier” years that occur, widely-interspersed, in the zone between the two clumps. The loadings plots indicate that the cluster separation is mainly related to dynamics in the middle range of woodland vegetation, which, coincidentally, is also the most productive range of vegetation in terms of edible biomass for ovicaprid grazing. Thus, it appears likely that ovicaprid grazing is the main driving factor for hysteresis between the two alternative stable states in the model. The presence of only a very dispersed set of points in the space between the two clusters indicates that the “flip” between these alternative states occurs very rapidly, over the space of only a

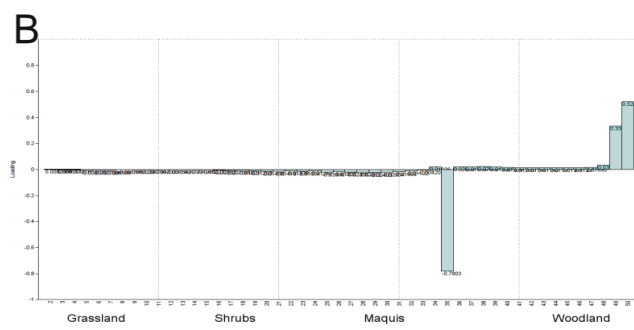
few years. Finally, the variation *within* each cluster (i.e., *within* each alternative stable vegetation state) seems to be driven mostly by dynamics at the top range of woodland vegetation, and to a lesser degree, by dynamics in the grass and shrublands.

“Unstable” experiment realizations (Figure 7.10) exhibit a “meandering” or “random-linear” pattern, where consecutive years seem to be mildly autocorrelated, but there is no distinct clustering over time. That is, the vegetation state “wanders” randomly over time, sometimes “doubling back” to a state it once occupied, but not with any regularity. The PCA loadings are less meaningful in this case, but they seem to indicate that vegetation variability

A



B



C

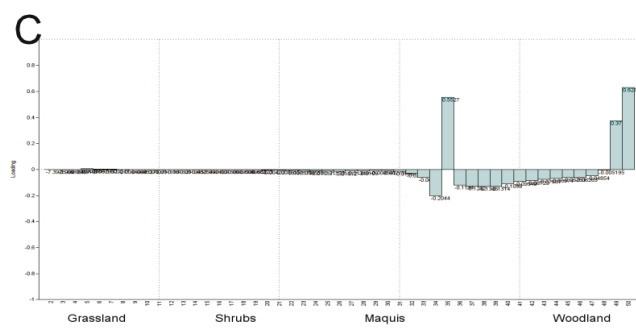


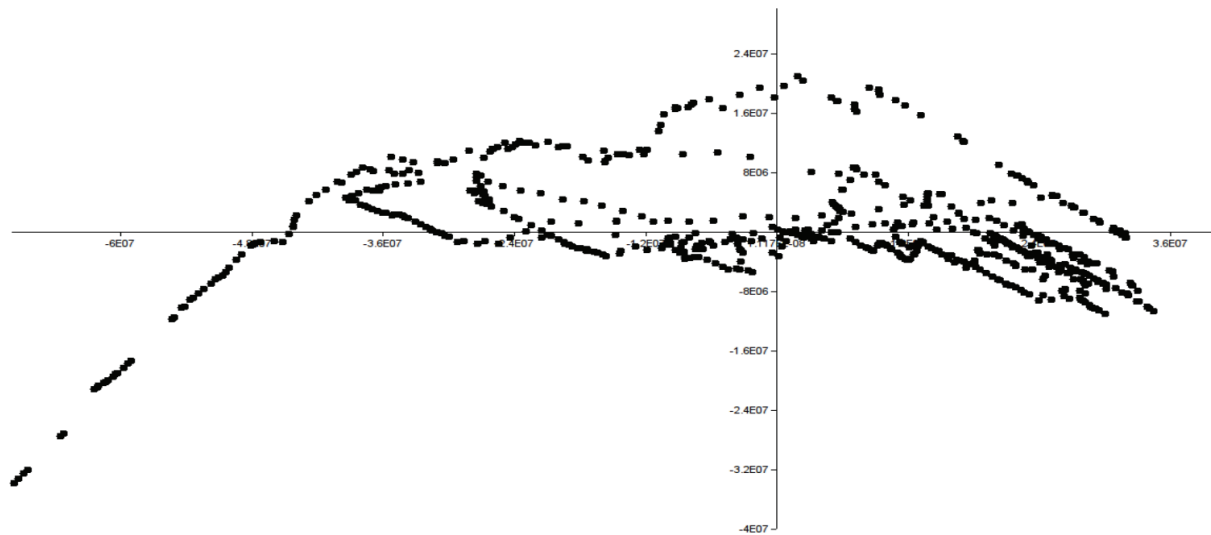
Fig. 7.10. A) A principle components analysis of the temporal patterning of vegetation variation for an example “unstable” experiment run shows that the experiment rarely attained the same configuration of vegetation more than once. Each dot represents an individual year of the experiment. **B)** The loadings for each vegetation class along principle component 1 (y-axis in PC plot). **C)** The loadings for each vegetation class along principle component 2 (x-axis in PC plot).

over time is driven by dynamics in the “maqui-immature woodland” zone, and at the “mature woodland”. This may be due to the competing needs of plot-clearance for “bottom up” farming, and the preferences of “top down” grazing in this “greedy-harworking” agropastoralists experiment.

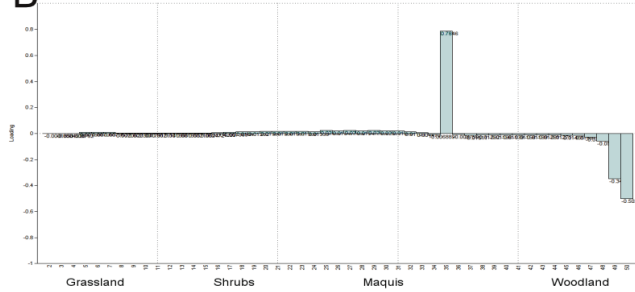
Finally, “Metastable trending to unstable” realizations exhibit a PCA plot pattern that has both the “tail and clump” of the “Metastable” experiments, and the “meandering” pattern of the “Unstable” experiments. The “clump” is much less autocorrelated than in the “Metastable” PCA plots and seems to show a pattern of increasing variation within the clump over time. This

is interesting because it would seem that the metastability achieved in the first years of these experiments is not completely stable. The internal dynamics in this supposedly “stable” vegetation state seem to be self-amplifying, until they reach the point where the entire system leaves the stable states, and enters into random, unstable movement through the vegetation spectrum over time. Again, the PCA loadings plots for this type of experiment must be interpreted with much caution, but it again seems that this patterning is being driven by two sets of dynamics at the top and middle end of the vegetation succession scheme.

A



B



C

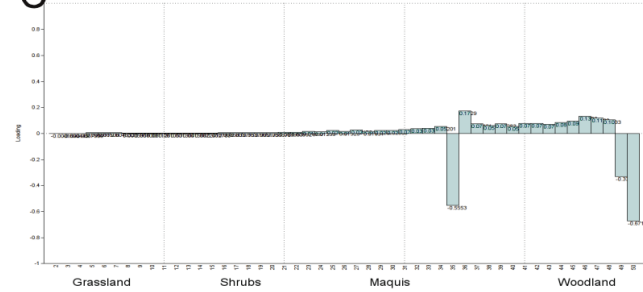


Fig. 7.11. A) A principle components analysis of the temporal patterning of vegetation variation for an example “stable trending to unstable” experiment run shows a small zone of initial vegetation stability followed by general instability. Each dot represents an individual year of the experiment. B) The loadings for each vegetation class along principle component 1 (y-axis in PC plot). C) The loadings for each vegetation class along principle component 2 (x-axis in PC plot).

7.3.4. Land-Cover Dynamics and Alternative Stable States

What is driving the hysteresis in the three models that resulted in more than one stable population state? Due to non-linear system dynamics, it is difficult to draw a direct causal link. Nevertheless, it is logical that some inherent cyclicity or other patterned variation in landcover dynamics may play a large role in controlling this hysteresis. A visual comparison of landcover maps from each stable state for a hysteretic model is a good starting point (Figure 7.12). Most strikingly, the size difference between the zone of impact for

high-population stable states and those for low-population stable states is not very large. This suggests that the landcover dynamics of only a relatively small portion of the landscape is largely responsible for determining the system-states of a particular subsistence strategy at any given time. These small regions seem to occur at the edges of the pastoral catchments, and thus may be the “critical impact zones” that are most responsible for controlling/triggering the (critical) transition between stable states. The vegetation-cover range in the pastoral “critical impact zones” are those in the middle-range of woodland, which are, again, those that produce the most edible

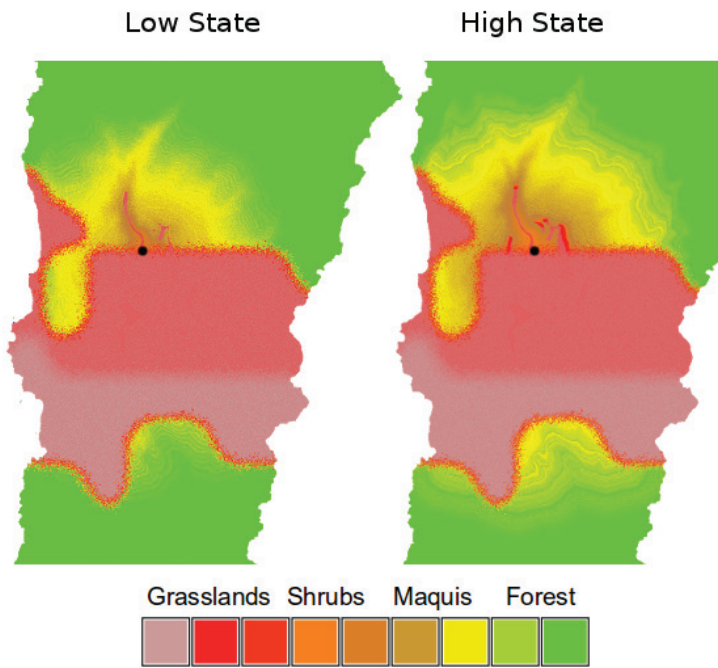


Fig. 7.12. Comparison of the landcover maps from a low population stable state (left) and a high population stable state (right) for the "Good" pastoralist experiment shows how population levels relate to vegetation impact. Higher population requires a larger footprint, which reduces vegetation cover in the area around the site.

biomass for ovicaprid grazing. This corresponds to the insights gained from the PCA analysis of the temporal patterning in vegetation for “Multi-Stable” models described in Section 7.3.3, above.

Finally, some additional insights may be gained by examining the temporal dynamics in vegetation of hysteretic models as captured by the same type of “heat map” diagrams described in Section 7.3.2, above. Figure 7.13 shows vegetation heat map diagrams for all six realizations of a highly hysteretic experiment (“good” pastoralism). Alternative vegetation states are clearly visible on these diagrams, and their timing corresponds to that in the population time-series data (Figure 7.1). Occasional rapid, brief switches from one state to the other and then back appear on some of these plots. Scheffer (2012, 2009) suggests that this type of rapid phase flipping is an “early warning” sign of an impending critical transition.

7.4. LANDSCAPE EVOLUTION DYNAMICS

The spatial and temporal patterning of human-caused erosion is a related, yet different, way to understand long-term impacts and dynamics in the connection of humans and landscapes. In the MML, surface vegetation patterns have a direct impact on erosion and deposition through their mediation of the flow of water across the landscape. Human alteration of vegetation as explored in Section 7.3 above should therefore produce unique signatures in the record of erosion and deposition patterns as well.

7.4.1. Landscape Evolution Control Model and Sensitivity Analysis

The human contribution to erosion and deposition in each experiment is understood through comparison to a control model carried out in *r:landscape.evol*. This control model uses the same climatic, environmental, and topographic contexts as the other experiments, but with no human land-use so that initial patterning of reconstructed LPPNB vegetation remained static across the entire 700 years of the control run. This control model thereby provides a base-line from which to understand the human contribution to erosion and deposition caused by the different land-use choices in the other simulation experiments.

In addition to the “base-line” control model that used the reconstructed LPPNB vegetation pattern, I conducted a Sensitivity Analysis (SA) of the effect of vegetation on erosion and deposition rates in *r:landscape.evol*. This type of analysis iteratively changes the value of one key variable to provide a structured understanding of how that variable affects the model output. This also provides a framework for interpreting the results of more complex experiments conducted in the same modeling environment. Vegetation is the

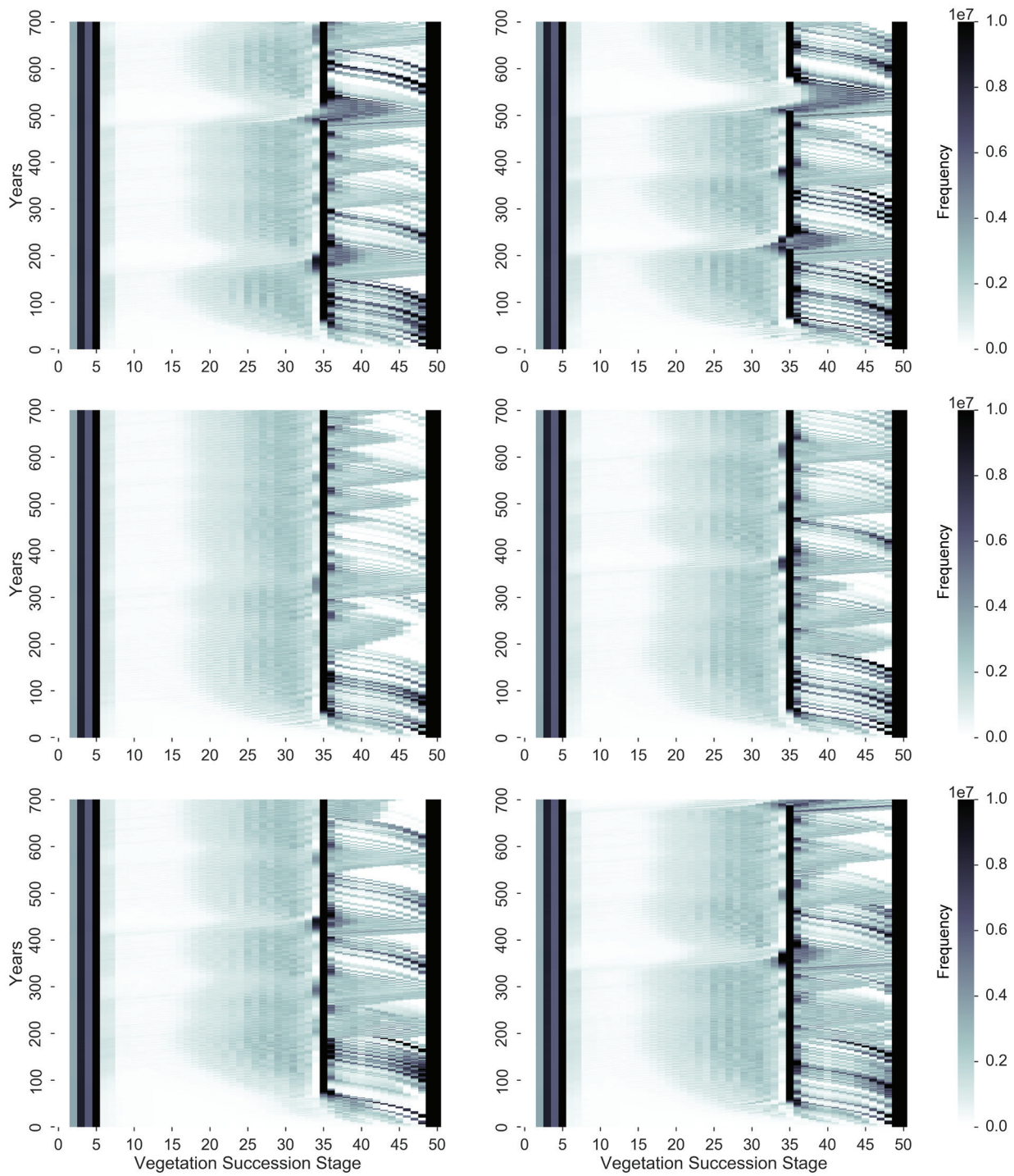


Fig. 7.13. “Heatmap” plots of the frequency of each vegetation type over time for six realizations runs of the “Good” pastoralism experiment. As in figure 7.7, bare and grasslands are on the left of the plots, whereas maquis and woodlands are on the right. Each row shows the frequency of these vegetation types in a particular year. Darker colors are higher frequencies, and lighter colors are lower frequencies. This comparison shows how temporal dynamics of human impacts on vegetation are different in each realization of each experiment. Note, in particular, how the top two realizations exhibit some larger “shocks” at years 500 and 600 of the experiment.

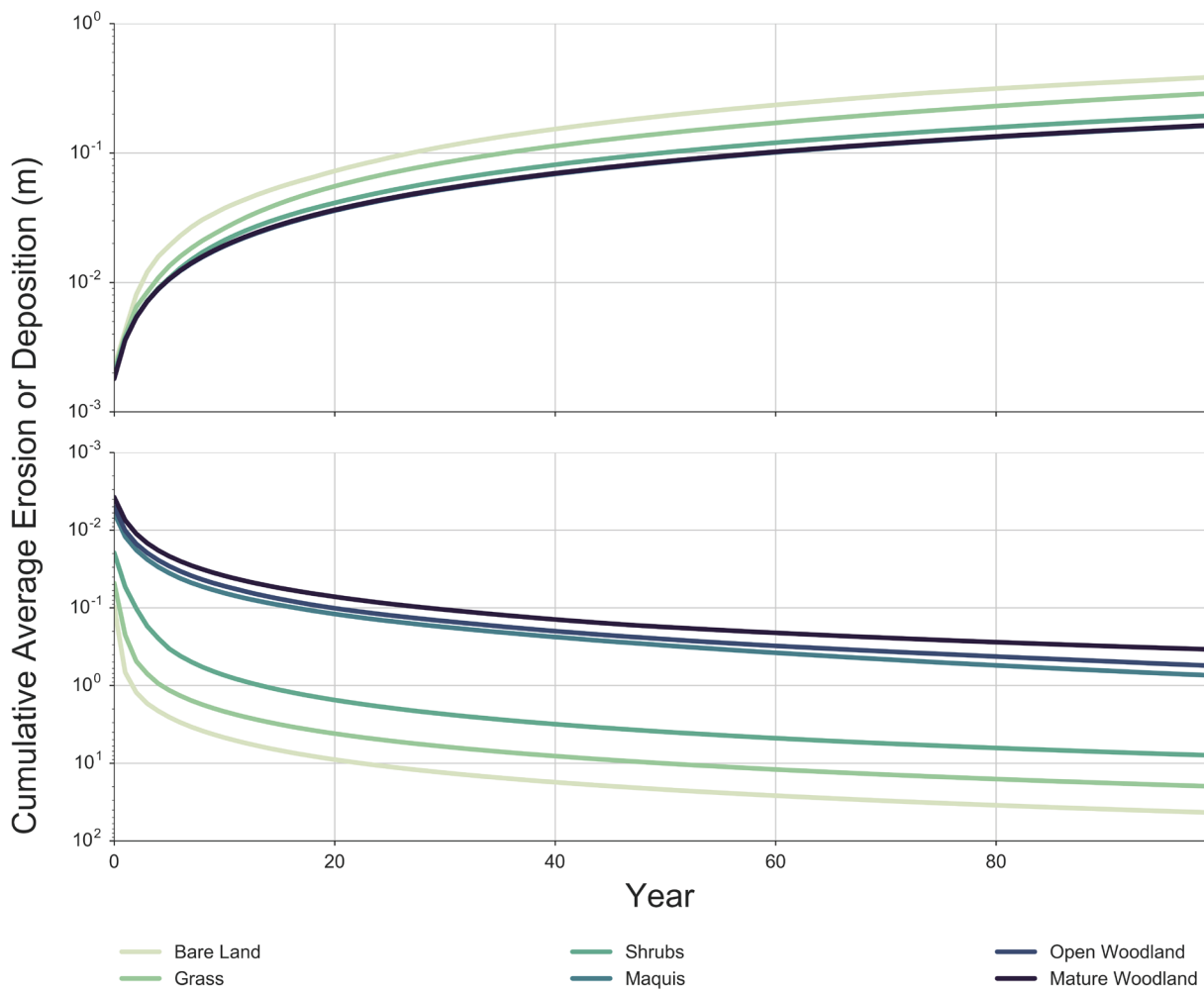


Fig. 7.14. Time-series trends for a series of short-term landscape evolution control models under different, but spatially homogeneous vegetation regimes show how vegetation influences rates of erosion and deposition.

key variable influencing erosion or deposition in the six modeling experiments investigated here, as climate and soil K-factor are held constant in these modeling runs. The SA therefore consisted of a series of short-term (100-year) model runs in *r:landscape.evol* with the same topographic and hydrological parameters used in all of the experiments, but using a series of static, homogeneous vegetation

Table 7.5. Table of average total sediment balance (sum of cumulative erosion and deposition) and average anthropogenic changes to sediment balance (compared to a control model) after 700 years for each experiment.

Raw Net Sediment Balance (m^3)			
	<i>Agriculturalists</i>	<i>Agropastoralists</i>	<i>Pastoralists</i>
<i>Good</i>	-217764	-202543	-200542
<i>Greedy</i>	-360307	-203820	-200694
Change in Sediment Balance due to Human land-use (m^3)			
	<i>Agriculturalists</i>	<i>Agropastoralists</i>	<i>Pastoralists</i>
<i>Good</i>	-14956	266	2267
<i>Greedy</i>	-157498	-1012	2114

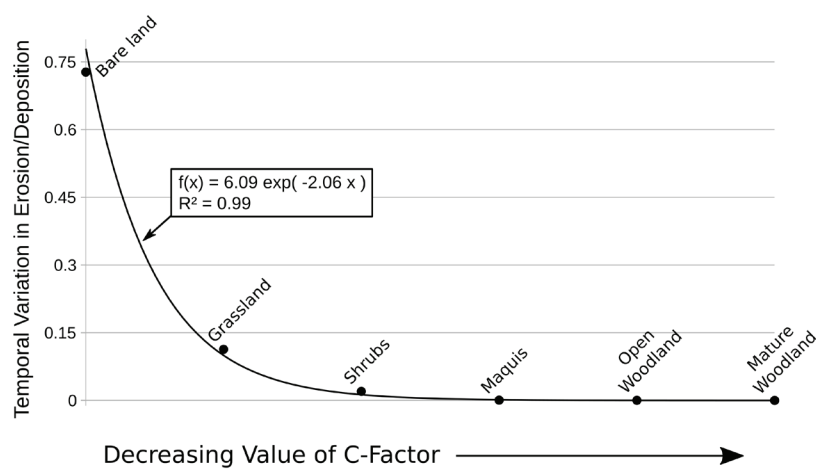


Fig. 7.15. The average (of all raster cells) temporal variance in net elevation change for each of the short -term homogeneous vegetation landscape evolution model runs show how the C-factor influences the stability of erosion and deposition rates over time.

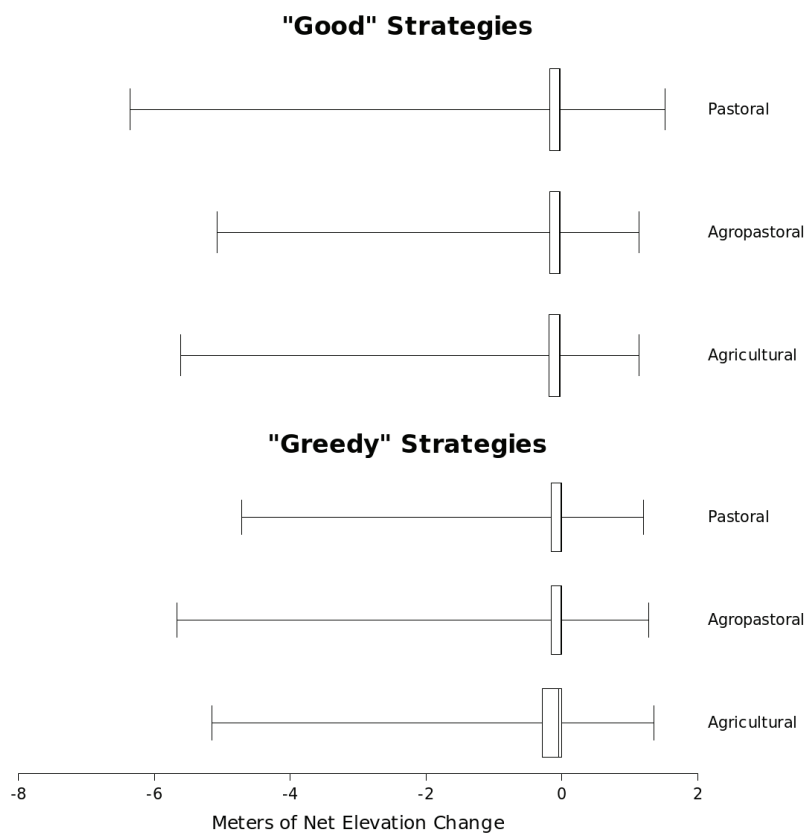


Fig. 7.16. Box-plots summarize the range of cumulative net elevation change values after 700 years in each of the modeling experiments. "Greedy" mindsets generally result in more erosion.

large impacts to erosion rates in affected areas. In particular, patterns of human landuse that lead to mosaicked shrub-maquis vegetation regimes – such as field fallowing or woodcutting – might produce distinct erosional features. Furthermore, when the temporal variation in erosion rates across time are calculated for these different static vegetation types (Figure 7.15), a very strong exponential relationship between erosion temporal variation and landcover can be seen. That is, the less-protective the landcover, the more likely it is that erosion will continually increase over time. Thus, experiments that reduce the amount of forest and maquis are more likely to experience increasingly large amounts of erosion over time.

7.4.2. Overall Human Affect on Sediment Balance

Table 7.5 lists the average sediment balance across all realizations of each experiment after 700 years of human landuse. The range of the inter-realization variability in this measure is shown as box-plots in Figure 7.16. This measure provides a good initial understanding of the cumulative impact of each of the potential LPPNB subsistence varieties could have had on mid-Holocene landscape evolution in the Wadi Ziqlab region.

These data are gathered by first aggregating a "cumulative net elevation-change map" for each experiment. To do this, the year-700 elevation map of each realization is subtracted from

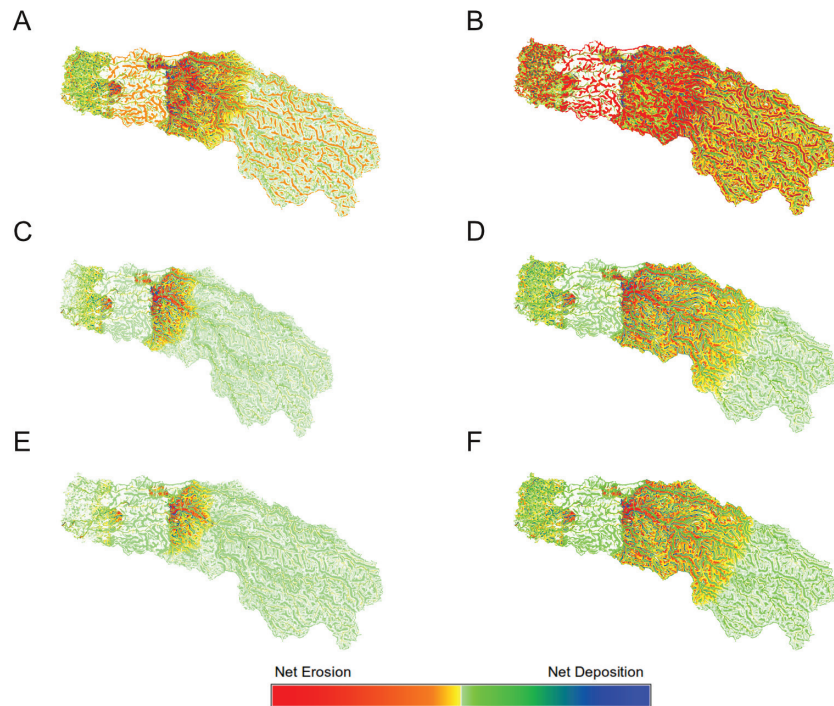


Fig. 7.17 Maps of the cumulative human-caused elevation change show the severity and extent of human impact on surface processes for each of the modeled scenarios.
A : Good Agriculture, B: Greedy Agriculture, C: Good Agropastoralism, D: Greedy Agropastoralism, E: Good Pastoralism, F: Greedy Pastoralism. Agricultural land-use produces the most severe impacts on erosion and deposition, and “Greedy” mindsets result in larger impacts than “Good” mindsets for every subsistence variant.

maps of different C-factor values each time. The median erosion and deposition rates from these SA runs are plotted as time-series in Figure 7.14. This shows the temporal trends in erosion and deposition rates under different homogeneous vegetation regimes. The overall impact of vegetation on erosion/deposition is as expected: erosion/deposition increases as landcover becomes more substantial and protective. But, an interesting phase-change appears in erosion rates between the “shrub” and “maquis” landcover types. Landcover of “shrubs” is substantially less protective than that of “maquis” or better, even though they are only separated by four succession-years in the vegetation succession regime implemented in the MML. Therefore, small human-caused changes in this range of vegetation might lead to very

the initial year-0 elevation. A second map is then produced by subtracting the cumulative net elevation change of the control model, leaving only the net contribution to elevation change caused by human activity (Figure 7.17). The total cumulative sediment balance is calculated as the sum of the values of all cells in the raw cumulative net elevation-change map, and the total human contribution to the final sediment balance is calculated as the sum of all values in the human contribution map. If erosion and deposition are perfectly balanced, the summed sediment balance would be 0. If the sum is negative, then erosion outpaced deposition. If the sum is positive, then deposition outpaced erosion.

The raw average net sediment values from each experiment (Table 7.5, top) show that each type of modeled human subsistence led to net erosion over the 700 simulated years. However, the absolute amount of erosion is greater

in the agricultural experiments than the other two subsistence suites, and also greater in the agropastoral models than in the pastoral ones.

Viewing the spread of these data in the box plots of Figure 7.18 shows that there is a fair amount of variability in the absolute range of erosion/deposition between the different experiments. In general, however, the inter-quartile range is larger for the “greedy” models than for their respective “good” variants and larger for agriculture than for either of the other subsistence strategies.

The human contributions to the sediment balance of each experiment allow a more accurate understanding of the impacts of the different subsistence systems (Table 7.5, bottom). Agriculture and “greedy” agropastoralism led to *more* erosion than would naturally occur

in the absence of humans, whereas pastoralism and “good” agropastoralism led to *less* net erosion and deposition than would naturally occur. These divisions match those derived from the analysis of the average variation in population over time (Figure 7.3). It is also worth noting that even within these two categories, the “greedy” model variants led to generally more erosion than their respective “good” counterparts.

7.4.3. Spatial Patterning of Landscape Evolution

Visual examination of the 700-year “human-caused” net elevation-change maps created in the above analysis (Figure 7.17) shows obvious differences in the spatial patterning in erosion/deposition between experiments. The spatial patterning in these maps shows general alignment with the spatial patterning of the peak-population vegetation maps for each experiment (Figure 7.4).

The general pattern shared by all subsistence strategies is for increased erosion in the farming catchment. The relationship of vegetation cover to erosion rates shown in the SA (Figures 7.14 and 7.15) shows that this increase in erosion is due the removal of more protective types of landcover, and the maintenance of anthropogenic grasslands and shrublands in these areas from year to year. This helps to explain why the area of increased erosion rates scales with the degree of agriculture in the subsistence system: it is largest in the agriculturalist models, second largest in the agropastoral models, and smallest in the pastoralist models. It may also explain why the “greedy” models also had more extensive eroded areas than the “good” models: these mindsets led to larger amounts of cultivated land than with their respective “good” counterparts.

Knowing that patterns of erosion and

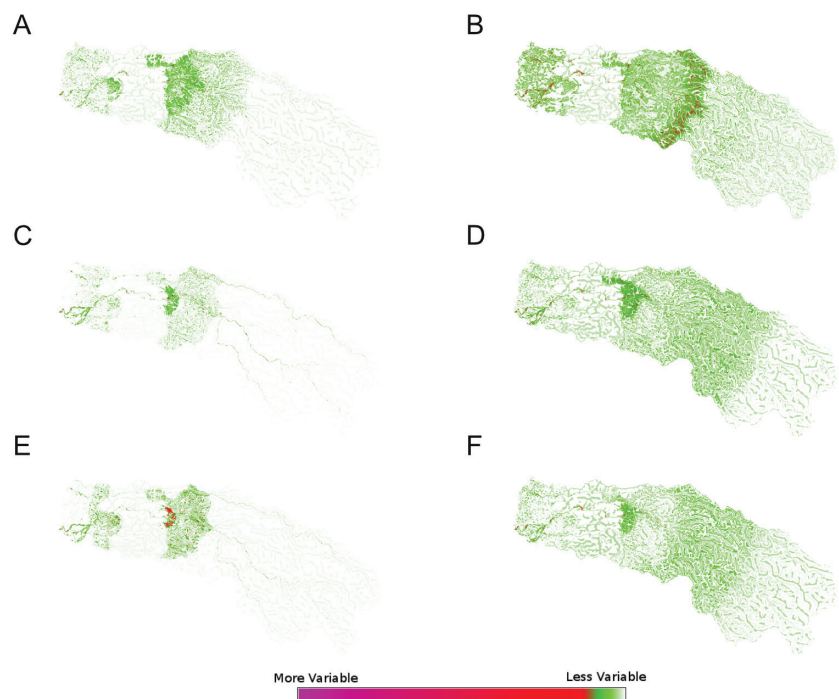


Fig. 7.18. Maps of the inter-realization variance in cumulative elevation change show the portions of the landscape most sensitive to variability in human land-use in each of the modeled scenarios. A : Good Agriculture, B: Greedy Agriculture, C: Good Agropastoralism, D: Greedy Agropastoralism, E: Good Pastoralism, F: Greedy Pastoralism. “Greedy” mindsets result in larger inter-realization variability.

deposition are linked to patterns of human vegetation use, it is as important to understand how the spatiality of erosion changes between realizations of each experiment as it is to see how the spatiality of erosion is different between the different experiments. To do this, I used map algebra to calculate the standard deviation in net elevation change at each cell between all the realizations for each experiment. In the output maps, areas with high standard deviations are those that have widely different values of net elevation change across all realizations of that experiment (Figure 7.18). These maps both summarize the general variability in net elevation-change due to divergent trajectories in each experiment and identify highly variable areas. These highly variable areas are those parts of the landscape where the amount of human-induced erosion or deposition is

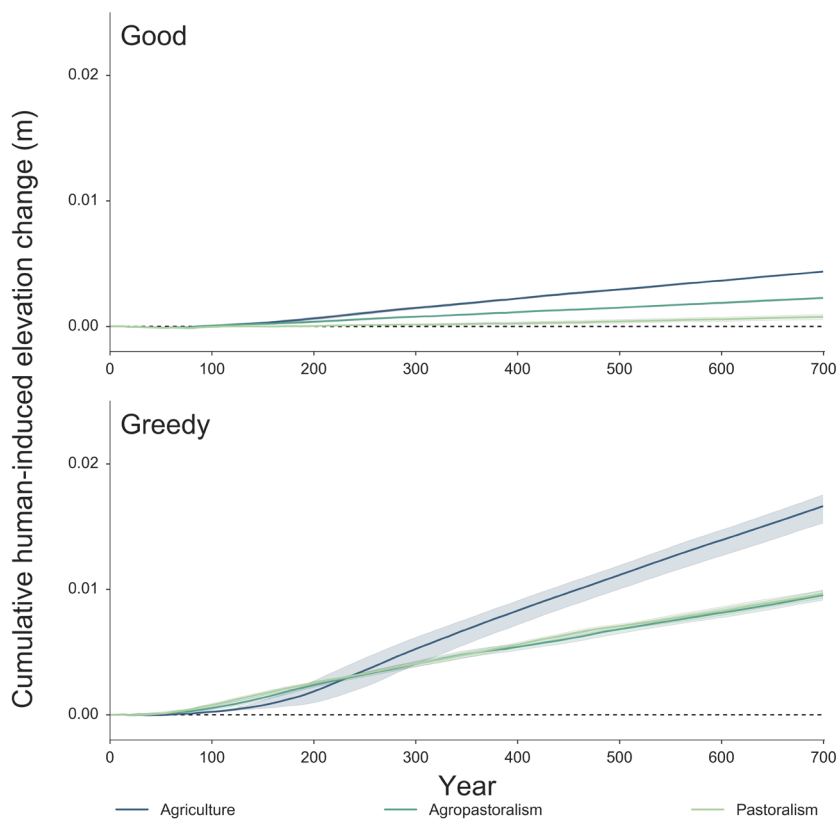


Fig. 7.19. Plotting the cumulative human-caused deposition for each modeled scenario shows how human land-use influences deposition rates over time. Solid lines show the mean of all realizations of each experiment. Shaded regions are the 99% confidence interval of these means. “Greedy” mindsets greatly increase rates of deposition for all modeled scenarios.

unpredictable and thus are quite sensitive to the potential for emergence in the modeled subsistence suite. These sensitive areas appear most frequently at the outer fringes of the agricultural and pastoral catchments, respectively. This is particularly interesting in comparison to the patterning in vegetation dynamics in section 7.3 above, which indicated that dynamics/variability in these areas are also responsible for controlling/triggering the timing and nature of the transition between stable states in models that have multiple stable states. This all suggests that under certain subsistence regimes, these areas may be key locations in the ecological “memory” (i.e., “ecological inheritance”) of the system, where random effects may “take root”, self-amplify, and produce

path-dependent trajectories that can lead to hysteresis.

There are some other interesting patterns in these data as well. First, erosion/deposition on agricultural land seems to be more variable than on pastoral land. Second, variability on pastoral land is higher in those models that had a larger pastoral component (i.e., agropastoralism, and pastoralism). Thirdly, variability is more widespread in the “greedy” models than in the “good” models. Finally, in models that resulted in “Unstable” or “Trending to Unstable” human population trends (“greedy” agropastoralism and pastoralism) the pastoral catchment is very large and seems to exhibit interesting and highly variable sensitivity between model runs. This suggests that the instability in these models derives from the increased effect of stochasticity in larger pastoral catchments.

7.4.4. Temporal Patterning of Landscape Evolution

Previous MedLanD research has identified several important indicators in the temporal patterns of erosion and deposition output by the MML (Barton et al., 2010b). Temporal patterning of the human impact to erosion and deposition rates is most simply viewed by subtracting the mean erosion/deposition values of the control model from those of each modeling run in a spreadsheet *post facto*⁴. These values are iteratively summed

⁴ Tests undertaken by MedLanD project staff in preparation for the analyses presented in Barton et al. (2010b) showed that there was no statistical difference between “human contribution” values produced by post facto subtraction of yearly median control model values in a spreadsheet and “human contribution” values generated directly from maps made by subtracting control model erosion/deposition maps from experiment erosion/

to calculate a cumulative time-series of the human-caused erosion and deposition in each realization of each experiment. As before, the average trendline for each experiment is plotted, with an associated 95% confidence interval shown as a shaded region around the trendline (Figures 7.20 and 7.21, for deposition and erosion, respectively). The cumulative amount of human-caused deposition and erosion is a good gauge for the how the overall environmental impact of different subsistence practices change over time. It is important to note that because this is the net *human* impact to erosion/deposition, it is possible to achieve negative values, which indicate that *less* erosion or deposition occurred in the simulation than would have happened with no human land-use.

The resulting time-series curves show another aspect of the different ways each of the models affect erosion and deposition. The most apparent pattern in these data

deposition maps in a GIS. The huge increase in calculation time needed to accomplish the latter is thus unwarranted. What are that all “good” experiments had significantly smaller impacts on erosion/deposition than did their “greedy” counterparts. Because climatic variables are held constant in these simulations, changes to erosion and deposition rates are intrinsically tied to changes in the landcover of the project area. Clearly, the large expansion of artificial grassland (wheat and barley fields) in the agricultural experiments lead to greatly increased erosion and reduced deposition. Even the “good” agricultural models result in very high amounts of erosion and deposition, which is not clear in the other measures examined above.

Pastoralism seems to result in the lowest human contribution to erosion in both the “good”

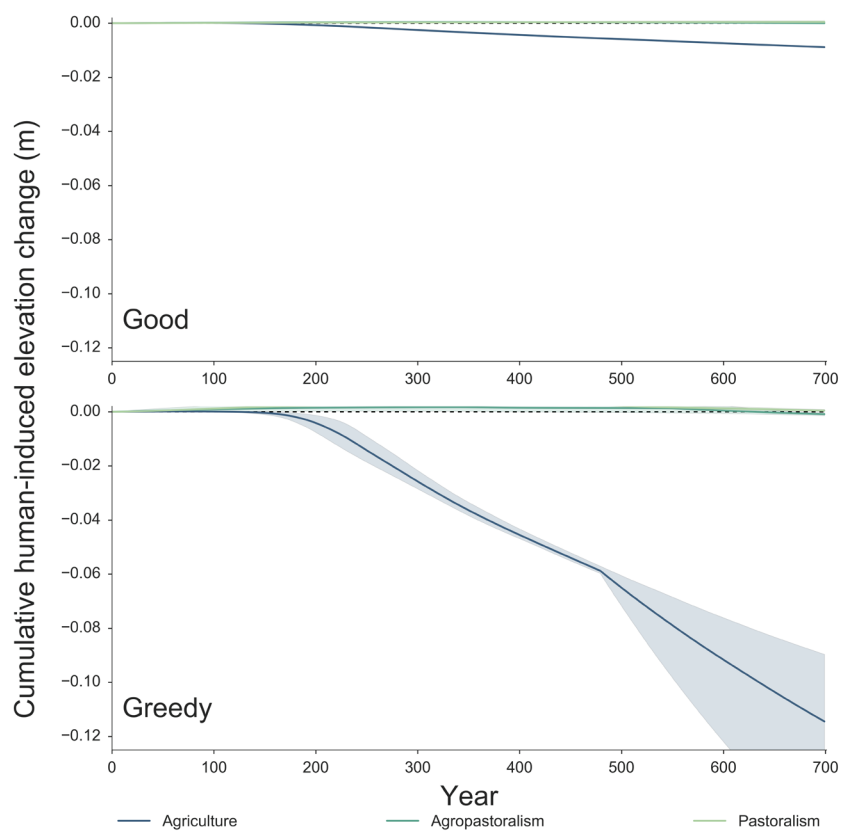


Fig. 7.20. Plotting the cumulative human-caused erosion for each modeled scenario shows how human land-use influences erosion rates over time. Solid lines show the mean of all realizations of each experiment. Shaded regions are the 99% confidence interval of these means. A “Greedy” mindset increases erosion rates for agriculture, but decreases them for pastoralism and agropastoralism.

and “greedy” model-suites. In fact, pastoralism at times produced *less* erosion than would have occurred without human land-use, while simultaneously increasing levels of deposition. Agropastoralism shows a similar, although less drastic pattern. This is particularly interesting in the light of the temporal vegetation patterns (Figure 7.7), which indicates that, at least in the “greedy” variants of these models, significant deforestation occurs periodically throughout the simulation. This would be expected to lead to *increased* erosion rates, but seems not to have had that effect. One possible reason for this counterintuitive result may be that grazing tends to create a “patchy” landscape, rather than a uniformly cleared one.

This increased heterogeneity of vegetation (i.e., “mosaicking”) may provide a series of vegetated “check dams”, which may sufficiently reduce the stream power of flowing water and thus lead to lower-than-expected erosion.

Finally, all of the realizations of “greedy” pastoralism initially yielded rates of erosion much lower than would have occurred naturally, these rates eventually began to drop back towards the level of the control model, and some even

surpassed this level. Interestingly, the This model also showed relatively high inter-run variability in erosion rates, which is notable because it was also the run with the least stable population over time.

The shape of these curves can illustrate the of amount of connectedness between parts of the system. Increases in average human-caused cumulative erosion and deposition are due to human manipulation of landcover. Thus, increasing connectedness between humans and vegetation should be visible on the time-series plots as continual increase in average human-caused cumulative erosion and deposition over time. This is, in fact, the exact pattern that occurs for all agriculturalist models. Neutrality or reduction in erosion, on the other hand, is indicative of increased biodiversity, and thus decreased connectedness, and this is what we see in the agropastoral and pastoral models.

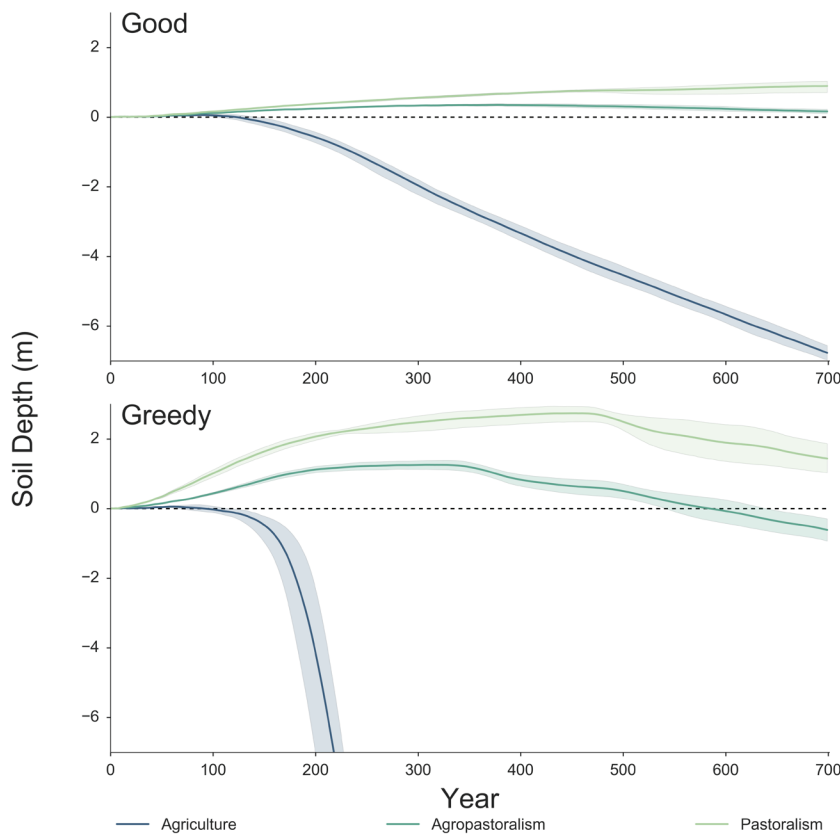


Fig. 7.21. Plotting the deviation in depth of anthropogenic soils from natural soils for each modeled scenario shows how human land-use influences soil availability over time. Solid lines show the mean of all realizations of each experiment. Shaded regions are the 99% confidence interval of these means. Agriculture always results in shallower soils than would exist without humans, whereas pastoralism and agropastoralism tend to produce thicker than natural soils. A “Greedy” mindset initially produces much thicker than natural soils in pastoralism and agropastoralism, but then these soils eventually get shallower. Greedy mindsets also produce greater inter-realization variability.

7.5. SOIL DYNAMICS

In the model, soil fertility and depth are the variables that control vegetation regrowth and farming yields, so it is very important to understand spatial and temporal patterning in soil dynamics and how these relate to the patterns noted in the other analyses.

7.5.1. Temporal Variability in Soil Depth

Figure 7.21 show time-series graphs of the net human effect on average soil depths for each model. These statistics were calculated by subtracting the yearly average soil depth in the control model (i.e., with no human land-use) from the yearly average soil depth of each model

(i.e., with different types of human land-use). In these graphs, positive numbers mean that human land-use resulted in generally deeper soils than would have naturally occurred, while negative numbers mean the human land-use resulted in generally shallower soils than would have naturally occurred. The patterns of human effect on soil depths unsurprisingly track very well with those erosion and deposition (see Section 7.4, above).

Notably, all agriculturalists models resulted in extreme reduction of natural soils over time. On the other hand, pastoralism and agropastoralism tended to produce *thicker* than natural soils. In all experiments, the “greedy” model variants had more extreme impacts on soil depths than did the “good” model variants. “Good” models also had very low inter-run variability, whereas variability in the “greedy” ones became more substantial over time.

Of note, the two agropastoral experiments both initially resulted in deeper-than-natural soils. However, this did not last. In the “good” agropastoral variant, net human effect on soil depth eventually became negative after about 300 years, so that the anthropogenically thickened soils began to thin again after this time. A similar effect is seen for the “greedy” agropastoral variant, although the change is much more pronounced and occurs at around 350 years. After this time, the rate becomes sharply negative, and is also quite variable between experiment realizations. Between about 550 to 650 years after the initiation of the experiment, all realizations of the “greedy” agropastoral subsistence variant have lost all anthropogenic thickening of soils, and start to actually reduce the depth of soils to thinner-than-natural levels.

The difference between the “good” and

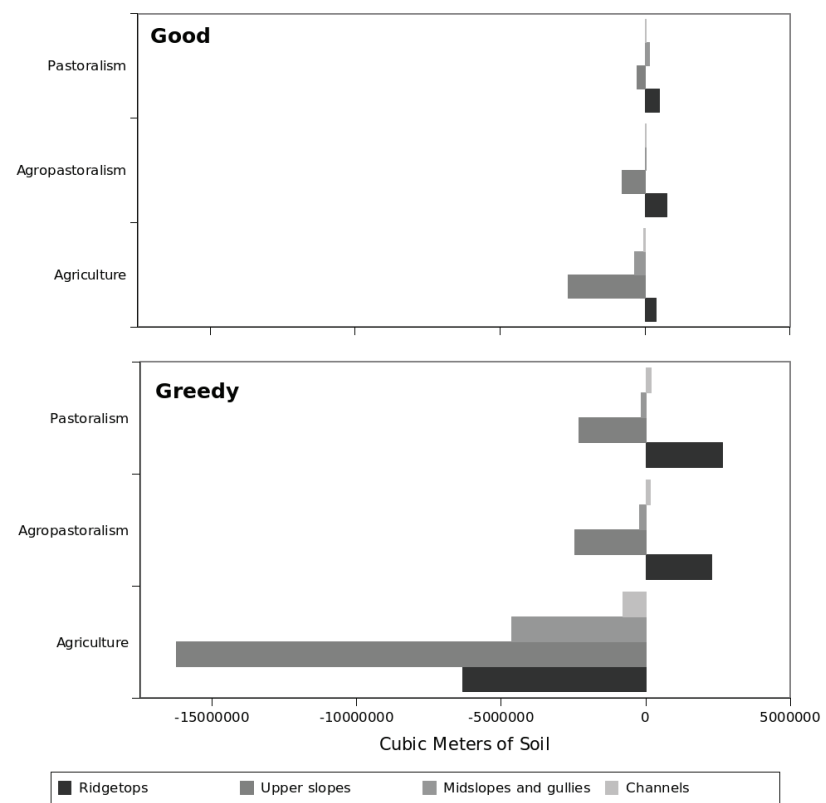


Fig. 7.22. Human land-use affects soil depths on some landforms more than others. This plot shows the difference in total volume of sediment on different landforms between each land-use scenario and the non-human control model. Human land-use can create thicker than natural soils on ridgetops, but typically produces thinner than natural soils on all other landforms. A “Greedy” mindset enhances this trend, especially for agricultural land-use.

“greedy” pastoralists models is similar to that of the agropastoralists models, except that “good” pastoralism seems to result in continued net increase of soil depth over time. The “good” pastoralist models also had very low inter-run variability. The “greedy” pastoral models resulted in soil depth impact patterns very similar to the “greedy” agropastoral models except that none of the experiment realizations had reduced soils to thinner-than-natural levels by the end of the simulation time period. However, it appears likely that this would have occurred given a longer simulation timespan.

Another interesting difference between the pastoral and agropastoral experiments is that the

“peak” amount of human-caused increased soil depth was higher in the pastoral models than in the agropastoral ones, suggesting that it is pastoral landuse that creates artificially thickened soils. Also interesting, the inter-realization variability became much higher in the “greedy” pastoral model over time than the “greedy” agropastoral one. This largely mirrors the changes in population that occurred in these models, and also suggests that a “greedy” mindset produces unpredictability in largely pastoral subsistence systems.

7.5.2. Spatial Patterning in Soil Depth

An investigation of the spatiality of anthropogenic impacts on soil depth can shed further light on the temporal patterns seen in the previous section. To do so, I first created maps of the average human effect on soil-depth across all runs of each experiment by subtracting the map of final soil depths from the control model from the final soil maps for each experiment realization. I then used the same landscape parsing rules used to determine surface-process breakpoints procedure described in Appendix A, Section A.2 to create a map of four major landforms (see Figure A.3): 1) ridges, 2) upper slopes, 3) mid-slopes and gullies, and 4) channels. I then extracted the average human effect on soil-depth for these four landform types in all realizations of each of the six experiments. The across-

realization averaged amounts of anthropogenic change to soils on the four landforms in each experiment is shown in Figure 7.22. In this figure, it is clear that all variants of every subsistence type produced thinner-than-natural soils on the upper slopes. But, the amount by which they thinned these upper-slope soils varied quite widely. “Greedy” agriculture had a much more severe impact on upper-slope soil-depths than any other subsistence variant. “Good” agriculture, “greedy” agropastoralism, and “greedy” pastoralism all thinned upper-slope soils to a similar, moderate degree. “Good” agropastoralism and “good” pastoralism thinned soils only marginally. Another pattern visible in Figure 7.22 is that all variants of pastoralism and agropastoralism, and the “good” variant of agriculture all actually *increased* soil depths on ridges (which also includes other flat areas, like plateaus and large terraces). However, “greedy” agriculture *decreased* soil-depths in these same areas. Finally, while agriculture reduced soil-depths on midslopes and in channels, pastoralism and agropastoralism did not.

Figure 7.23 shows the range of inter-experiment variability in the human contribution to soil depths in the four types of land-forms. Unsurprisingly, upper-slopes show the widest range of values followed by ridges and then midslopes. Interestingly, human landuse seems to have little impact to channels in the current set of experiments – perhaps due to the nature of the

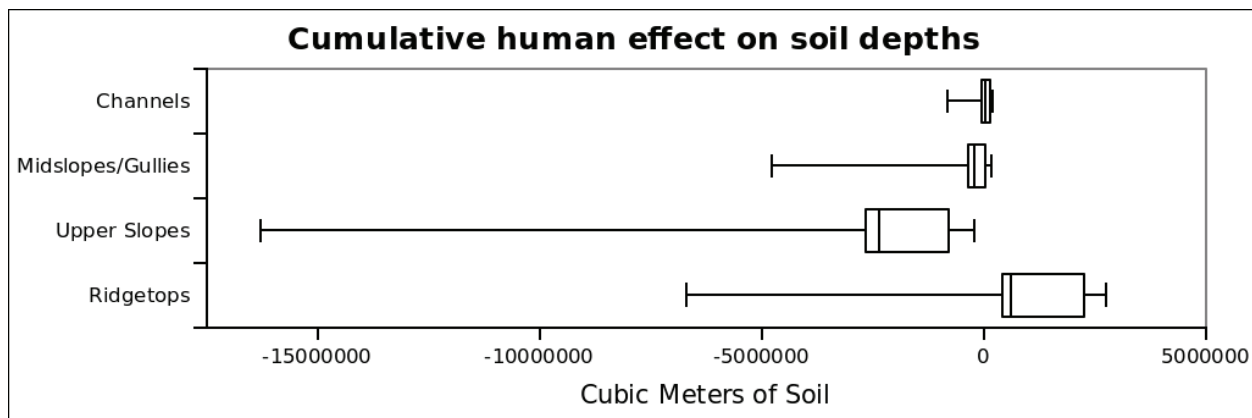


Fig. 7.23. Viewing the total human impact on soil depths as box-plots for the different landforms shows that human land-use mostly affects the upper slopes.

process models used in this version of the MML (see Barton, Ullah, and Heimsath, 2016, for the results of an updated process model for channel erosion). Upper-slopes may also be the areas most affected by pastoral land-use, since that land is typically too steep for farming.

To further test this idea further, I repeated this procedure, but broke the landscape apart by groupings of low-slope ($< 10^\circ$), medium-slope ($10^\circ - 20^\circ$), and high-slope ($> 20^\circ$). Low-slope regions are more preferred farming locations by agents in the MML, whereas medium-slope areas are farmable, but not preferred. High-slope areas are not farmable at all in the model, and so may be preferred as grazing territory. Figures 7.24 shows the inter-realization average net human effect on soil-depths in each of these slope-zones for each of the six experiment types. Agriculture results in thinner-than natural soils in all slope-zones, but “greedy” agriculture does so to a much higher degree than “good” agriculture. Pastoralism and agropastoralism all *increase* soil-depths in low-slope areas, but *decrease* them in high-slope areas. They have a variable, but minimal effect on the medium slope-zones.

The inter-experiment variability in net human impact to the three slope-zones (Figure 7.25) shows that the low-slope areas experience the widest range of human impacts. The range of human impacts on the upper-slopes is more narrowly constrained, but the average anthropogenic effect is quite negative, indicating that soils are almost always

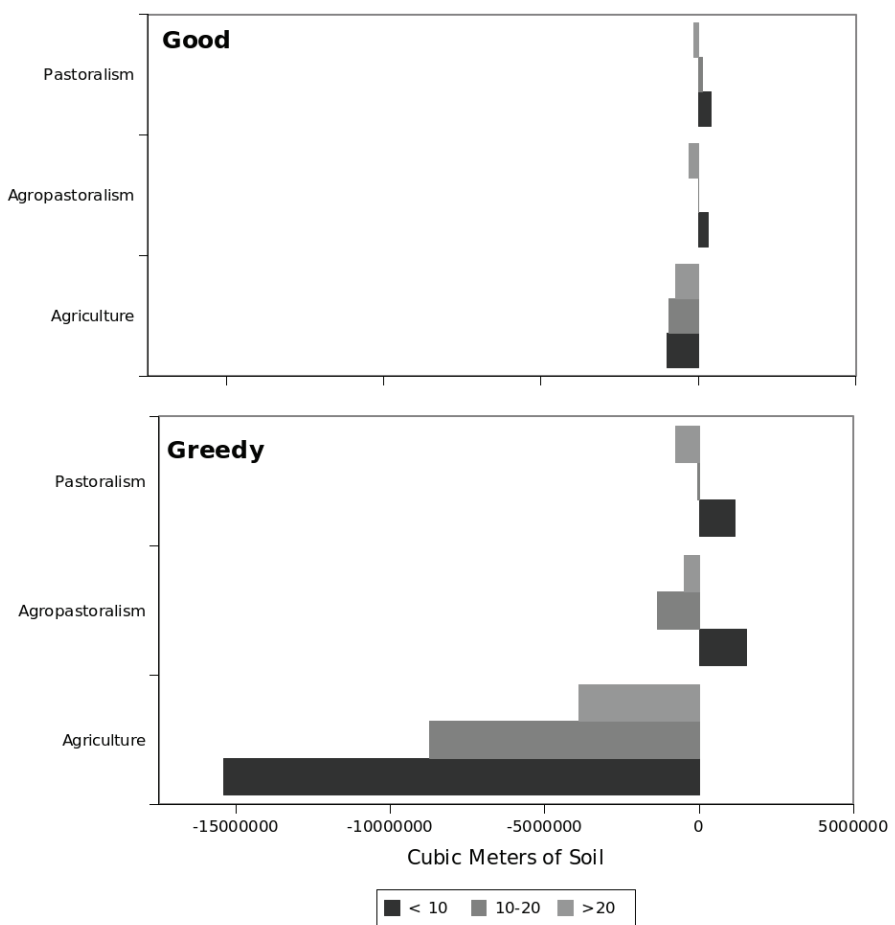


Fig. 7.24. Human land-use alters the relationship of slope to erosion. This plot shows the difference in total volume of sediment on terrain of three different intervals of slope between each land-use scenario and the non-human control model. Agropastoral and pastoral land-use can create thicker than natural soils on low slope areas, but agriculture typically produces thinner than natural soils in these areas. All land-use produce thinner than natural soils in medium and high-slope areas. A “Greedy” mindset enhances these trends.

thinned in these areas after human use of them.

All in all, the data indicates that grazing on the steeper areas increases erosion in these areas, but that the loosened sediment does not travel far (i.e., it is deposited at the base of the slope). It also indicates that farming – especially “greedy” farming – greatly increases erosion on farmed fields and may lead to serious reduction in soil-depth of these fields over time.

7.5.3. Temporal Patterning in Soil Fertility

Soil fertility provides another proxy for system potential, and is a particularly good indicator of the health of the agricultural component of human subsistence systems. Further, tracking soil fertility dynamics is important because the amount of yearly human-caused reduction to soil fertility is one of the aspects that was used to separate “good” subsistence mindsets from “greedy” ones. In the MML, summary soil fertility statistics are recorded every year. Figure 7.26 shows time series of soil fertility for the six experiments. As before, the inter-realization averages are depicted by the solid lines, and the inter-realization variability is shown by the shaded areas. The main observation from these plots is that there was only a very narrow range of impact to the overall soil fertility in these experiments. No experiment produced soil fertility values in farmed areas of lower than 98% of full fertility in any given year. When averaged across the entire landscape, this yields averages of greater than 99.9% soil fertility in the project region after 700 years even in the most intensive “greedy” agricultural scenario. This is likely because farm plots were not tenured in any of the models, and so the farmplot choice logic in the model (see Chapter 4) allowed agents to establish an efficient bi- or tri-annual fallow-rotation cycle that prevented significant reduction in soil fertility over time. This

is significant because it means that no experiments reached a point where fertile agricultural land was a limited resource (i.e., when an extensive land-use system would no longer be tenable).

The second thing of note is that the time-series patterns for fertility track very well with those for population for all experiments. This is unsurprising, considering that soil fertility is a major component of grain yield, and that population levels are tied to the amount of grain that can be grown (see Chapter 4). Thus all of the differences between the experiments noted for population (see section 7.2, above) hold true for soil fertility (i.e., those experiments that resulted in larger village populations also had an overall larger impact to soil fertility). Finally, it seems that “greedy” variants experienced a slightly more rapid decline in soil fertility at the start of the simulation than did their “good” counterparts. Thus, “greedy” mindsets more quickly reduced the yield-potential of the close by fields, which is likely why all of the “greedy” experiments eventually needed larger farming catchments than did their the “good” counterparts.

Finally, it is also interesting to use Figure 7.26 to compare the inter-realization variability in soil fertility between experiments over time. All of “good” model variants have steady, low amounts of variation over time. The “greedy” model variants, on the other hand, show significant amounts

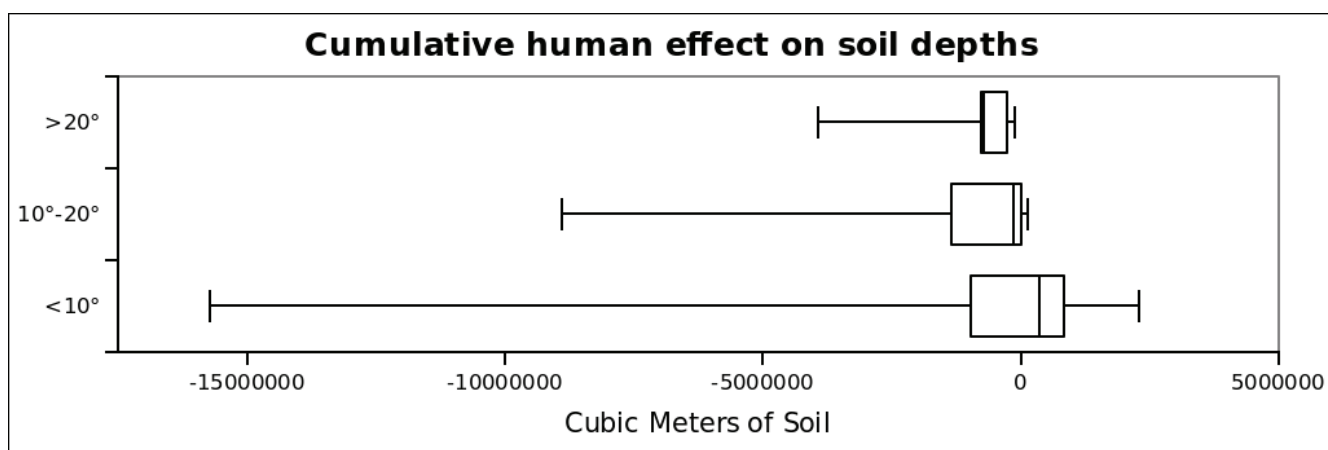


Fig. 7.25. Viewing the total human impact on soil depths as box-plots for the different slope intervals shows that there is a wide range of variability in the human impact on soil depths in shallow areas.

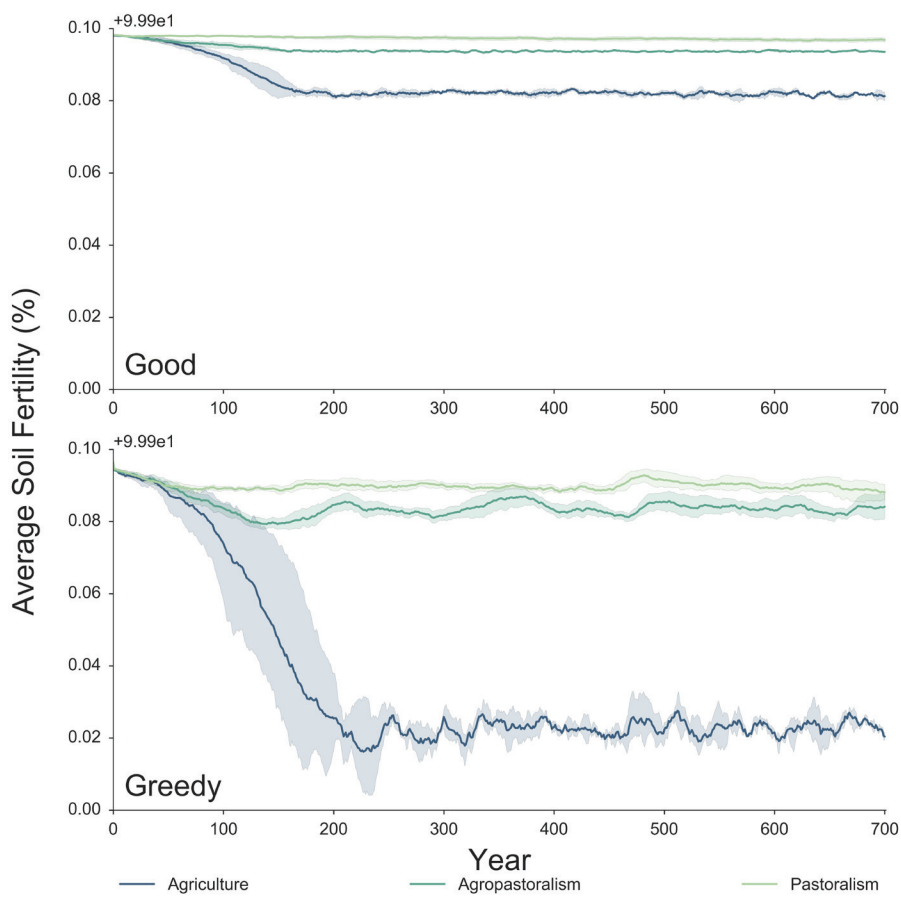


Fig. 7.26. Plotting the average fertility of soils shows the temporal dynamics of soil degradation and regeneration for each modeled scenario over time. Solid lines show the mean of all realizations of each experiment. Shaded regions are the 99% confidence interval of these means. Agricultural land-use has a more severe impact on the general fertility of soils in the experiment region than does agropastoral or pastoral land-use. A “Greedy” mindset increases this impact, and also induces visible degradation and regeneration cycles in each land-use scenario.

of variability. This means that being greedy significantly affects predictability, and triggers emergence/divergence in soil-fertility dynamics. Finally, even though all “greedy” variants maintain highly dynamic patterns in inter-run fertility variability through time, “greedy” pastoralism exhibits a clear trend towards increasingly higher values of inter-run variation, “greedy” agriculture shows a clear trend of *decreasing* values of inter-run variation over time, and “greedy” agropastoralism maintains a relatively even spread of variation values over time. This is interesting, as

it suggests that the fertility of agricultural land of even “greedy” agriculture is become *more* predictable over time, whereas those of “greedy” pastoralism are becoming *less* predictable.

7.6. DISCUSSION

Some common trends occur in the analysis presented in the preceding sections, and there are several important insights that can be made from these observations about stability, predictability, emergence, stress, resilience, and critical transitions in low-level food-producing SES. The modeling experiments presented here show that fairly small differences in either subsistence behavior or the mindset of subsistence choices can lead to highly divergent socio-natural dynamics. Small differences in the stocking density of animals and the impact farming practices on soil fertility can have

very large impacts on the size of the ecological footprint. This, in turn affects temporal trends in system stability over the long-term, and the degree to which emergent phenomena can begin to self-amplify and affect directionality in these trends.

The results of these experiments make it clear that the main limiting factor on population growth in the MML is uncertainty in subsistence yields from year to year. The MML agents are “satisficing” – they are only trying to meet their basic needs, and no more. The more accurately an agent can predict its required number of farming

and grazing plots in a given year, the greater the chance that they will successfully satisfy their subsistence need. Most of the experiments achieved one or more stable population states. It is clear that this stability is regulated by a sort of dynamic “carrying-capacity” threshold that emerges from the interaction of each suite of subsistence choices with the natural components of the modeled system. Stability is achieved once the human population surpasses a threshold, beyond which further growth cannot be sustained for long periods of time. Beyond this threshold, agents must use a large enough number of sub-optimal farming and/or grazing patches so that a significant discrepancy between the returns from the planned subsistence activities and the actual subsistence need of the agents occurs. After this point, stochasticity in subsistence returns couples with lag-times between poor-return/high-return years and decreased/increased population growth rates to induce a cyclical “dynamic equilibrium,” sinusoidally hovering near a long-term population mean.

This is not to say that the “stable” systems identified in the simulation experiments will remain “balanced” in the very long term. These stable systems have very large maximum potential, and so have larger ecological footprints. This, as we have seen, means that they have more drastic effects on biodiversity, soil fertility, and erosion dynamics in their local catchments. These stable systems also seem to be path-dependent, as all indicators point to a general reduction in system resilience over time, with a concomitant increase in system connectedness and potential. “Greediness” exacerbates this. For example, the “greedy” agricultural agents had completely exhausted their woodland resources at a very early point in the simulation, whereas the “good” agriculturalists never did so. “Greedy” agricultural landuse also tended to reduce the depth and fertility of soils in agricultural land. The combined impact of forest removal and thinning, de-fertilized soil would eventually have made it very difficult for these “greedy” agricultural agents to smoothly switch to another style of food production when or if agricultural production ceases to be able to sustain the population. In other words, this

“greedy agricultural” system is at a continually growing risk of undergoing a major critical transition. While no such critical transitions were observed in the time span modeled in these experiments, I should reiterate that the current round of experiments was conducted under stable environmental conditions. It is unclear if any of these systems would achieve or keep stability in the face of gradual or rapid climate change.

Some of the modeling experiments achieved multiple stable states within a single subsistence strategy. The analysis of the output of these experiments suggests that under certain combinations of subsistence and mindset, the vegetation dynamics of the far edges of the site’s catchment may induce hysteresis in the rest of the system. There is likely a threshold in site catchment size which precipitates this. Smaller catchments are efficiently used, but larger ones are more difficult to fully exploit. As human populations grow, certain styles of landuse achieve catchment configurations right at the border of efficiency. As land-use begins to exhaust the productivity of the inner portion of the catchment, a new “ring” of landuse is added, which equals or increases the amount of land already being used. This produces a short-term surplus, which leads to population growth. Once this new region begins to be exhausted, however, subsistence returns can no longer support the number of mouths that need to be fed, and so population reduces. Meanwhile, the formerly exhausted regions have recovered, and the cycle can begin anew.

Only in certain combinations of subsistence and environmental dynamics does this result in a medium-term oscillation, or hysteresis. Under other circumstances, cycling may occur more rapidly or more slowly. In the range of experiments conducted in this analysis, it appears that agricultural landuse led to fast cycling, or “dynamic equilibrium.” Pastoralism, on the other hand, seems to generally lead to medium or slow cycling, or true hysteresis. Agropastoralism can lead to either fast or slow cycling, depending upon the mindset of resource exploitation.

What is perhaps most interesting about the true hysteretic cycles is that they do not necessarily

occur at the same times or intervals in the different experiments. However, when they occur, it is clear that the system has fallen into a true alternative stable state, in that it cannot immediately return to its previous configuration. In other words, a true critical transition has occurred. This means that it would be almost impossible for an agent to predict when one of these state transitions may occur, or even if one will occur at all. Further, it would be equally impossible for an agent to predict when or if the system may transition back to the old state. Unpredictability is a hallmark of complexity, and it is clear that the emergence of hysteresis in these systems are complex phenomena. The “level” (e.g., equilibrium population) of each of the alternative stable states is basically the same between runs, however, suggesting that the states themselves are well defined “natural” attractors.

In unstable systems, subsistence choices—and the impacts that occur from them—balance the system towards uncertainty. Although clearly there is a “preferred” system state (for example, the unstable “greedy” agropastoralist model still tended to achieve an population levels of about 200 people), remaining at that state is difficult for long periods of time. Unstable models are therefore characterized by periodic crashes in system state. The accrual of deleterious impacts occurs at a faster rate than in other subsistence combinations, leading to short, variably-sized cycle-widths. Unlike multistable models, the “crashes” in the unstable models do not meet the criteria for true hysteresis even though they can occur at similar cycle widths. This is because the system does not remain at the lowered system state for a lengthy period of time; rather, it begins to recover almost immediately. Furthermore, unstable models are characterized by very high inter-run variability, which means that they are highly unpredictable systems. The “crashes” in system-state do not occur on a regular interval and are spaced very differently in each of the five model-runs, so it is highly unlikely that agents operating within them would be able to predict them. Instability does not equate to lower system resilience, however; on the contrary, unstable models were characterized by fairly high system

resilience. In fact, the “instability” of these models may be linked to their ability to quickly adapt to changing conditions (i.e., to their resilience).

Perhaps most interestingly of all, some models were initially stable in the early years of the simulation but trended towards instability in the latter years. This illustrates that the specific type or nature of “stability” or “multistability” in a regional SES is not an immutable characteristic but can change over time. It is particularly interesting that in these models, the trend towards instability was an emergent property of the system (i.e., instability was *not* induced by external perturbation from climate, war, etc.). Further, the advent of instability seems to have been coincident with a general increase in system potential and decrease in system resilience over time. However, in these cases, system potential was extremely variable between realizations. Thus, the transition from stability to instability was accompanied by a rapid and extreme increase in divergence between model runs, indicating that the system switched from fairly predictable to wildly unpredictable.

How do these trends relate to the amount of stress that individuals would encounter under the various modeled subsistence regimes? Resource scarcity or unpredictability is a major source of stress in low-level food-producing SES, and is likely the major stressor driving change in these modeling experiments. Looking at the patterning in population, vegetation, and soil over time, several subsistence strategies have correlated frequent high amplitude surges and declines in these measures. These strategies can be understood to be experiencing a recurring resource imbalance, and thus are more likely to experience resource stress, than those with lower amplitudes or less frequent surges (i.e., stability over time). By this measure, agriculture and “good” agropastoralism would seem to have the lowest levels of this type of resource stress, “greedy” agropastoralism the highest levels of resource stress, with pastoralism intermediate between these. Also, all else being equal, a “greedy” subsistence mindset always produces more resource stress than a “good” mindset.

Another source of resource-related stress

Table 7.6. Summary of general system potential, resilience, and connectedness in each of the modeling experiments, based on the measures presented in this chapter.

System Potential			
	<i>Agriculturalists</i>	<i>Agropastoralists</i>	<i>Pastoralists</i>
<i>Good</i>	Medium-High	Medium	Low
<i>Greedy</i>	High	Medium	Low
System Resilience			
	<i>Agriculturalists</i>	<i>Agropastoralists</i>	<i>Pastoralists</i>
<i>Good</i>	Low	Low	High
<i>Greedy</i>	Low	High	High
System Connectedness			
	<i>Agriculturalists</i>	<i>Agropastoralists</i>	<i>Pastoralists</i>
<i>Good</i>	High	Medium	Low
<i>Greedy</i>	High	Medium-Low	Medium-Low

derives from inequalities that arise between households in sedentary agricultural societies due to small-scale resource variability (Kelly, 1991). This stress typically manifests in high levels of inter-household competition over a limited set of resources and would be visible archaeologically as large differences in maximum populations between households in a single community. Although this phenomenon could be directly measured in the output data of newer versions of the MML (i.e., by graphically comparing household “life histories”, or population trends, over time) it is not possible with the version used in this research. However, based on the patterning I have seen in vegetation and soil properties, I would expect “greedy” mindsets to produce more of this kind of stress as well. This is a topic that would be interesting to explore in future modeling experiments with newer versions of the MML.

Other types of more socially-derived stresses exist in real agropastoral SES, but because the social modeling engine of the MML is highly simplified, these types of stress have no effect in the current experiments. The general amount of social stress that may result from each of the subsistence variants can only be inferred through overall

population size and stability over time. The relationship between population size and social stress has been established by Johnson (1982), in his investigation of “scalar stress” among low-level food producers. As the overall population of a community increases, scalar communication stress also increases, potentially affecting social cohesion and igniting social strife (Johnson, 1982). Thus, subsistence strategies that allow for very high populations can be also be understood to result in higher levels of social stress, which can be a source of instability if not mitigated by

special social institutions (Kuijt, 2000b). By this measure, the two agricultural subsistence variants would lead to much greater levels of scalar stress than would the pastoral and agropastoral subsistence variants, and agropastoralism would lead to higher levels of scalar stress than pastoralism.

A final, more poorly understood source of stress is uncertainty due to emergence. This produces stress because the outcome of actions in highly emergent systems is very unpredictable. In other words, there would be little confidence that conducting the same action (e.g., farming) in the same set of circumstance (e.g., same field or on the same landform) would obtaining the same result every year. Pastoralism and “greedy” agropastoralism showed the largest capacity for emergence among the modeled subsistence systems. These types of subsistence should therefore also be subject to the largest amounts of stress due to unpredictability.

In the agricultural and “good” agropastoral models, however, the existence of a very stable “equilibrium” across all repeated model-runs in these subsistence variants would make long-term social planning and larger populations possible. Stability therfore begets larger populations, and larger populations lead to social stress and potential

resource scarcity. These stresses can be resolved either by a reduction in population, or an increase in social complexity or level of technology. Thus, these three sets of stressors are interconnected, so that change in one affects the others. They would have acted in a sort of dynamic “push-pull” on the LPPNB SES of Wadi Ziqlab, as a balance of forces that could induce change or promote stability. Stress from resource imbalance and emergence would tend to favor an increasing reliance on agriculture, which these modeling experiments show is a stable, predictable subsistence system. However, a greater reliance on agriculture seems to lead to higher populations, introducing more social stress which may push people towards an increased reliance on pastoralism. The other solution would be to mitigate these social stresses in a different way, such as by creating new and potentially complex social institutions.

7.7. SUMMARY

I have summarized the general amounts of system potential, resilience, and connectedness for each of the twelve models in Table 7.6. These experiments show two major subsistence attractors with different characteristics. Under the modeled conditions (stable Mediterranean climate), agriculture provides a quite stable subsistence base that allows for relatively high populations and increasing predictability over time. It seems to be relatively immune to fluctuations deriving from subsistence mindset, although there is some indication that territorial “packing” may occur as a result of mindsets that encourage less sustainable resource use. In the case of such packing, certain types of vegetation may become locally depleted, leading to a reduction in system resilience over time. Nevertheless, a subsistence system based mainly on agriculture seems to be the “best” solution if a large, relatively stable

population base is the measure of success. This is quite interesting in relation to the “mega-site” phenomenon of the LPPNB. Using those same measures, pastoralism is a much less attractive, although not altogether unattractive, option.

Secondly, it seems that the addition of domestic animals to the subsistence base has divergent effects, depending upon the ratio of agriculture to pastoralism. The inclusion of domestic animals seems to further-stabilize the resource base if the ratio is small. By the time agriculture and pastoralism become equally important to the resource base, an additional source of instability is introduced. Equally-mixed agropastoralism in stable Mediterranean ecosystems is thus the most sensitive of the three simulated subsistence strategies to differences in subsistence mindset. Under conservationist mindsets, agropastoralism can be extremely stable and predictable while being capable of supporting a relatively large population base. Interestingly, reducing conservationist ethics, and minimizing field-clearance labor makes it wildly unpredictable and unstable over time. This is very interesting in the light of the ethnographic research conducted in Chapter 3, which also suggested that certain forms of agropastoralism were inherently unstable.

Finally, under the modeled conditions, pastoralism can support far fewer people and tends to result in a kind of “hysteresis” between two alternative stable population levels at medium to long-term cycle-widths. Pastoralism is thus less predictable than agriculture over the long-term in stable Mediterranean ecosystems but is still fairly predictable at small or medium time-scales. Pastoralism is also fairly immune to perturbation due to subsistence mindset, although it seems to be sensitive to mindsets that encourage a combination of less sustainable resource use and minimization of field-clearing labor.

CHAPTER 8

CONCLUSION

8.1. IMPLICATIONS FOR SOCIETAL TRANSITION IN THE NEOLITHIC AND BEYOND

What implications do the outcome of these simulations have for our understanding of the cause of major social transitions in the Neolithic or in other times or places? Firstly, the simulation approach has provided a more nuanced picture of the dynamic and recursive set of relationships between people and local ecosystems during the Neolithic. Simulation makes clear that these relationships are capable of producing complex, non-linear system-behavior, including unpredictable emergent properties, hysteresis, and critical transitions. Importantly, the experiment-based approach showed that even relatively minor differences between potential Neolithic subsistence systems could have led to vastly different outcomes. Simulation highlights the roles of resilience, connectedness, and system potential in agropastoral subsistence. The results of the six modeling experiments reveal how these factors dynamically interconnect to produce stability or unpredictability in different potential Neolithic SES. These dynamics are not preserved in the archaeological record, and oversimplified narratives of change are simply inadequate if we really want to learn how and why change occurs in complex human systems.

From the simulation approach, we also learn that what actually happened in the past is very likely to have been just one of many potential scenarios that could have unfolded from the same beginnings. That is to say, the evidence we recover from archaeological survey and excavation is the record of just one realization of the course of events in a complex system that was could just as easily have proceeded differently. Finally, although some of the experiments did produced signs of

bifurcation to alternative states, it is significant that a total catastrophic depopulation never occurred in any of the modeled scenarios. This supports the idea that traditional ideas about societal transitions as “collapse” need to be rethought.

8.1.1. Implications for the PPN-LN Transition in Wadi Ziqlâb

In keeping with the goals of a modeling approach (see Chapter 5), it is not important if any of the six modeling experiments perfectly mimicked the true PPN SES of Wadi Ziqlâb. Instead, it is more important that they are simplified representations of SES’s that could have existed in the region at that time. Studying the dynamics produced in each of the experiments can tell us something about the kinds of dynamics produced by the real PPNB SES of Tell Rakkan I. Because the simplified SES in the simulations have fewer “moving parts” than do real world SES, we can possibly hope to more completely understand how these components interact to produce different dynamics under different conditions. We can then map this understanding to the tidbits of information we have gathered about the real human past in the region.

As explored in Chapters 2 and 3, the archaeological proxies of the level of system potential from Wadi Ziqlâb suggest only moderate population and agropastoral productivity. These best fit with the patterns of system potential produced by the pastoral and agropastoral simulation models. In particular, these models produce population sizes that are within the range of those estimated for Tell Rakkan I (less than 300 people), whereas the agriculturalist models all result in much higher “equilibrium” populations. Although we cannot rule out that the MML simply overestimates the number of people supported by a dominantly agricultural economy, the results

of these experiments would suggest that the population of PPN Tell Rakkan I was significantly lower than it should have been in a dominantly agricultural Neolithic subsistence system. However, the archaeological data relating to subsistence practices in the LPPNB in general and, to a lesser degree, from Tell Rakkan I in specific, suggests that agriculture was important, and was becoming more important over time. Moreover, there is no evidence at Tell Rakkan I to suggest that pastoralism was the dominant subsistence activity (scant faunal remains, no documented animal enclosures, etc.). Given the size of the site and the relative permanence of the architecture documented in the limited excavations of the site, it is very likely that agriculture was a major subsistence staple at the site. Combining these lines of evidence suggests that the mixed agropastoral economy is the simulated PPN SES that most closely matches that of PPNB Tell Rakkan I¹.

If this is true, some general conclusions about the nature of the LPPNB regional SES of Wadi Ziqlâb can be drawn from the results of the simulation experiments (see Chapter 7). First, the small differences in herd animal stocking rates and in farming impact between the “good” and “greedy” agropastoral models yielded wide differences in system potential, system resilience, system connectedness, cyclicity, divergence, stability, predictability, and the amount of cumulative human impacts over time.

Thus, while agropastoralism can be a highly stable, predictable subsistence system in some circumstances, it can be a wildly unstable and potentially vulnerable subsistence system in others. Although agents in the MML could not adapt their land-use decision-making criteria, real people do adapt to changing circumstance. Further, recent cross-cultural analysis of human subsistence strategies shows that mixed agropastoral strategies do not occur frequently in the ethnographic record of modern and historic peoples (Ullah et al., 2015). The fundamental tension between needing to provide for large numbers of herd animals (requiring mobility and flexibility), and needing to

tend farm plots (requiring sedentism and capital investment in a fixed place) makes a subsistence based equally on farming and herding inherently unstable over long time-spans. If the inhabitants wanted to increase predictability, stability, and system output (potential, in the form of increased grain yields, higher population, etc.), they could have consciously changed their subsistence logic in such a way as to increase reliance on agriculture over time. However, in doing so, they would have given up some of the resilience inherent to smaller-scale mixed systems. This would have been exacerbated over time as the cumulative effects of human land-use fundamentally altered their ability to return to a more pastoral way of life. This narrowing of options would potentially have put them at greater risk for a critical transition.

So, was the PPN-LN transition in Wadi Ziqlâb a critical transition? The evidence from the simulation models do not prove it to have been such. But, they do offer tantalizing clues that suggest that it could have been. If it was a critical transition, then the small-scale LN subsistence system could be understood as the alternative stable state in a hysteretic cycle of a more general suite of Neolithic SES.

8.1.2. Implications for the PPN-LN Transition in General

Although situated in Wadi Ziqlâb, the results of this simulation experiment nevertheless have some implications for the nature of the PPN-LN transition in other parts of the Southern Levant and in the “Mega-sites” of the Jordanian Highlands in particular. It seems fairly certain that the very large populations assumed to have been housed in the Mega-sites could only be supported by a dominantly agricultural subsistence system. High population-levels require massive site catchments, however, and the two agricultural simulations that achieved the largest populations were utilizing the entire Wadi Ziqlâb watershed by the end of the PPNB. These systems were quite stable throughout the length of the simulations, but this stability, and the large system-potential, came at the cost of increasing connectedness and rigidity over time.

¹ Missing, of course, any of the wild resources that PPNB people still relied on.

In short, these highly agricultural systems began to lose resilience over time and, thus, were at ever-greater risk of falling or being pushed into a catastrophic system transformation. Although these systems appear very stable and predictable in the short- and medium-term, the cost of this stability is increased risk of catastrophic failure in the long-term. The experiments conducted in this research did not result in a critical transitions for agriculturalists, so it is not possible to estimate what the characteristics of a purely agricultural alternative stable state might be. One possibility is for a complete return to one of the other major human subsistence systems (e.g., agropastoralism, pastoralism, or hunting and gathering). Another, more intriguing possibility, is that an alternative state is, in fact, a more intensive investment in agriculture – one requiring more complex social arrangements to manage labor and capital. Although that clearly did not occur across the PPN-LN transition in Wadi Ziqlâb or elsewhere, it does seem to have happened all across the Neolithic world at the end of the Late Neolithic when we see a fluorescence of intensively agricultural societies in the Chalcolithic and Bronze Ages.

A final implication of the research presented in this monograph is that while rigidity may have made the PPN SES more vulnerable to outside influence (rapid climate change, warfare, etc.), outside influence would not have been a necessary trigger of the transition. Further, if a series of Neolithic towns were indeed connected in a regional network, increased connectivity in the system would mean that the dissolution of only one town—whether due to a self-imposed critical transition or external disturbance—could have affected them all. Any such disturbance would have been exacerbated by the accumulation of 700 years of increasing rigidity and decreasing resilience in the subsistence system of all the large LPPNB towns. What may have started as a single critical failure of one component of the regional system could have initialized a cascade of failure throughout the entire LPPNB network.

8.2. FUTURE RESEARCH DIRECTIONS

The simple simulation experiments presented in this monograph have provided many useful insights into the dynamics of Neolithic SES in Northern Jordan, but were ultimately limited by the structure of the MML and the structure of the specific experiments formulated for this research. Nevertheless, the experiments presented here to-date represent the largest-scale use of simulation modeling to understand the dynamics of subsistence and environment in one of the world's oldest SES. They also represent the largest set of experiments conducted with the MML, and so have exposed a number of shortcomings in the modeling infrastructure (e.g., the inability to recover from interrupted runs, internal errors disrupting statistical output, malformed or cumbrosomely-formatted statistical output, human error associated with managing the arrangement of simulation experiments on multiple desktop computers, etc.). Steps are already being taken to mitigate some of these issues (Barton et al., 2016), however, and future versions of the MML will greatly expand the flexibility and reliability of the modeling framework.

The current round of modeling experiments were intentionally limited in scope. For example, climate (and consequently vegetation climax limits) and site location were held constant for the entire 700 years of the simulation run. Clearly, these are critical variables for understanding the nature of the PPN-LN transition and feature prominently in two of the five existing hypotheses for the instigation of the transition (i.e., the “climatic forcing” and “settlement reorganization” hypotheses). These experiments can (and do) inform us of the extent to which a PPNB SES of Wadi Ziqlâb may have been vulnerable to rapid climate change, but cannot (and do not) reveal the intricacies of the effect of climate change on the different potential Neolithic SES. Likewise, the experiments can (and do) reveal the limitations and opportunities afforded by the central location of a PPNB SES at Tell Rakkan I, but cannot (and do not) reveal the potential benefits and costs of a multi-sited SES during the Late Neolithic period that followed.

These are two clear avenues for future research.

The construction of the early version of the MML used in this research also presented some important limitations on the scope of the experiments that could be conducted. For example, because the number of households can never change in a simulation, in many of the simulations, they simply grow in size until they no longer represent a realistic “household”. This means that analysis of inter-household differences becomes meaningless because the variability in access to land between households is greatly reduced because of averaging effects across the very large catchments they now hold. Thus, it is not possible to analyze the amount of synchronicity in the adaptive cycle of the households which is a major indicator for the risk of critical transitions. These limitations would be circumvented if households were allowed to fission. Another limitation of this version of the MML is that there are no land-tenure restrictions, so agents are free to exchange farm parcels whenever it seems beneficial to do so. This seems to inevitably lead to a quick “swiddening” style of agriculture, which may be a reasonable model for Neolithic farming, but is clearly not the only style of rain-fed agriculture possible. Additionally, it means that, unless the entire catchment is given over to agriculture, agents will always choose to swidden. If land access was more restricted (e.g., through, tenure) it is likely that soil fertility levels would be more drastically affected over time which might lead to quite different population dynamics than were produced in the current set of experiments. Furthermore, agent behavior in this version of the MML is only determined by a “satisficing” style of decision making (i.e., while agents do try to minimize costs, they only try to meet their minimum requirements). Different decision strategies (e.g., profit maximizing, pure cost minimizing, etc.) would also likely lead to different outcomes (Barton et al., 2015, 2016). Finally, agents in this version of the MML are not allowed to modify their basic subsistence goals during the simulation. This necessarily reduces the amount of variability in model runs (which is good for the initial set of modeling experiments conducted here), but it means that an essential

component of subsistence dynamics cannot be modeled. It is impossible, therefore, to determine under which conditions agents might switch subsistence strategies (e.g., in a critical transition between agriculture and pastoralism). These issues are being addressed in the next version of the MML, and so future modeling experiments into the PPN-LN transition can capitalize on this improved functionality to investigate the effects of more nuanced and complex agent behavior.

Finally, the experiments conducted in this research reiterated the need for multiple runs. Emergence is a powerful component of complex systems, and many repeated runs are needed in order to better understand its influences. In future research, it will be prudent to conduct many more repeated runs than the 2-10 realizations of the current research.

8.3. CONCLUSION

This research has suggested that the PPN-LN transition in Northern Jordan can potentially be explained as a critical transition between fundamentally different states of Neolithic SES. The simulation models used in this research are admittedly simple and lack sophisticated social components. Nonetheless, it is clear that the Neolithic subsistence and land-use were complex phenomena, and that recursive and dynamic feedback between the human and natural portions of the system produced emergent properties that could not be predicted or planned-for by Neolithic peoples. In the simulations, we can see how the everyday decisions of farmers and herders, intent on feeding their families for another year, could manifest in drastic and lasting change in a coupled human-natural system. The simulation approach taken in this research dovetails with the explanatory power of complexity theory to provide a powerful analytical tool to approach and disentangle previously intransigent archaeological problems. The work presented here has barely scratched the proverbial surface of this technique and will serve as a launching off point for much future research.

BIBLIOGRAPHY

- Abel, N., Cumming, D.H.M., Andries, J.M., 2006. Collapse and reorganization in socialecological systems: questions, some ideas, and policy implications. *Ecology and Society* 11, 17.
- Abrantes, F., Voelker, A. (Helga L., Sierro, F.J., Naughton, F., Rodrigues, T., Cacho, I., Ariztegui, D., Brayshaw, D., Sicre, M.-A., Batista, L., 2012. Paleoclimate Variability in the Mediterranean Region, in: P. Lionello (Ed.), *The Climate of the Mediterranean Region*. Elsevier, Oxford, pp. 1–86.
- Adler, P., Raff, D., Lauenroth, W., 2001. The effect of grazing on the spatial heterogeneity of vegetation. *Oecologia* 128, 465–479.
- Al-Jaloudy, M.A., 2006. Country Pasture/Forage Resource Profiles: Jordan [WWW Document]. Food and Agriculture Organization of the United Nations Country Pasture Profiles. URL <http://www.fao.org/ag/AGP/agpc/doc/Counprof/Jordan/Jordan.htm#4.%20RUMINANT%20LIVESTOCK%20PRODUCTION%20SYSTEMS> (accessed 5.13.10).
- Al-Nahar, M., 2010. Tell Abu Suwan, A Neolithic Site in Jordan: Preliminary Report on the 2005 and 2006 Field Seasons. *Bulletin of the American Schools of Oriental Research* 1–18.
- Al-Shreideh, A.M., 1992. Water Resources and Systems in the Wadi Abu Ziyad basin and their Relationship with Human Settlement: A Hydrological and Archaeological Study (Unpublished MA thesis). Yarmouk University.
- Altaweel, M., 2008. Investigating agricultural sustainability and strategies in northern Mesopotamia: results produced using a socio-ecological modeling approach. *Journal of Archaeological Science* 35, 821–835.
- Anderson, P.M., Barnosky, C.W., Bartlein, P.J., Behling, P.J., Brubaker, L., Cushing, E.J., Dodson, J., Dworetzky, B., Guetter, P.J., Harrison, S.P., others, 1988. Climatic changes of the last 18,000 years: Observations and model simulations. *Science* 241, 1043–1052.
- Araus, J.L., Amaro, T., Voltas, J., Nakkoul, H., Nachit, M.M., 1998. Chlorophyll fluorescence as a selection criterion for grain yield in durum wheat under Mediterranean conditions. *Field Crops Research* 55, 209–223.
- Araus, J.L., Amaro, T., Zuhair, Y., Nachit, M.M., 1997a. Effect of leaf structure and water status on carbon isotope discrimination in field-grown durum wheat. *Plant Cell Environ* 20, 1484–1494.
- Araus, J.L., Febrero, A., Buxó, R., Camalich, M.D., Martin, D., Molina, F., RODRIGUEZ-ARIZA, M., Romagosa, I., 1997b. Changes in carbon isotope discrimination in grain cereals from different regions of the western Mediterranean Basin during the past seven millennia. Palaeoenvironmental evidence of a differential change in aridity during the late Holocene. *Global Change Biology* 3, 107–118.
- Araus, J.L., Slafer, G.A., Romagosa, I., Molist, M., 2001. FOCUS: estimated wheat yields during the emergence of agriculture based on the carbon isotope discrimination of grains: evidence from a 10th millennium BP site on the Euphrates. *Journal of Archaeological Science* 28, 341–350.
- Argonne National Laboratory, 2012. Repast Symphony. <http://repast.sourceforge.net/>.
- Arrowsmith, R., DiMaggio, E., Barton, C.M., Sarjoughian, H.S., Fall, P., Falconer, S.E., Ullah, I.I.T., 2006. Geomorphic

- mapping and paleoterrain generation for use in modeling Holocene (8,000–1,500 yr) agropastoral land-use and landscape interactions in southeast Spain. *Am Geophys Union*, San Francisco, CA.
- Asouti, E., Austin, P., 2005. Reconstructing woodland vegetation and its exploitation by past societies, based on the analysis and interpretation of archaeological wood charcoal macro-remains. *Environmental Archaeology* 10, 1–18.
- Asouti, E., 2006. Beyond the Pre-Pottery Neolithic B interaction sphere. *Journal of World Prehistory* 20, 87–126.
- Asouti, E., Fuller, D., 2012. From foraging to farming in the southern Levant: the development of Epipalaeolithic and Pre-pottery Neolithic plant management strategies. *Vegetation History and Archaeobotany* 21, 149–162.
- Banning, E.B., 1982. The research design of the Wadi Ziqlâb Survey, 1981. *American Schools of Oriental Research Newsletter* 8, 4–8.
- Banning, E.B., 1983. Wadi Ziqlâb Survey, in: Keller, D.R., Rupp, D.W. (Eds.), *Archaeological Survey in the Mediterranean Area, BAR International Series*. British Archaeological Reports, Oxford, pp. 341–344.
- Banning, E.B., 1985. Pastoral and Agricultural Land Use in the Wadi Ziqlâb, Jordan: An Archaeological and Ecological Survey (Doctoral Thesis). University of Toronto, Toronto.
- Banning, E.B., 1992a. Tabaqat al-Bûma, Wadi Ziqlâb. *American Journal of Archaeology* 96, 506–507.
- Banning, E.B., 1992b. 1992 Excavations at Wadi Ziqlâb, al-Kura, Jordan. *Canadian Archaeological Association Newsletter* 12, 3–4.
- Banning, E.B., 1995. Herders or Homesteaders? A Neolithic Farm in Wadi Ziqlâb, Jordan. *Biblical Archaeologist* 58, 2–13.
- Banning, E.B., 1996. Highlands and Lowlands: Problems and Survey Frameworks for Rural Archaeology in the Near East. *Bulletin of the American Schools of Oriental Research* 301, 25–45.
- Banning, E.B., 1998. The Neolithic Period: Triumphs of Architecture, Agriculture, and Art. *Near Eastern Archaeology* 61, 188–237.
- Banning, E.B., 1999. Neolithic and Chalcolithic Archaeology in Wadi Ziqlâb, Northern Jordan. *Occident & Orient* 4, 46–48.
- Banning, E.B., 2001. Settlement and Economy in Wadi Ziqlâb During the Late Neolithic, in: Amr, K. (Ed.), *Studies in the History and Archaeology of Jordan VII: Jordan by the Millennia*, 7. Department of Antiquities, Amman, pp. 149–156.
- Banning, E.B., 2003. Housing Neolithic Farmers. *Near Eastern Archaeology* 66, 4–21.
- Banning, E.B., 2007a. Wadi Rabah and related assemblages in the southern Levant: Interpreting the radiocarbon evidence. *Paléorient* 33, 77–101.
- Banning, E.B., 2007b. Time and Tradition in the Transition from Late Neolithic to Chalcolithic: Summary and Conclusions. *paleo* 33, 137–142.
- Banning, E.B., 2010. Houses, households, and changing society in the Late Neolithic and Chalcolithic of the Southern Levant. *Paleorient* 36, 46–87.
- Banning, E.B., Blackham, M., Lasby, D., 1998. Excavations at WZ 121, A Chalcolithic Site at Tubna, In Wadi Ziqlâb. *Annual of the Department of Antiquities of Jordan* 42, 141–159.
- Banning, E.B., Byrd, B.F., 1987. Houses and the Changing Residential Unit: Domestic Architecture at PPNB 'Ain Ghazâl, Jordan. *Proceedings of the Prehistoric Society* 53, 309–325.
- Banning, E.B., Dodds, R.R., Field, J., Kuijt, I., McCorriston, J., Siggers, Julien, Taani, H., Triggs, J., 1992. Tabaqat al Bûma: 1990 excavations at a Kebaran and Late Neolithic site in Wadi Ziqlâb. *Annual of the Department of Antiquities of Jordan* 36, 43–69.

- Banning, E.B., Dodds, R.R., Field, J., Maltby, S., McCorriston, J., Monckton, S., Rubenstein, R., Sheppard, P.J., 1989. Wadi Ziqlâb Project 1987: A Preliminary Report. Annual of the Department of Antiquities of Jordan 33, 43–58.
- Banning, E.B., Fawcett, C., 1983. Man-land relationships in the ancient Wadi Ziqlâb: report of the 1981 survey. Annual of the Department of Antiquities of Jordan 27, 291–309.
- Banning, E.B., Gibbs, K., Gregg, M., Kadowaki, S., Rhodes, S., 2002. Excavations at al-Basatin, Wadi Ziqlâb, Jordan. Neolithics 2, 13–14.
- Banning, E.B., Gibbs, K., Kadowaki, S., 2011. Changes in material culture at Late Neolithic Tabaqat al Bûma, in Wadi Ziqlâb, northern Jordan, in: Lovell, J., Yorke, R.M. (Eds.), Culture, Chronology and the Chalcolithic: Theory and Transition., Council for British Research in the Levant Supplementary Series. Oxbow Books, Oxford, pp. 36–60.
- Banning, E.B., Gibbs, K., Kadowaki, S., 2003. Excavations at a Late Neolithic site, al-Basatin, in Wadi Ziqlâb, Jordan. Annual of the Department of Antiquities of Jordan 47.
- Banning, E.B., Gibbs, K., Ullah I.I., Hitchings, P., Abu Jayyab, K., Edwards, S., and Rhodes, S., 2015. Archaeological Excavations in Wadi Quseiba and Wadi al-Bîr, northern Jordan. Antiquity Project Gallery. 344. <http://antiquity.ac.uk/projgall/508>
- Banning, E.B., Maher, L.A., Kadowaki, S., Gibbs, K., 2004. Excavations at a Late Neolithic site in Wadi Ziqlâb, Northern Jordan. Antiquity 308.
- Banning, E.B., Najjar, M., 1999. Excavations at Tell Rakan I, a Neolithic site in Wadi Ziqlâb. Neo-Lithics 99, 1–3.
- Banning, E.B., Rahimi, D., Siggers, Julian, 1994. The Late Neolithic of the Southern Levant: Hiatus, Settlement Shift or Observer Bias? The Perspective from Wadi Ziqlâb. Paléorient 20, 151–164.
- Banning, E.B., Rahimi, D., Siggers, Julian, Taani, H., 1996. The 1992 Season of Excavations in Wadi Ziqlâb, Jordan. Annual of the Department of Antiquities of Jordan 40, 29–49.
- Banning, E.B., Siggers, Julian, 1997. Technological Strategies at a Late Neolithic Farmstead in Wadi Ziqlâb, Jordan, in: Gebel, Hans G, Kafafi, Zedan, Rollefson, G.O. (Eds.), The Prehistory of Jordan II: Perspectives from 1997. Ex Oriente, Berlin.
- Barlett, P.F., 1980. Adaptive Strategies in Peasant Agricultural Production. Annual Review of Anthropology 9, 545–573.
- Bar, S., Rosenberg, D., 2011. Newly Discovered Yarmukian and Wadi Rabah Sites in the Southern Jordan Valley and The Desert Fringes of Samaria During the 7th and 6th Millennia BC: Preliminary Report. Archaeology, Ethnology and Anthropology of Eurasia 39, 32–39.
- Bartolome, J., Franch, J., Plaixats, J., Seligman, N. G., 1998. Diet Selection by Sheep and Goats on Mediterranean Heath-Woodland Range. Journal of Range Management 51, 383–391.
- Barton, C.M., Ullah, I.I.T., Bergin, S., 2010a. Land use, water and Mediterranean landscapes: modelling long-term dynamics of complex socio-ecological systems. Philosophical Transactions of the Royal Society A: Mathematical, Physical and Engineering Sciences 368, 5275 –5297.
- Barton, C.M., Ullah, I.I.T., Bergin, S.M., Mitasova, H., Sarjoughian, H., 2012. Looking for the future in the past: Long-term change in socioecological systems. Ecological Modelling 241, 42–53.
- Barton, C.M., Ullah, I.I.T., Mitasova, H., 2010b. Computational modeling and Neolithic socioecological dynamics: a case study from Southwest Asia. American Antiquity 75, 364–386.
- Barton, C.M., Ullah, I.I.T., Mayer G., Bergin, S., Sarjoughian, H., and Mitasova, H., 2015. MedLand Modeling Laboratory v.1 - A hybrid modeling environment that couples an agent-based model of small-holder agropastoral households and a cellular

- landscape evolution model that simulates changes in erosion/deposition, soils, and vegetation. Retrievable from: CoMSES Computational Model Library, www.openabm.org/model/4609/version/1
- Barton, C.M., Ullah, I.I.T., Bergin, S.M., Sarjoughian, H.S., Mayer, G.R., Bernabeu Auban, J.E., Heimsath, A.M., Acevedo, M.F., Riel-Salvatore, J.G., and Arrowsmith, J.R., 2016. Experimental Socioecology: Integrative Science for Anthropocene Landscape Dynamics. *Anthropocene*. Pre-press online: 10.1016/j.ancene.2015.12.004.
- Bar-Yosef, O., 1985. A Cave in the Desert: Nahal Hemar: 9,000-year-old-finds. Israel Museum.
- Bar-Yosef, O., 2001. Lithics and the social geographical configurations identifying Neolithic tribes in the Levant. Beyond tools. Redefining PPN Lithic assemblages of the Levant 437–448.
- Bar-Yosef, O., 2002. The Natufian culture and the early Neolithic: Social and economic trends in Southwestern Asia. Examining the Farming/Language Dispersal Hypothesis, McDonald Institute Monographs, University of Cambridge, Cambridge 113–126.
- Bar-Yosef, O., Alon, D., 1988. Nahal Hemar Cave: the excavations.
- Bar-Yosef, O., Meadow, R.H., 1995. The Origins of Agriculture in the Near East, in: Price, T.D., Gebaur, A. (Eds.), *Last Hunters-First Farmers: New Perspectives on the Prehistoric Transition to Agriculture*. School of American Research Press, Santa Fe, pp. 39–94.
- Barzegar, A.R., Yousefi, A., Daryashenas, A., 2002. The effect of addition of different amounts and types of organic materials on soil physical properties and yield of wheat. *Plant and soil* 247, 295–301.
- Batjes, N.H., Rawajfih, Z., Al-Adamat, R., 2003. Soil data derived from SOTER for studies of carbon stocks and change in Jordan. Version (1.0), ISRIC. The Netherlands: World Soil Information.
- Bazzaz, F.A., 1979. The Physiological Ecology of Plant Succession. *Annual Review of Ecology and Systematics* 10, 351–371.
- Belfer-Cohen, A., Goring-Morris, N., 1997. The articulation of cultural processes and Late Quaternary environmental changes in Cisjordan. *paleo* 23, 71–93.
- Bender, F., 1975. Geology of the Arabian Peninsula: Jordan. United States Government Printing Office.
- Bender, F., Khdeir, M.K., 1974. Geology of Jordan. Gebrueder Borntraeger.
- Bentley, R.A., 2003. Complex systems and archaeology: empirical and theoretical applications. University of Utah Press, Salt Lake City.
- Bentley, R. Alexander, Maschner, H.D.G., 2003. Complex systems and archaeology. University of Utah Press, Salt Lake City.
- Berger, J.-F., Guilaine, J., 2009. The 8200 cal BP abrupt environmental change and the Neolithic transition: A Mediterranean perspective. *Quaternary International* 200, 31–49.
- Bergin, S., Ullah, I.I.T., Barton, C.M., Gravel-Miguel, C., 2012. Human-Environment Interactions in a Changing Environment: A Computational Model of Agropastoral Practices and Landscapes in Neolithic Spain, in: *Socio-natural Systems in Pastoral and Agro-pastoral Societies: Archaeological Investigations of Pastoral Landscapes*. Presented at the 77th annual meeting of the Society of American Archaeology, Memphis.
- Berthold, M.R., Cebron, N., Dill, F., Gabriel, T.R., Kötter, T., Meinl, T., Ohl, P., Sieb, C., Thiel, K., Wiswedel, B., 2008. KNIME: The Konstanz information miner. *Data Analysis, Machine Learning and Applications* 319–326.
- Berthold, M.R., Cebron, N., Dill, F., Gabriel, T.R., Kötter, T., Meinl, T., Ohl, P., Thiel, K., Wiswedel, B., 2009. KNIME-the Konstanz information miner: version 2.0 and beyond. *AcM SIGKDD explorations Newsletter* 11, 26–31.

- Bettinger, R.L., 1987. Archaeological approaches to hunter-gatherers. *Annual Review of Anthropology* 16, 121–142.
- Bhatt, B.P., Sachan, M.S., 2004. Firewood consumption pattern of different tribal communities in Northeast India. *Energy Policy* 32, 1–6.
- Binford, L.R., 1977. Forty-seven trips: A case study in the character of archaeological formation processes, in: Wright, R.V.S. (Ed.), *Stone Tools as Cultural Markers*. Australian Institute of Aboriginal Studies, Canberra, pp. 24–36.
- Binford, L.R., 1980. Willow Smoke and Dogs' Tails: Hunter-Gatherer Settlement Systems and Archaeological Site Formation. *American Antiquity* 45, 4–20.
- Binford, L.R., 2001. Constructing frames of reference: an analytical method for archaeological theory building using ethnographic and environmental data sets. University of California Press, Berkeley.
- Binford, L.R., 1977. For theory building in archaeology: essays on faunal remains, aquatic resources, spatial analysis, and systemic modeling. Academic Pr.
- Binford, L.R., 1983. Working at archaeology. Academic Press New York.
- Blackham, M., 1997. Changing Settlement at Tabaqat al-Bûma in Wadi Ziqlâb, Jordan: A Stratigraphic Analysis, in: H. G. Gebel, Z.K., Rollefson, G.O. (Eds.), *Prehistory of Jordan II: Perspectives from 1997, Studies in Early Near Eastern Production, Subsistent, and Environment 4*. Ex Oriente, Berlin, pp. 345–360.
- Blackham, M., Fisher, K., Lasby, D., 1997. Excavations at Tell Fendi, a Late Chalcolithic Site in the Jordan Valley, Jordan. *Echos Du Monde Classique/Classical Views* 41, 1–4.
- Bledsoe, B.P., 2002. Stream Erosion Potential and Stormwater Management Strategies. *Journal of Water Resources Planning & Management* 128, 451.
- Bocquet-Appel, J.P., 2002. Paleoanthropological Traces of a Neolithic Demographic Transition. *Current Anthropology* 43, 637–650.
- Boellstorff, D., Benito, G., 2005. Impacts of set-aside policy on the risk of soil erosion in central Spain. *Agriculture, Ecosystems and Environment* 107, 231–243.
- Bonabeau, E., 2002. Agent-based modeling: Methods and techniques for simulating human systems. *Proceedings of the National Academy of Sciences* 99, 7280–7287.
- Bonet, A., 2004. Secondary succession of semi-arid Mediterranean old-fields in south-eastern Spain: insights for conservation and restoration of degraded lands. *Journal of Arid Environments* 56, 213–233.
- Bonet, A., Pausas, Juli G, 2004. Species richness and cover along a 60-year chronosequence in old-fields of southeastern Spain. *Plant Ecology* 174, 257–270.
- Bonet, A., Pausas, J. G, 2007. Old Field Dynamics on the Dry Side of the Mediterranean Basin: Patterns and Processes in Semiarid Southeast Spain. *Old Fields: Dynamics and Restoration of Abandoned Farmland* 247.
- Borg, I., Groenen, P.J.F., 2005. Modern multidimensional scaling: Theory and applications. Springer Verlag.
- Boserup, E., 1965. *The Conditions of Agricultural Growth: The Economics of Agrarian Change Under Population Pressure*. George, Allen, and Unwin, London.
- Bourgeron, P.S., Humphries, H.C., Riboli-Sasco, L., 2009. Regional analysis of social-ecological systems. *Natures Sciences Sociétés* Vol. 17, 185–193.
- Bradley, R.S., 1999. *Paleoclimatology: Reconstructing Climates of the Quaternary*. Academic Press.
- Braun, J., Heimsath, A.M., Chappell, J., 2001. Sediment transport mechanisms on soil-mantled hillslopes. *Geology* 29, 683–686.
- Brayshaw, D.J., Rambeau, C.M.C., Smith, S.J., 2011. Changes in Mediterranean climate during the Holocene: Insights from global and regional climate modelling. *The Holocene* 21, 15–31.

- Brooks, A., Yellen, J., 1987. The Preservation of Activity Areas in the Archaeological Record: Ethnoarchaeological and Archaeological Work in Northwest Ngamiland, Botswana, in: Kent, S. (Ed.), *Method and Theory for Activity Area Research: An Ethnoarchaeological Approach*. Columbia University Press, New York, pp. 63–106.
- Bryson, R.A., Bryson, R.U., 1996. High resolution simulations of regional Holocene climate: North Africa and the Near East, in: Nüzhett Dalfes, H., Kukla, G. (Eds.), *Third Millennium BC Climate Change and Old World Collapse*, Nato ASI Series I: Global Environmental Change. Springer Verlag, Berlin, pp. 565–593.
- Bryson, R.A., McEnaney-DeWall, K., 2007. An Introduction to the Archaeoclimatology Macrophysical Climate Model. University of Wisconsin.
- Burdon, D.J., Quennell, A.M., 1959. *Handbook of the Geology of Jordan*. Government of the Hashemite Kingdom of Jordan.
- Burke, B.C., Heimsath, Arjun M, White, A.F., 2007. Coupling chemical weathering with soil production across soil-mantled landscapes. *Earth Surface Processes and Landforms* 32, 853–873.
- Burrough, P.A., 1989. Fuzzy mathematical methods for soil survey and land evaluation. *Journal of Soil Science* 40, 477–492.
- Burrough, P.A., Macmillan, R.A., van DEURSEN, W., 1992. Fuzzy classification methods for determining land suitability from soil profile observations and topography. *Journal of Soil Science* 43, 193–210.
- Butzer, K.W., 1982. *Archaeology as human ecology: method and theory for a contextual approach*. Cambridge University Press, Cambridge.
- Byrd, B.F., 1994. Public and Private, Domestic and Corporate: The Emergence of the Southwest Asian Village. *American Antiquity* 59, 639–666.
- Byrd, B.F., Banning, E.B., 1988. Southern Levantine Pier Houses: Intersite Architectural Patterning during the Pre-Pottery Neolithic B. *paleo* 14, 65–72.
- Byrne D., Callaghan G., 2014. *Complexity Theory and the Social Sciences: The State of the Art*. Routledge, New York.
- Campbell, D., 2010. Modelling the Agricultural Impacts of the Earliest Large Villages at the Pre-Pottery Neolithic–Pottery Neolithic Transition, in: Finlayson, B., Warren, G. (Eds.), *Landscapes in Transistion*. Oxbow Books, Oxford, pp. 173–183.
- Campin, J.-M., Fichefet, T., Duplessy, J.-C., 1999. Problems with using radiocarbon to infer ocean ventilation rates for past and present climates. *Earth and Planetary Science Letters* 165, 17–24.
- Carmel, Y., Kadmon, R., 1999. Effects of grazing and topography on long-term vegetation changes in a Mediterranean ecosystem in Israel. *Plant Ecology* 145, 243–254.
- Carter, D.L., Berg, R.D., Sanders, B.J., 1985. The effect of furrow irrigation erosion on crop productivity. *Soil Science Society of America Journal* 49, 207–211.
- Casado, M.A., Miguel, J.M., Sterling, A., Peco, B., Galiano, E.F., Pineda, F.D., 1986. Production and spatial structure of Mediterranean pastures in different stages of ecological succession. *Plant Ecology* 64, 75–86.
- Chapman, H., Adcock, J., Gater, J., 2009. An approach to mapping buried prehistoric palaeosols of the Atlantic seaboard in Northwest Europe using GPR, geoarchaeology and GIS and the implications for heritage management. *Journal of Archaeological Science* 36, 2308–2313.
- Christensen, L.A., McElyea, D.E., 1988. Toward a general method of estimating productivity-soil depth response relationships. *Journal of soil and water conservation* 43, 199–202.
- Christiansen, J.H., Altaweel, M.R., 2005. Understanding Ancient Societies: A New Approach Using Agent-Based Holistic Modeling. *Structure and Dynamics* 1.

- Cioffi-Revilla, C., Luke, S., Parker, D.C., Rogers, J.D., Fitzhugh, W.W., Honeychurch, W., Frohlich, B., Depriest, P., Amartuvshin, C., 2007. Agent-based modeling simulation of social adaptation and long-term change in Inner Asia, in: Advancing Social Simulation: The First World Congress in Social Simulation, Edited by T. Terano and D. Sallach. Tokyo, New York, and Heidelberg: Springer Verlag.
- Cioffi-Revilla, C., Rogers, J.D., Latek, M., 2010. The MASON HouseholdsWorld Model of Pastoral Nomad Societies. Simulating Interacting Agents and Social Phenomena 193–204.
- Cioffi-Revilla, C., Rogers, J.D., Wilcox, S.P., Alterman, J., 2008. ‘Computing the Steppes: Data Analysis for Agent-Based Modeling of Polities in Inner Asia, in: Annual Conference of the American Political Science Association.
- Clare, Lee, 2010. Pastoral Clashes: Conflict risk and mitigation at the Pottery Neolithic Transition in the Southern Levant. *Neolithics* 10, 13–31.
- Clevis, Q., Tucker, G.E., Lock, G., Lancaster, S.T., Gasparini, N., Desitter, A., Bras, R.L., 2006. Geoarchaeological simulation of meandering river deposits and settlement distributions: a three-dimensional approach. *Geoarchaeology* 21, 843–874.
- Colledge, S., 2001. Plant exploitation on epipalaeolithic and early neolithic sites in the Levant, BAR International. Oxford.
- Colledge, S., Conolly, J., Shennan, S., 2004. Archaeobotanical Evidence for the Spread of Farming in the Eastern Mediterranean. *Current Anthropology* 45, S35–S58.
- Conolly, J., Colledge, S., Dobney, K., Vigne, J.-D., Peters, J., Stopp, B., Manning, K., Shennan, S., 2011. Meta-analysis of zooarchaeological data from SW Asia and SE Europe provides insight into the origins and spread of animal husbandry. *Journal of Archaeological Science* 38, 538–545.
- Contreras, D.A., 2009. Reconstructing landscape at Chavín de Huántar, Perú: A GIS-based approach. *Journal of Archaeological Science* 36, 1006–1017.
- Corbeels, M., Shiferaw, A., Haile, M., 2000. Farmers’ knowledge of soil fertility and local management strategies in Tigray, Ethiopia, Managing Africa’s Soils. Russell Press, Nottingham.
- Cordova, C.E., 2007. Millennial Landscape Change in Jordan: Geoarchaeology and Cultural Ecology. University of Arizona Press.
- Cowgill, G.L., 1975. On Causes and Consequences of Ancient and Modern Population Changes. *American Anthropologist* 77, 505–525.
- Culling, W.E.H., 1960. Analytical Theory of Erosion. *The Journal of Geology* 68, 336–344.
- Culling, W.E.H., 1963. Soil Creep and the Development of Hillside Slopes. *The Journal of Geology* 71, 127–161.
- Culling, W.E.H., 1965. Theory of Erosion on Soil-Covered Slopes. *The Journal of Geology* 73, 230–254.
- Dabasi-Scheng, L., 1978. Economic aspects of shifting cultivation, in: FAO/SIDA Regional Seminar on Shifting Cultivation and Soil Conservation in Africa, Ibadan (Nigeria), 2-21 Jul 1973. Presented at the FAO/SIDA Regional Seminar on Shifting Cultivation and Soil Conservation in Africa, FAO, Ibadan, pp. 78–99.
- David, P.A., 1988. Path-dependence: putting the past into the future of economics, Institute for mathematical studies in the social sciences Technical Report. Stanford University.
- David, P.A., 1993. Path-dependence and predictability in dynamic systems with local network externalities: a paradigm for historical economics, in: Technology and the Wealth of Nations. Pinter, London, pp. 208–231.
- David, P.A., 2001. Path dependence, its critics and the quest for “historical economics”, in: Garrouste, P., Ioannides, S. (Eds.), Evolution and Path Dependence in Economic Ideas:

- Past and Present. Edward Elgar Publishing , Inc., Northhampton, pp. 15–40.
- David, P.A., 2007. Path dependence: a foundational concept for historical social science. *Cliometrica* 1, 91–114.
- Davies, C.P., Fall, P.L., 2001. Modern pollen precipitation from an elevational transect in central Jordan and its relationship to vegetation. *Journal of Biogeography* 28, 1195–1210.
- Davis, F., Goetz, S., 1990. Modeling vegetation pattern using digital terrain data. *Landscape Ecology* 4, 69–80.
- Davis, J., Simmons, A.H., Mandel, R.D., Rollefson, Gary, Kafafi, Zeidan, 1990. A postulated Early Holocene summer precipitation episode in the Levant: Effects on Neolithic adaptations. Presented at the 55th annual meeting of the Society for American Archaeology, Las Vegas.
- Day, R.L., Laland, K.N., Odling-Smee, F.J., 2003. Rethinking adaptation: the niche-construction perspective. *Perspectives in Biology and Medicine* 46, 80–95.
- Deal, M., 1985. Household Pottery Disposal in the Maya Highlands: An Ethnoarchaeological Interpretation. *Journal of Anthropological Archaeology* 4, 243–291.
- Debussche, M., Escarré, J., Lepart, J., Houssard, C., Lavorel, S., 1996. Changes in Mediterranean plant succession: old-fields revisited. *Journal of Vegetation Science* 7, 519–526.
- Degani, A., Lewis, L.A., Downing, B.B., 1979. Interactive Computer Simulation of the Spatial Process of Soil Erosion. *Professional Geographer* 31, 184–190.
- Degen, A.A., 2007. Sheep and goat milk in pastoral societies. *Small Ruminant Research* 68, 7–19.
- De Jong, S.M., Pebesma, E.J., Lacaze, B., 2003. Above-ground biomass assessment of Mediterranean forests using airborne imaging spectrometry: the DAIS Payne experiment. *International Journal of Remote Sensing* 24, 1505–1520.
- Dietrich, W.E., Bellugi, D.G., Sklar, L.S., Stock, J.D., Heimsath, A.M., Roering, J.J., 2003. Geomorphic transport laws for predicting landscape form and dynamics. *Geophysical Monograph* 135, 103–132.
- Dodds, R.R., 1987. Wadi Ziqlâb Project 1987; Tabaqat al Bûma- 200.
- Donner, L., Schubert, W., 2011. The Development of Atmospheric General Circulation Models: Complexity, Synthesis, and Computation. Cambridge University Press.
- Edwards, P.C., Thorpe, S., 1986. Surface lithic finds from Kharaysin, Jordan. *paleo* 12, 85–87.
- Edwards, P., Meadows, J., Sayej, G., Westaway, M., 2004. From the PPNA to the PPNB : new views from the Southern Levant after excavations at Zahrat adh-Dhra' 2 in Jordan. *paleo* 30, 21–60.
- El-Naqa, A., 2001. Engineering geology assessment of El-Rabweh landslide, south-east of Amman City, Jordan. *Bulletin of Engineering Geology and the Environment* 60, 109–116.
- Enloe, J.G., 2003. Food sharing past and present: archaeological evidence for economic and social interactions. *Before Farming: the Archaeology and Anthropology of Hunter-Gatherers* 1, 1–23.
- Epstein, H., 1982. Awassi Sheep. *World Animal Review* 44, 11–27.
- Eshed, A.N., Hershkovitz, I., Goring-Morris, A.N., 2008. A Re-Evaluation of Burial Customs in the Pre- Pottery Neolithic B in light of Paleodemographic Analysis of the Human Remains from Kfar HaHoresh, Israel. *paleo* 34, 91–103.
- Eshed, Vered, Gopher, A., Gage, T.B., Hershkovitz, Israel, 2004. Has the transition to agriculture reshaped the demographic structure of prehistoric populations? New evidence from the Levant. *American Journal of Physical Anthropology* 124, 315–329.
- Essa, S., 2004. GIS modeling of land degradation in Northern-Jordan using Landsat imagery, in: *Proceedings of XXth ISPRS Congress*.

- Istanbul.
- Evans, T.P., Kelley, H., 2004. Multi-scale analysis of a household level agent-based model of landcover change. *Journal of Environmental Management* 72, 57–72.
- Fairbairn, S.L., Patience, J.F., Classen, H.L., Zijlstra, R.T., 1999. The energy content of barley fed to growing pigs: characterizing the nature of its variability and developing prediction equations for its estimation. *J. Anim Sci.* 77, 1502–1512.
- Fall, P.L., Falconer, S.E., Lines, L., 2002. Agricultural intensification and the secondary products revolution along the Jordan Rift. *Human Ecology* 30, 445–482.
- Farhan, Y., 1986. Landslides in Central Jordan with Special Reference to the March 1983 Rainstorm. *Singapore Journal of Tropical Geography* 7, 80–97.
- Feinman, G., Neitzel, J.E., 1984. Too Many Types: An Overview of Sedentary Prestate Societies in the Americas. *Advances in Archaeological Method and Theory* 7, 39–102.
- Fenner, J.N., 2005. Cross-cultural estimation of the human generation interval for use in genetics-based population divergence studies. *American Journal of Physical Anthropology* 128, 415–423.
- Field, J., 1994. Rainfall patterns and landscape changes in Wadi Ziqlâb, Jordan, in: Jamieson, R., Abonyi, S., Mirau, N. (Eds.), *Archaeology and the Environment: A Fragile Coexistence*. Proceedings of the 24th Annual Chacmool Conference. Department of Archaeology, University of Calgary, Calgary, pp. 257–59.
- Field, J., Banning, E. B, 1998. Hillslope processes and archaeology in Wadi Ziqlâb, Jordan. *Geoarchaeology* 13, 595–616.
- Fisher, W., Atkinson, D., Beaumont, P., Coles, A., Gilchrist-Shirlaw, D., 1966. Soil Survey of Wadi Ziqlâb, Jordan. Durham University, Durham.
- Flanagan, L.J.M., Meyer, L.D., 2003. Honoring the Universal Soil Loss Equation Booklet. American Society of Agricultural and Biological Engineers and Purdue University, West Lafayette, IN.
- Flannery, K.V., 1993. Will the real model please stand up: comments on Saidel's "Round house or square". *Journal of Mediterranean Archaeology* 6, 109–117.
- Fleuret, P.C., Fleuret, A.K., 1978. Fuelwood Use in a Peasant Community: A Tanzanian Case Study. *The Journal of Developing Areas* 12, 315–322.
- Folke, C., 2006. Resilience: The emergence of a perspective for social-ecological systems analyses. *Global environmental change* 16, 253–267.
- Folke, C., Carpenter, S., Walker, B., Scheffer, M., Elmqvist, T., Gunderson, L., Holling, C. S., 2004. Regime shifts, resilience, and biodiversity in ecosystem management. *Annual Review of Ecology, Evolution, and Systematics* 557–581.
- Förster, H., Wunderlich, J., 2009. Holocene sediment budgets for upland catchments: The problem of soilscape model and data availability. *CATENA* 77, 143–149.
- Foster, G. R., Meyer, L.D., Shen, 1972. A closed-form soil erosion equation for upland areas, in: *Sedimentation: Symposium to Honor Professor HA Einstein*. Ft. Collins, CO. pp. 12.1–12.19.
- Fox, J., 1984. Firewood consumption in a Nepali village. *Environmental Management* 8, 243–249.
- Fuller, D., Asouti, E., Purugganan, M., 2012. Cultivation as slow evolutionary entanglement: comparative data on rate and sequence of domestication. *Vegetation History and Archaeobotany* 21, 131–145.
- Gaili, E.S., Ali, A.E., 1985. Meat from Sudan desert sheep and goats: Part 2—Composition of the muscular and fatty tissues. *Meat Science* 13, 229–236.
- Galán, J.M., Izquierdo, L.R., Izquierdo, S.S., Santos, J.I., Del Olmo, R., López-Paredes, A., Edmonds, B., 2009. Errors and artefacts in agent-based modelling. *Journal of Artificial Societies and Social Simulation* 12, 1.

- García Puchol, O., Baton, C.M., Bernabeu Aubán, J., 2008. Programa de prospección geofísica, microsondeos y catas para la caracterización de un gran foso del IV milenio cal AC en Alt del Punxó (Muro de l'Alcoi, Alacant). *Trabajos de prehistoria* 65, 143–154.
- Garfinkel, Y., 1987. Yiftahel: a Neolithic village from the seventh millennium BC in Lower Galilee, Israel. *Journal of Field Archaeology* 14, 199–212.
- Gasparini, N.M., Bras, R.L., Whipple, K.X., 2006. Numerical modeling of non-steady-state river profile evolution using a sediment-flux-dependent incision model. *Special Paper - Geological Society of America* 398, 127–141.
- Gebel, H.G., 2004. Central to what? The centrality issue of the LPPNB Mega-Site phenomenon in Jordan, in: Bienert, H.-D., Gebel, H.G., Neef, Reinder (Eds.), *Central Settlements in Neolithic Jordan, Studies in Early Near Eastern Production, Subsistence, and Environment. Ex oriente*, Berlin, pp. 1–19.
- Gibbon, D., 1981. Rainfed farming systems in the Mediterranean region. *Plant Soil* 58, 59–80.
- Gibbs, K., 2008. Understanding Community: A Comparison of Three Late Neolithic Pottery Assemblages from Wadi Ziqlâb, Jordan (Ph.D.). University of Toronto, Toronto.
- Gibbs, K., Kaduwaki, S., Banning, E.B., 2006. The Late Neolithic at al-Basatîn in Wadi Ziqlâb, northern Jordan. *Antiquity* 80, <http://antiquity.ac.uk/projgall/gibbs/index.html>.
- Gibbs, K., Kaduwaki, S., Banning, E.B., 2010. Excavations at al-Basatîn, a Late Neolithic and Early Bronze I Site in Wadi Ziqlâb, Northern Jordan. *Annual of the Department of Antiquities of Jordan* 54, 461–476.
- Glaser, M., Ratter, B.M.W., Krause, G., Welp, M., 2012. New approaches to the analysis of human–nature relations, in: Glaser, M., Ratter, B.M.W., Krause, G., Welp, M. (Eds.), *Human-nature Interactions in the Anthropocene: Potentials of Social-ecological Systems Analysis*. Routledge, New York, pp. 1–12.
- Goodale, N.B., Kuijt, I., 2006. Chronological Frameworks and Disparate Technology: an Exploration of Chipped Stone Variability and the Forager to Farmer Transition at ‘Iraq ed-Dubb, Jordan. *paleo* 32, 27–45.
- Goodale, N.B., 2009. Convergence in the Neolithic: Human population growth at the dawn of agriculture. Washington State University.
- Goodchild, M., Haining, R., STEPHEN, W., 1992. Integrating GIS and spatial data analysis: problems and possibilities. *International Journal of Geographical Information Systems* 6, 407–423.
- Gordon, R.L., Knauf, E.A., 1987. Er-Rumman Survey 1985. *Annual of the Department of Antiquities of Jordan* 31 289–93.
- Goring-Morris, A. N., Burns, R., Davidzon, A., Eshed, V., Goren, Y., Herskovitz, I., Kangas, S., Kelecevic, J., 1998. The 1997 season of excavations at the mortuary site of Kfar HaHoresh, Galilee, Israel. *Neo-Lithics* 3, 1–4.
- Goring-Morris, N., Belfer-Cohen, A., 2010. “Great Expectations,” or the Inevitable Collapse of the Early Neolithic in the Near East N. Goring-Morris and Anna Belfer-Cohen, in: Brandy, M.S., Fox, J.R. (Eds.), *Becoming Villagers: Comparing Early Village Societies*. University of Arizona Press, Tucson, pp. 62–80.
- Gotts, N.M., 2007. Resilience, panarchy, and world-systems analysis. *Ecology and Society* 12, 24.
- Gould, R.A., 1978. Beyond analogy in ethnoarchaeology, in: *Explorations in Ethnoarchaeology, SAR Advanced Seminars*. University of New Mexico Press, Albuquerque, pp. 249–321.
- GRASS Development Team, 2016. Geographic Resources Analysis Support System [WWW Document]. URL <http://grass.osgeo.org> (accessed 02.25.16).
- Greer, J., Thorbecke, E., 1986. A methodology for measuring food poverty applied to Kenya. *Journal of Development Economics*

- 24, 59–74.
- Gregg, M.W., Banning, E.B., Gibbs, K., Slater, G.F., 2009. Subsistence practices and pottery use in Neolithic Jordan: molecular and isotopic evidence. *Journal of Archaeological Science* 36, 937–946.
- Griggs, D.J., Noguer, M., 2002. Climate Change 2001: The Scientific Basis. Contribution of Working Group I to the Third Assessment Report of the Intergovernmental Panel on Climate Change. *Weather* 57, 267–269.
- Grisley, W., Kellogg, E.D., 1983. Farmers' Subjective Probabilities in Northern Thailand: An Elicitation Analysis. *American Journal of Agricultural Economics* 65, 74–82.
- Gunderson, L.H., Allen, C.R., Holling, C.S., 2010. Foundations of ecological resilience. Island Press.
- Gunderson, L.H., Holling, C.S. (Eds.), 2002. Panarchy: understanding transformations in human and natural systems. Island Press, Washington D.C.
- Gustafson, E.J., Shifley, S.R., Mladenoff, D.J., Nimerfro, K.K., He, H.S., others, 2000. Spatial simulation of forest succession and timber harvesting using LANDIS. *Canadian Journal of Forest Research* 30, 32–43.
- Halstead, P., 1999. Neighbours from hell? The household in Neolithic Greece. *Neolithic society in Greece* 77–95.
- Hammad, A.A., Lundkvam, H., Børresen, T., 2004. Adaptation of RUSLE in the Eastern Part of the Mediterranean Region. *Environmental Management* 34, 829–841.
- Hammad, A.H.A., Børresen, T., Haugen, L.E., 2006. Effects of rain characteristics and terracing on runoff and erosion under the Mediterranean. *Soil and Tillage Research* 87, 39–47.
- Hartter, J., Boston, K., 2007. An integrated approach to modeling resource utilization for rural communities in developing countries. *Journal of Environmental Management* 85, 78–92.
- Hartter, J., Boston, K., 2008. Consuming Fuel and Fuelling Consumption: Modelling Human Caloric Demands and Fuelwood Use. *Small-scale Forestry* 7, 1–15.
- Hayden, B., Cannon, A., 1983. Where the garbage goes: Refuse disposal in the Maya Highlands. *Journal of Anthropological Archaeology* 2, 117–163.
- Hegmon, M., 1991. The Risks of Sharing and Sharing as Risk Reduction: Interhousehold Food Sharing in Egalitarian Societies, in: Gregg, S.A. (Ed.), *Between Bands and States*, Occasional Paper No. 9. Center for Archaeological Investigation, Southern Illinois University, Carbondale, pp. 309–332.
- Heimsath, A.M., Chappell, J., Dietrich, W.E., Nishiizumi, K., Finkel, R.C., 2000. Soil production on a retreating escarpment in southeastern Australia. *Geology* 28, 787–790.
- Heimsath, A.M., Chappell, J., Spooner, N.A., Questiaux, D.G., 2002. Creeping soil. *Geology* 30, 111–114.
- Heimsath, A.M., Dietrich, W.E., Nishiizumi, K., Finkel, R.C., 1997. The soil production function and landscape equilibrium. *Nature* 338, 358–361.
- Heimsath, A.M., Dietrich, W.E., Nishiizumi, K., Finkel, R.C., 2001. Stochastic Processes of Soil Production and Transport: Erosion Rates, Topographic Variation and Cosmogenic Nuclides in the Oregon Coast Range. *Earth Surface Processes and Landforms* 26, 531–552.
- Heimsath, A.M., Dietrich, W.E., Nishiizumi, K., Finkel, R.C., 1999. Cosmogenic nuclides, topography, and the spatial variation of soil depth. *Geomorphology* 27, 151–172.
- Henry, D.O., White, J.J., Beaver, J.E., Kaduwaki, S., Nowell, A., Cordova, C.E., Dean, R.M., Ekstrom, H., McCorriston, J., Scott-Cummings, L., 2003. The Early Neolithic Site of Ayn Abu Nukhayla, Southern Jordan. *Bulletin of the American Schools of Oriental Research* 330, 1–30.
- HilleRisLambers, R., Rietkerk, M., van den Bosch, F., Prins, H.H.T., de Kroon, H., 2001. Vegetation Pattern Formation in Semi-Arid

- Grazing Systems. *Ecology* 82, 50–61.
- Hill, J.B., Miller, A.E., Wentz, E., Barton, C.M., 2008. Archaeoclimatology and Ancient Mediterranean Landscape Dynamics. Paper presented at Annual Meetings of the Society for American Archaeology. Presented at the The 74th Meeting of the Society for American Archaeology, Vancouver, Canada.
- Hillman, G., 1973. Agricultural Productivity and Past Population Potential at Aşvan: An Exercise in the Calculation of Carrying Capacities. *Anatolian Studies* 23, 225–240.
- Hirata, M., Fujita, H., Miyazaki, A., 1998. Changes in grazing areas and feed resources in a dry area of north-eastern Syria. *Journal of Arid Environments* 40, 319–329.
- Hitchcock, R.K., 1987. Sedentism and site structure: Organizational changes in Kalahari Basarwa residential locations. *Method and Theory for Activity Area Research* 374–423.
- Holling, C.S., 1973. Resilience and stability of ecological systems. *Annual review of ecology and systematics* 1–23.
- Holling, C.S., Gunderson, L.H., 2002. Resilience and adaptive cycles, in: Gunderson, L.H., Holling, C. S. (Eds.), *Panarchy: Understanding Transformations in Human and Natural Systems*. Island Press, Washington D.C., pp. 25–62.
- Holling, C.S., Gunderson, L.H., Peterson, G.D., 2002. Sustainability and panarchies, in: Gunderson, L.H., Holling, C. S. (Eds.), *Panarchy: Understanding Transformations in Human and Natural Systems*. Island Press, Washington D.C., pp. 63–102.
- Horowitz, A., 2001. *The Jordan Rift Valley*. A.A. Balkema Publishers, Lisse ; Exton, PA.
- Horwitz, L.K., Lernau, O., 2003. Temporal and spatial variation in Neolithic animal exploitation strategies: a case study of fauna from the site of Yiftah'el (Israel). *Paléorient* 29, 19–58.
- Howard, A.D., Kerby, G., 1983. Channel changes in badlands. *Geological Society of America Bulletin* 94, 739–752.
- Huston, M., Smith, T., 1987. Plant Succession: Life History and Competition. *The American Naturalist* 130, 168–198.
- Ibáñez, J.J., González Urquijo, J., Rodríguez, A., 2007. The evolution of technology during the PPN in the Middle euphrates. A view from use wear analysis of lithic tools, in: Astruc, L., Binder, D., Briois, F. (Eds.), *Technical Systems and Near Eastern PPN Communities*. Editions APDCA, Antibes, pp. 153–165.
- Ivanyi, M., Boci, R., Gulyas, L., Kozma, V., Legendi, R., 2007. The multi-agent simulation suite, in: *Emergent Agents and Socialities: Social and Organizational Aspects of Intelligence*. Papers from the 2007 AAAI Fall Symposium. pp. 57–64.
- Janssen, M.A., Kohler, T.A., Scheffer, M., 2003. Sunk-Cost Effects and Vulnerability to Collapse in Ancient Societies. *Current Anthropology* 44, 722–728.
- Janssen, M. A., Scheffer, M., 2004. Overexploitation of renewable resources by ancient societies and the role of sunk-cost effects. *Ecology and Society* 9, 6.
- Johnson, A.L., 2002. Cross-Cultural Analysis of Pastoral Adaptations and Organizational States: A Preliminary Study. *Cross-Cultural Research* 36, 151–180.
- Johnson, D.L., 1969. *The Nature of Nomadism: A Comparative Study of Pastoral Migrations in Southwestern Asia and Northern Africa*, Department of Geography Research Papers. The Department of Geography, The University of Chicago, Chicago.
- Johnson, G., 1982. Organisational Structure and Scalar Stress, in: Renfrew, C. (Ed.), *Theory & Explanation in Archaeology*. Academic Press, New York, pp. 389–421.
- Kadowaki, S., 2005. Designs and production technology of sickle elements in Late Neolithic Wadi Ziqlâb, Northern Jordan. *Paléorient* 31, 69–85.
- Kadowaki, S., 2007. Changing Community Life at a Late Neolithic Farmstead: Built environments and the use of Space at Tabaqat al-Bûma in Wadi Ziqlâb, Northern

- Jordan (PhD Diss.). University of Toronto, Toronto.
- Kadowaki, S., Gibbs, K., Allentuck, A., Banning, E.B., 2008. Late Neolithic Settlement in Wadi Ziqlâb, Jordan: al-Basatîn. *paleo* 34, 105–129.
- Kafafi, Z., 1993. The Yarmoukians in Jordan. *paleo* 19, 101–114.
- Kafafi, Z., 1992. Pottery Neolithic settlement patterns in Jordan, in: Studies in the History and Archaeology of Jordan IV. Department of Antiquities of Jordan, Amman, pp. 115–122.
- Kaliszan, L.R., Hermansen, B.D., Jensen, C.H., Skulbøl, T.B.B., Bille Petersen, M., Bangsgaard, P., Ihr, A., Sørensen Mette, L., Markussen, B., others, 2002. Shaqarat Mazyad-The village on the edge.
- Kamp, K.A., 2000. From Village to Tell: Household Ethnoarchaeology in Syria. *Near Eastern Archaeology* 63, 84–93.
- Kamp, K.A., 1987. Affluence and image: Ethnoarchaeology in a Syrian village. *Journal of field archaeology* 14, 283–296.
- Karanth, K.K., Curran, L.M., Reuning-Scherer, J.D., 2006. Village size and forest disturbance in Bhadra Wildlife Sanctuary, Western Ghats, India. *Biological Conservation* 128, 147–157.
- Keane, R.E., Cary, G.J., Davies, I.D., Flannigan, M.D., Gardner, R.H., Lavorel, S., Lenihan, J.M., Li, C., Rupp, T.S., 2004. A classification of landscape fire succession models: spatial simulations of fire and vegetation dynamics. *Ecological Modelling* 179, 3–27.
- Kelly, R.L., 1983. Hunter-Gatherer Mobility Strategies. *Journal of Anthropological Research* 39, 277–306.
- Kelly, R.L., 1991. Sedentism, socio-political inequality, and resource fluctuations, in: Gregg, S.A. (Ed.), Between Bands and States, Occasional Paper No.9. Center for Archaeological Investigations, Southern Illinois University, Carbondale, pp. 135–158.
- Kelly, R.L., 1995. The Foraging Spectrum: Diversity in Hunter-Gatherer Liveways, in: Foraging and Subsistence. Smithsonian Institution Press, Washington D.C., pp. 65–110.
- Kent, S., 1993. Sharing in an Egalitarian Kalahari Community. *Man* 28, 479–514.
- Kenyon, K.M., 1960. Archaeology in the Holy Land, 3d ed. Praeger, New York.
- Khazanov, A., 1994. Nomads and the Outside World. University of Wisconsin Press, Madison.
- Khresat, S., Al-Bakri, J., Al-Tahhan, R., 2008. Impacts of land use/cover change on soil properties in the Mediterranean region of northwestern Jordan. *Land Degradation & Development* 19, 397–407.
- Khresat, S.A., Rawajfh, Z., Mohammad, M., 1998a. Land degradation in north-western Jordan: causes and processes. *Journal of Arid Environments* 39, 623–629.
- Khresat, S.A., Rawajfh, Z., Mohammad, M., 1998b. Morphological, physical and chemical properties of selected soils in the arid and semi-arid region in north-western Jordan. *Journal of Arid Environments* 40, 15–25.
- Kim, S., Sarjoughian, H.S., Elamvazhuthi, V., 2009. DEVS-Suite: A Simulator for Visual Experimentation and Behavior Monitoring, in: High Performance Computing & Simulation Symposium, Proceedings of the Spring Simulation Conference. ACM Press.
- Kinzig, A. P., Ryan, P.A., Etienne, M., Allison, H.E., Elmquist, T., Walker, B.H., 2006. Resilience and regime shifts: assessing cascading effects. *Ecology and Society* 11.
- Kirkby, M.J., 1971. Hillslope process-response models based on the continuity equation, in: Brunsden, D. (Ed.), Hillslopes: Form and Process, Institute of British Geographers Special Publications Series. Oxford, pp. 15–30.
- Kohler-Rollefson, I., 1992. A model for the development of nomadic pastoralism on the Transjordanian Plateau, in: Yosef, O.B., Khazanov, A. (Eds.), Pastoralism in

- the Levant: Archaeological Materials in Anthropological Perspectives, Monographs in World Archaeology. Prehistory Press, Madison, pp. 11–18.
- Kohler-Rollefson, I., 1988. The Aftermath of the Levantine Neolithic Revolution in the Light of Ecological and Ethnographic Evidence. *paleo* 14, 87–93.
- Kohler-Rollefson, I., Rollefson, G.O., 1990. The impact of Neolithic subsistence strategies on the environment: The case of ‘Ain Ghazâl, Jordan, in: Bottema, S., Entjes-Nieborg, Zeist, W. van (Eds.), *Man’s Role in the Shaping of the Eastern Mediterranean Landscape*. Balkema., Rotterdam, pp. 3–14.
- Kohler, T.A., 2012. Complex Systems and Archaeology. Santa Fe Institute Working Papers.
- Kohler, T.A., Johnson, C.D., Varien, M., Ortman, S., Reynolds, R., Kobti, Z., Cowan, J., Kolm, K., Smith, S., Yap, L., 2007. Settlement ecodynamics in the prehispanic central Mesa Verde region, in: Kohler, T A, van der Leeuw, S. (Eds.), *The Model-Based Archaeology of Socionatural Systems*. SAR Press, Santa Fe, pp. 61–104.
- Kohler, T.A., Varien, M.D., 2012. Emergence and Collapse of Early Villages: Models of Central Mesa Verde Technology. University of California Press.
- Kohler, T.A., van der Leeuw (Eds.), 2007. *The Model-Based Archaeology of Socionatural Systems*. School for Advanced Research Press., Santa Fe, NM.
- Koriat, A., Goldsmith, M., Pansky, A., 2000. Toward a Psychology of Memory Accuracy. *Annual Review of Psychology* 51, 481–537.
- Kramer, C., 1980. Estimating prehistoric populations: An ethnoarchaeological approach, in: Barrelet, M.T. (Ed.), *L’archéologie de l’Iraq: Du Début de L’époque Néolithique à 333 Avant Notre Ère, Perspectives Et Limites de L’interprétation Anthropologiques Des Documents. Colloques Internationaux du CNRS* 580, Paris, pp. 315–334.
- Kramer, C., 1982. *Village Ethnoarchaeology: Rural Iran in Archaeological Perspective*. Academic Press, New York.
- Krysanova, V., Hattermann, F., Wechsung, F., 2005. Development of the ecohydrological model SWIM for regional impact studies and vulnerability assessment. *Hydrological Processes* 19, 763–783.
- Kuijt, I., 2000a. *Life in Neolithic Farming Communities: Social Organization, Identity, and Differentiation*. Springer.
- Kuijt, I., 2000b. People and Space in Early Agricultural Villages: Exploring Daily Lives, Community Size, and Architecture in the Late Pre-Pottery Neolithic. *Journal of Anthropological Archaeology* 19, 75–102.
- Kuijt, I., 2004. Pre-Pottery Neolithic A and Late Natufian at ’Iraq ed-Dubb, Jordan. *Journal of Field Archaeology* 29, 291–308.
- Kuijt, I., 2008a. The Regeneration of Life. *CURRENT ANTHROPOLOGY* 49, 171–197.
- Kuijt, I., 2008b. Demography and Storage Systems During the Southern Levantine Neolithic Demographic Transition, in: Bocquet-Appel, J.-P., Bar-Yosef, O. (Eds.), *The Neolithic Demographic Transition and Its Consequences*. Springer Netherlands, pp. 287–313.
- Kuijt, I., 2009. What Do We Really Know about Food Storage, Surplus, and Feasting in Preagricultural Communities? *Current Anthropology* 50, 641–644.
- Kuijt, I., Finlayson, B., 2009. Evidence for food storage and predomestication granaries 11,000 years ago in the Jordan Valley. *PNAS* 106, 10966–10970.
- Kuijt, I., Goring-Morris, N., 2002. Foraging, Farming, and Social Complexity in the Pre-Pottery Neolithic of the Southern Levant: A Review and Synthesis. *Journal of World Prehistory* 16, 361–440.
- Kuijt, I., Mabry, J., Palumbo, G., 1991. Early Neolithic use of upland areas of Wadi El-Yabis : preliminary evidence from the excavations of ’Iraq Ed-Dubb, Jordan. *paleo* 17, 99–108.

- Kupfer, J., Farris, C., 2007. Incorporating spatial non-stationarity of regression coefficients into predictive vegetation models. *Landscape Ecology* 22, 837–852.
- Laland, K.N., Odling-Smee, F.J., Feldman, M.W., 1999. Evolutionary consequences of niche construction and their implications for ecology. *Proceedings of the National Academy of Sciences* 96, 10242–10247.
- Laland, K.N., Odling-Smee, F.J., Feldman, M.W., 2001. Niche construction, ecological inheritance, and cycles of contingency in evolution, in: Oyama, S., Griffiths, P.E., Gray, R.D. (Eds.), *Cycles of Contingency: Developmental Systems and Evolution*. The MIT Press, Cambridge, pp. 117–126.
- Lamberson, P.J., Page, S.E., 2012. Tipping Points. Santa Fe Institute Working Papers.
- Lansing, J.S., 2003. Complex adaptive systems. *Annual Review of Anthropology* 183–204.
- Le Houérou, H.N., 1980. The role of browse in the management of natural grazing lands, in: Le Houérou, H.N. (Ed.), *Browse in Africa: The Current State of Knowledge*. International Livestock Center for Africa, Addis Ababa.
- Lilburne, L., Hewitt, A., McIntosh, P., Lynn, I., 1998. GIS-driven models of soil properties in the high country of the south island, in: 10th Colloquium of the Spatial Information Research Centre, University of Otago, New Zealand. pp. 173–180.
- Lim, K., Deadman, P.J., Moran, E., Brondizio, E., McCracken, S., 2002. Agent-based simulations of household decision making and land use change near Altamira, Brazil, in: Gimblett, H.R. (Ed.), *Integrating Geographic Information Systems and Agent-Based Modeling: Techniques for Simulating Social and Ecological Processes*. Oxford University Press, Cary, pp. 277–310.
- Lovell, J., Dollfus, G., Kafafi, Zeidan, 2007. The Ceramics of the Late Neolithic and Chalcolithic: Abu Hamid and the Burnished Tradition. *paleo* 33, 51–76.
- Luke, S., Cioffi-Revilla, C., Panait, L., Sullivan, K., Balan, G., 2005. MASON: A multiagent simulation environment. *Simulation* 81, 517–527.
- Maher, L.A., 2000. *Analysing Quaternary Deposits: Problems in Determining Particle Size for Palaeosols at an Epipalaeolithic Site in Northern Jordan*. York University.
- Maher, L.A., 2005. The Epipalaeolithic in Context: Palaeolandscapes and Prehistoric Occupation of Wadi Ziqlâb, Northern Jordan (PhD). University of Toronto.
- Maher, L.A., 2007. 2005 Excavations at the Geometric Kebaran site of ‘Uyun al-Hammam, al-Koura District, northern Jordan. *Annual of the Department of Antiquities of Jordan* 51, 263–272.
- Maher, L.A., 2011. Reconstructing paleolandscapes and prehistoric occupation of Wadi Ziqlâb, northern Jordan. *Geoarchaeology* 26, 649–692.
- Maher, L.A., Banning, E. B., Chazan, M., 2011. Oasis or mirage? Assessing the role of abrupt climate change in the prehistory of the southern Levant. *Cambridge Archaeological Journal* 21, 1–29.
- Maher, L.A., Banning, E.B., 2001. Geoarchaeological Survey in Wadi Ziqlâb, Jordan, in: Zayadine, F. (Ed.), *Annual of the Department of Antiquities of Jordan*. Department of Antiquities of Jordan, Amman, pp. 61–69.
- Maher, L.A., Löhr, M., Betts, M., Parslow, C., Banning, E.B., 2002. Middle Epipalaeolithic Sites in Wadi Ziqlâb, Northern Jordan. *Paléorient* 27, 5–19.
- Maltz, E., Shkolnik, A., 1980. Milk production in the desert: lactation and water economy in the black Bedouin goat. *Physiological zoology* 53, 12–18.
- Manson, S.M., 2001. Simplifying complexity: a review of complexity theory. *Geoforum* 32(3), 405–414.
- Manson, S.M., 2003. Epistemological possibilities and imperatives of complexity research: a reply to Reitsma. *Geoforum* 34(1), 17–20.
- Marom, N., Bar-Oz, G., 2009. Culling profiles: the indeterminacy of archaeozoological

- data to survivorship curve modelling of sheep and goat herd maintenance strategies. *Journal of Archaeological Science* 36, 1184–1187.
- Martínez-Casasnovas, J.A., Sánchez-Bosch, I., 2000. Impact assessment of changes in land use/conservation practices on soil erosion in the Penedès-Anoia vineyard region (NE Spain). *Soil and Tillage Research* 57, 101–106.
- Martin, L., Edwards, Y.H., 2007. Fauna from the Natufian and PPNA Cave Site of Iraq ed-Dubb in Highland Jordan. *paleo* 33, 143–174.
- Mavrogenis, A.P., Papachristoforou, C., 1988. Estimation of the energy value of milk and prediction of fat-corrected milk yield in sheep and goats. *Small Ruminant Research* 1, 229–236.
- Mayer, G.R., Sarjoughian, H., 2007. Complexities of Simulating a Hybrid Agent-Landscape Model Using Multi-Formalism Composability, in: Spring Simulation Conference: Agent-Directed Simulation. IEEE Press, Norfolk, Virginia, pp. 161–168.
- McBratney, A. B, Mendonca Santos, M.L., Minasny, B., 2003. On digital soil mapping. *Geoderma* 117, 3–52.
- McCall, M.K., 1985. The significance of distance constraints in peasant farming systems with special reference to sub-Saharan Africa. *Applied Geography* 5, 325–345.
- McIntosh, R.J., 1991. Early Urban Clusters in China and Africa: The Arbitration of Social Ambiguity. *Journal of Field Archaeology* 18, 199–212.
- McShane, B.B., 2011. A statistical analysis of multiple temperature proxies: Are reconstructions of surface temperatures over the last 1000 years reliable? *Ann. Appl. Stat.* 5, 5–44.
- Meged', S.S., Torkaev, A.N., Egorov, S.V., Storozhuk, S.I., 2008. Milk productivity of breeding sheep of the Altai finewool breed. *Russ. Agricult. Sci.* 34, 52–54.
- Merah, O., Araus, J.L., Souyris, I., Nachit, M.M., Deléens, E., Monneveux, P., 2000. Carbon isotope discrimination: potential interest for grain yield improvement in durum wheat. *Durum Wheat Improvement in the Mediterranean Region: New Challenges. Options Méditerranéennes* 40.
- Migowski, C., Stein, M., Prasad, S., Negendank, J.F.W., Agnon, A., 2006. Holocene climate variability and cultural evolution in the Near East from the Dead Sea sedimentary record. *Quaternary Research* 66, 421–431.
- Miller, J., Franklin, J., 2002. Modeling the distribution of four vegetation alliances using generalized linear models and classification trees with spatial dependence. *Ecological Modelling* 157, 227–247.
- Miller, J., Franklin, J., Aspinall, R., 2007. Incorporating spatial dependence in predictive vegetation models. *Ecological Modelling* 202, 225–242.
- Miller, J.H., Page, S.E., 2007. Complex adaptive systems: An introduction to computational models of social life. Princeton University Press, Princeton.
- Minasny, Budiman, McBratney, Alex B, 1999. A rudimentary mechanistic model for soil production and landscape development. *Geoderma* 90, 3–21.
- Minasny, Budiman, McBratney, Alex B, 2006. Mechanistic soil-landscape modelling as an approach to developing pedogenetic classifications. *Geoderma* 133, 138–149.
- Mitasova, H., Hofierka, J., Zlocha, M., Iverson, L.R., 1996a. Modelling topographic potential for erosion and deposition using GIS. *International Journal of Geographical Information Systems* 10, 629–641.
- Mitasova, H., Mitas, L., 1993. Interpolation by Regularized Splines with Tension: I. Theory and implementation. *Mathematical Geology* 25, 641–655.
- Mitasova, H., Mitas, L., Brown, W M, Johnston, D., 1996b. Multidimensional Soil Erosion/Deposition Modeling Part III: Process based erosion simulation. *Geographic Modeling and Systems Laboratory, University of Illinois at Urbana-Champaign*.

- Mitasova, H., Mitas, Lubos, Brown, William M, 2001. Multiscale Simulation of Land Use Impact on Soil Erosion and Deposition Patterns, in: Stott, D.E., Mohtar, R.H., Steinhardt, G.C. (Eds.), Sustaining the Global Farm: 10th International Soil Conservation Organization Meeting Held May 24-29, 1999. Purdue University and the USDA-ARS National Soil Erosion Research Laboratory, pp. 1163–1169.
- Mitasova, H., Barton, C.M., Ullah, I.I.T., Hofierka, J., Harmon, R.S., 2013. GIS-based soil erosion modeling, in: Shrader, J., Bishop, M.P. (Eds.), Remote Sensing and GIScience in Geomorphology, Treatise in Geomorphology. Academic Press, San Diego, pp. 228–258.
- Mitchell, M., 2009. Complexity: a guided tour. Oxford University Press, Oxford.
- Moore, I.D., Burch, G.J., 1986. Physical Basis of the Length-slope Factor in the Universal Soil Loss Equation. *Soil Sci Soc Am J* 50, 1294–1298.
- Muheisen, M., Gebel, H. G., Hannss, C., Neef, R., 1988. Ain Rahub, a new final Natufian and Yarmoukian site near Irbid, in: Garrard, A., Gebel, H.G. (Eds.), The Prehistory of Jordan, British Archaeological Reports International Series. BAR, Oxford, pp. 572–502.
- Murdock, G.P., White, D.R., 2006. Standard Cross-Cultural Sample: online edition, in: Social Dynamics and Complexity, Working Paper Series. Institute for Mathematical Behavioral Sciences, University of California Irvine, Irvine.
- Nablusi, H., Ali, J.M., Abu Nahleh, J., 1993. Sheep and goat management systems in Jordan: traditional and feedlot, a case study. Task Force Documents, Amman.
- Naughton-Treves, L., Kammen, D.M., Chapman, C., 2007. Burning biodiversity: Woody biomass use by commercial and subsistence groups in western Uganda's forests. *Biological Conservation* 134, 232–241.
- Neteler, M., Mitasova, H., 2007a. Open Source GIS: A GRASS GIS Approach. The International Series in Engineering and Computer Science: Volume 773. New York.
- Neteler, M., Mitasova, H., 2007b. Open Source GIS: A GRASS GIS Approach. The International Series in Engineering and Computer Science: Volume 773. New York.
- Ngwa, A.T., Pone, D.K., Mafeni, J.M., 2000. Feed selection and dietary preferences of forage by small ruminants grazing natural pastures in the Sahelian zone of Cameroon. *Animal Feed Science and Technology* 88, 253 – 266.
- Nordblom, T.L., Goodchild, A.V., Shomo, F., 1995. Livestock feeds and mixed farming systems in West Asia and North Africa.
- Nyerges, A.E., 1980. Traditional pastoralism: an evolutionary perspective. *Expedition* 22, 36–41.
- Oba, G., 2012. Harnessing pastoralists' indigenous knowledge for rangeland management: three African case studies. *Pastoralism: Research, Policy and Practice* 2, 1.
- Odling-Smee, F.J., Laland, K.N., Feldman, M.W., 2003. Niche construction: the neglected process in evolution (MPB-37). Princeton University Press.
- Onori, F., De Bonis, P., Grauso, S., 2006. Soil erosion prediction at the basin scale using the revised universal soil loss equation (RUSLE) in a catchment of Sicily (southern Italy). *Environmental Geology* 50, 1129–1140.
- Osem, Y., Perevolotsky, A., Kigel, J., 2002. Grazing Effect on Diversity of Annual Plant Communities in a Semi-Arid Rangeland: Interactions with Small-Scale Spatial and Temporal Variation in Primary Productivity. *The Journal of Ecology* 90, 936–946.
- Otto-Bliesner, B.L., Schulz, M., 2009. New Methods to Integrate Paleodata Into Climate Models: Data-Assimilation Techniques for Paleoclimate Data; Vienna, Austria, 25 April 2009. *Eos Trans. AGU* 90, 300.
- Pachauri, R.K., 2007. Climate Change 2007: Synthesis Report. Contribution of Working Groups I, II and III to the Fourth Assessment

- Report of the Intergovernmental Panel on Climate Change. Intergovernmental Panel on Climate Change.
- Parker, D.C., Manson, S.M., Janssen, M.A., Hoffmann, M.J., Deadman, P., 2003. Multi-agent systems for the simulation of land-use and land-cover change: a review. *Annals of the Association of American Geographers* 93, 314–337.
- Pausas, Juli G., 1999a. Response of plant functional types to changes in the fire regime in Mediterranean ecosystems: A simulation approach. *Journal of Vegetation Science* 10, 717–722.
- Pausas, Juli G., 1999b. Mediterranean vegetation dynamics: modelling problems and functional types. *Plant Ecology* 140, 27–39.
- Payne, S., 1973. Kill-off patterns in sheep and goats: the mandibles from A\csvan Kale. *Anatolian studies* 281–303.
- Perevolotsky, A., Seligman, No'am G, 1998. Role of Grazing in Mediterranean Rangeland Ecosystems. *BioScience* 48, 1007–1017.
- Phillips, S., Dudik, M., Schapire, R., 2010. MaxEnt 3.3. Princeton University.
- Phillips, S.J., Anderson, R.P., Schapire, R.E., 2006. Maximum entropy modeling of species geographic distributions. *Ecological Modelling* 190, 231–259.
- Prochnow, S.J., Mullins, M., Capello, S.V., Perry, A.F., Ahr, S.W., Westfield, I.T., Fallert, K.L., Gao, S., Hartzell, K.T., Lang, K.R., 2007. Gis Interpolation of Stratigraphic Contact Data to Reconstruct Paleogeography: Deriving a Paleolandscape Model of the Base Zuni Sequence and Subsequent Cretaceous Islands in Central Texas, in: 2007 GSA Denver Annual Meeting.
- Pross, J., Kotthoff, U., Müller, U.C., Peyron, O., Dormoy, I., Schmiedl, G., Kalaitzidis, S., Smith, A.M., 2009. Massive perturbation in terrestrial ecosystems of the Eastern Mediterranean region associated with the 8.2 kyr B.P. climatic event. *Geology* 37, 887–890.
- Pswarayi, A., van Eeuwijk, F.A., Ceccarelli, S., Grando, S., Comadran, J., Russell, J.R., Francia, E., Pecchioni, N., Li Destri, O., Akar, T., Al-Yassin, A., Benbelkacem, A., Choumane, W., Karrou, M., Ouabbou, H., Bort, J., Araus, J.L., Molina-Cano, J.L., Thomas, W.T.B., Romagosa, I., 2008. Barley adaptation and improvement in the Mediterranean basin. *Plant Breeding* 127, 554–560.
- Quiroga, A., Funaro, D., Noellemeyer, E., Peinemann, N., 2006. Barley yield response to soil organic matter and texture in the Pampas of Argentina. *Soil and Tillage Research* 90, 63–68.
- Rapp, M., Santa Regina, I., Rico, M., Gallego, H.A., 1999. Biomass, nutrient content, litterfall and nutrient return to the soil in Mediterranean oak forests. *Forest Ecology and Management* 119, 39–49.
- Rawls, W.J., 1983. Estimating soil bulk density from particle size analysis and organic matter content. *Soil Science* 135, 123.
- Reddy, A.K.N., 1981. An Indian village agricultural ecosystem- case study of Ungra village, Part II: Discussion. *Biomass* 1, 77–88.
- Redman, C., 2005. Resilience Theory in Archaeology. *American Anthropologist* 107, 70–77.
- Redman, C.L., Nelson, M.C., Kinzig, Ann P, 2009. The resilience of socioecological landscapes: Lessons from the Hohokam, in: Fisher, C.T., Hill, J. B., Feinman, G.M. (Eds.), *The Archaeology of Environmental Change: Socionatural Legacies of Degradation and Resilience*. University of Arizona Press, Tucson.
- Reitsma, F., 2003. A response to simplifying complexity. *Geoforum* 34, 13–16.
- Renard, K.G., Foster, G.R., Weesies, G.A., Porter, J.P., 1991. RUSLE: Revised Universal Soil Loss Equation. *Journal of Soil and Water Conservation* 46, 30–33.
- Renard, K.G., Freimund, J.R., 1994. Using monthly precipitation data to estimate the R-factor in the revised USLE. *Journal of Hydrology* 157, 287–306.

- Renard, K. G., Foster, G. R., Weesies, G. A, McCool, D.K., Yoder, D.C., 1997. Predicting soil erosion by water: a guide to conservation planning with the Revised Universal Soil Loss Equation (RUSLE), in: Agriculture Handbook. US Department of Agriculture, Washington, DC, pp. 1–251.
- Řezanková, H., 2009. Cluster analysis and categorical data. *Statistika* 216–232.
- Rhoton, F.E., Lindbo, D.L., 1997. A soil depth approach to soil quality assessment. *Journal of soil and water conservation* 52, 66–72.
- Robinson, S.A., Black, S., Sellwood, B.W., Valdes, P.J., 2006. A review of palaeoclimates and palaeoenvironments in the Levant and Eastern Mediterranean from 25,000 to 5000 years BP: setting the environmental background for the evolution of human civilisation. *Quaternary Science Reviews* 25, 1517–1541.
- Rogers, J.D., Nichols, T., Emmerich, T., Latek, M., Cioffi-Revilla, C., 2012. Modeling scale and variability in human–environmental interactions in Inner Asia. *Ecological Modelling*.
- Rogosic, J., Pfister, J.A., Provenza, F.D., Grbesa, D., 2006. Sheep and goat preference for and nutritional value of Mediterranean maquis shrubs. *Small Ruminant Research* 64, 169–179.
- Rollefson, G.O., 1989. The Aceramic Neolithic of the Southern Levant : The View from 'Ain Ghazâl. *paleo* 15, 135–140.
- Rollefson, G.O., 1990. Neolithic Chipped Stone Technology at 'Ain Ghazâl, Jordan : The Status of the PPNC Phase. *paleo* 16, 119–124.
- Rollefson, G.O., 1993. The Origins of the Yarmoukian at 'Ain Ghazâl. *paleo* 19, 91–100.
- Rollefson, G.O., 1997. Neolithic 'Ayn Ghazâl in its landscape. *Studies in the History and Archaeology of Jordan* 6, 241–244.
- Rollefson, G.O., 2001. The Neolithic Period, in: B. MacDonald, R.A., Bienkowski, P., Adams, R. (Eds.), *The Archaeology of Jordan*, Levantine Archaeology. Sheffield Academic Press, Sheffield, pp. 67–105.
- Rollefson, G.O., 2004. A reconsideration of the PPN koine: Cultural diversity and centralities. *Neo-Lithics* 1, 46–48.
- Rollefson, G.O., 2009. Slippery slope: the Late Neolithic rubble layer in the Southern Levant. *Neo-Lithics* 9.
- Rollefson, G.O., Kafafi, Zeidan, 2007. The rediscovery of the Neolithic Period in Jordan, in: Levy, T.E., Daviau, P.M.M., Younker, R.W., Shaer, M. (Eds.), *Crossing Jordan. North American Contributions to the Archaeology of Jordan*. Equinox Publishing, London, pp. 211–218.
- Rollefson, G.O., Köhler-Rollefson, I., 1993. PPNC adaptations in the first half of the 6th millennium B.C. *paleo* 19, 33–42.
- Rollefson, G.O., Kohler-Rollefson, Ilse, 1989. Collapse of Early Neolithic settlements in the southern Levant, in: *People and Culture in Change*. Oxford : B.A.R, pp. 73–89.
- Rollefson, G.O., Kohler-Rollefson, Ilse, 1992. Early neolithic exploitation patterns in the Levant: Cultural impact on the environment. *Population & Environment* 13, 243–254.
- Rollefson, G.O., Schmandt-Besserat, D., Rose, J. c., 1998. A Decorated Skull from MPPNB 'Ain Ghazâl. *paleo* 24, 99–104.
- Rollefson, G.O., Simmons, A.H., Kafafi, Zeidan, 1992. Neolithic Cultures at 'Ain Ghazâl, Jordan. *Journal of Field Archaeology* 19, 443–470.
- Ruter, A., Arzt, J., Vavrus, S., Bryson, R.A., Kutzbach, J.E., 2004. Climate and environment of the subtropical and tropical Americas (NH) in the mid-Holocene: comparison of observations with climate model simulations. *Quaternary Science Reviews* 23, 663–679.
- Sadras, V.O., Calvino, P.A., 2001. Quantification of grain yield response to soil depth in soybean, maize, sunflower, and wheat. *Agronomy Journal* 93, 577–583.
- Sarjoughian, H.S., Meyer, G.R., Ullah, I.I.T., and Barton, C.M., 2015. Managing Hybrid Model Composition Complexity: Human–Environment Simulation Models, in:

- Concepts and Methodologies for Modeling and Simulation. *Simulation Foundations, Methods and Applications*. Levent Yilmaz, ed. Springer International Publishing. pp. 107–134.
- Savory, A., 2013. The Grazing Revolution: A Radical Plan to Save the Earth. TED Conferences.
- Schacter, D.L., 1999. The seven sins of memory: Insights from psychology and cognitive neuroscience. *American Psychologist* 54, 182–203.
- Scheffer, M., 2009. Critical transitions in nature and society, Princeton Studies in Complexity. Princeton University Press, Princeton.
- Scheffer, M., 2010. Complex systems: Foreseeing tipping points. *Nature* 467, 411–412.
- Scheffer, M., Bascompte, J., Brock, W.A., Brovkin, V., Carpenter, Stephen R., Dakos, V., Held, H., Nes, E.H. van, Rietkerk, M., Sugihara, G., 2009. Early-warning signals for critical transitions. *Nature* 461, 53–59.
- Scheffer, M., Carpenter, S.R., 2003. Catastrophic regime shifts in ecosystems: linking theory to observation. *Trends in Ecology & Evolution* 18, 648–656.
- Scheffer, M., Carpenter, S.R., Lenton, T.M., Bascompte, J., Brock, W., Dakos, V., Koppell, J. van de, Leemput, I.A. van de, Levin, S.A., Nes, E.H. van, Pascual, M., Vandermeer, J., 2012. Anticipating Critical Transitions. *Science* 338, 344–348.
- Schiffer, M.B., 1987. Formation processes of the archaeological record. University of New Mexico Press, Albuquerque.
- Schuldenrein, J., 2007. A Reassessment of the holocene stratigraphy of the Wadi Hasa Terrace and Hasa formation, Jordan. *Geoarchaeology* 22, 559–588.
- Schulman, N., 1962. The geology of the central Jordan Valley. Hebrew University (Jerusalem).
- Sen, A.R., Santra, A., Karim, S.A., 2004. Carcass yield, composition and meat quality attributes of sheep and goat under semiarid conditions. *Meat Science* 66, 757–763.
- Shoup, J., 1990. Middle Eastern Sheep Production and the Hima System, in: Galaty, J.G., Johnson, D.L. (Eds.), *World of Pastoralism: Herding Systems in Comparative Perspective*. Guilford Press, New York, pp. 195–215.
- Simmons, A.H., 2000. Villages on the edge: Regional settlement change and the end of the Levantine Pre-Pottery Neolithic, in: Kuijt, I. (Ed.), *Life in Neolithic Farming Communities: Social Organization, Identity and Differentiation*. Kluwer Academic/Plenum Publishers, New York, pp. 211–230.
- Simmons, A.H., 2007. The Neolithic Revolution in the Near East: Transforming the Human Landscape. University of Arizona Press, Tucson.
- Simmons, A.H., Rollefson, G.O., Kafafi, Zeidan, Mandel, R.D., Al-Nahar, M., Cooper, J., Kohler-Rollefson, Ilse, Durand, K.R., 2001. Wadi Shu'eib, a large Neolithic community in central Jordan: final report of test investigations. *Bulletin, American Schools of Oriental Research* 321, 1–39.
- Singh, R., Phadke, V.S., 2006. Assessing soil loss by water erosion in Jamni River Basin, Bundelkhand region, India, adopting universal soilloss equation using GIS. *Current Science* 90, 1431–1435.
- Smith, A.B., 1992. *Pastoralism in Africa : origins and development ecology*. Christopher Hurst ; Ohio University Press, London : Athens :
- Smith, M.L., 2006. How Ancient Agriculturalists Managed Yield Fluctuations through Crop Selection and Reliance on Wild Plants: An Example from Central India. *Economic Botany* 60, 39–48.
- Sneh, A., Bartov, Y., Weissbrod, T., Rosensaft, M., 1998. Geological Map of Israel, 1:200,000. Israeli Geological Survey, (4 sheets).
- Solomon, S., 2007. Climate change 2007: the physical science basis: contribution of Working Group I to the Fourth Assessment Report of the Intergovernmental Panel on Climate Change. Intergovernmental Panel

- on Climate Change.
- Soto-Berelov, M., 2011. Vegetation Modeling of Holocene Landscapes in the Southern Levant (Ph.D., Geography). Arizona State University, United States -- Arizona.
- Spielmann, K.A., Nelson, M., Ingram, S., Peeples, M.A., 2011. Sustainable small-scale agriculture in semi-arid environments. *Ecology and Society* 16, 26.
- Staubwasser, M., Weiss, H., 2006. Holocene climate and cultural evolution in late prehistoric–early historic West Asia. *Quaternary Research* 66, 372–387.
- Stewart, B.A., Woolhiser, D.A., Wischmeier, W.H., Caro, J.H., Frere, M.H., 1975. Control of Water Pollution from Cropland, Volume 1—A Manual for Guideline Development, EPA-600/2-75-026a. US Environmental Protection Agency, Washington D.C.
- Stuth, J.W., Kamau, P.N., 1989. Influence of Woody Plant Cover on Dietary Selection by Goats in an Acacia senegal Savanna of East Africa. *Small Ruminant Research* 3, 211–225.
- Stuth, J.W., Sheffield, W.J., 1991. Determining Carrying Capacity for Combinations of Livestock, White-tailed Deer and Exotic Ungulates, in: Wildlife Management Handbook. Texas A&M University Department of Wildlife and Fisheries Sciences, College Station, pp. 5–12.
- Swarm Development Group, 1999. Swarm. www. swarm.org, Santa Fe.
- Tabuti, J.R.S., Dhillon, S.S., Lye, K.A., 2003. Firewood use in Bulamogi County, Uganda: species selection, harvesting and consumption patterns. *Biomass and Bioenergy* 25, 581–596.
- Tachikawa, T., Kaku, M., Iwasaki, A., Gesch, D., Oimoen, M., Zhang, Z., Danielson, J., Krieger, T., Curtis, B., Haase, J., others, 2011. ASTER Global Digital Elevation Model Version 2—Summary of Validation Results August 31, 2011.
- Terradas, J., 1992. Mediterranean woody plant growth-forms, biomass and production in the eastern part of the Iberian Peninsula, in: Homage to Ramon Margalef or Why Is There Such Pleasure in Studying Nature. University of Barcelona, Barcelona, pp. 337–349.
- Thomson, E.F., Bahhady, F., Termanini, A., Mokbel, M., 1986. Availability of home-produced wheat, milk products and meat to sheep-owning families at the cultivated margin of the NW Syrian steppe. *Ecology of Food and Nutrition* 19, 113–121.
- Thomson, E.F., 1987. Feeding systems and sheep husbandry in the barley belt of Syria. ICARDA, Aleppo.
- Thomson, E.F., Bahhady, F., 1983. Aspects of sheep husbandry systems in Aleppo Province of Northwest Syria, Farming systems program research reports. ICARDA, Aleppo.
- Tucker, G., Lancaster, S., Gasparini, N., Bras, R., 2001. The Channel-Hillslope Integrated Landscape Development model (CHILD), Landscape erosion and evolution modeling. Kluwer Academic/Plenum Publishers, New York, NY.
- Turner, M.G., Baker, W.L., Peterson, C.J., Peet, R.K., 1998. Factors influencing succession: lessons from large, infrequent natural disturbances. *Ecosystems* 1, 511–523.
- Tversky, A., Kahneman, D., 1974. Judgment Under Uncertainty: Heuristics and Biases. *Science* 185, 1124–1131.
- Twiss, K. C., 2007. The Neolithic of the southern Levant. *Evolutionary Anthropology: Issues, News, and Reviews* 16, 24–35.
- Twiss, K. C., 2007. The Zooarchaeology of Tel Tif'dan (Wadi Fidan 001), Southern Jordan. *Paléorient* 33, 127–145.
- Ullah, I.I.T., 2009. Within-room spatial analysis of activity areas at Late Neolithic Tabaqat Al-Bûma, Wadi Ziqlâb, Al Koura, Jordan, in: Studies in the History and Archaeology of Jordan, X. The Department of Antiquities of Jordan, Amman, pp. 87–95.
- Ullah, I.I.T., 2011. A GIS method for assessing the zone of human-environmental impact around archaeological sites: a test case from the Late Neolithic of Wadi Ziqlâb, Jordan.

- Journal of Archaeological Science 38, 623–632.
- Ullah, I.I.T., 2012. Particles from the past: microarchaeological spatial analysis of ancient house floors, in: Parker, B.J., Foster, C.P. (Eds.), New Perspectives in Household Archaeology. Eisenbrauns, Winona Lake, pp. 123–138.
- Ullah, I.I.T., Kuijt, I., and Freeman, J., 2015. Toward a theory of punctuated subsistence change. PNAS 112(31), 9579–9584.
- Ullah, I.I.T., Bergin, S.M., 2012. Modeling the Consequences of Village Site Location: Least Cost Path Modeling in a Coupled GIS and Agent-Based Model of Village Agropastoralism in Eastern Spain, in: White, D.A., Surface-Evans, S.L. (Eds.), Least Cost Analysis of Social Landscapes: Archaeological Case Studies. University of Utah Press, Salt Lake City, pp. 155–173.
- USDA, 2010. Nutrient Data Laboratory [WWW Document]. URL http://www.ars.usda.gov/main/site_main.htm?modecode=12-35-45-00 (accessed 12.9.10).
- USDA, N.R.C. services, 2012. Soil Texture Calculator.
- Usher, M.B., 1981. Modelling ecological succession, with particular reference to Markovian models. Plant Ecology 46–47, 11–18.
- Van Dyke P.H., Savit, R., Riolo, R., 1998. Agent-Based Modeling vs. Equation-Based Modeling: A Case Study and Users' Guide, in: Sichman, J., Conte, R., Gilbert, N. (Eds.), Multi-Agent Systems and Agent-Based Simulation, Lecture Notes in Computer Science. Springer Berlin / Heidelberg, pp. 277–283.
- Van Nes, E.H., Scheffer, M., 2005. Implications of Spatial Heterogeneity for Catastrophic Regime Shifts in Ecosystems. Ecology 86, 1797–1807.
- Varien, M.D., Ortman, S.G., Kohler, T. A., Glowacki, D.M., Johnson, C.D., 2007. Historical ecology in the Mesa Verde region: Results from the village ecodynamics project. American Antiquity 273–299.
- Verhoeven, M., 2002. Transformations of society : the changing role of ritual and symbolism in the PPNB and the PN in the Levant, Syria and south-east Anatolia. paleo 28, 5–13.
- Vigne, J.-D., 2011. The origins of animal domestication and husbandry: A major change in the history of humanity and the biosphere. Comptes Rendus Biologies 334, 171–181.
- Vigne, J.-D., Helmer, D., 2007. Was milk a "secondary product" in the Old World Neolithisation process ? Its role in the domestication of cattle, sheep and goats. Anthropozoologica 42, 9–40.
- Volohonsky, H., Kaplanovsky, A., Serruya, S., 1983. Storms on Lake Kinneret: Observations and mathematical model. Ecological Modelling 18, 141–153.
- Wagner, W., 2011. Groundwater in the arab middle east. Springer Verlag.
- Wainwright, J., 2008. Can modelling enable us to understand the rôle of humans in landscape evolution? Geoforum 39, 659–674.
- Walker, B., Gunderson, L., Kinzig, A., Folke, C., Carpenter, S., Schultz, L., 2006. A Handful of Heuristics and Some Propositions for Understanding Resilience in Social-Ecological Systems. Ecology and Society 11, 13.
- Warren, S.D., Mitasova, H., Hohmann, M.G., Landsberger, S., Skander, F.Y., Ruzycki, T.S., Senseman, G.M., 2005. Validation of a 3-D enhancement of the Universal Soil Loss Equation for prediction of soil erosion and sediment deposition. Catena 64, 281–296.
- Wasse, A., 2002. Final results of an analysis of the sheep and goat bones from Ain Ghazâl, Jordan. Levant 34, 59–82.
- Watson, P.J., 1979. Archaeological Ethnography in Western Iran, Viking Fund Publications in Anthropology. University of Arizona Press, Tucson.
- Weninger, B., Alram-Stern, E., Bauer, E., Clare, L., Danzeglocke, U., Jöris, O., Kubatzki, C., Rollefson, G., Todorova, H., van Andel, T.,

2006. Climate forcing due to the 8200 cal yr BP event observed at Early Neolithic sites in the eastern Mediterranean. *Quaternary Research* 66, 401–420.
- Weninger, B., Clare, L., Rohling, E.J., Bar-Yosef, O., Böhner, U., Budja, M., Bundschuh, M., Feurdean, A., Gebel, H. G., Jöris, O., 2009. The impact of rapid climate change on prehistoric societies during the Holocene in the Eastern Mediterranean. *Documenta Praehistorica* 36, 7–59.
- Wilensky, U., 1999. NetLogo. Center for Connected Learning and Computer-Based Modeling, Northwestern University, Evanston, <http://ccl.northwestern.edu/netlogo/>.
- Wilkinson, T.J., Gibson, M., Christiansen, J. H., Widell, M., Schloen, D., Kouchoukos, N., Woods, C., Sanders, J., Simumich, K.-L., Altaweeil, M.R., Ur, J.A., Hritz, C., Lauinger, J., Paulette, T., Tenney, J., 2007. Modeling Settlement Systems in a Dynamic Environment, in: Kohler, Timothy A., van der Leeuw, S. (Eds.), *The Model-Based Archaeology of Socionatural Systems*. SAR Press, Santa Fe, pp. 175–208.
- Wilk, R.R., Rathje, W.L., 1982. Household archaeology. *American behavioral scientist* 25, 617.
- Wilson, J.P., 2012. Digital terrain modeling. *Geomorphology* 137, 107–121.
- Wilson, R., Frank, D., Topham, J., Nicolussi, K., Esper, J., 2005. Spatial reconstruction of summer temperatures in Central Europe for the last 500 years using annually resolved proxy records: problems and opportunities. *Boreas* 34, 490–497.
- Wilson, R.T., 1982. Husbandry, nutrition and productivity of goats and sheep in tropical Africa, in: Gatenby, R.M., Trail, J.C.. (Eds.), *Small Ruminant Breed Productivity in Africa*. International Livestock Center for Africa, ILCA, Addis Ababa.
- Wischmeier, W.H., 1976. Use and Misuse of the Universal Soil Loss Equation. *Journal of Soil and Water Conservation* 31, 5–9.
- Wischmeier, W.H., Johnson, C.B., Cross, B.V., 1971. A Soil Erodibility Nomograph for Farmland and Construction Sites. *Journal of Soil and Water Conservation* 26, 189–92.
- Wischmeier, W.H., Smith, D.D., 1978. Predicting Rainfall-Erosion Losses - A Guide to Conservation Planning, USDA Agriculture Handbook.
- Wolfram, S., 2002. A new kind of science.
- Wong, M.T.F., Asseng, S., 2007. Yield and environmental benefits of ameliorating subsoil constraints under variable rainfall in a Mediterranean environment. *Plant Soil* 297, 29–42.
- World Meteorological Organization, National Climatic Data Center (U.S.), 1998. 1961–1990 global climate normals.
- Wright, K.I., 2000. The social origins of cooking and dining in early villages of Western Asia, in: *Proceedings of the Prehistoric Society*. pp. 89–122.
- Wylie, A., 1985. The Reaction against Analogy. *Advances in Archaeological Method and Theory* 8, 63–111.
- Yellen, J.E., 1977. *Archaeological Approaches to the Present: Models for Reconstructing the Past*. Academic Press, New York.
- Zeder, M.A., 2008. Domestication and early agriculture in the Mediterranean Basin: Origins, diffusion, and impact. *Proceedings of the National Academy of Sciences* 105, 11597.
- ZielhO., C., Clare, Lee, Rollefson, G.O., Wächter, S., Hoffmeister, D., Bareth, G., Roettig, C., Bullmann, H., Schneider, B., Berke, H., Weninger, Bernhard, 2012. The decline of the early Neolithic population center of 'Ain Ghazâl and corresponding earth-surface processes, Jordan Rift Valley. *Quaternary Research*.

APPENDIX A

SUBSIDIARY FORMULAS AND MODELING ROUTINES

A.1. ESTIMATING STREAM DEPTHS

Depth of flow is difficult to estimate accurately because it is the depth of flowing water in a cell at any moment and changes over the course of a rainfall event (Bledsoe, 2002). Iterative cellular automata routines, such as SIMWE (see Chapter 4), provide the most accurate way to estimate h in a GIS but are computationally very expensive, and thus impractical for long-term iterated landscape evolution simulations (such as that employed by the MML) where minimization of run-time length is important. Therefore MML estimates h in each cell from an idealized “unit hydrograph” for that cell, which is a graphical representation of flow depth over time during a simulation interval. Although a real unit hydrograph curve may take one of many different shapes (e.g., skewed, bimodal, etc.) the idealized unit hydrograph for a cell in the MML is assumed to be normally distributed with a base equal to the length of the time of a hydrologic event (such as a storm). The area under the curve is the total accumulated vertical meters of runoff from the event passing through the cell over the entire hydrological event, and the apex of the curve represents the peak flow depth during the event (Figure A.1), which is a good estimation of h . Thus, h can be estimated according to the following function:

$$\text{Eq. A.1} \quad h = \frac{R_e \cdot A}{0.595 \cdot t}$$

In this equation, R_e [m] is the excess rainfall (meters precipitation minus infiltration) during the hydrologic event, and A [m^2] is the upslope accumulated area so that $R_e \cdot A$ is the accumulated runoff (vertical meters of water) that passed over the cell during the simulation

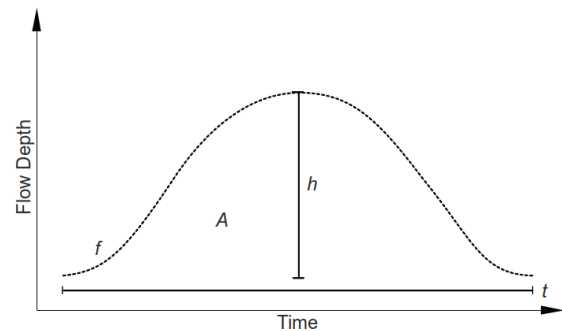


Fig. A.1. Method of approximation of peak flow depth from an idealized unit hydrograph. Dashed line “ f ” is flow depth over the course of a storm of time “ t ”. The area “ A ” under the curve is the total accumulated flow, and the length of the line at its peak, is the peak flow depth “ h ”.

interval¹. The value of t is the number of “hydrologic instants” in the simulation interval. The hydrologic instant is the time it takes water to cross one cell of a raster DEM, which can be determined by multiplying the average velocity of flowing water in the watershed (e.g., as derived with Manning’s equation) by the cell resolution.

A.2. DETERMINING BREAKPOINTS IN NET ACCUMULATED FLOW FOR PROCESS PHASE CHANGES

The location for surface process phase changes is based on the determination of series of breakpoints in net accumulated flow (A), which is the accumulated flow of all upslope precipitation minus infiltration (see Chapter 4).

¹ A is calculated by the GRASS hydrological modeling module “r.watershed”. See Chapter 4, Section 4.5.2 for more information about the calculation of accumulated runoff.

A series of three breakpoints are needed: one between diffusive soil creep and overland flow, the second between overland flow and rilling/gullying, and the third between rilling/gullying and channelized stream flow.

The first two breakpoints are determined by plotting A against local topographic curvatures in the direction of slope – the profile curvature (pc) – for each cell. Positive values of pc indicate a marked increase in slope (a convex profile), negative values indicate a marked decrease in slope (a concave profile), while values of $pc \sim 0$ represent cells where there is little change in slope. This is shown in Figure A.2a with A on the y -axis and pc on the x -axis. Drainage divides have little accumulation and little change of slope, plotting near 0 on the x and y axes; hillslopes also have little change in slope, but have higher accumulation, plotting near 0 on the x -axis but higher on the y -axis. The transition between the drainage divide and hillslopes has the maximum convex curvature (positive pc) and relatively low values of A , while the transition between hillslopes and gully heads at the base of slopes has concave curvature (negative pc) and higher accumulation values. Hence, for a given landscape and hydrologic regime, the value of A for the maximum value of pc is a good estimate for the transition from equation diffusion to USPED with exponents m and n for overland flow (sheetwash), and the value of A for the minimum value of pc is a good estimate for the transition from sheetwash to USPED with exponents m and n for rill/gully flow (Figure A.2a).

In a similar way, A can be plotted against the tangential curvature (tc) of each cell – the curvature perpendicular to the direction of slope – to identify the accumulation value for the transition from USPED to a shear-stress equation for channelized flow. The beginning of channelized flow can be identified as the location where very negative values of tc (concave) are associated with high

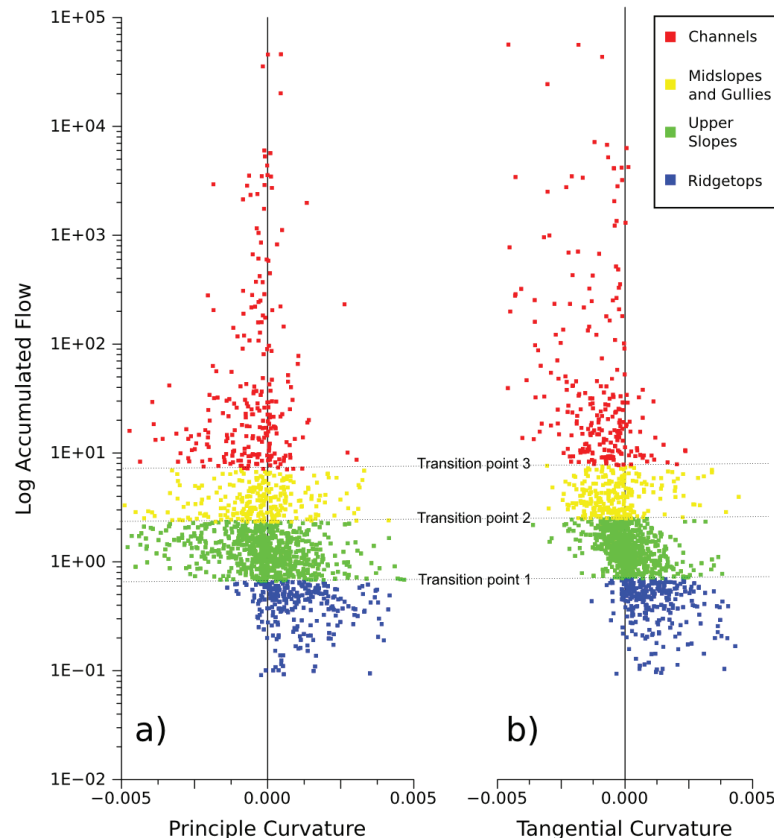


Fig. A.2. Graphical display of profile curvature and tangential curvature versus log flow accumulation.

values of A . Slightly negative values of tc that are associated with lower values of A represent the larger gullies and gully-heads (i.e., that occur higher in the drainage network than the real stream channels), and even higher values of A where tc has decreased indicate a widening channel carrying more water (Figure A.2b). Figure A.3 shows the locations of the transition points identified in Figure A.2 on the DEM for which they were derived.

A.3. THE ADAPTIVE “SOFT-KNEE” NET-dz SMOOTHING ALGORITHM

The smoothing procedure used to remove “spikes” from the net dz map is carried out over three stages. In the first stage, global univariate statistics are separately calculated for all values in the dz map below 0 (i.e., for all areas of net erosion), and all areas in the dz map above 0 (i.e., for all areas of net deposition). Then, the routine identifies values from the 1st quartile of erosion to the minimum

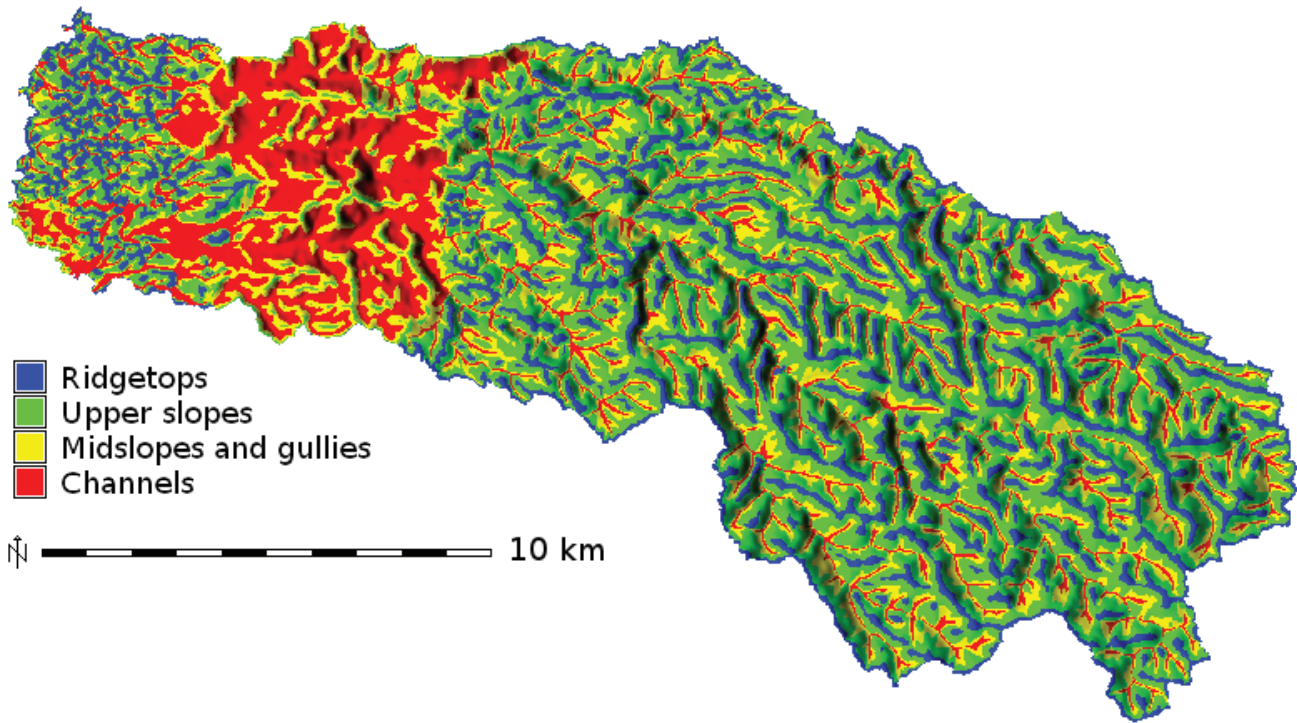


Fig. A.3. Map showing the locations of surface process transitions as determined from the graphs in Figure A.2.

(i.e., the very large negative numbers) and values from the 3rd quartile of deposition to the maximum (i.e., the very large positive numbers). The numerical values in these areas are then linearly rescaled from the 1st quartile to the 1st percentile and the 3rd quartile to the 99th percentile respectively. Unlike “brick wall” single threshold limiting, this “soft-knee” style of limiting retains some of the original scaling at the ends of the distribution but brings the highest values (i.e., the “spikes”) into the range of a normally distributed dataset.

A.4. CALCULATION OF SOIL-DEPTH “RATES”

The soil depth “rate” maps are created in a two-stage process, illustrated in Figure A.4. First, the relationship between the slope of a cell and the base-line soil-depth is established using a “graphing function”, which is a method that uses sequential linear equations to approximate the equation of a more complex curve. The segments of the linear graphing function are tied to breakpoints (Figure

A.4, points a, b, c, and d), which control the shape of the curve they approximate, in this case, the baseline relationship between the topographic slope in the neighborhood of the raster cell and soil-depths. In the r.soildepth.py script, the modeler may adjust these breakpoints to suit the particular landscape in question. Once this baseline relationship is established, a localized “offset” of the soil depth curve is calculated based on the amount and type of average topographic curvature (i.e., the average of the profile and tangential curvatures) present in the neighborhood of the raster cell. As the local curvature becomes increasingly concave, the curve is offset in the positive direction until the maximum positive offset is reached (points +b', +c', and +d' in Figure A.4), or, as the local curvature becomes increasingly concave, the curve is offset in the negative direction until the maximum negative offset is reached (points -a', -b', and -c' in Figure A.4). The relationship between the numerical amount of curvature and the numerical amount of offset is defined by a simple linear function, which can be adjusted by the modeler depending

upon the particular landscape in question (which essentially changes the locations of +b', +c', +d', -a', -b', and -c' in Figure A.4). Once the localized “soil depth rate curve” is established for all cells in the input raster map, the “r.soildepth.py” script then converts these values to actual units of soil depth (meters of sediment) through a simple linear

transformation. This transformation essentially sets the endpoints of the curve (points “a” and “d” in Figure A.4) to the actual maximum and minimum soil depths observed in the project area, and then estimates the depth of the particular raster cell based upon its position along the curve.

APPENDIX B

A GEOARCHAEOLOGICAL GAZETTEER OF THE WADI ZIQLÂB REGION

B.1. GEOARCHAEOLOGICAL SURVEY OF WADI-ZIQLÂB

In Wadi Ziqlâb, the wadi-bottom and the lower and middle terraces were surveyed on foot from its outlet to about 1 km beyond the confluence of the two main tributaries, Wadi ed-Dimna and Wadi ‘Ain Zubiya. Portions of the upper regions of the Wadi, especially around the hilltop town of Tubna, were also visited, although contiguous survey of this region was not carried out. The purpose of this work was to better understand the relationship between the lower and middle terraces and the active channel in all parts of the Wadi, and to gain an understanding of the depth of soils/sediments on different landforms in the Wadi and the areas of the plateau and uplands associated with the Wadi.

Figure B.1 shows an overview of part of Wadi ‘Ain Zubiya, above its confluence with Wadi ed-Dimna. The wadi is a seasonally inundated wash at this point, and the most prominent geomorphological features in this portion of the greater Ziqlâb drainage are a series of small alluvial terraces right along the drainage channel in the narrow wadi-bottom (Figure B.1). These small terraces are actually Maher’s “middle terrace”, but are still partially fluvially connected to the current fluvial regime in this portion of the Wadi, mainly through lateral erosion (Figure B.2). Exposed profiles of this terrace show about 50 cm of interbedded alluvial pebbles, gravels, and sands with silt lenses, overlain by another 50 cm of lightly reworked colluvium with larger cobbles and boulders in a matrix of red clays and silts (Figure B.1). The color and consistency of the colluvial fines suggest a dual origin in the grey slope Rendzinas and the red Terra Rossa soils of the plateau region. Fluvial and colluvial processes seemed to be well balanced in this portion of the Wadi, resulting in minimal Holocene colluviation



Fig B.1. Upper section of Wadi ‘Ayn Zubia.
Arrow points to a good example of the middle terrace in this section of the Wadi.



Fig B.2. Cutbank into a middle terrace remnant in the Upper Ziqlâb, showing the stratigraphy of the terrace.

on terraces, and only minor Holocene channel incision. It is likely that much of the colluvial material that is deposited in this portion of the Wadi is incorporated into the sediment supply of the channel during winter storm events and stored as a series of channel bars. These bars are the only equivalent of the lower terrace in this region. Also present in this portion of the Wadi are a series of

small bench-terraces which occur intermittently at about 10 to 20 m above the current channel, occurring most frequently at the inside of bends in the wadi. These are Maher's "upper terrace". Many of them have been completely depleted of surface sediments and are evidenced only by a mild break in the slope of the wadi walls (Figure B.2). The slopes above the upper terrace are covered in colluvium, and I found remnant, filled-in gully channels exposed in a road cut about half way up the slope (Figure B.3). This suggests that colluvial activity on the slope has alternated with gully erosion over time, but it is unclear if these gullies were active during the Neolithic.

At the confluence of Wadi 'Ain Zubiya and Wadi ed-Dimna (see Chapter 2, Figure 2.5), the channel becomes mildly incised, with banks of between 2-5 m. The lower terraces become more pronounced, and the system tends toward net erosion in this section of the Wadi. The middle terraces are now thickly mantled by colluvium, and several archaeological sites are preserved on them in this portion of the Wadi, notably the Late Neolithic sites of Tabaqat al-Bûma and al Aqaba, and the Epipaleolithic site of 'Uyun al-Hammam (see Chapter 2). Excavation at these sites indicates that the red Epipaleolithic paleosol is present on most of the middle terrace remnants in this section of the wadi (Maher, 2011) and this was confirmed at several exposures (road cuts and agricultural terrace cuts) in this section of the Wadi (Figure B.5).



Fig B.3. An example of a remnant of the upper terrace in the Upper Ziqlâb region.



Fig B.4. A filled gully on the slopes of the Upper Ziqlâb. Dotted line shows the outline of the ancient gully channel. Note that the fill derives from the red Terra Rossa soils of the upper plateau.



Fig B.5. This recent agricultural terrace cut in the Upper Ziqlâb region has exposed a section showing the red Epipaleolithic paleosol directly (and unconformably) overlain by tan Holocene colluvium.

Below 'Uyun al-Hammam, the Wadi-bottom broadens significantly, the channel is no longer incised, and the channel itself is also much wider than in the upper portions of the Wadi system (Figure B.6). 'Uyun al-Hammam is an active spring, but is currently being pumped by the town of Dayr Abu Sa'id, and though water no longer



Fig B.6. Overview of the middle section of the Wadi Ziqlâb drainage. The arrow points to a good example of the middle terrace in this section of the Wadi.

flows perennially in this section of the Wadi, it certainly did so before the pumping began in modern times. The lower terrace is still in active connection with the channel, but it appears in larger sections. The middle terraces are now quite large and broad (Figure B.6), but retain similar bedding character to the lower terraces in the upper reaches of the wadi (Figure B.7). Portions of the middle terrace are being actively eroded by bank-undercut in this section of the Wadi which has also led to large-scale stepped-slumping of the eroded edges of these terraces (Figure B.8). Mass-wasting occurs very frequently on the slopes in this portion of the wadi. There is a broad “piedmont” of colluvium at the base of these slopes in many parts of this portion of the Wadi and can be seen directly overlaying the middle terrace in many cutbanks (Figure B.9). The Epipaleolithic paleosol can be also seen in many of the cutbanks of the middle terrace, sometimes overlain by massive amounts of Holocene colluvium (Figure B.10), and in some places, reworked deposits clearly derived from the paleosol occur in larger alluvial profiles (Figure B.11). Several large and sometimes cross-cutting rotational slumps are evident in this portion of the wadi, and some appear to be quite recent (Figure B.12). Rilling/gullying and associated translational sliding is also very common (Figures B.12 and B.13).

After almost 4 km, the wadi-bottom narrows



Fig B.7. This cutbank has exposed a small stratigraphic section of the middle terrace in the mid-reaches of the Ziqlâb drainage.



Fig B.8. An excellent example of terrace edge-slump caused by bank undercut in the middle section of the Ziqlâb drainage.



Fig B.9. An example of Late Holocene colluvium directly overlaying alluvial deposits of the middle terrace in the mid-section of the Ziqlâb drainage.



Fig B.10. An example of the Late Holocene colluvium directly and unconformably overlying the Epipaleolithic red paleosol in the middle section of the Wadi Ziqlâb drainage.

again and although the channel is not greatly incised in this section, it occupies the entirety of the wadi-bottom. The naturally flowing perennial spring of ‘Ain Jahjah adds its waters to the Wadi about 1 km after the narrowing and, from this point onward, water flows in the wadi channel all year round. The upper of the two lower knick points occurs about 500 m past ‘Ain Jahjah, forming a beautiful waterfall encrusted with travertines (Figure B.14). A smaller tributary wadi joins the main channel just past the ‘Ain Jahjah knick point, and the site of Tell Rakkan I is located on the small promontory formed by this confluence (See Chapter 2, Figure 2.4). The Tell Rakkan promontory is also a remnant of the middle terrace, and, like other middle terrace remnants in this section of the Wadi, is covered by a substantial layer of colluvium (Figure B.15).

Below the ‘Ain Jahjah knickpoint, the channel becomes very incised (Figure B.16). The lower terraces are again mostly represented as sand and gravel bars, and the channel seems to be actively downcutting into bedrock in several areas. The middle terrace remnants are suspended perhaps 50-100 m above the active channel and



Fig B.11. The outlined band of red alluvium likely represents reworked sediments eroded from the red Epipaleolithic paleosol further up the Wadi. This stratigraphic section was studied by Maher (2005, 2011).



Fig B.12. This photograph shows multiple slumps on the flank of the middle section of the Ziqlâb drainage. The dotted lines outline the individual slump scars, and the arrow shows a small rill/gully that is forming on the same slope.

are covered by thick deposits of colluvium. Excavations at the LN site of al-Basatîn, located on one of the middle terrace remnants in this section of the wadi, did not encounter the red paleosol, however the presence of small quantities of Epipaleolithic artifacts (Gibbs et al., 2006) at the site suggests that it does exist here too, but is likely very deeply buried. The modern surface of the al-Basatîn terrace is fairly steep: typically above 15 degrees, and approaching 30 degrees in its upper portions. Neolithic cobble surfaces



Fig B.13. This photograph shows a small alluvial fan in the middle section of the Ziqlâb drainage. This fan was created by repeated translational debris flows. The arrow points to a small gully that is now forming at the head of the fan.



Fig B.15. This bulldozer cut on the Tell Rakkan terrace exposes a large section of the Late Holocene colluvium. Note the presence of a portion of stone LPPNB wall appearing in this section.



Fig B.14. A photograph of the spectacular waterfall that occurs at the Tell Rakkan knick point. Image courtesy of S. Kadowaki.

discovered at the site (Banning et al., 2003, 2002; Gibbs et al., 2006) are relatively level, suggesting the terrace surface was flatter in the Neolithic. A ~2-meter deep geological sounding excavated on the upper portion of the terrace revealed that the colluvial deposits are at least that deep, and are likely several meters deeper. The buried remnants



Fig B.16. An overview of the lower portion of the Ziqlâb drainage, showing how incised the channel is at this point. The arrow points to the location of the Tell Rakkan terrace in the distance.

of ancient rills and gullies are preserved within the colluvium. Several of these ancient rills had cut into archaeological layers at the site, and could be traced horizontally for up to 30 m as they crossed through several of the excavation trenches (Figure B.17). Thus, it seems that, while colluviation at this location was likely fairly constant throughout the Holocene, there were episodes of increased fluvial rilling and gullying that occurred here some point after the Neolithic period.



Fig B.17. Several ancient rills/gullies are preserved in the al-Basatin terrace. The dashed line outlines an ancient gully that cut into the Late Neolithic layers. The dotted line (back wall of excavation unit) outlines the remnants of a later gully that cut into the Early Bronze age layers at the site.

The lowest and final knick point occurs about 1.7 km downstream from the ‘Ain Jahjah knick point. This knick point is also marked by a magnificent waterfall shrouded in travertines. In 2004, the waterfall at this knick point had two tiers, first falling about 10 m over and into a small travertine cave, before falling another 5 m into a wide pool (Figure B.18, left side). By 2006, the cave had collapsed, and the head of the waterfall had retreated several meters upstream (Figure B.18, right side), confirming that headward channel incision at the knick points is still active and is proceeding at a fairly rapid rate. Below this final knick point, for the remaining 3 km before its outlet into the Jordan Valley, the Wadi is at its most incised. Extensive remnants of the middle terrace



Fig B.18. Photographs of the waterfall that forms at the lower knick point in Wadi Ziqlâb. The image on the left was taken in 2004, and the image on the right was taken in 2006. The arrow points to approximately the same location in both photographs, and indicates the amount of erosion that had occurred in the space of two years. Left image courtesy of Lisa Maher, right image courtesy of Adam Allentuck.

exist along the northern edge of the wadi for about a kilometer below the knick point, but are stranded at least 60-80 m above the current channel. The lowest two kilometers of this section of the Wadi and the former Wadi-mouth are now covered by an artificial lake that forms behind a dam built in the 1960’s, but apparently there were extensive sand and gravel delta deposits in this section of the wadi (W. Fisher et al., 1966). From the Wadi-mouth, the channel meanders across the floor of the Jordan Valley, flowing past the Chalcolithic site of Tell Fendi, until it empties into the Jordan River. In this section the channel margins are defined by levies covered in riparian vegetation and surrounded by silty overbank deposits.

B.2. GEOARCHAEOLOGICAL SURVEY OF WADI TAYYIBA

A 4 km section of the middle and lower Wadi Tayyiba drainage—from the town of At-Tayyiba to the unexcavated Neolithic site of WT-4 (about 3 km from the outlet)—was surveyed mainly with pedestrian methods. The main purpose of the



Fig B.19. Overview of the middle section of Wadi Tayyiba.

survey was to obtain GPS location information for the lower knick points in Wadi Tayyiba to study the WT-4 terrace landform noted in the 2000 geoarchaeological survey of the Wadi and to assess the general terrace sequence in the Wadi. Although quite a bit narrower and deeper than the middle section of Wadi Ziqlâb, there are some similarities between the two wadis. Tayyiba's wadi bottom is a more V-shaped in this section than is the U-shaped bottom of Ziqlâb (Figure B.19), but, like Ziqlâb, there is a “middle terrace” that seems to date from the Early to Middle Holocene. The remnants of this terrace are in a similar geomorphological context with regard to the current active channel (3-10 m above it) as can be seen in Figure B.20. Also like Ziqlâb, this portion of the Wadi is currently a seasonally dry stream bed¹, and has an equivalent “lower terrace”, that is mainly composed of channel bars and spits. There may be some remnants of a highly eroded “upper terrace” in Tayyiba but, if it exists at all, it is rare, shallow, and difficult to differentiate from other breaks in slope on the Wadi flanks.

As in Wadi Ziqlâb, the lower two knick points occur below the level of the currently-flowing perennial springs. Although the upper of the two Tayyiba knick points is shallower than the ‘Ain Jahjah knick point in Ziqlâb, it nevertheless marks the point of the same notable change in character of the Tayyiba drainage that occurs in the Ziqlâb drainage; after this knick point

¹ Although it likely was perennial in the past, before extensive groundwater pumping by the nearby town of at-Tayyiba.



Fig B.20. Close up of a section of the middle Wadi Tayyiba drainage. The arrow points to a good example of the Tayyiba middle terrace, which is analogous to the middle terrace of Wadi Ziqlâb.



Fig B.21. Overview of lower Tayyiba knickpoint. Notice the presence of an Ottoman period mill.

it becomes moderately incised with perennial stream flow from a spring that bubbles up very close to the top of the knick point. The lower knick point is quite a bit steeper, and this was taken advantage of in the Ottoman period by the construction of a water driven mill (Figure B.21). The Wadi becomes quite deeply incised past this point and access to the wadi-bottom from the middle terrace is very restricted (Figure B.22).

Interestingly, WT-4, the only known Neolithic site in Wadi Tayyiba (dated only by surface finds),



Fig B.22. Overview of the lower section of the Wadi Tayyiba drainage. Note how incised the channel is in this section.

is located in this lower region of the Wadi at a similar distance from the Wadi's outlet as Tell Rakkan I in Wadi Ziqlâb. Similarly to Tell Rakkan I, WT-4 is situated on a hanging terrace framed by the confluence of a smaller tributary wadi that feeds from the north into the main Tayyiba drainage (Figure B.23). The WT-4 terraces is quite large (15 ha), and a very long north-south bulldozer cut has exposed a stratigraphic sequence along one of its edges (see Chapter 2, Figure 2.9). Interestingly, the strata are dipping to the north

(i.e., away from the main Tayyiba drainage and against the direction of flow from the tributary wadi) at a 25-15 degree angle (Figure B.24). The stratigraphically lowest portion of the exposed profile appears at the southern end of the bulldozer cut and consists of several 10-50 cm thick bands of greyish and buff colluvium with rounded to subangular pebbles and cobbles (Figure B.24). These layers are cut by a small normal fault, with an offset of about 65 cm, and a fault plane trending roughly east-west (i.e., perpendicular to the dip of the strata, and parallel with the flow of the Wadi) (Figure 2.24). Stratigraphically above these layers is a 3-4 m thick layer of red silts with abundant archaeological material (likely dating to the Neolithic). There is a marked unconformity at the upper bound of this archaeological layer, topped by a massive layer of very lightly bedded tan silts with isolated cobbles and pebbles, which occupies the remainder of the very large exposed section. The severe "backwards" dip of all the layers suggests that this "terrace" may actually be a very large ancient rotational earth slump, of the type described by Field and Banning (1998). This hypothesis is supported by presence of microfaulting at the "toe" of the formation and

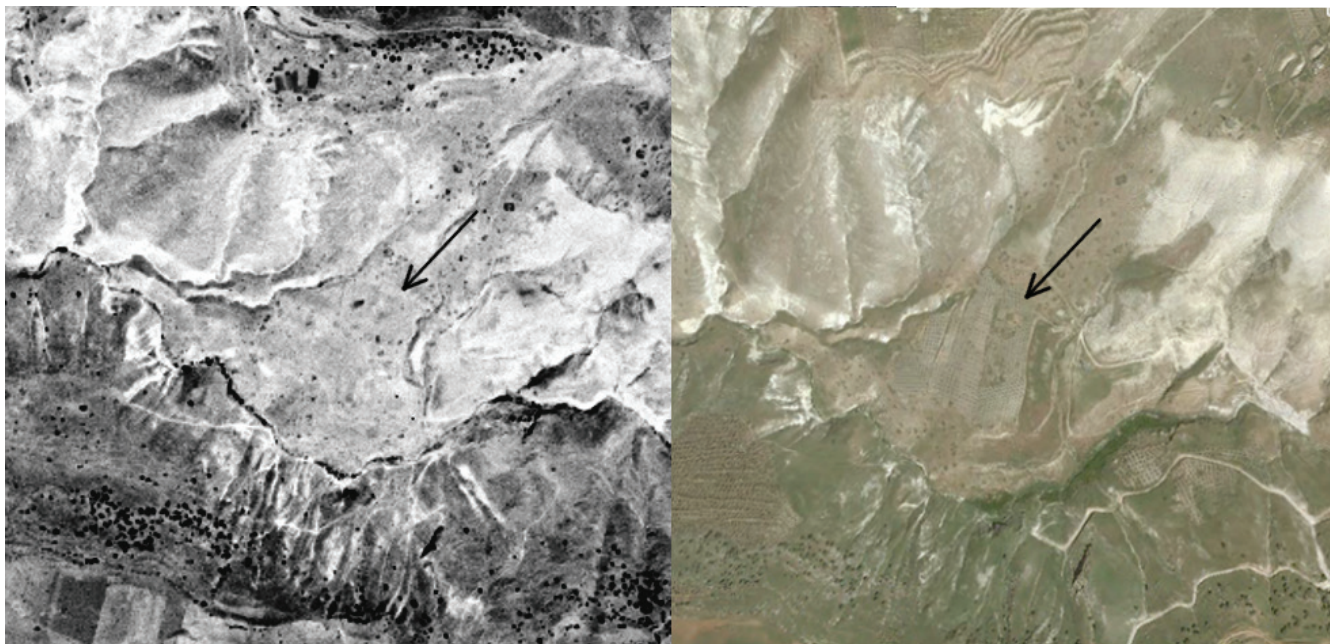


Fig B.23. CORONA (left) and GeoEye (right) imagery of the WT-4 terrace landform. The whole landform may be a rotational slump, and the arrow points to the possible point of detachment. Note that the slump may have originally blocked the entire Wadi channel.



Fig B.24. Close up of the stratigraphy of the “toe” of the WT-4 landform. The photo is looking downstream. Note the “backwards” dipping strata (outlined by the white dotted lines), and the fault (black dashed line). The arrow indicates the amount of slippage that has occurred along the fault line.

by the overall shape of the landform as seen on CORONA and GeoEye imagery (Figure B.23). The slump may have originally been a hanging alluvial terrace (perhaps the middle terrace?), left stranded and vulnerable to mass movement after the incision of the Tayyiba drainage in this section of the Wadi, which today is about 30-40 m below the edge of the terrace. The unconformable boundary of the archaeological layer with the massive silts suggests a period of post-Neolithic erosion of the surface of the ancient terrace, likely due to increased outwash from the small tributary wadi. This may have led to increased saturation which induced the slump to occur. The slump would have created a “sediment trap”, capturing silts carried by outwash from the small tributary. This would explain the accumulation of the massive silts behind the bedded front portion of the formation. Finally, an examination of the CORONA and GeoEye imagery (Figure B.23) suggests that it is also possible that the slump created a natural dam in the main Tayyiba channel², perhaps creating a small lake in this section of the Wadi which may have been an attractive

² It is also likely that a natural dam of this sort also occurred near the ‘Ain Jahjah knick point in Wadi Ziqlâb, and another in the upper part of Wadi Quseiba to the north of Wadi Tayyiba.



Fig B.25. Overview of the middle Wadi Abu Ziad drainage. Note the V-shape of the Wadi.

natural feature for later occupants of the region.

B.3. GEOARCHAEOLOGICAL SURVEY OF WADI ABU ZIAD

Wadi Abu Ziad differs from the previous two Wadis in that it is entirely located within the plateau region and does not transgress into the uplands. There are also no knick points in Wadi Abu Ziad, and there is a relative lack of small alluvial terraces along most of the length of the Wadi. The Wadi has a more V-shaped profile than the other two wadis (Figure B.25), which likely has to do with two geomorphological aspects of the Wadi itself. Firstly the short traverse of the Wadi means that it has a relatively steeper fall from source to outlet, and thus is more likely to experience high-energy, erosive flow along its entire length. Thus, there was little chance for substantial alluviation to occur in the wadi-bottom. Secondly, one of the main tributaries of the Wadi sources at a high-flowing perennial spring, now located directly beneath the road just north of the main masjid (mosque) in the center of the town of Dayr Abu Sayeed and which currently supplies most of that town’s water needs. The continual outflow from this spring, combined with the steep descent of the wadi channel, would have further exacerbated downcutting.

Another interesting feature of Wadi Abu Ziad is the presence of multiple types of tool-quality flint. Kaduwaki et al. (2008) have identified two



Fig B.26. Arrows point to probable ancient flint quarries at 'Ain Beidha.



Fig B.27. Overview of large alluvial deposits at the mouth of Wadi Abu Ziad.

sources of flint in Wadi Abu Ziad. The first is a band of fine- to medium-quality pinkish grey flint of the kind also appearing in outcrops in Wadi Ziqlâb. In Abu Ziad, the main outcrop of this flint occurs in the lower stretch of the Wadi opposite one of the perennial springs ('Ain Beidah) near the Bronze Age site of 'Ain Beidah (see Chapter 2, Figure 2.2). The hillside where this outcrop occurs is scarred by half-moon-shaped quarry diggings (Figure B.26) that are likely contemporaneous with the site of 'Ain Beidah, but flint could have also been quarried there in the Neolithic. The second flint source identified by Kadowaki et al. (2008) is located a few hundred meters upstream from 'Ain Beidha (see map in Chapter 2, Figure



Fig B.28. The large exposed section of alluvium at the mouth of Wadi Abu Ziad.



Fig B.29. Close up of the dated strata from the large alluvial deposit at the mouth of Wadi Abu Ziad. The upper dated strata had stone tools and abundant charcoal.

2.2), and is a source of fine-grained, lustrous, chocolate-brown, flint in nodule form. This type of fine-grained flint is required in order to make more technologically complex tool-forms, such as sickle-elements made on blades (Kadowaki, 2007).

It is only near the Wadi's outlet to the Jordan Valley that it widens sufficiently for alluviation to occur and for terraces to develop. Thus, the main geoarchaeological work conducted in Wadi Abu Ziad took place at a large, stream-cut terrace riser on the south bank of the Wadi (Figure B.27), almost directly opposite the Bronze Age site of 'Ain Beidha located on another small terrace on the northern side of the Wadi. This stream cut exposed roughly 5 m of alluvial deposits, grading into another overlaying 5-10 m of colluvium (Figure B.28). Close to the bottom of this stratigraphic sequence is a high-energy alluvial stratum composed of large imbricated cobbles, bounded below and above by

thin fine-grained, low-energy alluvial layers that contained large amounts of organic materials and charcoal (Figure B.29). The upper alluvial layer also contained flints of indeterminate age or provenience. Radiocarbon samples collected from the low-energy organic-rich alluvial layers date the lower alluvial stratum at 20,550 (± 410) cal BP, and the upper alluvial stratum 16,365 (± 455) cal BP, suggesting that, in Wadi Abu Ziad, there were alternating periods of high- and low-energy alluviation in the Epipaleolithic. These layers thus predate the unconformity in Wadi Ziqlâb, which Maher places some time between 14,600 and 11,500 cal BP (Maher, 2011, 2005), and, although it is impossible to be certain, the high charcoal content of the low-energy layers may relate to human alteration of the landcover via burning in this early period and which may have some implications for the causes of erosion at the end of this period.

ARIZONA STATE UNIVERSITY
ANTHROPOLOGICAL RESEARCH PAPERS

1. A CULTURAL INVENTORY OF THE PROPOSED GRANITE REEF AND SALT-GILA AQUEDUCTS, AGUA FRIA RIVER TO GILA RIVER, ARIZONA by A.E.Dittert, P. Fish and D. Simonis (1969), 26 pp., 14 figs. O.P.
2. PATTERN MATHEMATICS AND ARCHAEOLOGY by B. Zaslow and A.E. Dittert (1977), x + 90 pp., 39 figs., 5 tables, bibliogr. O.P.
3. SURFICIAL POLLEN RECORDS FOR CENTRAL ARIZONA by J. Schoenwetter and L. Doerschlag (1970), 22 pp., 1 table, bibliogr. O.P.
4. HECLA I: A PRELIMINARY REPORT ON THE ARCHAEOLOGICAL INVESTIGATIONS AT THE LAKESHORE PROJECT, PAPAGO RESERVATION, SOUTH-CENTRAL ARIZ-ONA by A. Goodyear and A.E. Dittert (1973), iv + 81 pp., 15 figs., bibliogr. O.P.
5. PALYNOLOGY OF THE ROBINSON SITE, NORTH-CENTRAL WISCONSIN by J. Gish (1976), viii + 76 pp., 11 figs., 5 tables, app., bibliogr. O.P.
6. DEFINITION AND PRELIMINARY STUDY OF THE MIDVALE SITE by J. Schoenwetter, S.W. Gaines and D. Weaver (1973), viii + 173 pp., 9 maps, 22 figs., 29 tables, bibliogr. O.P.
7. ARCHAEOLOGICAL INVESTIGATIONS AT THE WESTWING SITE, AZ T:7:27 (ASU), AGUA FRIA RIVER VALLEY, ARIZONA by D. Weaver (1974), v + 84 pp., 24 figs., 2 app., bibliogr. O.P.
8. AN ARCHAEOLOGICAL SURVEY OF THE CAVE BUTTES DAM ALTERNATIVE SITE AND RESERVOIR, ARIZONA by J. Rodgers (1974), vi + 92 pp., 30 figs., 2 app., bibliogr. ... O.P.
9. HECLA II AND III: AN INTERPRETIVE STUDY OF THE ARCHAEOLOGICAL REMAINS FROM THE LAKESHORE PROJECT, PAPAGO RESERVATION, SOUTH-CENTRAL ARIZONA by A. Goodyear (1975), xvii + 401 pp., 47 figs., 50 tables, 9 app., bibliogr. \$20.00
10. AN ARCHAEOLOGICAL INVESTIGATION OF BUCKEYE HILLS EAST, MARICOPA COUNTY, ARIZONA by J. Rodgers (1976), vii + 116 pp., 18 figs., 6 tables, 2 app. \$10.00
11. ARCHAEOLOGY IN COPPER BASIN, YAVAPAI COUNTY, ARIZONA: MODEL BUIL-DING FOR THE PREHISTORY OF THE PRESCOTT REGION by M. Jeter (1977), xv + 434 pp., 47 figs., 15 tables, 8 app., bibliogr. O.P.
12. ARCHAEOLOGICAL INVESTIGATIONS ALONG THE GRANITE REEF AQUEDUCT, CAVE CREEK ARCHAEOLOGICAL DISTRICT, ARIZONA by J. Rodgers (1977), ix + 185 pp., 31 figs., 33 tables, 3 app., bibliogr. \$15.00
13. AN ANALYTICAL APPROACH TO CULTURAL RESOURCE MANAGEMENT: THE LIT-TLE COLORADO PLANNING UNIT, F. Plog, Editor (1978), xiv + 293 pp., 67 figs., 96 tables, 4 app., bibliogr. O.P.
14. ARCHAEOLOGICAL INVESTIGATIONS AT SENECA LAKE, SAN CARLOS INDIAN RESERVATION, ARIZONA by R. C. Stafford (1978), vi + 96 pp., 31 figs., 11 tables, 3 app., bibliogr. \$10.00
15. COMPUTER GRAPHICS IN ARCHAEOLOGY: STATISTICAL CARTOGRAPHIC APPLICATIONS TO SPATIAL ANALYSIS IN ARCHAEOLOGICAL CONTEXTS, S. Upham, Editor (1979), vi + 156 pp., 75 figs., 18 tables, bibliogr. \$15.00

16. THE INTERPRETIVE POTENTIAL OF MOUSTERIAN DEBITAGE by P. Fish (1979), ix + 167 pp., 17 figs., 27 tables, 4 app., bibliogr. O.P.
17. ARCHAEOLOGICAL INVESTIGATIONS IN THE CAVE CREEK AREA, MARICOPA COUNTY, SOUTH-CENTRAL ARIZONA by T. Kathleen Henderson and James B. Rodgers (1979), xii + 198 pp., 33 figs., 34 tables, 19 plates, 4 app., bibliogr. \$20.00
18. AN ARCHAEOLOGICAL TEST OF SITES IN THE GILA BUTTE-SANTAN REGION, SOUTH-CENTRAL ARIZONA by G. Rice et al. (1979), x + 258 pp., 65 figs., 33 tables, bibliogr. O.P.
19. THE NORTH BURGOS ARCHAEOLOGICAL SURVEY: BRONZE AND IRON AGE ARCHAEOLOGY ON THE MESETA DEL NORTE (PROVINCE OF BURGOS, NORTH-CENTRAL SPAIN), G.A. Clark, Editor (1979), xviii + 307 pp., 98 figs., 40 tables, 9 plates, 4 app., bibliogr. O.P.
20. SPEAKING, SINGING AND TEACHING: A MULTIDISCIPLINARY APPROACH TO LANGUAGE VARIATION (SWALLOW VIII), F. Barkin and E. Brandt, Editors (1980), vi + 482 pp., bibliogr. O.P.
21. ARCHAEOLOGICAL INVESTIGATIONS AT AZ U:6:61 (ASU), A PREHISTORIC LIMIT-ED ACTIVITY SITE IN SOUTH-CENTRAL ARIZONA by P. Brown and A.E. Rogge (1980), viii + 83 pp., 17 figs., 17 tables, 4 plates, 1 app., bibliogr. \$10.00
22. PROCEEDINGS: EIGHTH INTERNATIONAL CONGRESS FOR THE STUDY OF THE PRECOLUMBIAN CULTURES OF THE LESSER ANTILLES, S. Lewenstein, Editor (1980), xiv + 624 pp., 106 figs., 46 tables, 90 plates, bibliogr. O.P.
23. CURRENT ISSUES IN HOHOKAM PREHISTORY: PROCEEDINGS OF A SYMPOSIUM, D. Doyel and F. Plog, Editors (1980), iv + 281 pp., 24 figs., 19 tables, 1 app., bibliogr. O.P.
24. THE PROTOHISTORIC PERIOD IN THE NORTH AMERICAN SOUTHWEST, A.D. 1450-1700, D. Wilcox and W.B. Masse, Editors (1981), vi + 445 pp., 12 figs., 8 tables, 10 plates, bibliogr. O.P.
25. PATTERN DISSEMINATION IN THE PREHISTORIC SOUTHWEST AND MESOAMERICA by Bert Zaslow (1981), vii + 57 pp., 28 figs., 2 tables, 3 app., bibliogr. \$10.00
26. CHIMPANZEE VISUAL COMMUNICATION by S. Berdecio and L. Nash (1981), xv + 159 pp., 15 figs., 60 tables, 80 plates, 2 app., bibliogr. O.P.
27. ANTHROPOLOGICAL STUDIES IN GREAT BRITAIN AND IRELAND, M. Firestone, Editor (1982), iii + 147 pp., 17 figs., 12 tables, bibliogr. \$12.00
28. GRANITE REEF: A STUDY IN DESERT ARCHAEOLOGY, P. Brown and C. Stone, Editors (1982), xvii + 443 pp., 71 figs., 69 tables, 20 plates, 4 app., bibliogr. \$25.00
29. ECOLOGICAL MODELS IN ECONOMIC PREHISTORY, G. Bronitsky, Editor (1983), iii + 290 pp., 36 figs., 36 tables, bibliogr. \$20.00
30. A PEASANT COMMUNITY IN CHANGING THAILAND by S. Piker (1983), ix + 157 pp., 5 figs., 19 tables, bibliogr. \$15.00
31. REGIONAL ANALYSIS OF PREHISTORIC CERAMIC VARIATION: CONTEMPORARY STUDIES OF THE CIBOLA WHITEWARES, A. Sullivan and J. Hantman, Editors (1984), vi + 149 pp., 16 figs., 11 tables, 12 plates, bibliogr. \$15.00
32. PREHISTORIC SUBSISTENCE AND POPULATION CHANGE ALONG THE LOWER AGUA FRIA RIVER, ARIZONA: A MODEL SIMULATION by D. Dove (1984), viii + 139 pp., 19 figs., 5 tables, 2 app., bibliogr. \$15.00

33. PREHISTORIC AGRICULTURAL STRATEGIES IN THE SOUTHWEST, S. Fish and P. Fish, Editors (1984), vii + 386 pp., 61 figs., 28 tables, 2 plates, bibliogr. \$25.00
34. HEALTH AND DISEASE IN THE PREHISTORIC SOUTHWEST, C. Merbs and R. Miller, Editors (1985), xix + 402 pp., 35 figs., 64 tables, 101 plates, 1 app., bibliogr. O.P.
35. POPULATION GROWTH AND SOCIAL COMPLEXITY: AN EXAMINATION OF SETTLEMENT AND ENVIRONMENT IN THE CENTRAL MAYA LOWLANDS by Anabel Ford (1986), xiii + 201 pp., 28 figs., 37 tables, 19 plates, 4 app., bibliogr., index \$15.00
36. LA RIERA CAVE: STONE AGE HUNTER-GATHERER ADAPTATIONS IN NORTHERN SPAIN L.G. Straus and G.A. Clark, Editors (1986), xvii + 498 pp., 244 figs., 107 tables, 35 plates, 2 app., bibliogr. \$25.00
37. POLITIES AND PARTITIONS: HUMAN BOUNDARIES AND THE GROWTH OF SOCIAL COMPLEXITY, K. Trinkaus, Editor (1987), iv + 251 pp., 43 figs., 11 tables, bibliogr. \$20.00
38. COASTS, PLAINS AND DESERTS: ESSAYS IN HONOR OF REYNOLD J. RUPPÉ, S.W. Gaines, Editor (1987), xii + 282 pp., 65 figs., 48 tables, 2 plates, bibliogr. \$25.00
39. NEW FRONTIERS IN THE ARCHAEOLOGY OF THE PACIFIC COAST OF SOUTHERN MESOAMERICA, F. Bové and L. Heller, Editors (1989), xvii + 292 pp., 81 figs., 40 tables, 44 plates, bibliogr. \$30.00
40. PERSPECTIVES ON ANTHROPOLOGICAL COLLECTIONS FROM THE AMERICAN SOUTHWEST, A.L. Hedlund, Editor (1989), iii + 158 pp., 2 figs., bibliogr. \$15.00
41. TECHNOLOGICAL CHANGE IN THE CHAVEZ PASS REGION, NORTH-CENTRAL ARIZONA, Gary Brown, Editor (1990), xiv + 226 pp., 48 figs., 90 tables, 2 plates, 6 app., bibliogr. \$20.00
42. THE ETHNOARCHAEOLOGY OF REFUSE DISPOSAL, E. Staski and L. Sutro, Editors (1991), vii + 92 pp., 11 figs., 13 tables, 8 plates, bibliogr. \$10.00
43. AN INVESTIGATION OF IMAGE PROCESSING TECHNIQUES AT PINCEVENT HABITATION NO. 1, AN UPPER MAGDALENIAN SITE IN NORTHERN FRANCE by Stephen A. Lang (1992), vii + 110 pp., 44 figs., 2 tables, 13 app., bibliogr. \$25.00
44. SHAMANS, PRIESTS AND WITCHES: A CROSS-CULTURAL STUDY OF MAGICO-RELIGIOUS PRACTITIONERS by Michael J. Winkelman (1992), viii + 191 pp., 11 figs., 4 tables, 3 app., bibliogr. \$27.50
45. MIDDLE PALEOLITHIC ASSEMBLAGE AND SETTLEMENT VARIABILITY IN WEST-CENTRAL JORDAN by James M. Potter (1993), v + 57 pp., 23 figs., 23 tables, bibliogr. \$10.00
46. EXPLORING SOCIAL, POLITICAL AND ECONOMIC ORGANIZATION IN THE ZUNI REGION, T. Howell and T. Stone, Editors (1994), ix + 126 pp., 39 figs., 28 tables, 3 plates, bibliogr. \$15.00
47. SUBSISTENCE AND STONE TOOL TECHNOLOGY: AN OLD WORLD PERSPECTIVE by B. J. Vierra (1995), xiv + 283 pp., 113 figs., 95 tables, 2 app., bibliogr. \$25.00
48. INTERPRETING SOUTHWESTERN DIVERSITY: UNDERLYING PRINCIPLES AND OVERARCHING PATTERNS, P. Fish and J. Reid, Editors (1996), ix + 320 pp., 61 figs., 20 tables, bibliogr. \$25.00
49. WANDERING VILLAGERS: PIT STRUCTURES, MOBILITY AND AGRICULTURE IN SOUTHEASTERN ARIZONA, P.A. Gilman (1997), xii + 216 pp., 53 figs., 54 tables, 2 app., bibliogr. O.P.

50. THE ARCHAEOLOGY OF THE WADI AL-HASA, WEST-CENTRAL JORDAN, VOLUME 1: SURVEYS, SETTLEMENT PATTERNS AND PALEOENVIRONMENTS, N. R. Coinman, Editor (1998), v + 228 pp., 63 figs., 20 plates, 37 tables, bibliogr.O.P.
51. MIGRATION AND REORGANIZATION: THE PUEBLO IV PERIOD IN THE AMERICAN SOUTHWEST, K. A. Spielmann, Editor (1998), x + 301 pp., 100 figs., 49 tables, 4 plates, 3 app., bibliogr.O.P.
52. THE ARCHAEOLOGY OF THE WADI AL-HASA, WEST-CENTRAL JORDAN, VOLUME 2: EXCAVATIONS AT MIDDLE, UPPER AND EPIPALEOLITHIC SITES, N. R. Coinman, Editor (2000), xiv + 391 pp., 143 figs., 13 plates, 167 tables, bibliogr.\$30.00
53. SOCIAL INTEGRATION IN THE ANCIENT MAYA HINTERLANDS: CERAMIC VARIABILITY IN THE BELIZE RIVER AREA by L. J. Lucero (2001), ix + 88 pp., 20 figs., 20 tables, bibliogr.\$15.00
54. BOUNDARIES AND TERRITORIES: PREHISTORY OF THE U. S. SOUTHWEST AND NORTHERN MEXICO, M. E. Villalpando, Editor (2002), xi + 186 pp., 15 maps, 46 figs., 12 tables, bibliogr., index....\$20.00
55. THE MESOLITHIC OF THE ATLANTIC FAÇADE: PROCEEDINGS OF THE SANTANDER SYMPOSIUM, M. R. González Morales and G. A. Clark, Editors (2004), xii + 260 pp., 83 figs., 5 plates, 20 tables, bibliogr.25.00
56. THE MOUSTERIAN OF THE ZAGROS: A REGIONAL PERSPECTIVE by J. M. Lindly (2005), vi + 116 pp., 29 figs., 26 tables, 1 app., bibliogr.\$20.00
57. MANAGING ARCHAEOLOGICAL DATA: ESSAYS IN HONOR OF SYLVIA W. GAINES, J. L. Hantman and R. Most, Editors (2006), ix + 201 pp., 37 figs., 42 tables, 1 app., bibliogr.\$25.00
58. EXPLORING VARIABILITY IN MOGOLLON PITHOUSES, B. J. Roth and R. J. Stokes, Editors (2007), v + 142 pp., 47 figs., 2 plates, 20 tables, bibliogr.\$20.00
59. REANALYSIS AND REINTERPRETATION IN SOUTHWESTERN BIOARCHAEOLOGY, A. Stodder, Editor (2008), vi + 237 pp., 35 figs., 44 tables, 3 app., index, site index, bibliogr.,\$30.00
60. THE CONSEQUENCES OF HUMAN LAND-USE STRATEGIES DURING THE PPNB-LN TRANSITION: A SIMULATION MODELING APPROACH by I. I. T. Ullah (2017), xiv + 177 pp., 93 figs, 14 tables, 3 app., bibliogr.\$30.00

Out-of-print numbers in the Arizona State University Anthropological Research Papers are available upon request in the form of pdfs at 15¢/page. Requests should be directed to the Editor, Anthropological Research Papers, School of Human Evolution & Social Change, Arizona State University, Tempe, AZ 85287-2402 [Tel: (480) 965-6215, 965-6957; Fax: (480) 965-7671].

Arizona State University vigorously pursues equal opportunity in its employment, activities and programs.

